

The Oxidation-Initiated Nazarov Cyclization and Other Pericyclic Transformations

by

Emily Schmidt

A thesis submitted in partial fulfillment of the requirements for the degree of

Master of Science

Department of Chemistry

University of Alberta

© Emily Schmidt, 2024

Abstract

The synthesis of interesting and useful cyclic structures is of high importance in chemistry. Strategies for their synthesis include pericyclic reactions, namely electrocyclizations and cycloadditions. This thesis will discuss the investigation towards the synthesis of cyclic structures via Nazarov cyclization, as well as a catalytic thermal [2+2] cycloaddition.

Chapter 1 describes recent advances in the Nazarov cyclization. A growing area is the use of non-traditional reagents to activate the divinyl ketone and derivatives towards cyclization. This provides alternative and sometimes milder conditions for the reaction. Another area of interest is the use of non-traditional substrates in the Nazarov cyclization, allowing access to interesting novel products.

Chapter 2 describes efforts towards the oxidation-initiated cyclization of non-traditional Nazarov substrates, such as silyl enol ethers and allylic ethers. Interestingly, products of these reactions when using DDQ as the oxidant resulted in DDQ adduct structures, via Diels-Alder reaction.

Chapter 3 describes the development of a catalytic Lewis acid mediated formal [2+2] cycloaddition of *o*-styrenyl chalcones, forming bicyclic structures. A preliminary investigation into an asymmetric transformation is also presented.

Preface

Part of chapter 1 of this thesis will be published as Schmidt, E; Khalifa, S.; West, F. G. “The Nazarov Reaction” in Comprehensive Organic Synthesis, 3rd edition. *Manuscript submitted.*

Acknowledgements

First, I would like to express my sincere gratitude to my supervisor, Professor Frederick G. West, for your continued support, guidance, and kindness during my graduate school journey. Thank you for helping me learn and grow; I feel like a completely different person and chemist from when I started.

To my undergraduate professors, Sharon and Norm who started me on this path, thank you for being the best mentors; your impact is significant.

To my colleagues and friends in the West group, thank you for always being there when needed, and for making me a better chemist. Carson, you were the best bench mate a person could ask for. Thank you for taking the time to teach me, and always being supportive and patient with my questions. Erin, thank you for the coffee, chats, and just generally everything. I am forever glad that you joined the group, and that we got to go through this together. Seif, Andrew, Karim, Christian and Richard, thank you for being great friends and colleagues, and for all for all the days spent together in lab. I have learned a lot and laughed a lot.

My friends in the department, Ashley and Madi, thank you for keeping me sane.

Liam, thank you for everything you have done for me in the last couple of years. Your support and sacrifices have been invaluable; I am so grateful that you were with me throughout this journey. Thank you.

Table of Contents

Chapter 1: The Nazarov Cyclization: Recent Advances in Activation Methods and Alternative Substrates	1
1.1 Introduction.....	1
1.2 Alternative Activation Strategies	2
1.2.1 Thermal Activation	3
1.2.2 Photochemical Activation	3
1.2.3 Oxidation-Initiated Cyclization	4
1.2.4 Halogen bond donors	5
1.2.5 Electrophilic phosphonium	6
1.2.6 Silylium-ion promoted cyclization	7
1.2.7 Activation via palladium enolate	8
1.2.8 Activation via formation of a Pd π -allyl complex.....	9
1.3 Alternative Substrates	10
1.3.1 Activation through trienes.....	10
1.3.2 Allenyl vinyl ketones	11
1.3.3 Aryl allenyl ketones	12
1.3.4 Activation through diketones	13
1.3.5 Activation by ring opening.....	14
1.3.6 Imino-Nazarov Cyclization.....	18
1.3.7 Halo Nazarov Cyclization.....	21
1.3.8 C–O bond ionization	22
1.3.9 Aza-Nazarov cyclization.....	25
1.3.10 Oxa-Nazarov cyclization	27
1.3.11 Iso-Nazarov cyclization	28
1.3.12 Vinylogous Nazarov cyclization	29
1.3.13 Metal mediated activation of alkynes	31
1.4 Summary	32
Chapter 2: Exploration of the Oxidative Entry to the Nazarov Cyclization	33
2.1 Introduction.....	33

2.1.1 Early examples of generation of carbocations via hydride abstraction using quinone oxidants	33
2.1.2 Mechanistic considerations of quinone oxidants	34
2.1.3 DDQ mediated oxidative C–C bond forming reactions	38
2.1.4 Other hydride abstraction oxidants	46
2.2 Background	50
2.3 Results and discussion	52
2.4 Conclusion	69
2.5 Future Directions	69
2.6 Experimental	70
2.6.1 General information	70
2.6.2 Characterization of compounds	71
Chapter 3: Development of a Catalytic Method for the Synthesis of Cyclobutanes via a Formal [2+2] Cycloaddition of o-Styrenyl Chalcones	90
3.1 Introduction	90
3.1.1 Applications of cyclobutane compounds in medicinal chemistry	90
3.1.2 Mechanistic considerations of [2+2] photocycloadditions	92
3.1.3 Thermal [2+2] cycloadditions	95
3.2 Background	103
3.3 Results and discussion	105
3.3.1 Development of a catalytic formal [2+2] cycloaddition	105
3.3.2 Preliminary investigations into an enantioselective transformation	114
3.4 Conclusion	117
3.5 Future Directions	118
3.6 Experimental	119
3.6.1 General information	119
3.6.2 Characterization of compounds	119
References	138
Appendix I: Selected NMR Spectra (Chapter 2)	152
Appendix II: Selected NMR Spectra (Chapter 3)	167

List of Tables

Chapter 2

Table 2.1 Screening of oxidant conditions for compound 41	54
Table 2.2 Screening of oxidant conditions for compound 48	60
Table 2.3 Screening of oxidant conditions for compound 52	65
Table 2.4 Screening of oxidant conditions for compound 57	67
Table 2.5 Screening of oxidant conditions for compound 61	68

Chapter 3

Table 3.1 Screening of catalytic conditions for the formal [2+2] cycloaddition of 23a	108
Table 3.2 Generality of the catalytic formal [2+2] cycloaddition	112
Table 3.3 Screening of chiral ligands for the formal [2+2] cycloaddition of 23a	115
Table 3.4 Screening of chiral ligands using In(OTf) ₃ for the formal [2+2] cycloaddition of 23a	117

List of Figures

Chapter 1

Figure 1.1 Select examples of natural products made using the Nazarov cyclization.....	2
---	---

Chapter 2

Figure 2.1 Secondary orbital interactions between hydride donor and DDQ.....	37
Figure 2.2 Oxoammonium ions	47
Figure 2.3 Carbocation oxidants	49
Figure 2.4 Key 2D NMR correlations for compound 50	61
Figure 2.5 Key carbon signals in compound 58	67

Chapter 3

Figure 3.1 FDA approved cyclobutane containing drugs.....	90
Figure 3.2 Examples of cyclobutanes as isosteres	91
Figure 3.3 Molecular orbitals involved in a [2+2] photocycloaddition	92
Figure 3.4 Excitation mechanism via triplet energy transfer from sensitizer	94
Figure 3.5 [2+2] photocycloaddition via photoredox catalysis.....	95
Figure 3.6 X-Ray crystal structure of 24a	104
Figure 3.7 Chiral ligands used in formal [2+2] cycloaddition screening study	116

List of Schemes

Chapter 1

Scheme 1.1 Vorländer ketal synthesis	1
Scheme 1.2 Synthesis of 2-cyclopentanone by Nazarov and coworkers	1
Scheme 1.3 Mechanism of the Nazarov cyclization	2
Scheme 1.4 Thermal activation of aryl allenyl ketones.....	3
Scheme 1.5 Photochemical activation of an aryl alkenyl ketone	4
Scheme 1.6 Synthesis of 16- <i>epi</i> -terpendole E via photochemical Nazarov cyclization	4
Scheme 1.7 Oxidative Nazarov cyclization of pentadienyl ethers	5
Scheme 1.8 Activation of divinyl ketones by halogen bond donors	6
Scheme 1.9 Activation using electrophilic phosphonium	7
Scheme 1.10 Activation using silylium ions	8
Scheme 1.11 Divergent reactivity of polarized dienones dependent on palladium(II) source	8
Scheme 1.12 Enantioselective palladium(0) catalyzed Nazarov cyclization	9
Scheme 1.13 Nazarov-type cyclization via formation of Pd π -allyl complex.....	9
Scheme 1.14 Nazarov cyclization of ethoxytrienes	10
Scheme 1.15 Nazarov cyclization of dimethoxytrienes	11
Scheme 1.16 Silica gel mediated cyclization of allenyl vinyl ketones.....	11
Scheme 1.17 Enantioselective cyclization of allenyl vinyl ketones.....	12
Scheme 1.18 Nazarov cyclization of aryl allenyl ketone via cationic iron complex	12
Scheme 1.19 Iron (III) chloride promoted cyclization of aryl allenyl ketones	13
Scheme 1.20 Magnesium methoxide cyclization of enediones.....	13
Scheme 1.21 Enantioselective cyclization of α -diketones	13
Scheme 1.22 Electrocyclization initiated by 1,6-conjugate addition to dienyl diketones.....	14
Scheme 1.23 Interrupted Nazarov cyclization of divinyl epoxides.....	15
Scheme 1.24 Peracid initiated Nazarov cyclization	15
Scheme 1.25 Unfavourable equilibrium of ring closure of 3-amino pentadienyl cations.....	16
Scheme 1.26 Formation of an indenyl glycine using asymmetric cyclization of a divinyl aziridine	16
Scheme 1.27 Nazarov cyclization via electrocyclic ring opening of dihalocyclopropanes	17
Scheme 1.28 General mechanism of the formal homo-Nazarov cyclization	18
Scheme 1.29 Yb(OTf) ₃ catalyzed ring opening of alkylidene cyclopropane-1,1-ketoesters	18
Scheme 1.30 First example of an Imino-Nazarov cyclization	19
Scheme 1.31 Silver assisted ring opening of 1-alkenyl-1-amino-2,2-dichlorocyclopropanes.....	19
Scheme 1.32 Imino-Nazarov cyclization of [2+2] annulation products	20
Scheme 1.33 Synthesis of cyclopentenamides from α -aryl substituted allenamides	20
Scheme 1.34 Imino-Nazarov cyclization of alkenyliminylation product.....	21
Scheme 1.35 Halo Nazarov cyclization via alkynyl halo-Prins reaction	21
Scheme 1.36 Tandem Prins cyclization/halo-Nazarov cyclization	22

Scheme 1.37 Boronic acid-catalyzed dehydrative Nazarov cyclization	22
Scheme 1.38 Enantioselective dehydrative Nazarov cyclization	23
Scheme 1.39 Dehydrative Nazarov cyclization of thioether bis(allylic) alcohols	23
Scheme 1.40 Interrupted Nazarov cyclization via Lewis acid mediated C–O bond ionization ...	24
Scheme 1.41 Decarboxylative generation of 2-oxidopentadienyl cation	24
Scheme 1.42 Aza-Nazarov cyclization of N-acylium ion salt.....	25
Scheme 1.43 Titanium mediated aza-Nazarov cyclization to form [6/6/5] tricycles	26
Scheme 1.44 Synthesis of N-hydroxy oxindoles by base assisted dehydrohalogenation	26
Scheme 1.45 Iodine catalyzed diaza-Nazarov cyclization	27
Scheme 1.46 Tandem oxa-Nazarov cyclization/Michael addition	27
Scheme 1.47 Mechanism of the iso-Nazarov cyclization	28
Scheme 1.48 Iso-Nazarov cyclization with formal oxygen shift from C1 to C3	29
Scheme 1.49 Interrupted iso-Nazarov cyclization.....	29
Scheme 1.50 The vinylogous Nazarov reaction	30
Scheme 1.51 Vinylogous iso-Nazarov cyclization	30
Scheme 1.52 Vinylogous iso-Nazarov cyclization	30
Scheme 1.53 Generation of a pentadienyl cation via gold mediated activation of alkynes	31
Scheme 1.54 Gold catalyzed imino-Nazarov cyclization.....	31
Scheme 1.55 Gold catalyzed aza-Nazarov cyclization.....	32

Chapter 2

Scheme 2.1 Quinone mediated dehydrogenation	33
Scheme 2.2 Lactone formation via intramolecular nucleophilic trapping of carbocation	34
Scheme 2.3 Cleavage of <i>para</i> -methoxy benzyl protecting group	34
Scheme 2.4 Proposed mechanisms for DDQ mediated C–H cleavage	35
Scheme 2.5 Effect of substrates on reaction rate of C–H oxidative cleavage reactions.....	37
Scheme 2.6 Carbocation trapping with silyl containing nucleophiles	38
Scheme 2.7 Carbocation trapping with Grignard nucleophiles.....	39
Scheme 2.8 Carbocation trapping with activated methylene nucleophiles	39
Scheme 2.9 Example of trapping of iminium ions generated by DDQ oxidation.....	40
Scheme 2.10 Total synthesis of clavosolide A	40
Scheme 2.11 One pot Ferrier-oxidative cyclization reaction	41
Scheme 2.12 Intramolecular oxidative Prins cyclization	42
Scheme 2.13 Oxidative intramolecular Friedel-Craft alkylation	42
Scheme 2.14 Temperature dependence of Diels-Alder product mixtures	43
Scheme 2.15 Dehydrogenative Diels-Alder reaction	43
Scheme 2.16 DDQ mediated tandem cyclization to form tricyclic benzoxa[3.2.1]octanes	44
Scheme 2.17 Regeneration of catalytic DDQ.....	45
Scheme 2.18 Cleavage of PMB ethers with catalytic DDQ.....	45

Scheme 2.19 MnO ₂ as a terminal oxidant for DDQ regeneration	46
Scheme 2.20 Oxidative coupling using a DDQ/NaNO ₂ /O ₂ system	46
Scheme 2.21 TEMPO salt oxidation of tetrahydroisoquinoline	47
Scheme 2.22 Diastereoselective functionalization of N-carbamoyl tetrahydropyridines	48
Scheme 2.23 Synthesis of 8-oxabicyclo[3.2.1]octanes via TEMPO mediated oxidation	48
Scheme 2.24 Conversion of enol silanes to enones using a carbocation oxidant	49
Scheme 2.25 Use of carbocation reagents for α functionalization of ethers	50
Scheme 2.26 Oxidative Nazarov cyclization	50
Scheme 2.27 Generation of pentadienyl cation	51
Scheme 2.28 Proposal of oxidative imino-Nazarov pathway	51
Scheme 2.29 Possible variations of oxidative imino-Nazarov cyclization	52
Scheme 2.30 Synthesis of silyl enol ether 41	52
Scheme 2.31 Proposed mechanism for the formation of product 42	53
Scheme 2.32 Attempted synthesis of various enol ethers	56
Scheme 2.33 Synthesis of enamine from aromatic ketone	57
Scheme 2.34 Enamine synthesis via cross coupling of alkenyl halides	57
Scheme 2.35 Attempted synthesis of alkenyl halides/pseudo halides	58
Scheme 2.36 Mechanism of iso-Nazarov cyclization with ethers	58
Scheme 2.37 Preparation of iso-Nazarov substrates	59
Scheme 2.38 Proposed mechanism for the formation of product 50	62
Scheme 2.39 Modification of iso-Nazarov substrates	63
Scheme 2.40 Steric properties favouring the U-conformer	63
Scheme 2.41 Synthesis of (<i>E</i>)-(2-(2-(1-ethoxypropyl)cyclohex-1-en-1-yl)vinyl)benzene	64
Scheme 2.42 Syntheses of compounds 57 and 61	66
Scheme 2.43 Synthesis of 3-halo-1,3-dienes via palladium catalysis	69
Scheme 2.44 Imino-iso-Nazarov substrates	70

Chapter 3

Scheme 3.1 [2+2] Photocycloaddition via direct excitation	92
Scheme 3.2 [2+2] Photocycloaddition via its triplet state (T ₁)	93
Scheme 3.3 Lewis acid assisted [2+2] cyclization of ketenes	96
Scheme 3.4 Regioisomers in a [2+2] dimerization of allenes	96
Scheme 3.5 Formal [2+2] cycloaddition of in situ generated cyclic allenes	97
Scheme 3.6 [2+2] Cycloaddition of sulphonyl-substituted allenes	97
Scheme 3.7 Ruthenium catalyzed [2+2] cycloaddition of norbornene	98
Scheme 3.8 Platinum catalyzed [2+2] reaction of ene-ynamides	98
Scheme 3.9 Ti(IV) catalyzed asymmetric [2+2] cycloaddition	99
Scheme 3.10 [2+2] cycloadditions of vinyl acetals	99
Scheme 3.11 [2+2] cyclization of silyl enol ethers and acrylates	100

Scheme 3.12 Silver(I) catalyzed cycloaddition of siloxy alkynes to enones	101
Scheme 3.13 Total synthesis of (+)-tricycloclavulone.....	101
Scheme 3.14 Chiral aluminum complex-catalyzed [2+2] cycloaddition	102
Scheme 3.15 Total synthesis of (+)-piperarborenine B	102
Scheme 3.16 Organocatalytic [2+2] cycloaddition via cooperative diamine/H-bond directing catalysis.....	103
Scheme 3.17 Formal crossed [2+2] cycloaddition of <i>o</i> -styrenyl chalcones.....	104
Scheme 3.18 Crossed [2+2] photocycloaddition via triplet energy transfer	105
Scheme 3.19 Preparation of <i>o</i> -styrenyl chalcones.....	106
Scheme 3.20 Proposed mechanism for the formation of products 24 and 24'	110
Scheme 3.21 Equilibration of diastereomers via cyclobutane ring opening	111
Scheme 3.22 Incorporation of another coordination site.....	118

List of Symbols and Abbreviations

^1H	proton
^{13}C	carbon-13
Å	angstrom
Ac	acetyl
Ac ₂ O	acetic anhydride
app	apparent (spectral)
aq	aqueous solution
Ar	aryl
atm	atmosphere
BArF	tetrakis[3,5-bis(trifluoromethyl)-phenyl]borate
Bn	benzyl
Boc	tert-butoxycarbonyl
Bpin	bis(pinacolato)boron
br	broad (spectral)
°C	degrees Celsius
calcd	calculated
CAN	ceric ammonium nitrate
cat.	indicates that the reagent was used in a catalytic amount
cm ⁻¹	wave number
COSY	H-H correlation spectroscopy
conc.	concentrated
d	day(s); doublet (spectral)
DART	Direct analysis in real time (mass spectrometry)
dba	tris(dibenzylideneacetone
DCE	1,2-dichloroethane
DCM	dichloromethane
DCP	dichloropropane
dd	doublet of doublets (spectral)
ddd	doublet of doublet of doublets (spectral)

dddd	doublet of doublet of doublet of doublets (spectral)
DDQ	2,3-dichloro-5,6-dicyano-1,4-benzoquinone
DFT	density functional theory
DIBAL-H	diisobutylaluminum hydride
DIPEA	<i>N,N</i> -Diisopropylethylamine
DMF	<i>N,N</i> -dimethylformamide
DMSO	dimethylsulfoxide
DMP	Dess-Martin periodinane
DMPU	<i>N, N'</i> -Dimethylpropyleneurea
dr	diastereomeric ratio
EDG	electron-donating group
EI	electron impact (mass spectrometry)
ee	enantiomeric excess
er	enantiomeric ratio
ESI	electrospray ionization (mass spectrometry)
Et	ethyl
EtOAc	ethyl acetate
equiv.	equivalent(s)
EWG	electron-withdrawing group
g	gram(s)
h	hour(s)
HAT	hydrogen atom transfer
HFIP	hexafluoroisopropanol
HMBC	heteronuclear multiple bond coherence (spectral)
HMPA	hexamethylphosphoramide
HOMO	highest occupied molecular orbital
HSQC	heteronuclear single quantum coherence (spectral)
HRMS	high resolution mass spectrometry
h ν	light
Hz	hertz
i-Pr	isopropyl

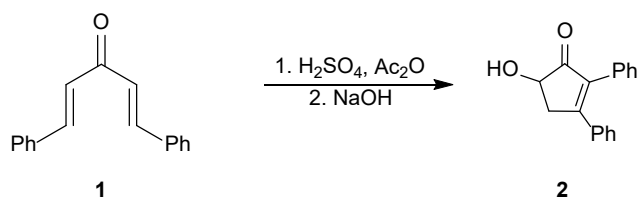
int	intermediate
IR	infrared
J	coupling constant
LA	Lewis acid
LD50	median lethal dose
LDA	lithium diisopropylamide
LiHMDS	lithium hexamethyldisilazide
M	molar
m	multiplet (spectral)
M ⁺	molecular ion
Me	methyl
<i>m</i> -CPBA	meta-chloroperoxybenzoic acid
MeCN	acetonitrile
MeOH	methanol
mg	milligram(s)
MHz	megahertz
min	minute(s)
mL	milliliter(s)
mmol	millimole(s)
MS	molecular sieves
<i>m/z</i>	mass to charge ratio
nm	nanometer
NMR	nuclear magnetic resonance
Nu	unspecified nucleophile
Ph	phenyl
PMB	para-methoxy benzyl
PMP	para-methoxy phenyl
PIFA	[bis(trifluoroacetoxy)iodo]benzene
ppm	parts per million
Pr	propyl
Py	pyridine

Pybox	pyridine bis(oxazoline) ligand
Pyox	pyridine oxazoline ligand
R	generalized alkyl group of substituent
R_f	retention factor (in chromatography)
rt	room temperature
s	singlet (spectral)
SET	single electron transfer
sept	Septet (spectral)
t	triplet (spectral)
T	temperature
TADDOL	α , α , α' , α' -tetraaryl-2,2-disubstituted 1,3-dioxolane-4,5-dimethanol
TBAB	tetrabutylammonium bromide
TBS	tert-butyldimethylsilyl
t-Bu	tert-butyl
Tf	trifluoromethanesulfonyl
TFA	trifluoroacetic acid
THF	tetrahydrofuran
TIPS	triisopropylsilyl
TLC	thin layer chromatography
TMEDA	tetramethylethylenediamine
TMS	trimethylsilyl
Ts	tosyl
δ	chemical shift

Chapter 1: The Nazarov Cyclization: Recent Advances in Activation Methods and Alternative Substrates

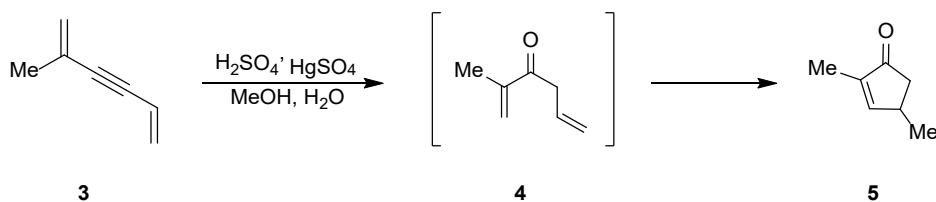
1.1 Introduction

The Nazarov cyclization details the transformation of cross-conjugated ketones into cyclopentenones. The first example of this reaction described in 1903 by Vorländer and Schroedter, involved the treatment of ketone **1** with sulfuric acid in the presence of acetic acid, followed by subsequent alkaline hydrolysis, furnishing ketol product **2** (Scheme 1.1).¹



Scheme 1.1 Vorländer ketal synthesis

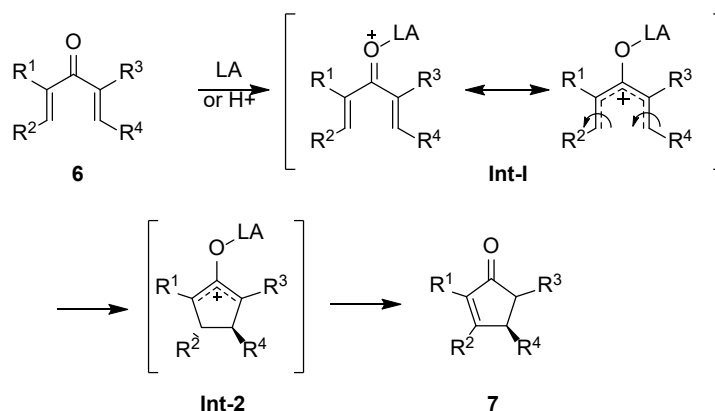
The structure of ketal **2**, originally misassigned by Vorländer and Schroedter, was corrected by Allen and coworkers.² Later, in the seminal work by Nazarov and coworkers, the hydration of diyne **3** to form allyl vinyl ketone **4** and subsequent acid catalyzed ring closure to generate 2-cyclopentanone **5** was investigated.



Scheme 1.2 Synthesis of 2-cyclopentanone by Nazarov and coworkers

In 1952, Braude and Coles published a report investigating the mechanism of the Nazarov cyclization.³ They correctly predicted the formation of a pentadienyl cation intermediate; further studies later confirmed this prediction, giving us mechanistic insight into the Nazarov cyclization. The Nazarov cyclization begins with activation of a cross-conjugated ketone **6** with Lewis or

Brønsted acid. Electrophilic activation of ketone **6** generates the key pentadienyl cation **Int-1**, which can subsequently undergo 4π conrotatory electrocyclic ring closure, furnishing oxyallyl cation **Int-2**. This species then undergoes proton elimination followed by enol tautomerization to furnish the cyclopentanone product **7** (Scheme 1.3).



Scheme 1.3 Mechanism of the Nazarov cyclization

In the last 70 years since its discovery, the Nazarov cyclization has realized vast synthetic utility in the synthesis of cyclopentanones, finding countless applications in natural product and pharmaceutical chemistry. Some recent applications are shown in Figure 1.1.^{4, 5, 6}

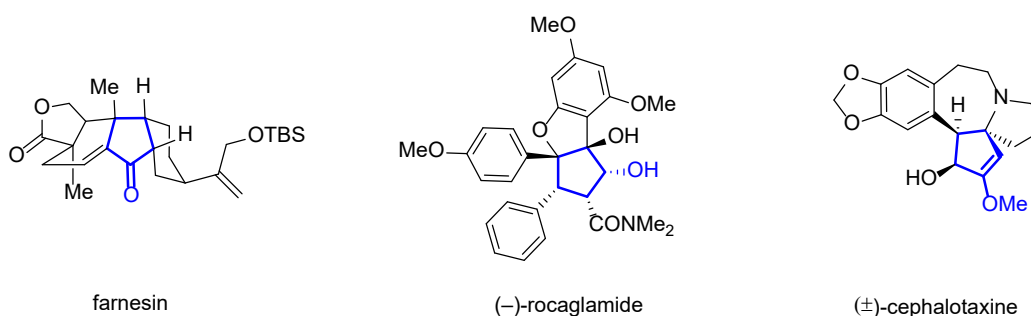


Figure 1.1 Select examples of natural products made using the Nazarov cyclization

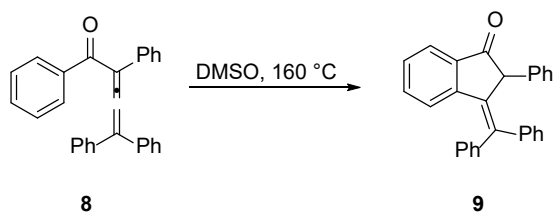
1.2 Alternative Activation Strategies

Traditionally, the Nazarov cyclization is carried out using stoichiometric quantities of Lewis or Brønsted acid. These conditions are often not compatible with sensitive functional groups. As a result, some attention has been dedicated to developing alternate methods to

activating the divinyl ketone and related structures. These strategies may provide milder/alternative conditions to obtain previously difficult to access products.

1.2.1 Thermal Activation

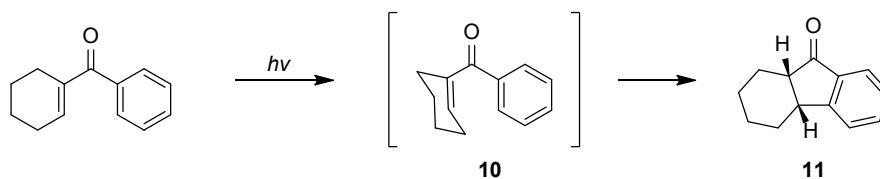
The first report of an acid free Nazarov cyclization came from the Greaney group in 2005.⁷ Briefly, the group demonstrated that subjecting dienones to high temperatures furnished the resulting cyclopentanones, in some cases. The Ren group later demonstrated that aryl allenyl ketones such as **8** undergo cyclization when heated to 160 °C in DMSO, to give 2,3-dihydroindanones **9** as the exclusive product (Scheme 1.4).⁸



Scheme 1.4 Thermal activation of aryl allenyl ketones

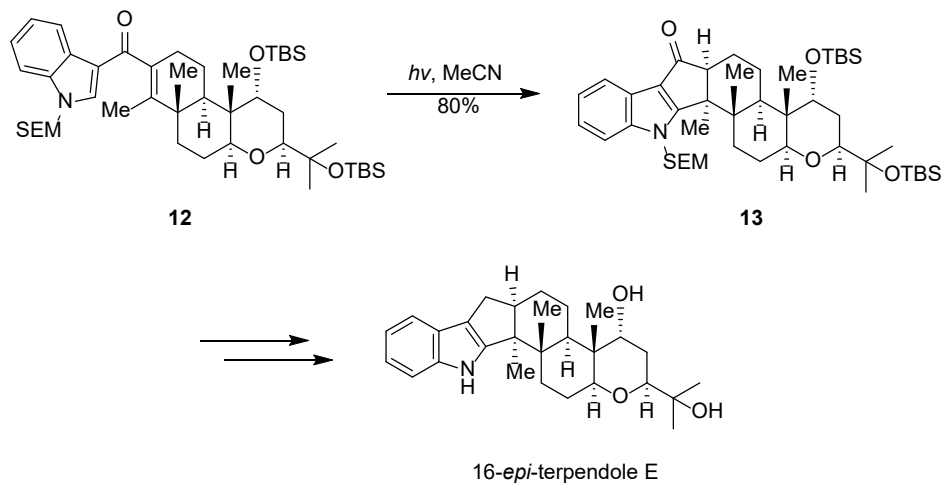
1.2.2 Photochemical Activation

As previously mentioned, the classical Nazarov cyclization proceeds in a conrotatory fashion, as determined by Woodward-Hoffmann rules. Photochemical irradiation has been shown to activate the divinyl ketone, furnishing the oxyallyl cation in a disrotatory ring closure process.⁹ This method has proven particularly useful for classes of substrates that are difficult to cyclize using traditional methods, such as aryl and heteroaryl vinyl ketones, as well as substrates containing acid-sensitive functional groups. A later study revealed mechanistic insights into this reaction; activation of dienones via irradiation leads to a highly strained isomerized intermediate **10**, which then undergoes cyclization to **11** (Scheme 1.5).¹⁰



Scheme 1.5 Photochemical activation of an aryl alkenyl ketone

This indicates that the vinyl moiety must be contained within a ring. Giannis et al. utilized this strategy to access indoloditerpenoid derivatives; irradiation of **12** with 350 nm light resulted in the formation of cyclization product **13** in 80% yield (Scheme 1.6).¹¹ Notably, when Lewis acid conditions were applied to the same compound, no reaction or decomposition of the substrate was observed, showcasing the importance of the photochemical activation, in this case.

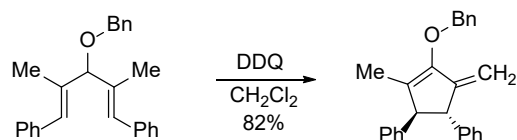


Scheme 1.6 Synthesis of 16-*epi*-terpendole E via photochemical Nazarov cyclization

1.2.3 Oxidation-Initiated Cyclization

West and coworkers explored oxidative conditions as an alternative entry to the key pentadienyl cation (Scheme 1.7).¹² This transformation employed pentadienyl ethers in place of the usual divinyl ketones. Upon oxidation with DDQ, the pentadienyl cation is generated via single electron transfer from the π system, followed by hydrogen atom abstraction. After cyclization to the oxyallyl cation, exclusive *exo*-elimination occurred, preserving both newly generated stereocenters. This transformation tolerated various ether groups including methyl, aryl, allyl and

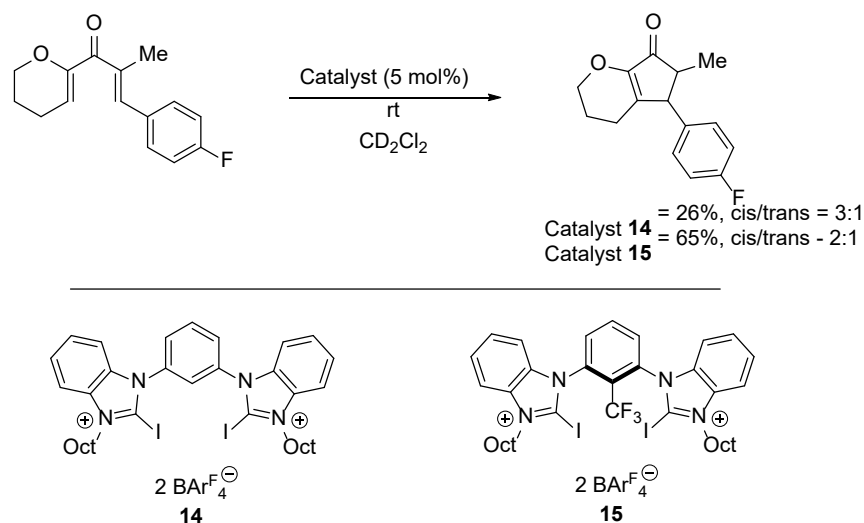
even benzyl ethers. The group also accomplished a catalytic version of the reaction, using substoichiometric amounts of DDQ and MnO₂ as the terminal oxidant.



Scheme 1.7 Oxidative Nazarov cyclization of pentadienyl ethers

1.2.4 Halogen bond donors

Halogen bond activation of organic molecules operates on the basis of non-covalent interactions between the electrophilic halogen and a suitable Lewis base. The electrophilic nature of halogen bond donor compounds can be explained in terms of anisotropy; some regions around the halogen are less negative, creating σ holes that can accept electron density. Additionally, computational studies show partial interaction between the non-bonding electrons of the Lewis base and the antibonding orbital (σ^*) of the C-X bond.¹³ The Huber group investigated a series of halogen bond donors for their ability to act as catalysts for the Nazarov reaction.¹⁴ Carbonyl activation via halogen bond donation catalysis has been reported previously for different transformations; Huber and coworkers hoped to expand this methodology to the Nazarov cyclization.^{15, 16, 17} A variety of halogen bond donor catalysts were screened, with **15** being the most active, giving complete conversion of starting material in less than 5 minutes (Scheme 1.8). This superior activity was observed when using a non-coordinating counterion such as tetrakis[3,5-bis(trifluoromethyl)-phenyl]borate (BAr^F₄), over triflate (OTf). The activity of this catalyst was partly due to the inclusion of the trifluoromethyl group in the center of the benzene core. This increases the Lewis acidity of the catalyst by preventing rotation of the halogen bond-donating moieties putting the catalyst into a pre-organized conformation. While still resulting in a productive reaction, the analog of **15** lacking the central trifluoromethyl group (catalyst **14**) showed only 70% conversion of starting material after 2 hours.

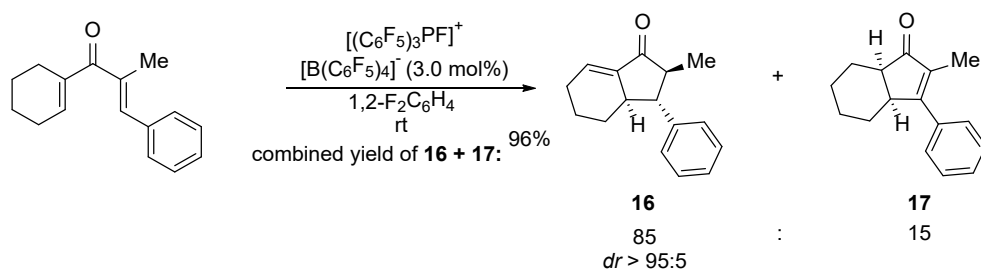


Scheme 1.8 Activation of divinyl ketones by halogen bond donors

The Breugst group later reported a similar halogen bond-activated cyclization, utilizing molecular iodine as the catalyst.¹⁸ For the most part, cyclized products were obtained as a single isomer in good to excellent yields. Mechanistic studies indicated that activation by halogen bond catalysis is the operative pathway; Brønsted acid catalysis was deemed unlikely. The use of molecular iodine provided an operationally simple means of accessing Nazarov cyclization products, resulting in products with comparable yields to other activation methods.

1.2.5 Electrophilic phosphonium

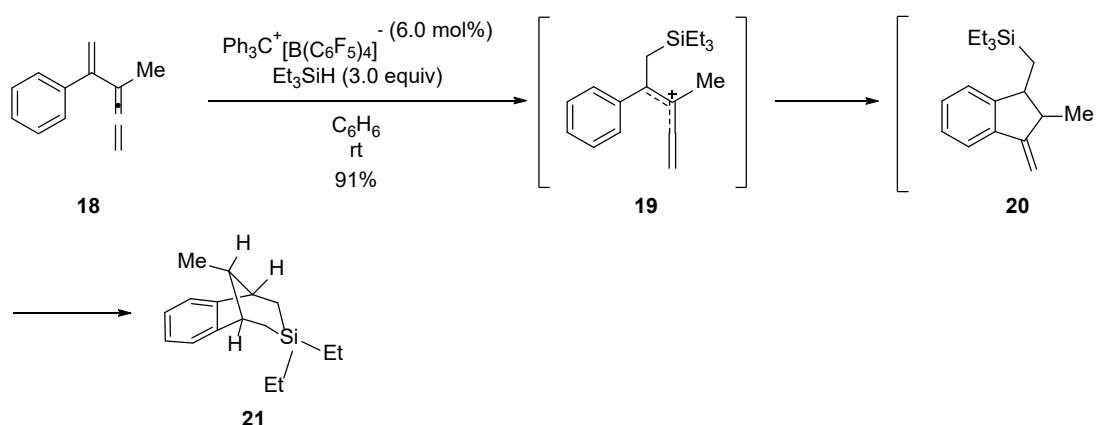
Electrophilic phosphonium cations have previously been explored for their ability to act as Lewis acid catalysts.¹⁹ The Oestreich group examined the use of fluorophosphonium cations to catalyze the Nazarov cyclization of activated and unactivated dienones (Scheme 1.9).²⁰ A range of unactivated dienones underwent cyclization in good yields to the trans isomer, with regioselectivity up to 85:15, as seen in the case of **16** and **17**. Activated dienones showed low yields and no diastereoselectivity.



Scheme 1.9 Activation using electrophilic phosphonium

1.2.6 Silylium-ion promoted cyclization

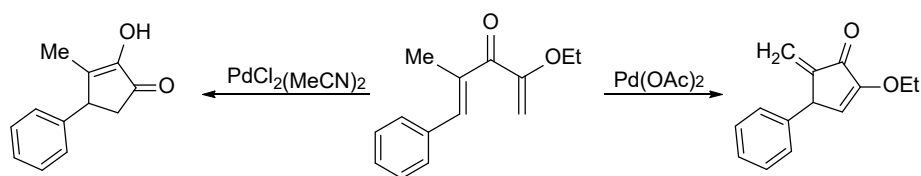
Oestreich and coworkers recently reported another alternative initiation method, being the use of silylium ions.²¹ The group described the activation of [3]dendralenes and hydrosilanes using catalytic amounts of $\text{Ph}_3\text{C}^+[\text{B}(\text{C}_6\text{F}_5)_4]^-$. The reaction began with the in situ generation of silylium ion $[\text{R}_3\text{Si}(\text{C}_6\text{H}_6)]^+$, which then effected electrophilic silylation of the starting material **18**, generating an α -allenyl benzylic carbocation intermediate **19** (Scheme 1.10). This species can then undergo Nazarov cyclization, followed by proton transfer and simultaneous re-aromatization, then finally a hydride abstraction from excess hydrosilane giving the Nazarov product **20**. Further reaction of intermediate **20** with excess in situ generated silylium ion yielded product **21** via fast dealkylation of the silicon, forming a silylium ion. Intramolecular silylation followed by hydride abstraction gave the product. This cascade reaction gives access to silicon-containing bicyclo[3.2.1]octane skeletons, through a Nazarov type cyclization followed by intramolecular hydrosilation. It was found that excess hydrosilane was key to this reaction, as less than 3 equivalents led to poor conversion.



Scheme 1.10 Activation using silylium ions

1.2.7 Activation via palladium enolate

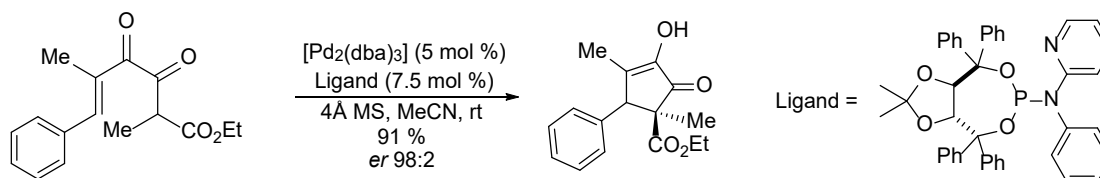
Several strategies have been developed over the past few years to generate Nazarov-type precursors via in situ activation. The first example of a palladium-catalyzed Nazarov cyclization was reported by the Tius group.²² The authors demonstrated the ability of Pd(II) to catalyze the cyclization of polarized dienones, proceeding through a palladium enolate intermediate. Notably, this reaction gave different products depending on the palladium source used, which was attributed to the difference in basicity of the counter ions (Scheme 1.11).



Scheme 1.11 Divergent reactivity of polarized dienones dependent on palladium(II) source

The same group later reported a Nazarov cyclization catalyzed by palladium(0).²³ This is the first example of a Nazarov-type cyclization catalyzed by a zerovalent metal. Of note, experiments from the group showed that when using Pd(II), the use of basic ligands completely suppresses the reaction. In this study, when using Pd(0), phosphine ligands were tolerated, suggesting the possibility of an asymmetric version utilizing chiral phosphines. In a subsequent report, the group applied this methodology to an asymmetric variant, utilizing TADDOL-derived phosphoramidite ligands and yielding products with up to 98:2 e.r. (Scheme 1.12).²⁴ The origin of

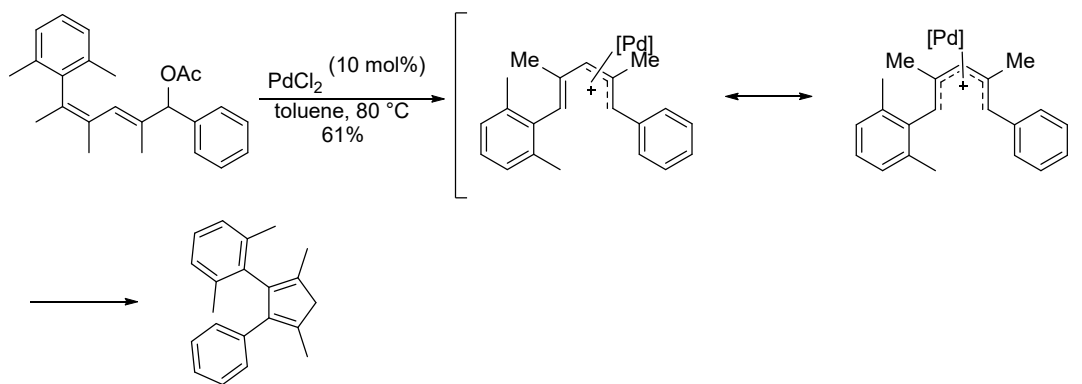
this enantioselectivity was thought to originate from the interaction between the C2 methyl group and one Ph group on the TADDOL ligand.



Scheme 1.12 Enantioselective palladium(0) catalyzed Nazarov cyclization

1.2.8 Activation via formation of a Pd π -allyl complex

The Ramasastry group demonstrated an alternative palladium activation strategy, utilizing 2,4-pentadienyl acetate compounds in a Tsuji-Trost like formation of a π -allyl complex, generating a pentadienyl cation-like intermediate (Scheme 1.13).²⁵ This reaction provided access to a variety of 1,2,3,4-tetrasubstituted cyclopentadienes, 1,2-disubstituted indenenes, and 1,2-disubstituted cyclopentannulated benzothiophenes and indoles, in good yields. This method provided a fascinating new entry to the Nazarov cyclization, yielding a variety of highly substituted cyclopentadiene products. The same group later reported a similar reaction utilizing instead (hetero)aryl allyl acetates to yield cyclopentene fused arenes and heteroarenes.²⁶



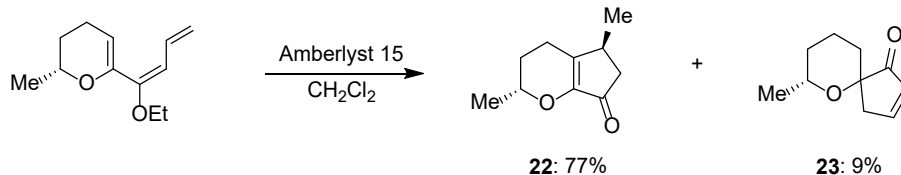
Scheme 1.13 Nazarov-type cyclization via formation of Pd π -allyl complex

1.3 Alternative Substrates

Considerable attention in the last several years has been focused on accessing diverse products using the Nazarov cyclization. Many research groups have put significant effort into developing reactions that diverge from the classic Nazarov reaction using divinyl ketones as precursors. Developing reactions that exhibit Nazarov-type reactivity on different substrates permits novel transformations and leads to new and interesting products.

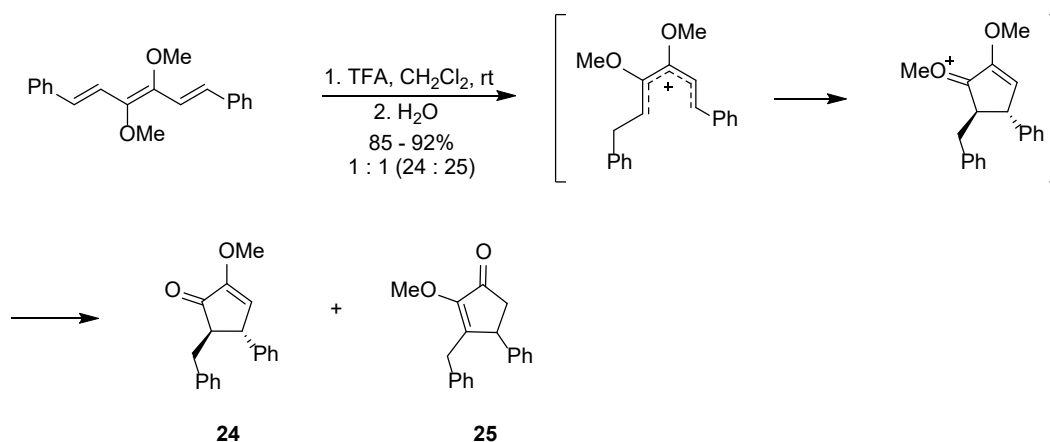
1.3.1 Activation through trienes

Occhiato and coworkers demonstrated that conjugated ethoxy trienes can be activated under mildly acidic conditions to obtain fused heterocycles, such as **22** (Scheme 1.14).²⁷ The mild conditions can be attributed to the stabilization given to the intermediate carbocation by the neighbouring heteroatom. Unexpected reactivity was observed for the dihydropyran derivative, in which a spirocyclic side-product **23** was also formed.²⁸ This is proposed to occur by competing protonation of the endocyclic double bond, followed by an alternative Nazarov cyclization.



Scheme 1.14 Nazarov cyclization of ethoxytrienes

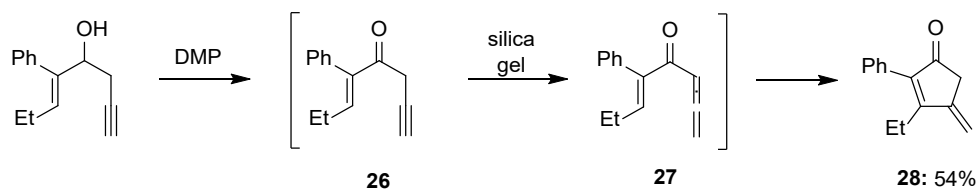
Another report, by Barluenga and coworkers described the treatment of dimethoxyhexatrienes with TFA leading to cyclopentanones **24** and **25** (Scheme 1.15).²⁹ Protonation of the terminal carbon-carbon double bonds generated a cationic intermediate, followed by ring closure. Direct hydrolysis gave product **24** or proton elimination followed by hydrolysis of the other enol ether yielded product **25**.



Scheme 1.15 Nazarov cyclization of dimethoxytrienes

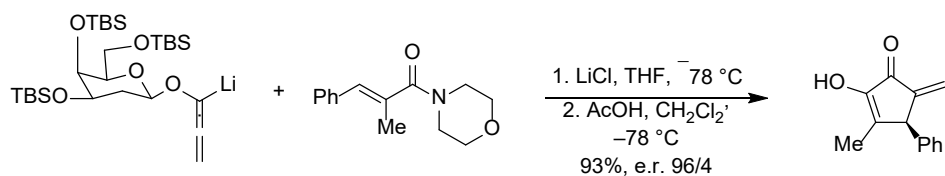
1.3.2 Allenyl vinyl ketones

A report by Hashmi and coworkers in 1998 described the first use of vinyl allenyl ketones as substrates for the Nazarov cyclization (Scheme 1.16).³⁰ Oxidation of propargyl vinyl carbinol to the corresponding ketone **26**, followed by silica gel mediated isomerization to **27**, permitted Nazarov cyclization of the activated allenyl vinyl ketone. The product **28** was obtained in 54% yield.



Scheme 1.16 Silica gel mediated cyclization of allenyl vinyl ketones

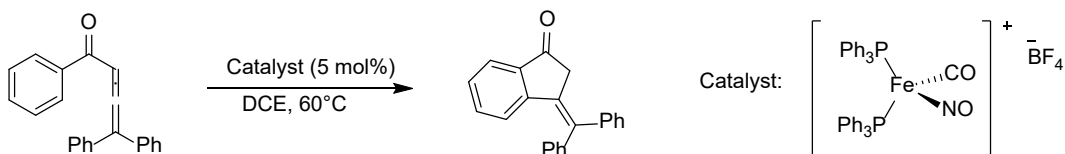
Tius and coworkers developed an enantioselective cyclization of *in situ* formed allyl vinyl ketones, using 2-deoxy-D-glucose as a traceless chiral auxiliary (Scheme 1.17).³¹ The same group has also demonstrated enantioselective versions of the reaction with camphor and chiral allenyl carbamates.^{32, 33}



Scheme 1.17 Enantioselective cyclization of allenyl vinyl ketones

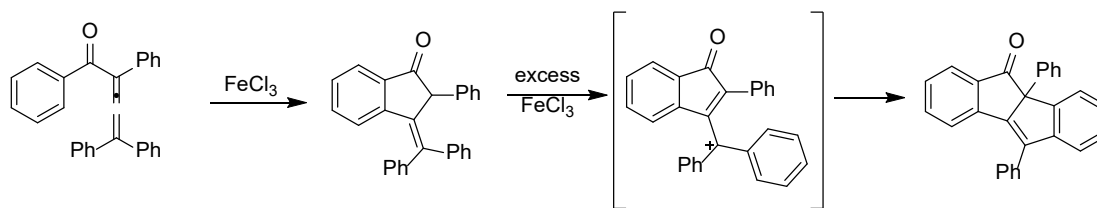
1.3.3 Aryl allenyl ketones

The cyclization of aromatic Nazarov substrates often proves to be slow and requires harsh conditions to effect the reaction, due to the temporary loss of aromaticity during the electrocyclization step. Further, it often requires the incorporation of electron donating groups on the aryl moiety to facilitate cyclization. A method to improve the cyclization of aryl substrates is to instead employ aryl allenyl ketones. Exchanging the vinyl group for an allenyl group increases reactivity of the substrate, by increasing the proportion of reactive conformers, due to the sp -hybridized central allenic carbon having less steric repulsion than the corresponding sp^2 -hybridized alkenyl carbon would have. Additionally, there is more stabilization provided to the resulting cyclized cation through added conjugation. Plietker and Teske effected the transformation of aryl allenyl ketones to 3-arylidene-indan-1-ones utilizing a cationic Fe complex $[(Ph_3P)_2Fe(CO)(NO)]BF_4$ (Scheme 1.18).³⁴



Scheme 1.18 Nazarov cyclization of aryl allenyl ketone via cationic iron complex

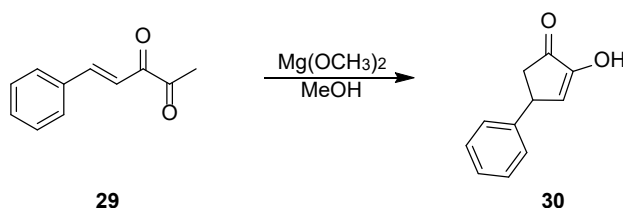
Miao and coworkers utilized an $FeCl_3$ system that promoted Nazarov cyclization of aryl allenyl ketones.³⁵ When the allenyl portion of the substrate is substituted with aryl groups, the cyclized product can undergo a formal hydride abstraction to furnish another pentadienyl cation, which undergoes a second Nazarov-type cyclization, giving polycyclic compounds (Scheme 1.19).



Scheme 1.19 Iron (III) chloride promoted cyclization of aryl allenyl ketones

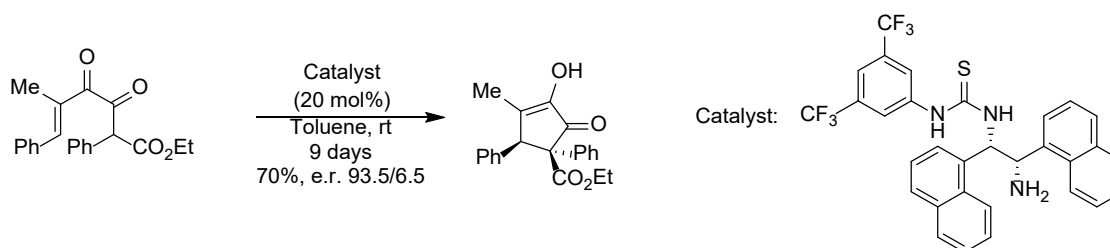
1.3.4 Activation through diketones

The inspiration for using α -diketones as substrates for the Nazarov cyclization came from a report by Muxfeldt and coworkers, in which they showed that enedione **29** is transformed into hydroxycyclopentanone **30** upon treatment with magnesium methoxide (Scheme 1.20).³⁶



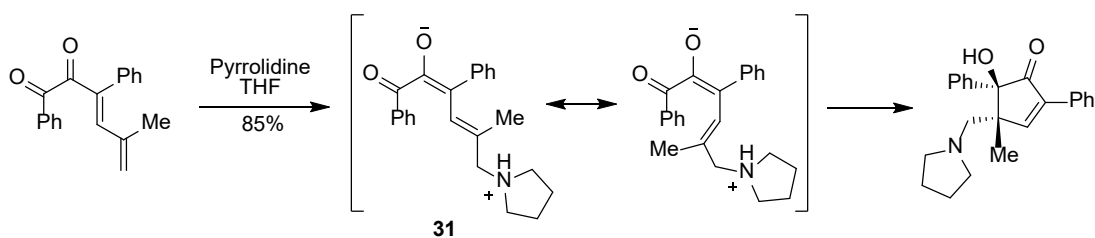
Scheme 1.20 Magnesium methoxide cyclization of enediones

Tius and coworkers later reported a cyclization of α -diketones that could be catalyzed by either LiTMP, or a Yb(OTf)₃/pyrrolidine system.³⁷ Further work on the subject by the Tius group showed that the use of a chiral thiourea organocatalyst could impose great enantioselectivity on the reaction, although reaction times were extremely long (Scheme 1.21).³⁸



Scheme 1.21 Enantioselective cyclization of α -diketones

Frontier and coworkers explored the 4π electrocyclization of dienyl diketones; this occurred by generating reactive 2-oxido-2,4-dien-1-ones via 1,6-conjugate addition of nucleophiles to the starting material (Scheme 1.22).³⁹ While these reactions do not go through the typical cationic intermediate, the authors rationalize that the intermediate **31** that results from the conjugate addition contains pentadienyl cation character. The observed diastereoselectivity in the products is consistent with a conrotatory electrocyclization. In a later report, the Frontier group expanded the scope of amine nucleophiles that can initiate the 4π cyclization, including electron-rich arylamines, electron-deficient arylamines and alkylamines.⁴⁰



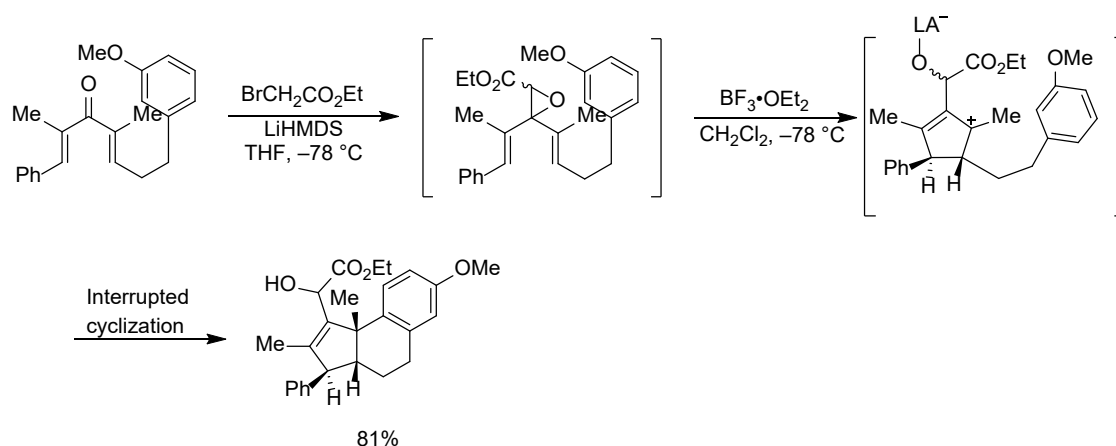
Scheme 1.22 Electrocyclization initiated by 1,6-conjugate addition to dienyl diketones

1.3.5 Activation by ring opening

Multiple research groups have leveraged the opening of small strained rings as an entry to the reactive pentadienyl cation.

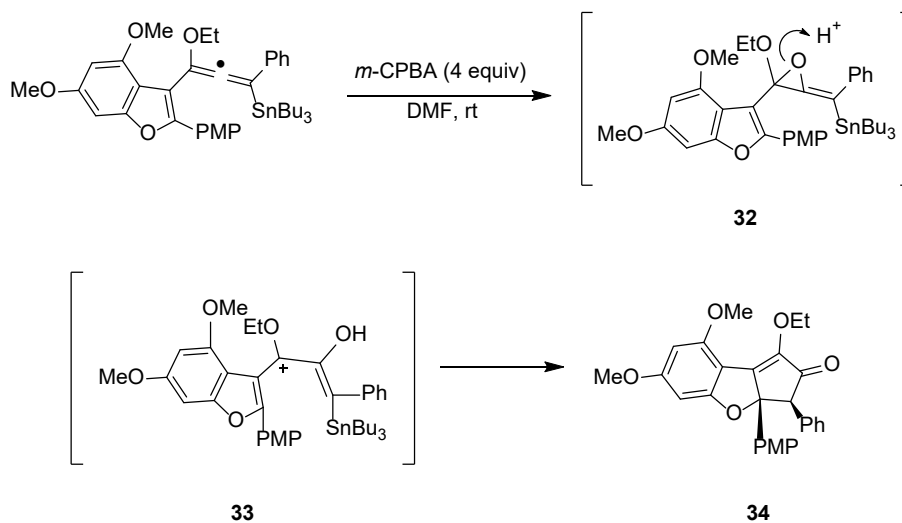
1.3.5.1 Epoxides

Sudhakar and Satish demonstrated an alternative method to access the pentadienyl cation, employing divinyl and aryl vinyl epoxides.⁴¹ The epoxide substrates, prepared by either Darzens or Corey-Chaykovsky reactions, were treated with Lewis acid to furnish a variety of substituted cyclopentadienes bearing allylic hydroxyl groups. The epoxide possessed sufficient steric bulk to enforce the reactive U conformation, allowing the reaction to proceed with substoichiometric amounts of promoter. The group also demonstrated an intramolecular interrupted version of the reaction, in which the cyclopentenyl cation was trapped with an electron-rich aromatic group (Scheme 1.23).



Scheme 1.23 Interrupted Nazarov cyclization of divinyl epoxides

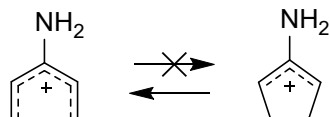
Frontier and coworkers achieved an interesting method to access the pentadienyl cation, via epoxidation of an allenol ether. Generation of intermediate **32** followed by epoxide opening under acidic conditions resulted in pentadienyl cation **33**, which then cyclized to form the product **34** (Scheme 1.24). Product **34** was further functionalized in a total synthesis sequence towards (\pm)-rocaglamide.⁴²



Scheme 1.24 Peracid initiated Nazarov cyclization

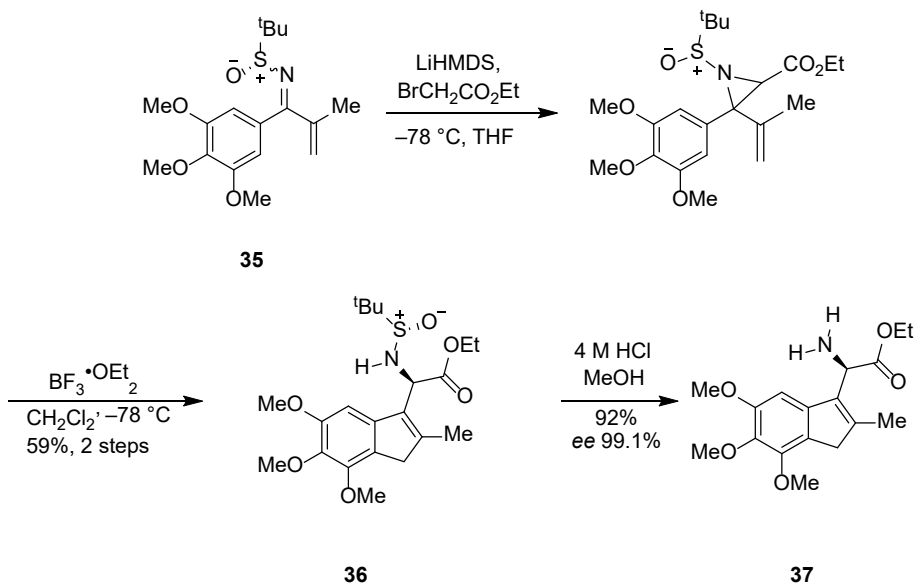
1.3.5.2 Divinyl Aziridines

After demonstrating the applicability of divinyl epoxides as Nazarov reaction precursors, Sudhakar and coworkers explored the use of dienylaziridines as pentadienyl cation precursors.⁴³ *Ab initio* calculations suggest that employing divinylimines as Nazarov precursors may be unfavourable due to the stabilization that the nitrogen provides to the amino-pentadienyl cation, preventing a productive cyclization (Scheme 1.25).⁴⁴



Scheme 1.25 Unfavourable equilibrium of ring closure of 3-amino pentadienyl cations

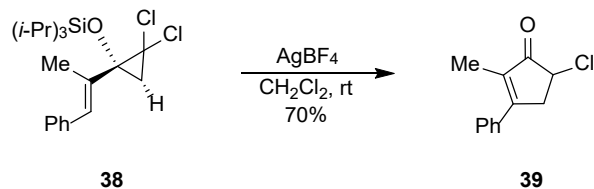
Utilizing aziridines circumvents this issue, as the nitrogen atom is bonded to a carbon atom adjacent to the pentadienyl system after aziridine cleavage. This reaction was realized by subjecting dienylimines to aza-Darzens conditions, to generate the divinylaziridine, followed by treatment with Brønsted or Lewis acid to promote the cyclization. An asymmetric version of the reaction was also accomplished, using chiral sulfinimine **35**, which was subjected to Darzens conditions followed by Nazarov cyclization to give **36** (Scheme 1.26). Deprotection of the chiral sulfinimide gave cyclopentadienyl and indenyl glycines **37**.



Scheme 1.26 Formation of an indenyl glycine using asymmetric cyclization of a divinyl aziridine

1.3.5.3 Dihalocyclopropanes

Grant and West established a ring-opening pathway to the pentadienyl cation using easily accessible alkenyl substituted dihalocyclopropanes.⁴⁵ Treatment of substrate **38** with AgBF₄ facilitated a 2 π electrocyclic ring opening of the cyclopropane, followed by 4 π electrocyclic ring closure to yield **39** (Scheme 1.27). A report the following year described the ability for tethered carbon nucleophiles to intercept the intermediate cation, furnishing tricyclic compounds.⁴⁶

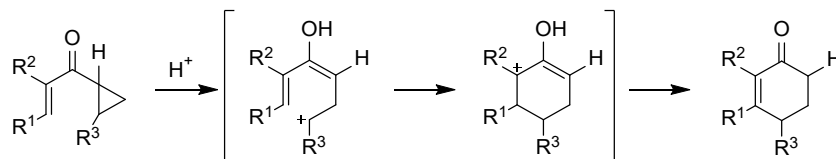


Scheme 1.27 Nazarov cyclization via electrocyclic ring opening of dihalocyclopropanes

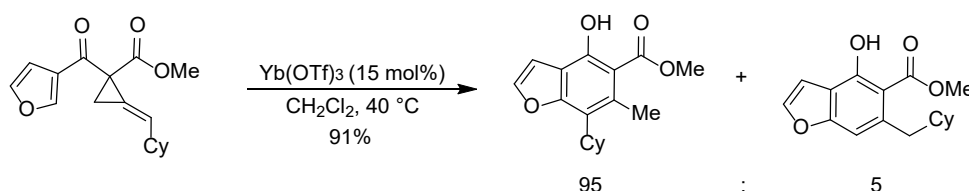
1.3.5.4 Formal homo-Nazarov cyclization

An analogous reaction to the Nazarov cyclization, the homo-Nazarov reaction, employs vinyl cyclopropyl ketones, effectively substituting one double bond of the classic Nazarov dienone substrate with a cyclopropane moiety. Upon activation of the carbonyl, the ring opening of the cyclopropane generates a carbocation, prompting the molecule to undergo ring closure to form a six membered ring instead of the five membered ring seen in typical Nazarov cyclizations. Eliminative termination gives the final cyclohexenone product (Scheme 1.28). While this reaction is comparable to the Nazarov cyclization, the mechanism is understood to occur in a stepwise manner in contrast to the concerted Nazarov cyclization process. The first example of this type of reaction was reported by Tsuge et al. in 1988, but necessitated harsh reaction conditions.⁴⁷ More recently, the Waser group reported a catalytic version of this reaction, requiring only 20 mol% Brønsted acid to facilitate the reaction.⁴⁸ The France group has studied the scope of this reaction extensively, demonstrating that indole and pyrrole cyclopropyl ketones, as well as alkylidene cyclopropane-1,1-ketoesters (Scheme 1.29) can efficiently undergo this reaction when treated with catalytic amounts of Lewis acid.^{49, 50, 51} The design of these substrates incorporated both an electron withdrawing group α to the ketone and a heteroatom substituted aromatic group (donor-acceptor cyclopropanes), affording ring opening of the cyclopropane under mild conditions. In the case of the alkylidene cyclopropane-1,1-ketoesters, two cyclized products were observed arising from

attack at either end of the allyl cation. Waser and coworkers showed the first example of an asymmetric homo-Nazarov cyclization using magnesium salts and PYBOX ligands, although the enantioselectivity was low.⁵²



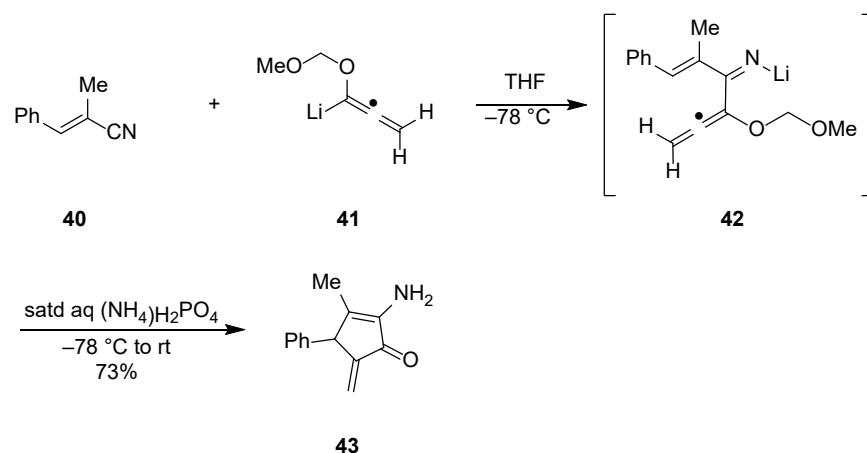
Scheme 1.28 General mechanism of the formal homo-Nazarov cyclization



Scheme 1.29 Yb(OTf)₃ catalyzed ring opening of alkylidene cyclopropane-1,1-ketoesters

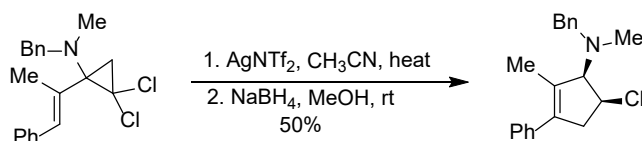
1.3.6 Imino-Nazarov Cyclization

As mentioned in section 1.3.5.3, replacement of the oxygen of a divinyl ketone with a nitrogen atom results in a divinyl imine, which was predicted computationally to be unproductive towards electrocyclization, albeit with unsubstituted substrates. Furthermore, divinyl imines lack robust methods for their synthesis. Several groups have overcome these issues by adding in structural elements that render the cyclization of the amino pentadienyl cation more favorable and designing clever methods to access 3-aminopentadienyl cations from divinyl imines, as well as alternative precursors. In 2001 Tius and coworkers described the addition of α -lithio- α -(methoxy)methoxyallene **41** to α -methylcinnamionitrile **40**, resulting in lithioamine **42**.⁵³ Protonation of this compound resulted in cyclization to give α -aminocyclopentenone **43** as the product (Scheme 1.30). This account is the first example of an imino-Nazarov reaction.



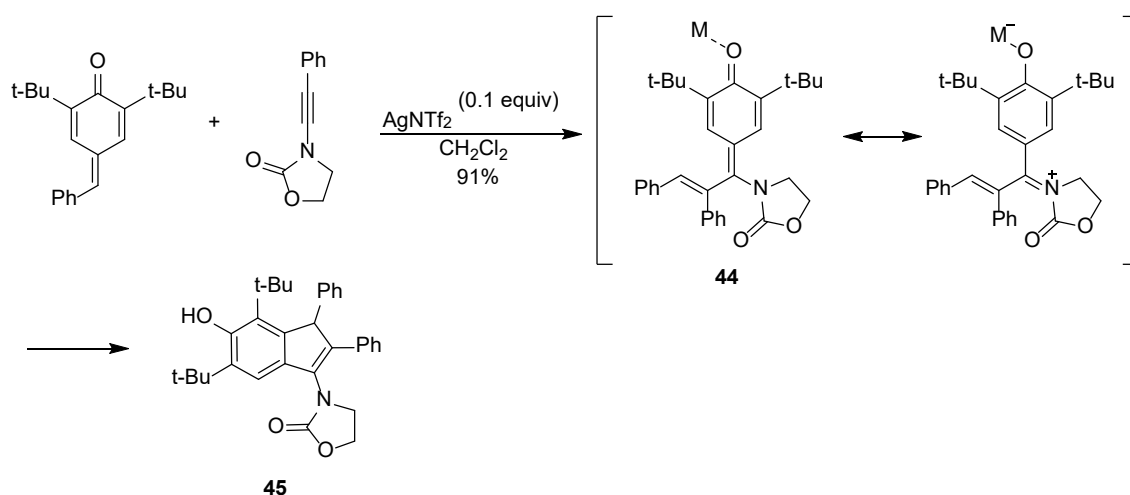
Scheme 1.30 First example of an Imino-Nazarov cyclization

Since this report in 2001, several groups have proposed solutions to the imino-Nazarov problem. The West group leveraged the silver assisted electrocyclic ring opening of 1-alkenyl-1-amino-2,2-dichlorocyclopropanes to give 3-aminopentadienyl cations.⁴⁵ These intermediates underwent Nazarov cyclization and elimination to form cyclopentenone-derived iminium salts, which could be reduced to the allylic amines (Scheme 1.31). It was noted that electron-rich amino groups were required to facilitate the initial cyclopropane opening.



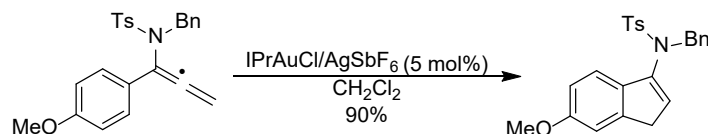
Scheme 1.31 Silver assisted ring opening of 1-alkenyl-1-amino-2,2-dichlorocyclopropanes

The Fan group utilized a tandem process involving [2+2] annulation of para-quinone methides and ynamides, followed by a 4π electrocyclic ring opening of the resulting cyclobutene to yield imino-Nazarov precursor **44**.⁵⁴ This intermediate then underwent cyclization to give highly functionalized aminoindenes, such as **45** (Scheme 1.32).



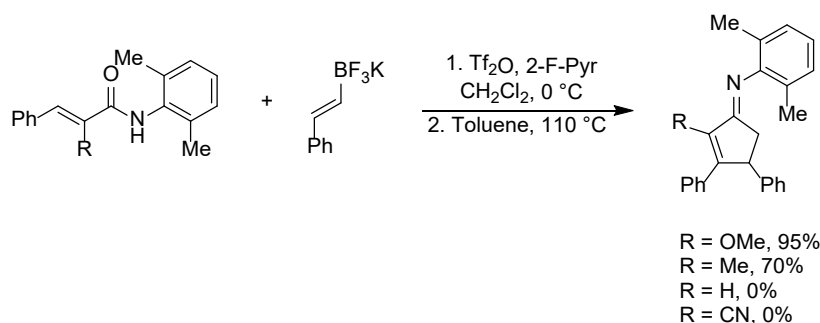
Scheme 1.32 Imino-Nazarov cyclization of [2+2] annulation products

The Hsung group examined a gold(I) catalyzed cascade of α -aryl substituted allenamides to form cyclopentenamides in high yields (Scheme 1.33).⁵⁵ Utilizing an *N*-acyl nitrogen atom would provide less stabilization to the open form of the pentadienyl cation (Scheme 1.25), encouraging cyclization. The authors initial attempts at Brønsted acid activation failed, as they were unable to overcome a competing hydrolysis pathway. This led them to utilizing gold catalysis.



Scheme 1.33 Synthesis of cyclopentenamides from α -aryl substituted allenamides

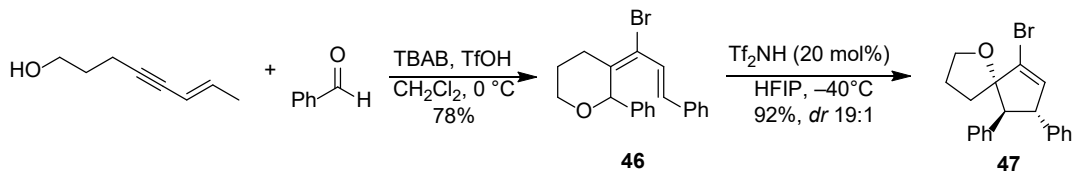
In a recent report, Huang and coworkers were successful in synthesizing a variety of penta-1,4-diene-3-imines, utilizing an alkenyliminylation approach on α,β -unsaturated secondary amides (Scheme 1.34).⁵⁶ The ease of preparation of these substrates allowed for investigation of effects that substituents α to the carbonyl had on cyclization. It was determined that strongly electron donating groups resulted in a fast cyclization at room temperature. Weakly electron donating groups required more forcing conditions, but still resulted in a productive cyclization. Substrates bearing an electron withdrawing group (cyano) or H did not participate in the cyclization reaction.



Scheme 1.34 Imino-Nazarov cyclization of alkenyliminylation product

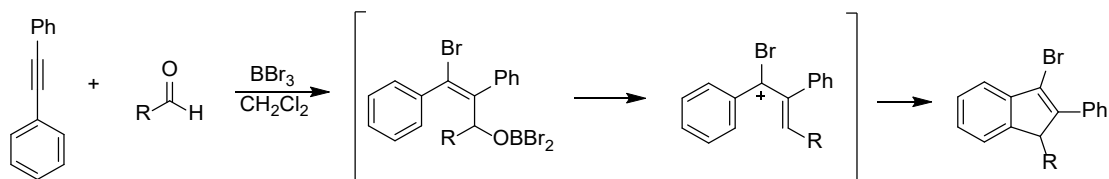
1.3.7 Halo Nazarov Cyclization

The halo Nazarov cyclization employs a 3-halo pentadienyl cation as the cyclization precursor. This pentadienyl cation intermediate is more reactive than the usual 3-oxopentadienyl cation as a result of the decreased amount of stabilization provided by the halo substituent. The reaction has remained largely underdeveloped despite the high reactivity of the intermediate, in part due to the lack of convenient precursors. The Frontier group found an interesting method to access dienyl halides with allylic leaving groups by employing an alkynyl halo-Prins reaction to generate compounds such as **46** (Scheme 1.35).⁵⁷ Treatment of this compound with triflimide in hexafluoroisopropanol (HFIP) furnished the 3-halopentadienyl cation by ionization of the C–O bond, followed by cyclization to the halocyclopentenyl cations, which could then be trapped by the pendent hydroxyl group in a net ring-contraction to form **47**. In a later report the group expanded the trapping scope to include carbon nucleophiles, building complex polycyclic molecules.⁵⁸ The same group later reported using similar methodology to synthesize halo-indenes.⁵⁹ This method took advantage of the lower barrier to cyclization associated with the 3-halopentadienyl cation, allowing for effective cyclization of substrates containing an arene as part of the pentadienyl unit.



Scheme 1.35 Halo Nazarov cyclization via alkynyl halo-Prins reaction

Sultana and Lee, as well as Kumari and Fernandez demonstrated an alternative method to access the 3-halo pentadienyl cation, via Lewis acid mediated cascade.^{60, 61} Both papers demonstrate the use of Lewis acid (BX_3) acting as both catalyst for the initial Prins cyclization, as well as halide source, in a single step to generate indenenes (Scheme 1.36).



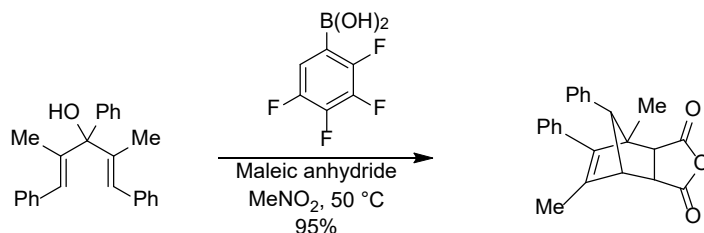
Scheme 1.36 Tandem Prins cyclization/halo-Nazarov cyclization

1.3.8 C–O bond ionization

An alternative entry to the pentadienyl cation that has been explored is via ionization of C–O alcohol and ether bonds.

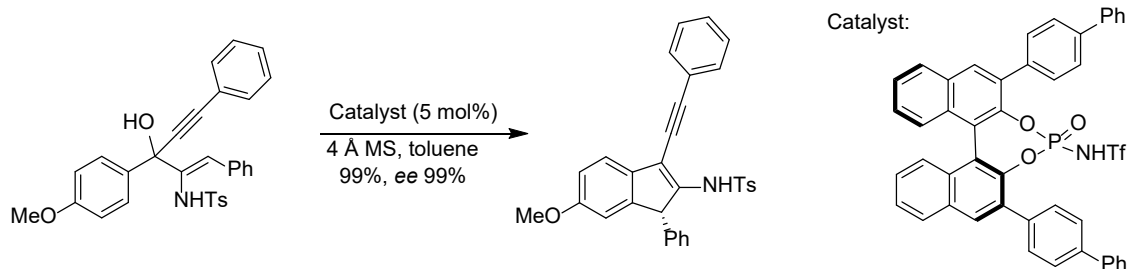
1.3.8.1 Dehydrative Nazarov cyclization

Employing a bis(allylic) alcohol that can be protonated and lose a water molecule to generate the pentadienyl cation constitutes a “dehydrative Nazarov” cyclization. The Hall group reported a boronic acid-catalyzed dehydrative Nazarov cyclization.⁶² The resulting cyclopentadiene products could undergo Diels-Alder reactions with maleic anhydride to form highly functionalized bicyclic compounds (Scheme 1.37).



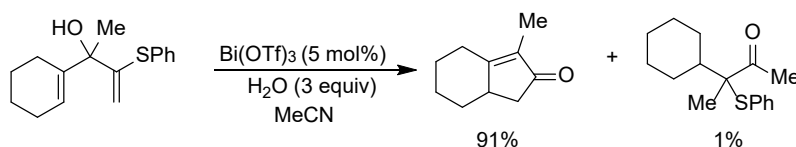
Scheme 1.37 Boronic acid-catalyzed dehydrative Nazarov cyclization

An example of an enantioselective dehydrative Nazarov cyclization was demonstrated by the Chan group, utilizing chiral Brønsted acid catalysis (Scheme 1.38).⁶³ Protonation of the alcohol is followed by loss of a water molecule. The presence of electron rich groups facilitated this step, providing stabilization to the resulting cation. The chiral catalyst can then form an ion pair species, enforcing the enantioselectivity in the ring closing step. This reaction was accomplished in very high yields, and enantiomeric excesses of up to 99%.



Scheme 1.38 Enantioselective dehydrative Nazarov cyclization

Lemière and coworkers demonstrated dehydrative-type Nazarov cyclization of thioether containing bis(allylic) alcohols.⁶⁴ Ionization of the C–O bond by Lewis acid, followed by cyclization and hydrolysis of the sulphenyl-diene intermediate gave the cyclopentenone products (Scheme 1.39). An alternate reactivity pathway was also observed under some conditions, resulting in a semipinacol rearrangement product. This side reactivity was almost completely suppressed when Bi(OTf)₃ in acetonitrile was employed.

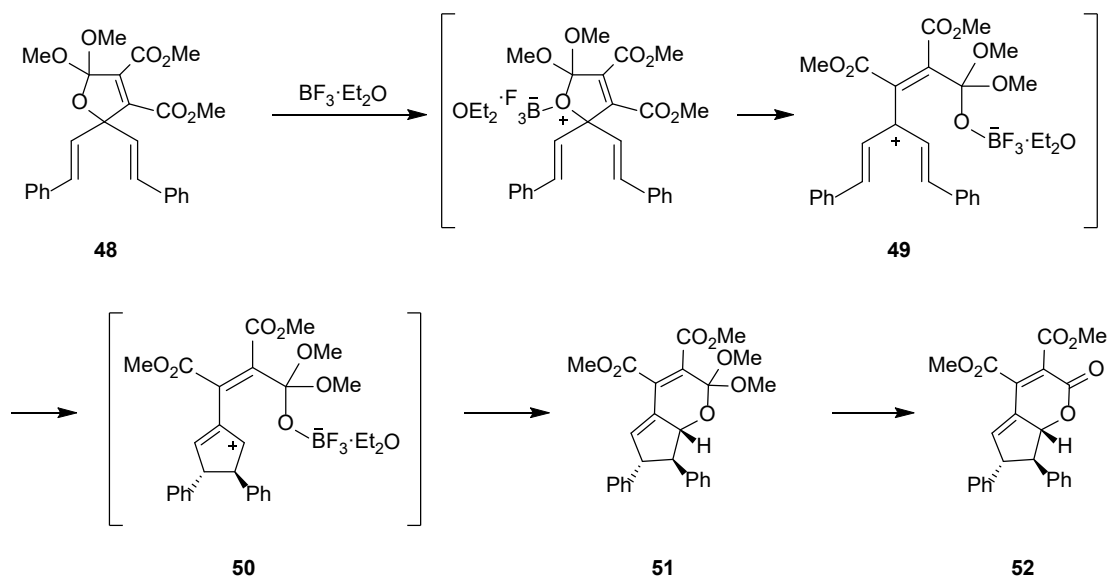


Scheme 1.39 Dehydrative Nazarov cyclization of thioether bis(allylic) alcohols

1.3.8.2 Ionization of C–O ether bonds

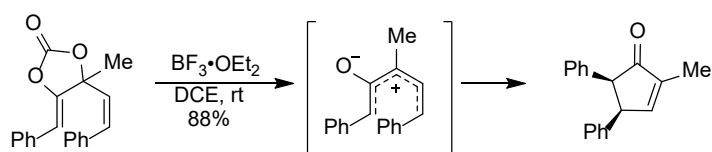
In 2002, Nair and coworkers described an interrupted Nazarov cyclization of *gem*-divinyl dihydrofurans (Scheme 1.40).⁶⁵ Coordination of Lewis acid with compound **48** results in ring opening of the dihydrofuran moiety, revealing pentadienyl cation **49**, which underwent 4π

electrocyclic ring closure, followed by trapping of the allyl cation **50** with the pendent nucleophile, giving compound **51**. Elimination of methanol gives the final bicyclic lactone **52**.



Scheme 1.40 Interrupted Nazarov cyclization via Lewis acid mediated C–O bond ionization

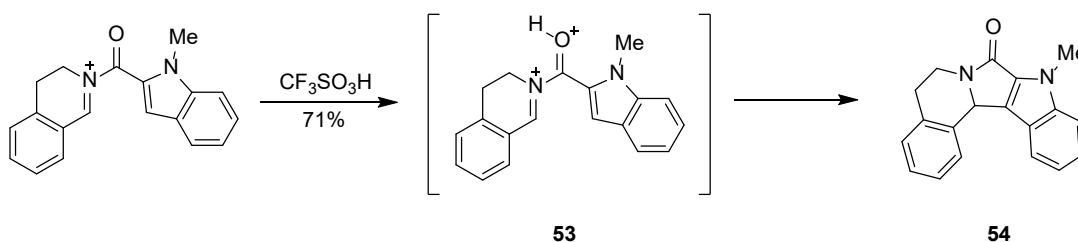
The Yamada group showed an interesting modification to these C–O bond cleavage initiated Nazarov cyclizations, involving a decarboxylative Nazarov process.⁶⁶ Cyclic carbonates were treated with Lewis acid, initiating ionization at the doubly allylic position followed by loss of CO₂, generating a 2-oxidopentadienyl cation. Ring closure gave substituted 2-cyclopentenone derivatives (Scheme 1.41). An important outcome of this reaction is that due to the different substitution seen in the pentadienyl cation compared to the classic Nazarov substrates, the non-typical product with the double bond forming on the less cation-stabilizing side can be obtained.



Scheme 1.41 Decarboxylative generation of 2-oxidopentadienyl cation

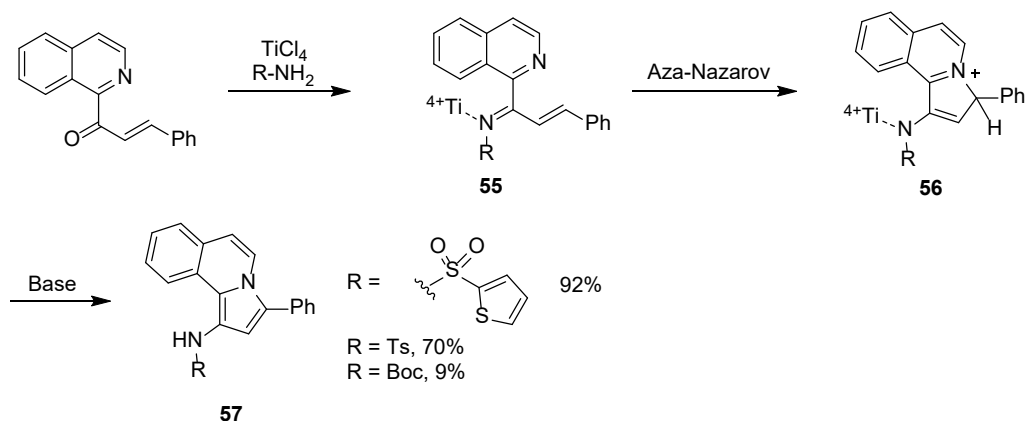
1.3.9 Aza-Nazarov cyclization

Substituting one carbon atom with a nitrogen in the dienone core constitutes an “aza-Nazarov” reaction. This method provides access to 5 membered nitrogen containing heterocycles. The first example was reported by Ciufolini and Roschager in a total synthesis of (+)-camptothecin; a quinoline containing enone underwent a facile aza-Nazarov cyclization to yield an indolizine.⁶⁷ Klump and coworkers later reported an aza-Nazarov cyclization of *N*-acylium ion salts via acid catalysis to form *N*-heterocyclic products **54** (Scheme 1.42).⁶⁸ The authors postulate the formation of a dicationic intermediate species **53**, which is crucial to a productive cyclization; the formation of the dicationic species destabilizes the *N*-acylium ion, leading to a large decrease in activation energy of cyclization.



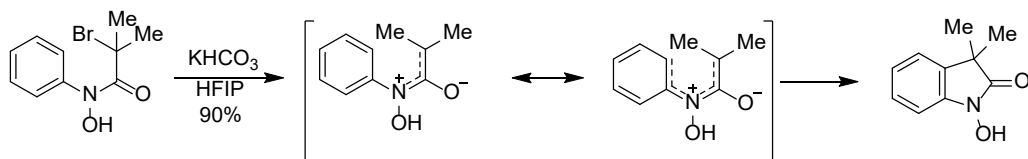
Scheme 1.42 Aza-Nazarov cyclization of *N*-acylium ion salt

Wang and coworkers utilized a titanium mediated aza-Nazarov cyclization towards the synthesis of [6/6/5] tricycles.⁶⁹ The starting materials, α,β -unsaturated isoquinoline ketones underwent titanium mediated imine formation with electron withdrawing amines to give **55** (Scheme 1.43), then the lone pair of the isoquinoline initiated the aza-Nazarov cyclization. A proton transfer followed by a cycloisomerization gave the product **57**. Evaluation of the scope of the reaction showed that more activated amines gave higher yields.



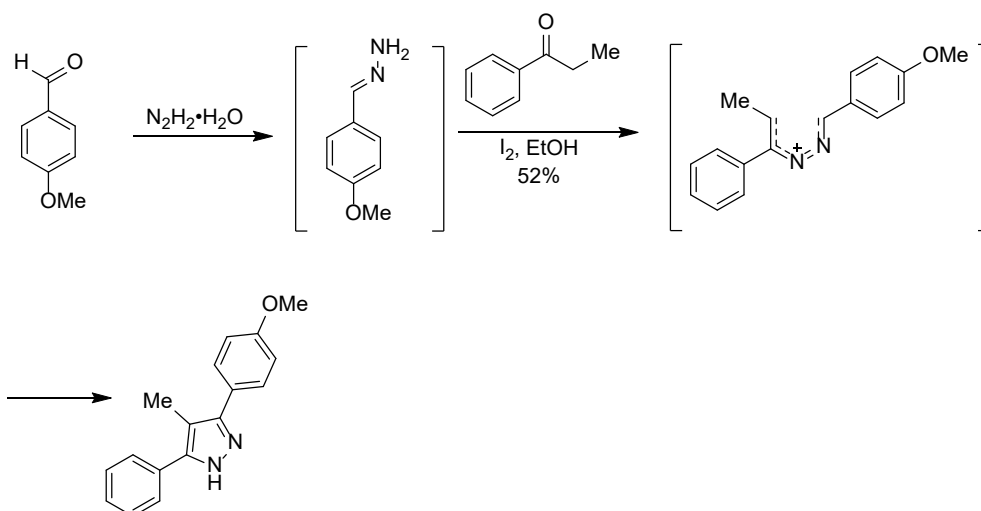
Scheme 1.43 Titanium mediated aza-Nazarov cyclization to form [6/6/5] tricycles

Recently, Liao and coworkers studied the formation of 2-oxido-3-azaallyl cations by base assisted dehydrohalogenation. These intermediates can then undergo cyclization via a pentadienyl system that includes a neighboring aryl ring to form N-hydroxy oxindoles (Scheme 1.44).⁷⁰ The hydroxyl substitution on the nitrogen proved to be crucial, as H, methyl, benzyl and methoxy substituted anilides resulted in no reaction. The mild conditions of this reaction are desirable, as alternative methods to access oxindoles require either harsh conditions or expensive metal catalysts.



Scheme 1.44 Synthesis of N-hydroxy oxindoles by base assisted dehydrohalogenation

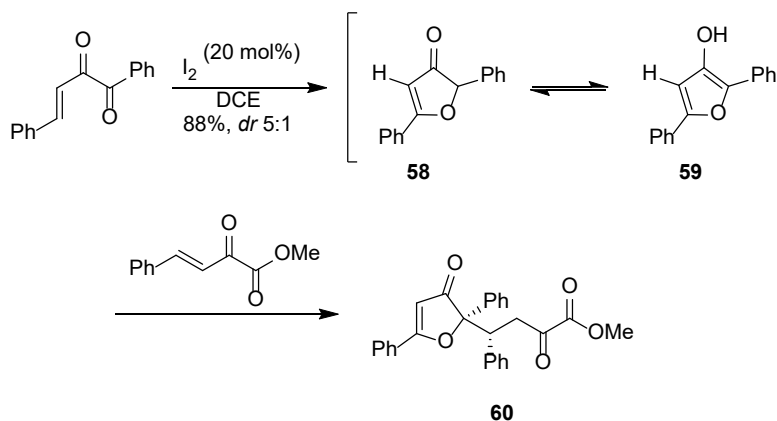
Peddinti and Aegurla reported the first example of a diaza-Nazarov cyclization, used to construct substituted pyrazoles.⁷¹ This method utilized *in situ* generated aldehyde hydrazones and acetophenone derivatives which condensed, followed by reaction with iodine to form a 2,3-diaza pentadienyl cation (Scheme 1.45).



Scheme 1.45 Iodine catalyzed diaza-Nazarov cyclization

1.3.10 Oxa-Nazarov cyclization

There has been significant development in the aza-Nazarov field in recent years, but the oxygen analogue, the oxa-Nazarov reaction has seen much less growth. The Fang group reported the first concrete example of substrates displaying this reactivity, where α -diketones were activated by I_2 , underwent cyclization to give intermediate **58**, tautomerization to **59** and subsequent Michael addition with enones to yield dihydrofuranones such as **60** (Scheme 1.46).⁷²

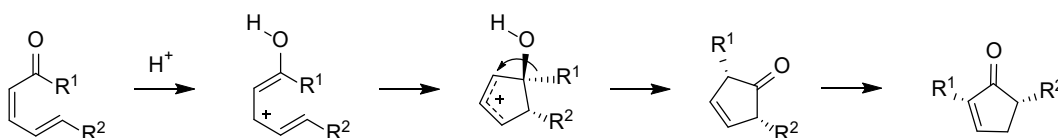


Scheme 1.46 Tandem oxa-Nazarov cyclization/Michael addition

Lv reported an asymmetric version of this transformation, utilizing the Lewis acid FeBr₃ and chiral phosphoric acids as the catalyst to yield 3(2H)-furanones in high yields and enantiomeric excesses of up to 96%.⁷³

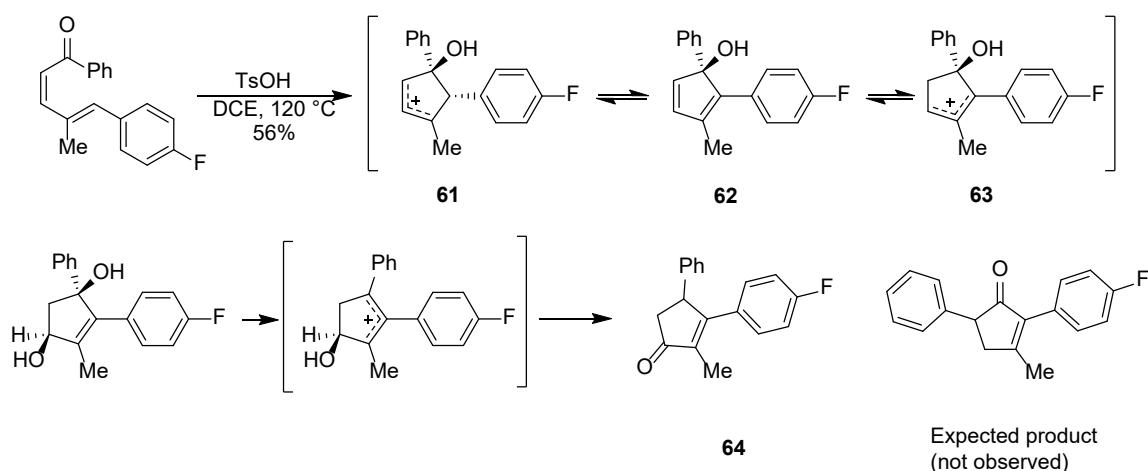
1.3.11 Iso-Nazarov cyclization

The iso-Nazarov cyclization employs linearly conjugated dienals or dienones. The reactivity of these substrates was first observed by Denmark in 1988 as an unexpected product while investigating silicon-directed Nazarov reactions, and subsequent explorations were undertaken by the Trauner group.⁷⁴ Activation by Lewis or Brønsted acid generates a pentadienyl cation with oxygen substitution at C1, ring closure, followed by an alkyl shift necessitated by the reformation of the carbonyl group (Scheme 1.47).⁷⁵ These reactions are frequently encountered with cis dienals, which readily undergo this cyclization process.



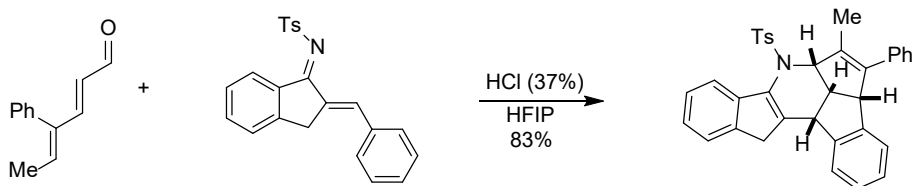
Scheme 1.47 Mechanism of the iso-Nazarov cyclization

The Riveira group demonstrated that linearly conjugated all trans dienals can be cyclized efficiently when reacted with iodine.⁷⁶ It is assumed that the substrate first isomerized into the reactive (2Z)-dienal, followed by carbonyl activation by two iodine molecules. This was determined computationally to be most likely pathway as it has an energetic cyclization barrier that would be accessible at the experimental reaction temperature. Later, the same group reported another all-trans dienal iso-Nazarov cyclization, this time using TsOH as the promoter.⁸¹ Interestingly, when these conditions were applied to dienones, the usual substitution pattern arising from a 1,2-shift was not observed (Scheme 1.48). The resulting product **64** appears to have undergone an oxygen shift from C1 to C3; the authors reasoned that after cyclization to form **61**, deprotonation at C5 gave **62**, which can subsequently be reprotonated at C2 resulting in **63**. A water molecule then attacked C3, followed by cleavage of the C–O bond at C1. The dienals screened gave the expected products.



Scheme 1.48 Iso-Nazarov cyclization with formal oxygen shift from C1 to C3

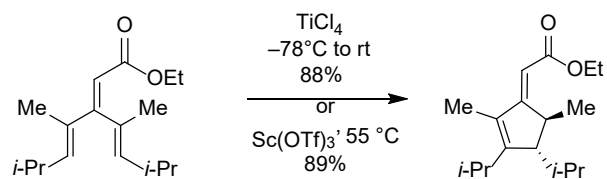
Moreau utilized the iso-Nazarov reaction to construct intricate fused hexacyclic ring systems, in an interrupted process.⁷⁷ This reaction proceeded via HCl activation of the dienal forming a cyclopentadienol which can then undergo [4+2] cycloaddition with azadienes followed by skeletal rearrangements to form the product (Scheme 1.49).



Scheme 1.49 Interrupted iso-Nazarov cyclization

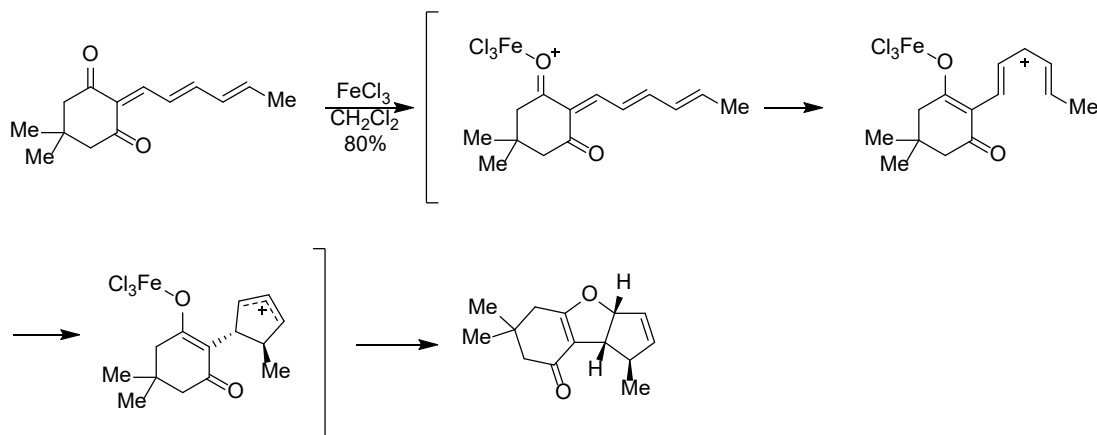
1.3.12 Vinylogous Nazarov cyclization

The vinylogous Nazarov cyclization, first introduced by West and coworkers, involves the use of cross-conjugated trienes ([3]dendralenes) that can be activated at a remote carbonyl site to initiate cyclization.⁷⁸ The substrates were subjected to TiCl_4 or $\text{Sc}(\text{OTf})_3$ conditions, resulting in a single stereoisomer of the exocyclic double bond (Scheme 1.50).



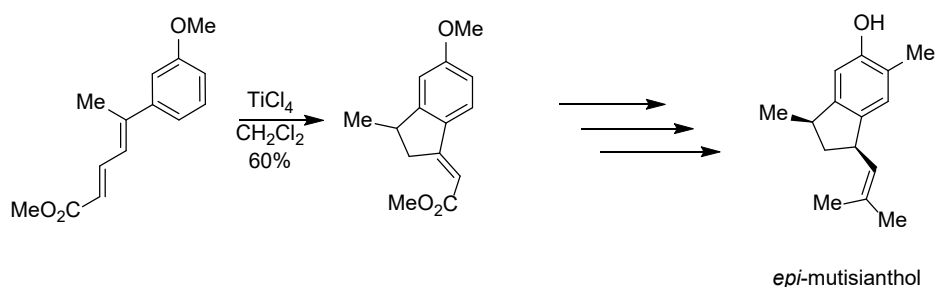
Scheme 1.50 The vinylogous Nazarov reaction

A recent advance in this field came from Riveira and Mischne, who described a vinylogous iso-Nazarov cyclization.⁷⁹ Upon activation of the carbonyl with a Lewis acid, the linearly conjugated triene isomerized to the reactive U conformer. Cyclization followed by trapping of the allyl cation with the enolic oxygen led to the product as a single diastereomer (Scheme 1.51).



Scheme 1.51 Vinylogous iso-Nazarov cyclization

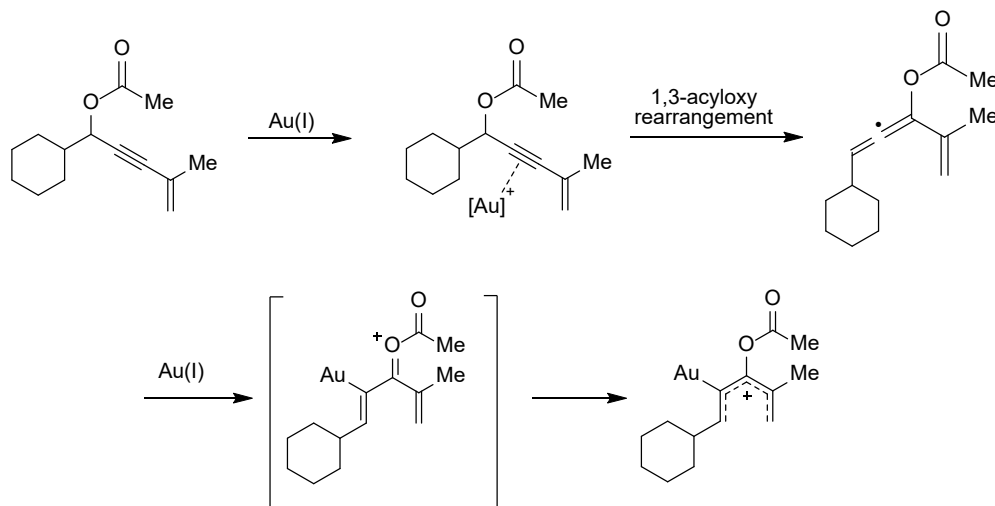
Dethe and coworkers reported a vinylogous iso-Nazarov cyclization in which the remote carbonyl was conjugated at C1, not at C3 as is typically seen.⁸⁰ This reaction provided access to substituted indanes, and was applied to a total synthesis of *epi*-mutisianthol (Scheme 1.52).



Scheme 1.52 Vinylogous iso-Nazarov cyclization

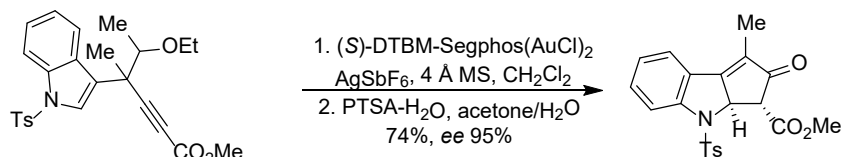
1.3.13 Metal mediated activation of alkynes

The first example of metal mediated activation of alkynes to form a Nazarov-type pentadienyl intermediate *in situ* was reported by Zhang, synthesizing cyclopentenones from propargyl acetates of enynes.⁸¹ This methodology took advantage of the tendency for acyloxy groups on gold activated alkynes to undergo 1,3-migration, resulting in an allene that can be activated by the gold complex to generate a reactive pentadienyl cation (Scheme 1.53).



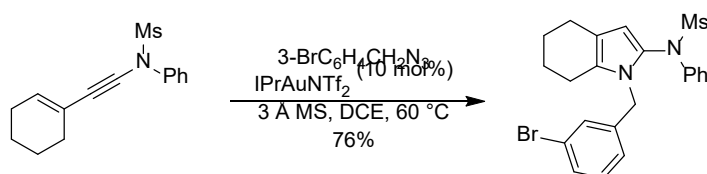
Scheme 1.53 Generation of a pentadienyl cation via gold mediated activation of alkynes

Since this pioneering study, this methodology has been used to furnish many interesting compounds. Toste reported the synthesis of cyclopenta[*b*]indoles via gold catalyzed imino-Nazarov type cyclization of propargyl acetates.⁸² Coordination of the gold to the alkyne initiated a 1,2-acetoxy migration producing an amino pentadienyl cation, which was stabilized by the indole moiety. The use of (*S*)-DTBM-Segphosgold(I) gave highly enantioenriched cyclization products (Scheme 1.54).



Scheme 1.54 Gold catalyzed imino-Nazarov cyclization

Lu and Ye described an interesting transformation to access 2-aminopyrroles. Activation of an ynamide with gold, followed by intermolecular amination using benzyl azides generated an imine-containing gold carbene intermediate that can subsequently undergo aza-Nazarov type cyclization (Scheme 1.55).⁸³



Scheme 1.55 Gold catalyzed aza-Nazarov cyclization

1.4 Summary

A considerable amount of work in the last 20 years in the field of Nazarov chemistry has been dedicated to expanding the scope of the reaction. This includes discovering alternative modes of activation, to provide products that are not compatible with traditional acid mediated reaction conditions. Alternative activation methods can sometimes reveal new modes of reactivity not observed under typical conditions. In addition, the discovery of many new classes of substrates that are amenable to Nazarov type reactivity has vastly expanded the synthetic utility of the reaction. Many classes of molecules have been synthesized using Nazarov chemistry that wouldn't have been possible using the divinyl ketone template. It is of interest to our research group to explore the types of substrates that are responsive to alternative activation methods, in particular oxidative activation.

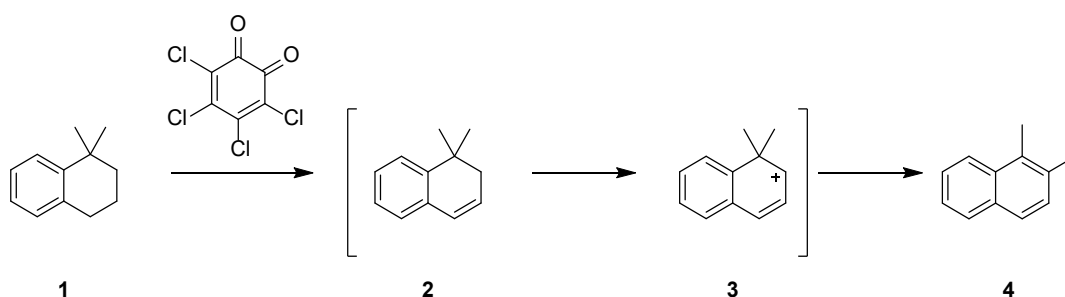
Chapter 2: Exploration of the Oxidative Entry to the Nazarov Cyclization

2.1 Introduction

As discussed in Section 1.2, the development of alternative activation strategies for the Nazarov cyclization is of great interest to many research groups, including ours. Of particular interest is the ability for certain substrates to undergo formal hydride abstraction to generate a reactive carbocation species, that may be able to undergo Nazarov cyclization. The development of C–H bond functionalization using organic oxidants has expanded significantly in recent years, providing ample precedent for its application to Nazarov chemistry; relevant mechanistic considerations and applications will be discussed in subsequent sections.

2.1.1 Early examples of generation of carbocations via hydride abstraction using quinone oxidants

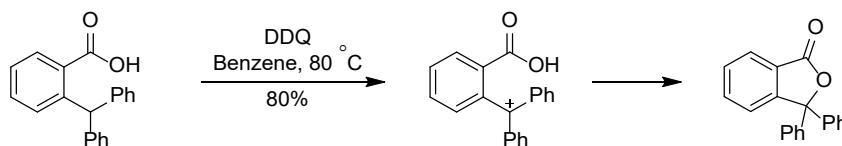
An early study on the use of quinones as dehydrogenating agents came from Braude and coworkers, who demonstrated that 1,1-dimethyl tetralin **1** formed 1,2-dimethylnaphthalene **4** when treated with *o*-chloranil (Scheme 2.1).⁸⁴



Scheme 2.1 Quinone mediated dehydrogenation

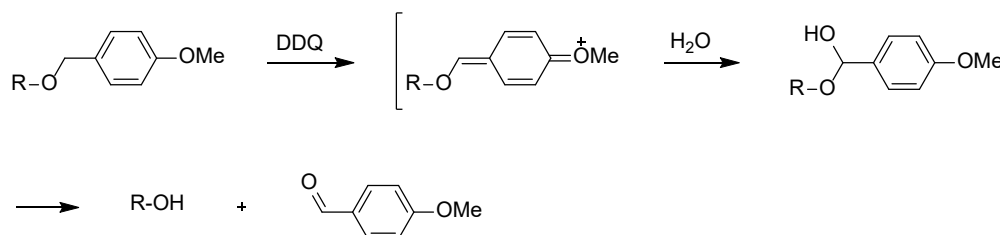
Although not discussed in the paper, the mechanism presumably began with hydride abstraction from **1** followed by deprotonation to form intermediate **2**, which can then undergo another hydride abstraction of an allylic hydride, generating intermediate **3**. Alkyl shift followed by loss of a proton formed the product **4**. Another report in the same year by Creighton and

trapping of the carbocation, resulting in a γ -lactone (Scheme 2.2).⁸⁵



Scheme 2.2 Lactone formation via intramolecular nucleophilic trapping of carbocation

Possibly one of the most well known uses of quinone oxidants is their use to cleave *para*-methoxy benzyl groups under aqueous conditions, demonstrated by Yonemitsu and coworkers (Scheme 2.3).⁸⁶ This makes PMB groups particularly useful for the protection of alcohols due to the orthogonal nature of the oxidizing conditions used for their removal.

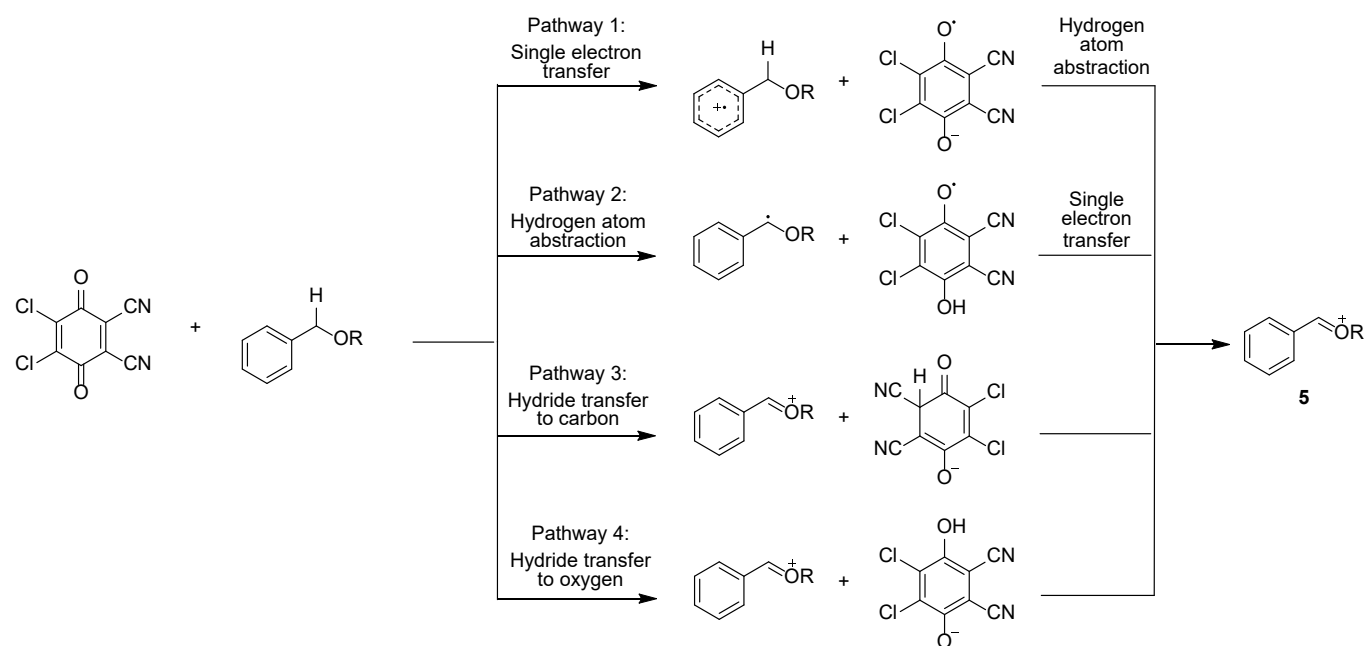


Scheme 2.3 Cleavage of *para*-methoxy benzyl protecting group

2.1.2 Mechanistic considerations of quinone oxidants

An increase in attention towards quinone based oxidants for C–H bond functionalization has resulted in comprehensive studies into the mechanism, to fully understand this important transformation. DDQ mediated C–H bond functionalization reactions occur first through the formation of a charge transfer complex between the oxidant and the substrate.^{87, 88, 89, 90} Following the formation of the charge transfer complex, a formal hydride abstraction from the substrate to the quinone occurs. The mechanism by which the formal hydride abstraction occurs has been the topic of some controversy.^{91, 92, 93, 94} The four proposed mechanisms are shown in Scheme 2.4.⁹⁵ The first possible pathway is a single electron transfer from the substrate to DDQ forming a radical cation, which then undergoes subsequent hydrogen atom transfer to form carbocation **5**. The second pathway is essentially the opposite; a hydrogen atom transfer followed by a single electron

transfer to form **5**. Pathways 3 and 4 are both direct hydride abstraction pathways, differing only in the location to which the hydride is transferred to DDQ. In pathway 3 the hydride is transferred to one of the CN bearing carbons, while in pathway 4 it is transferred directly to one of the quinone oxygen atoms.

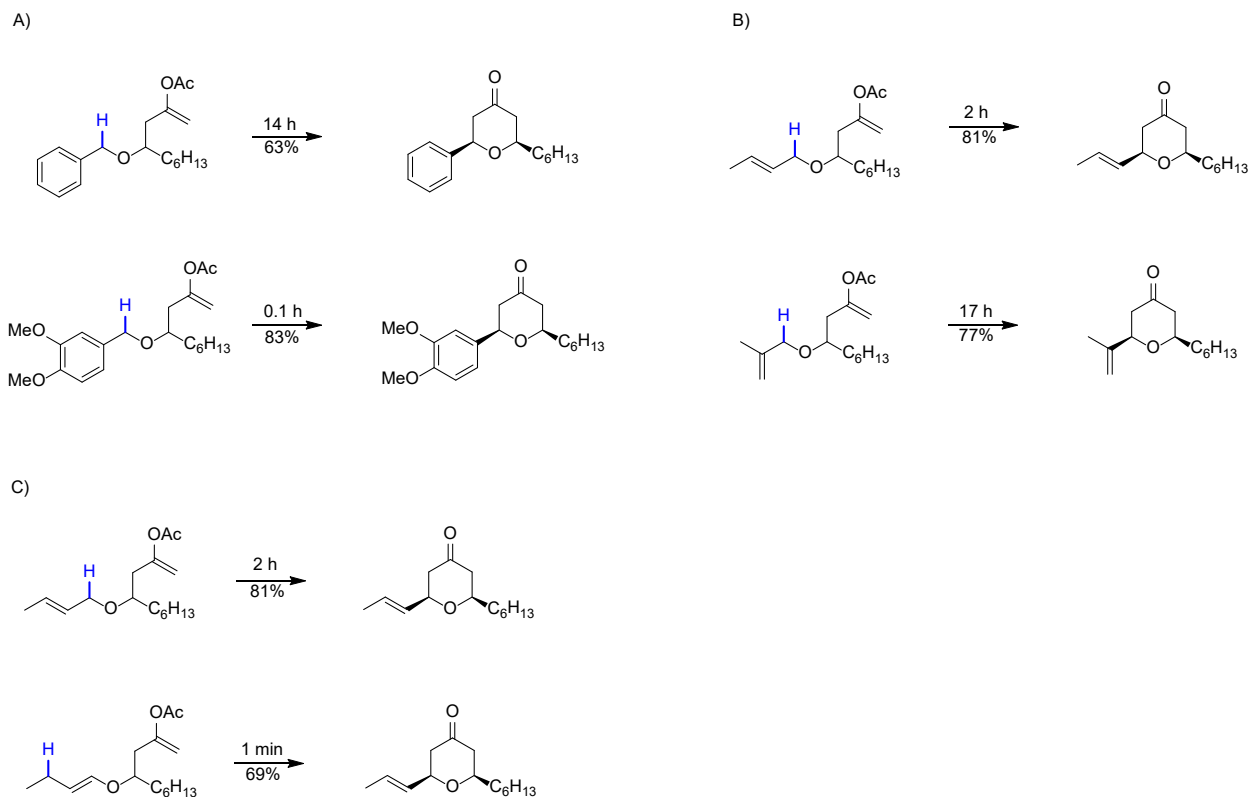


Scheme 2.4 Proposed mechanisms for DDQ mediated C–H cleavage

The proposal of pathway 2 arises from a report by Rüchardt in 1996 that observed trapping of intermediate radicals with nitrosobenzene.⁹⁶ This pathway can be largely discounted because when cation stabilizing groups are added, reaction rates increase. Pathway 2 does not adequately explain these observations.^{97, 98} Many computational studies have been published that support direct hydride abstraction over a single electron transfer pathway, whether it be transfer to the carbon or oxygen atom.^{99, 94, 100, 92} A detailed computational study by Floreancig in 2017 reveals that the O and C attack pathways are generally competitive and are substrate dependent.⁹⁵ Both the SET and HAT mechanisms had a higher energetic barrier than the hydride abstraction mechanisms in this study.

Experimental observations of the rate of DDQ-mediated oxidative C–H cleavage reactions can also give insight into the reaction mechanism. The Floreancig group has conducted extensive

studies on how different substrates affect the rate of DDQ mediated tetrahydropyran synthesis (Scheme 2.5).¹⁰¹ From these reactions a reactivity trend can be observed. In Scheme 2.5a, the addition of electron donating groups on the aromatic ring resulted in consumption of the starting material significantly faster than the unsubstituted substrate. Scheme 2.5b demonstrated the increased rate of C–H cleavage in internal alkenes vs. external alkenes. These two trends demonstrated the effect that increased cation stabilization has on reaction rate. In scheme 2.5c we see that allylic hydrides on enol ethers reacted much faster than allylic hydrides on allyl ethers. This cannot be explained by resulting carbocation stability, as both substrates yield the same intermediate carbocation. The authors hypothesized that the origin of increased reactivity for the enol ether hydride over the allyl ether hydride stem from increased electrostatic interactions and secondary orbital interactions between the substrate and DDQ.⁹⁵ Indeed the computational results indicate there is more electron transfer (i.e. electrostatic interaction) in the transition state of the enol ether substrate over the allylic ether (in both O- and C- attack mechanisms). Further, there are greater secondary orbital interactions between the enol ether substrate and DDQ. This is because the HOMO orbital is more polarized on the enol ether substrate **6**, resulting in a larger orbital coefficient on the carbon adjacent to the oxygen generating stronger secondary orbital interactions, and therefore increased reactivity (Figure 2.1).



Scheme 2.5 Effect of substrates on reaction rate of C–H oxidative cleavage reactions

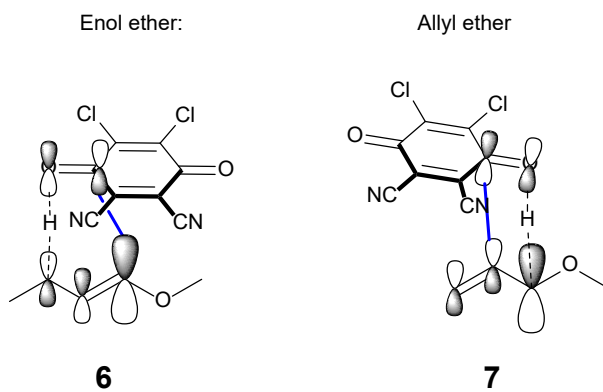


Figure 2.1 Secondary orbital interactions between hydride donor and DDQ

From these studies it can be concluded that the mechanism of DDQ-mediated C–H cleavage likely proceeds through a direct hydride abstraction pathway. The rate of the reaction

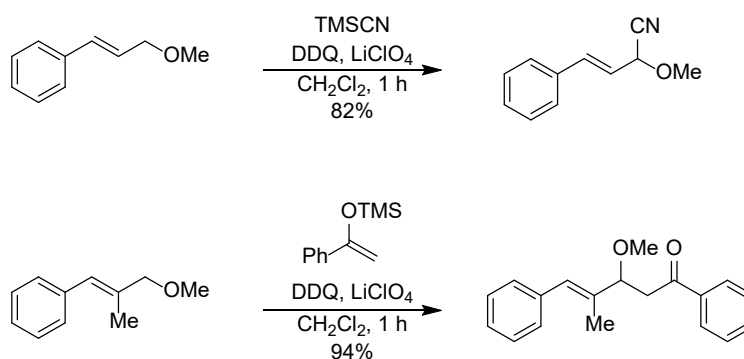
depends largely on how much stabilization is given to the resulting carbocation. An interesting case is observed for allylic substrates, in which increased electrostatic interactions as well as secondary orbital interactions also have significant impacts on the rate of the reaction.

2.1.3 DDQ mediated oxidative C–C bond forming reactions

DDQ mediated C–H bond activation reactions have shown great synthetic utility in recent years, and have been applied to a wide variety of transformations. These transformations include alkylations, arylations, and Prins cyclizations, among others. Using organic hydride abstraction reagents such as quinones is beneficial because significant functionality can be introduced into a molecule without need for multiple functional group interconversions, or activating groups. This improves atom economy, lowers step economy, and decreases likelihood of reagent incompatibility within a synthetic scheme.

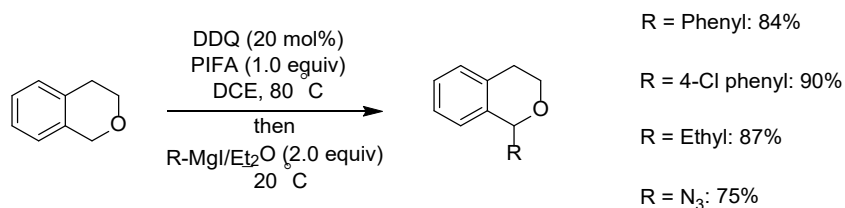
2.1.3.1 Intermolecular reactions

The most common application of this chemistry is generation of the carbocation, followed by nucleophilic trapping. An early study from Hayashi and Mukaiyama showed the compatibility of various silyl containing nucleophiles with DDQ.¹⁰² Cinnamyl ether was reacted with DDQ, followed by cation trapping with silyl nucleophiles (Scheme 2.6).



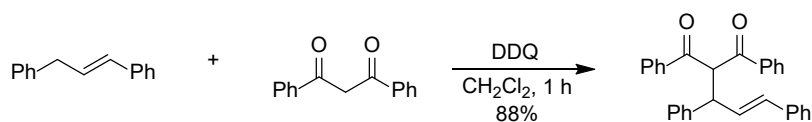
Scheme 2.6 Carbocation trapping with silyl containing nucleophiles

Muramatsu and Nakano demonstrated nucleophilic trapping of cations generated from isochroman derivatives with aryl, alkyl and vinyl Grignard reagents (Scheme 2.7).¹⁰³ With the addition of PIFA ([bis(trifluoroacetoxy)iodo]benzene) as a co-oxidant, the loading of DDQ could be decreased to 20 mol%.



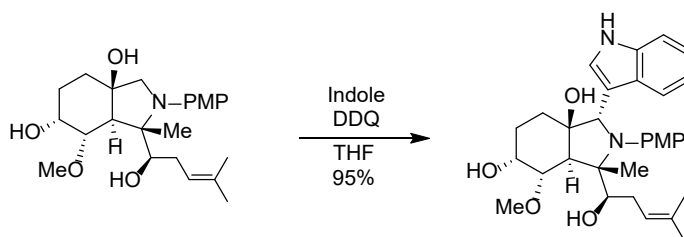
Scheme 2.7 Carbocation trapping with Grignard nucleophiles

Bao reported the ability of active methylenic compounds to trap oxidatively formed carbocations (Scheme 2.8).¹⁰⁴ Various substituents on the β -diketone were tolerated, including thienyl, furanyl, and alkyl groups.



Scheme 2.8 Carbocation trapping with activated methylene nucleophiles

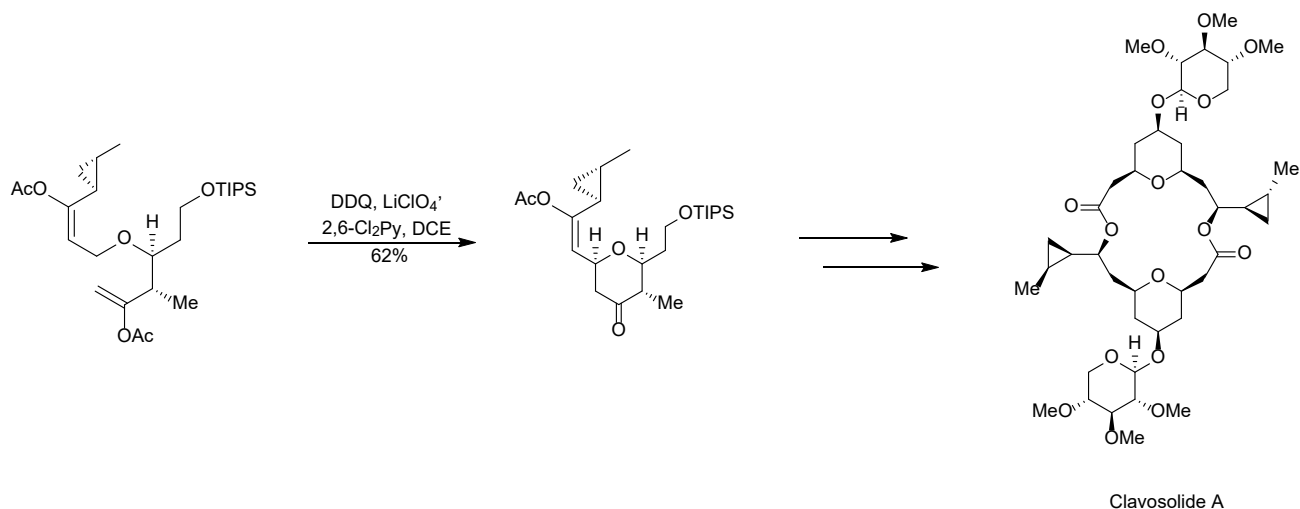
In 2014 the Grenning group utilized this methodology in an oxidative-Mannich reaction (Scheme 2.9).¹⁰⁵ The oxidatively generated intermediate iminium ion could be trapped with a variety of nucleophiles, including indole, diethylphosphite, cyclohexane silyl enol ether, and methylenecyclopentane. These compounds are a part of a two-step diversity-oriented synthesis from natural product fumagillol.



Scheme 2.9 Example of trapping of iminium ions generated by DDQ oxidation

2.1.3.2 Intramolecular reactions

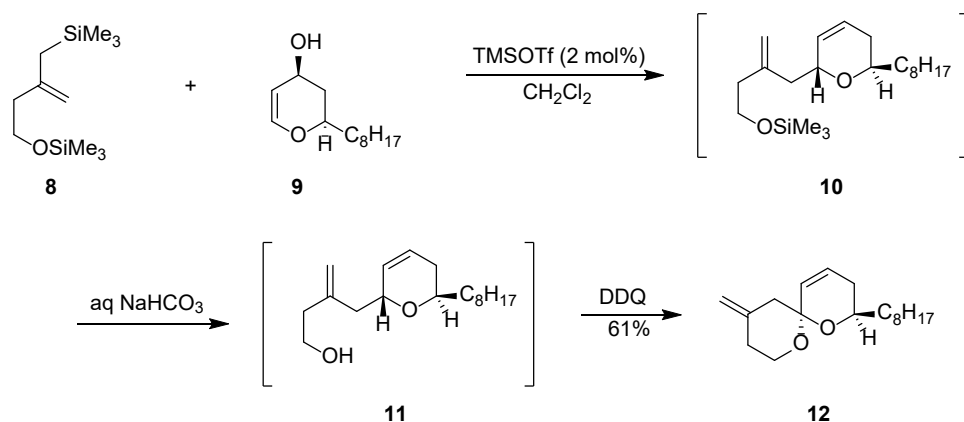
As highlighted in Scheme 2.5, the Floreancig group has accomplished significant work in this field towards tetrahydropyran synthesis, as well as other scaffolds.^{101, 106, 107, 108, 109} They have applied their methodology towards several total synthesis schemes, including clavosolide A (Scheme 2.10).¹¹⁰ This reaction demonstrated that the oxidative conditions used were compatible with cyclopropane groups. The oxidative cyclization to tetrahydropyrans with an enol acetate as the nucleophile was achieved without any competitive ring opening.



Scheme 2.10 Total synthesis of clavosolide A

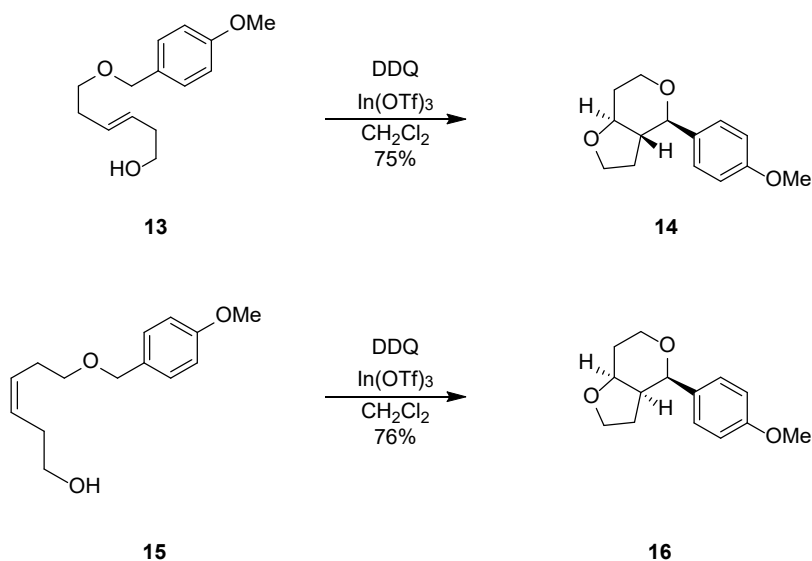
The group has also demonstrated the ability to generate the reactive intermediates, followed by ring closure to form spirocycles in a one pot fashion (Scheme 2.11).¹¹¹ Allylsilane **8** reacted with dihydropyran **9** under Lewis acid mediated conditions in a Ferrier rearrangement reaction,

yielding intermediate **10**. Cleavage of silyl ether resulted in **11**, followed by DDQ mediated cyclization to give product **12** in 61% yield.



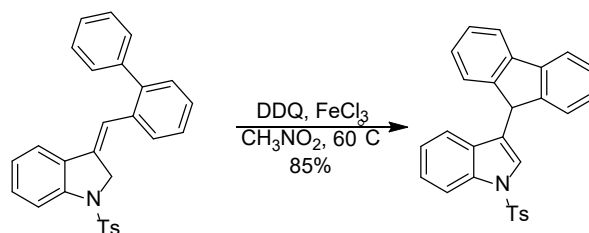
Scheme 2.11 One pot Ferrier-oxidative cyclization reaction

Reddy and coworkers demonstrated an intramolecular oxidative Prins cyclization, mediated by DDQ and a Lewis acid.¹¹² The reaction did not proceed without a Lewis acid – the authors hypothesized that the role of the acid is to further activate DDQ to increase its oxidative potential. The use of Lewis acids in conjunction with DDQ has been reported by others, for similar transformations.^{113, 114, 115} The authors demonstrated that the geometry of the alkene determined the stereochemical outcome of the transformation (Scheme 2.12). The *trans* alkene **13** resulted in the *trans* product **14**. Likewise, the *cis* alkene **15** gave the *cis* product **16**.



Scheme 2.12 Intramolecular oxidative Prins cyclization

Jana and coworkers demonstrated the synthesis of various fluorene compounds utilizing a DDQ/ FeCl_3 system (Scheme 2.13).¹¹⁵ Oxidation, followed by intramolecular Friedel-Crafts alkylation furnished the fluorene substituted indole product in high yield. Similar to above, the exact role of the Lewis acid is not fully understood, but likely activated DDQ.

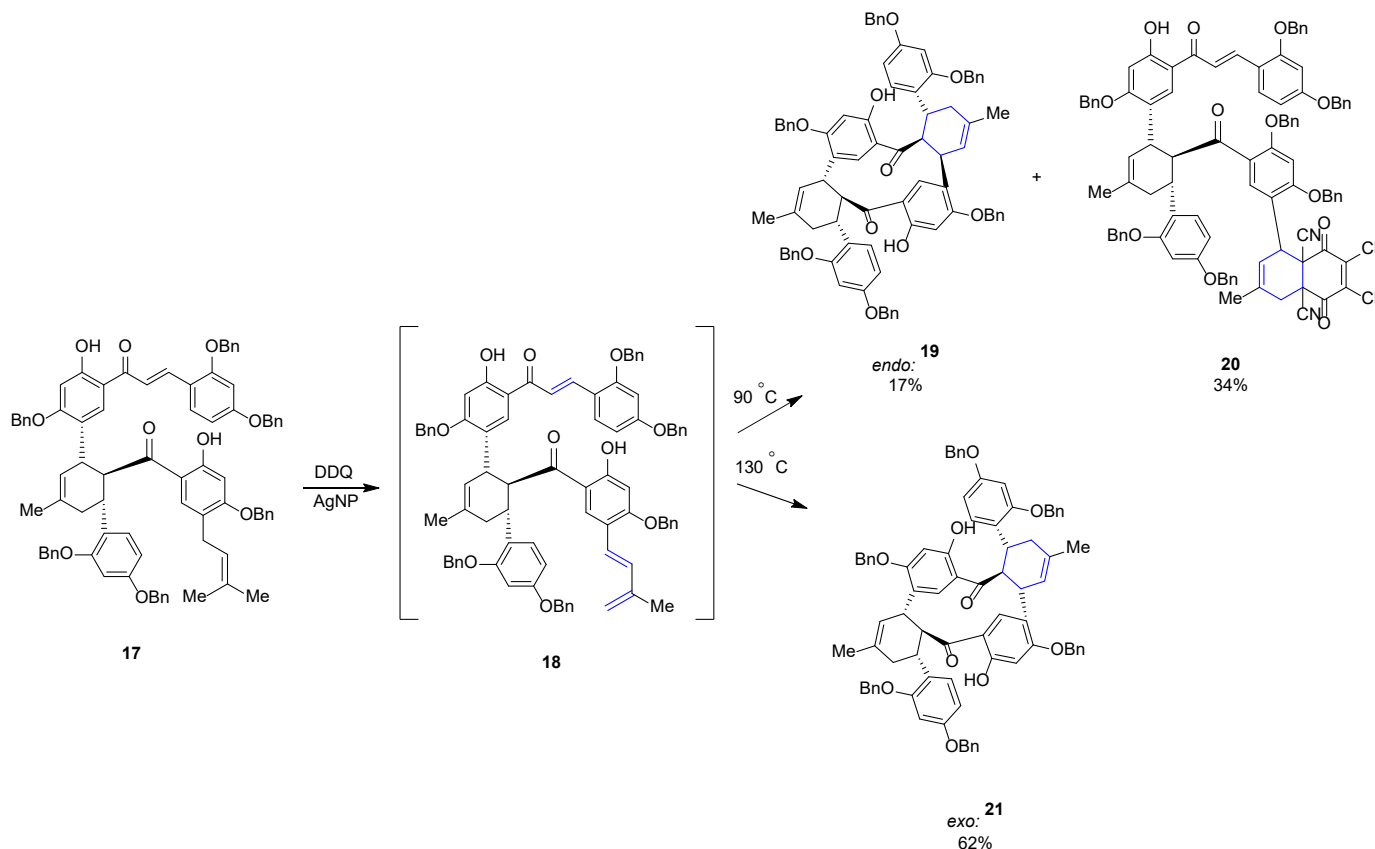


Scheme 2.13 Oxidative intramolecular Friedel-Craft alkylation

2.1.3.3 Cycloadditions and bond reorganizations

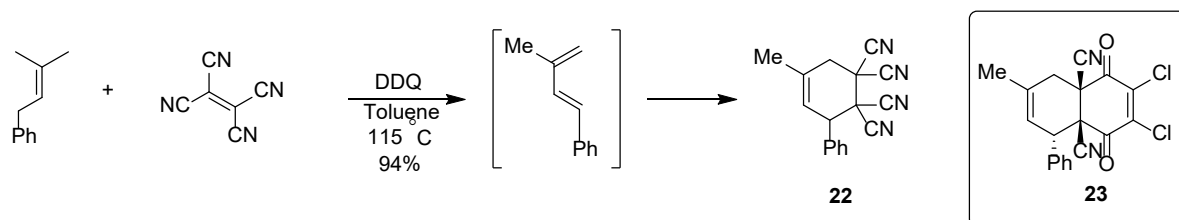
There have been multiple examples of DDQ mediated dehydrogenative Diels Alder reactions. These reactions can sometimes be problematic as DDQ itself can compete as dienophile. Porco and coworkers found that when subjecting compound **17** to DDQ/AgNPs (silver nanoparticles) at 90 °C, the *endo* Diels-Alder product **19** was obtained in 17% yield, along with a

DDQ adduct **20** in 34% yield (Scheme 2.14).¹¹⁶ Increasing the temperature to 130 °C allowed for a retro Diels-Alder reaction to occur, followed by reaction with the desired dienophile. This gave the *exo* adduct as the major product in 62% yield.



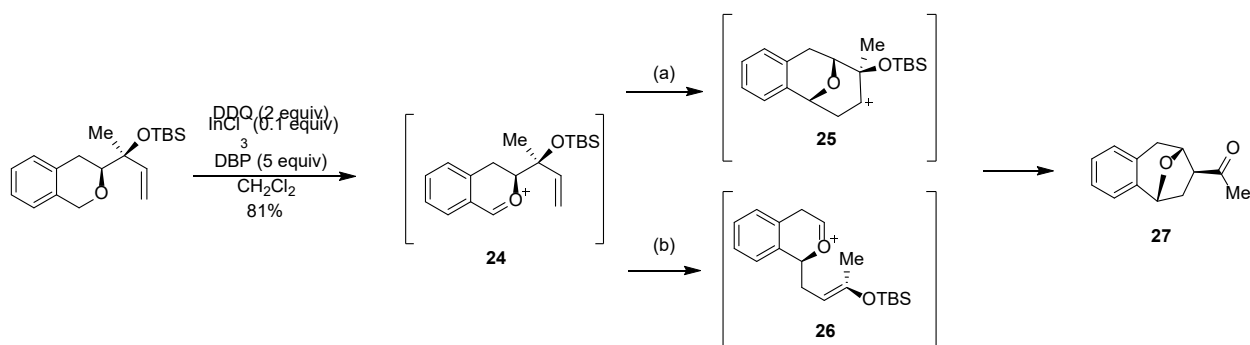
Scheme 2.14 Temperature dependence of Diels-Alder product mixtures

Zhou and Coworkers also observed this thermally reversible process.¹¹⁷ Reaction at lower temperatures gave the desired product **22** as well as DDQ adduct **23**. Upon raising the temperature to 115 °C no DDQ adduct was observed, and the product was isolated in 94% yield (Scheme 2.15).



Scheme 2.15 Dehydrogenative Diels-Alder reaction

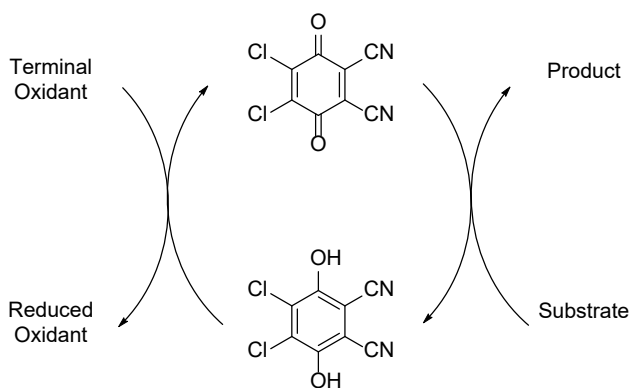
An interesting bond reorganization reaction came from Jiao et al., in which isochroman derivatives underwent C–H bond activation, resulting in tricyclic benzoxa[3.2.1]octanes (Scheme 2.16).¹¹³ There are two possible mechanistic pathways to arrive to the product. First, oxidation of the benzylic C–H bond gives intermediate **24**. From this intermediate, pathway (a) involves cyclization to intermediate **25**, followed by semipinacol rearrangement to give the product **27**. In pathway (b), intermediate **24** undergoes an oxonia-Cope rearrangement to **26**, followed by aldol reaction to give the product. The authors propose that pathway (b) is more likely, as no competing migration was observed when using electron rich groups in the allylic position, which would be expected if a semipinacol rearrangement process was operative. This process was used towards the total synthesis of (–)-brussonol and (–)-przewalskine E.



Scheme 2.16 DDQ mediated tandem cyclization to form tricyclic benzoxa[3.2.1]octanes

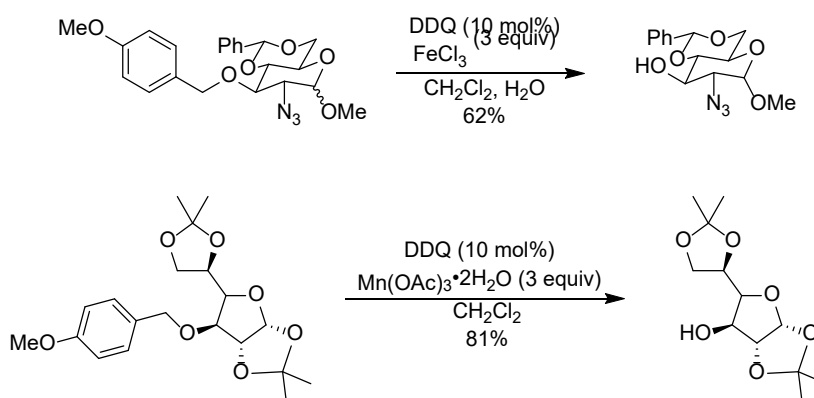
2.1.3.4 Catalytic Methods

While the use of DDQ and other quinone oxidants has been able to effect interesting and important synthetic transformations, the moderate toxicity of DDQ (LD₅₀ of 82 mg/Kg in rats) has encouraged the development of catalytic methods (Scheme 2.17).



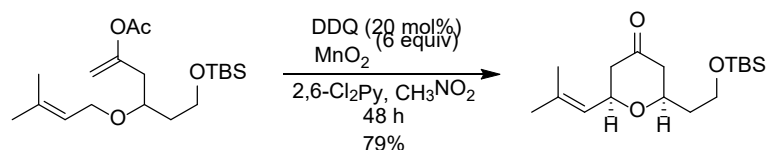
Scheme 2.17 Regeneration of catalytic DDQ

The first examples of substoichiometric use of DDQ with a terminal oxidant were used to cleave PMB groups.^{118, 119} Two such examples were published, using FeCl_3 and $\text{Mn}(\text{OAc})_3 \cdot 2\text{H}_2\text{O}$, both with only 10 mol% DDQ, and 3 equivalents of the terminal oxidant (Scheme 2.18).



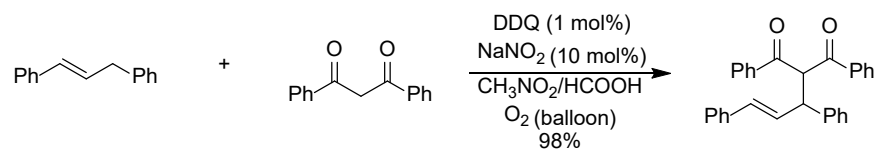
Scheme 2.18 Cleavage of PMB ethers with catalytic DDQ

Hu and coworkers utilized a DDQ/*tert*-butyl nitrite/oxygen system to oxidize benzylic alcohols to their respective aldehyde/ketone.¹²⁰ In this catalytic system, *tert*-butyl nitrite acted as an NO equivalent, which functioned as a bridge between molecular oxygen and DDQ/DDQH. Inspired by these reports, Floreancig and coworkers applied this methodology to carbon-carbon bond forming reactions (Scheme 2.19).¹²¹ A variety of terminal oxidants were screened; MnO_2 was chosen due to its low cost and negligible toxicity, although reaction times were long. This protocol was applied to a variety of transformations, including PMB ether cleavage, dehydrogenations, and cross dehydrogenative coupling.



Scheme 2.19 MnO₂ as a terminal oxidant for DDQ regeneration

Cheng et al. also reported a C–C bond forming reaction utilizing catalytic DDQ; benzylic compounds and β -diketones were coupled in the presence of catalytic DDQ, NaNO₂, molecular oxygen and formic acid (Scheme 2.20).¹²² The products of this reaction were obtained in high yields in short reaction times. Notably, only 1% DDQ was required to effect these transformations.



Scheme 2.20 Oxidative coupling using a DDQ/NaNO₂/O₂ system

2.1.4 Other hydride abstraction oxidants

DDQ has received much attention when it comes to hydride abstraction mediated transformations, but other reagents are capable of generating the same reactive cation intermediates. These reagents, namely oxoammonium ions and trityl cations can provide different reactivity patterns in response to steric or electronic factors, making them complementary oxidation reagents to DDQ.

2.1.4.1 Oxoammonium ions

Oxoammonium ions have long been used for the oxidation of alcohols.¹²³ The first example of ether oxidation using oxoammonium ions was by Pradhan et al., who used Bobbitt's salt **29** to cleave benzyl ether groups in the presence of water.¹²⁴ Notably, the ability for Bobbitt's salt to cleave unsubstituted benzyl groups indicates that Bobbitt's salt is a more powerful oxidant than

DDQ. A computational study by Miller et al. showed that oxidations by oxoammonium ions are not sensitive to substrate oxidation potential; cation stability is the determining factor in reaction rates.¹²⁵ This study also showed that oxidations by Bobbitt's salt are less sensitive to steric restrictions imposed by the substrate than DDQ oxidations, as the transition state places the bulky *gem*-dimethyl groups distal to the oxidation site. This is in contrast to DDQ oxidations, which exhibit a stacked geometry.

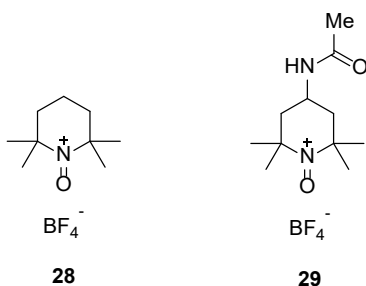
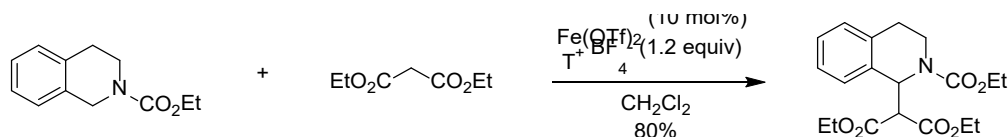


Figure 2.2 Oxoammonium ions

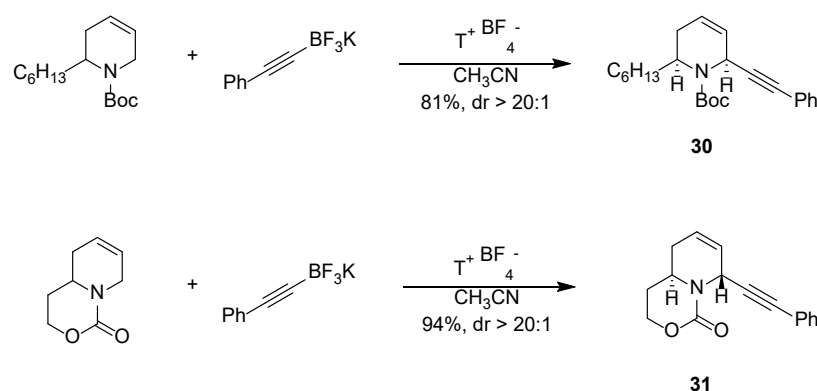
Richter and Mancheño described the use of oxoammonium salts in a dehydrogenative coupling reaction.¹²⁶ TEMPO salts (T^+BF_4^-) were used to oxidize $\text{C-H}(\text{sp}^3)$ bonds that were adjacent to heteroatoms, and coupled them to enolate nucleophiles in the presence of an iron catalyst (Scheme 2.21). The iron catalyst was necessary to activate the nucleophile – the reaction did not proceed without it. This method was utilized to functionalize a variety of isochroman derivatives as well as tetrahydroisoquinoline derivatives, with enolate-type nucleophiles. They also demonstrated the ability to oxidize acyclic benzyl ethers, although the yields were lower.



Scheme 2.21 TEMPO salt oxidation of tetrahydroisoquinoline

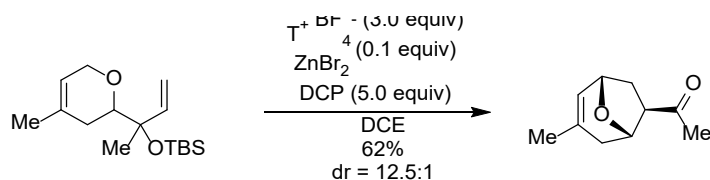
Oxidations with oxoammonium ions are also possible on substrates lacking the cation stabilizing benzo-fusion groups. Liu and coworkers facilitated the functionalization of *N*-carbamoyl tetrahydropyridines using TEMPO salts.¹²⁷ Notably, this transformation failed using

other common oxidants, including DDQ. Utilizing BOC protected tetrahydropyridine in the presence of TEMPO and potassium trifluoroborate nucleophiles furnished products **30** in high yield, and excellent *cis* diastereoselectivity (Scheme 2.22). The authors were able to generate the complementary *trans* products by incorporating the acyl group into a fused ring. This afforded the *trans* products in high diastereoselectivity (>20:1). Incorporating the acyl group into a ring resulted in an inversion of stereoselectivity arising from a difference in intermediate N-acyliminium conformation stabilities.



Scheme 2.22 Diastereoselective functionalization of N-carbamoyl tetrahydropyridines

As previously discussed, Jiao et al. demonstrated the ability for DDQ to oxidize isochroman derivatives, whose oxocarbenium products undergo a subsequent [3,3]-Cope rearrangement followed by aldol reaction (Scheme 2.16). When the aromatic ring was removed from the substrate, DDQ was no longer able to facilitate the reaction. This led the group to explore stronger oxidizing agents; they landed on TEMPO salts used in conjunction with ZnBr_2 and DCP as the optimal conditions for this reaction (Scheme 2.23).¹²⁸ The development of this methodology demonstrated that oxoammonium salts are able to facilitate reactions that DDQ cannot.



Scheme 2.23 Synthesis of 8-oxabicyclo[3.2.1]octanes via TEMPO mediated oxidation

2.1.4.2 Carbocation Oxidants

Another class of reagents capable of oxidation via hydride abstraction are carbocation oxidants (Figure 2.3). Similar to the history of DDQ and oxoammonium ions, early uses of the reagent include its ability to cleave PMB groups in the presence of water, as well as the ability to cleave acetal and ketal groups.^{129, 130, 131}

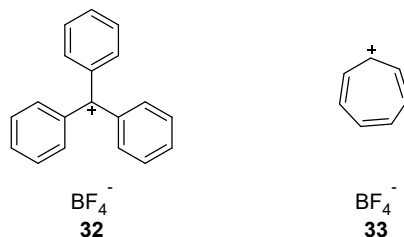
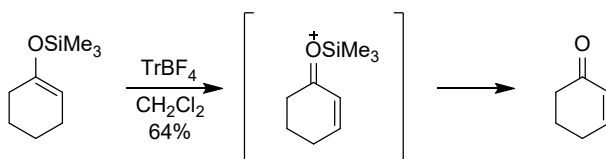


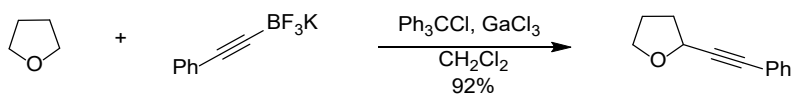
Figure 2.3 Carbocation oxidants

Jung and coworkers described the ability for TrBF_4 **32** to convert enolsilanes into enones via hydride abstraction mechanism (Scheme 2.24).¹³² The group even demonstrated the ability of TrBF_4 to transform acyclic enolsilanes into enones, albeit in lower yields.



Scheme 2.24 Conversion of enol silanes to enones using a carbocation oxidant

More recently these reagents have been used in the application of C–C bond forming reactions. The most common application is the oxidation of C–H bonds adjacent to heteroatoms. In 2014 Liu and coworkers demonstrated the first example of carbocation oxidants being used to facilitate oxidative coupling of ethers with carbon nucleophiles (Scheme 2.25).¹³³ The most effective system was an *in situ* generated carbocation oxidant, from TrCl and GaCl_3 . Nucleophilic attack of alkynyltrifluoroborates on the oxidatively generated cation gave products in high yields. This methodology was also applied to various ring sized cyclic ethers, cyclic sulfides, pyrrolidine, among others.

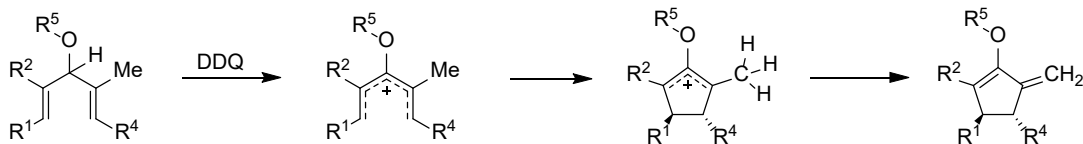


Scheme 2.25 Use of carbocation reagents for α functionalization of ethers

Sections 2.1.3 and 2.1.4 have described the applications of three hydride abstraction reagents classes to bond forming reactions. These three reagents can react with a substrate to form the same reactive carbocation species. The ability for multiple reagents to effect the same transformation increases the number of suitable substrates, due to mechanistic nuances between oxidants.

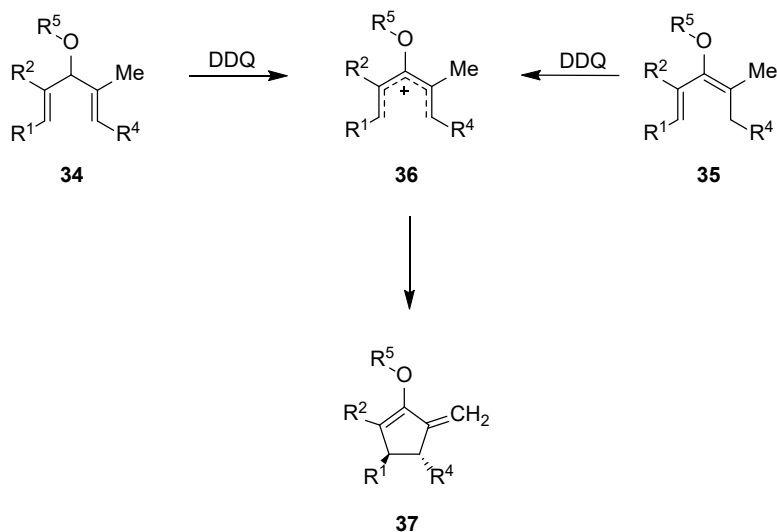
2.2 Background

As mentioned in section 1.2.3, our group recently described the oxidative Nazarov cyclization of dienyl ethers (Scheme 2.26).¹² This reaction tolerated a variety of ether groups, including benzyl and allyl ethers. Notably, the elimination step resulted in exclusive formation of the exocyclic double bond, resulting in a highly regioselective outcome that also preserved the two stereocenters generated in the electrocyclization step.



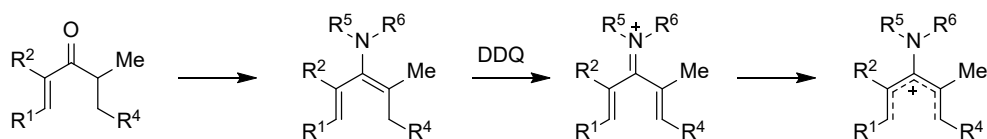
Scheme 2.26 Oxidative Nazarov cyclization

This study prompted us in thinking what other substrates may be oxidized by DDQ to allow for cyclizations that may not be possible using traditional methods. We envisioned the use of enol ethers as substrates for this reaction; the expectation is that **35** would undergo formal hydride abstraction to generate the pentadienyl cation **36**, which should undergo conversion to **37** (Scheme 2.27).



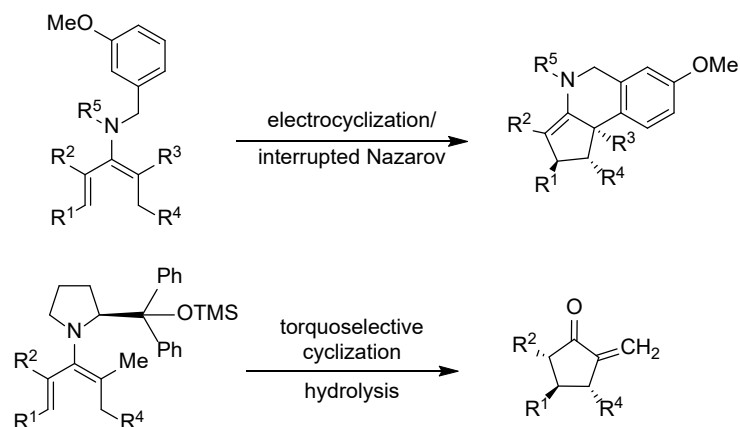
Scheme 2.27 Generation of pentadienyl cation

The ultimate goal of this project was to develop an oxidatively initiated imino-Nazarov transformation. This would be advantageous for several reasons. First, the direct nitrogen analogs of the commonly employed Nazarov substrates, which are divinyl imines, are difficult to access. Employing enamines may provide a more direct access to the desired 3-amino pentadienyl cation (Scheme 2.28).



Scheme 2.28 Proposal of oxidative imino-Nazarov pathway

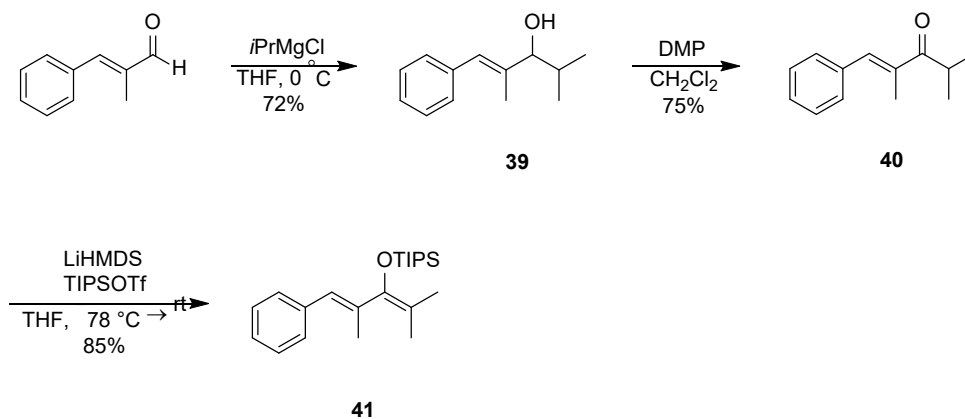
Second, utilizing amines provides the opportunity to incorporate tethered trapping groups on the amine, allowing for interrupted variants of the reaction. Lastly, there is the possibility of utilizing chiral secondary amines, which may allow for a torquoselective ring closure (Scheme 2.29).



Scheme 2.29 Possible variations of oxidative imino-Nazarov cyclization

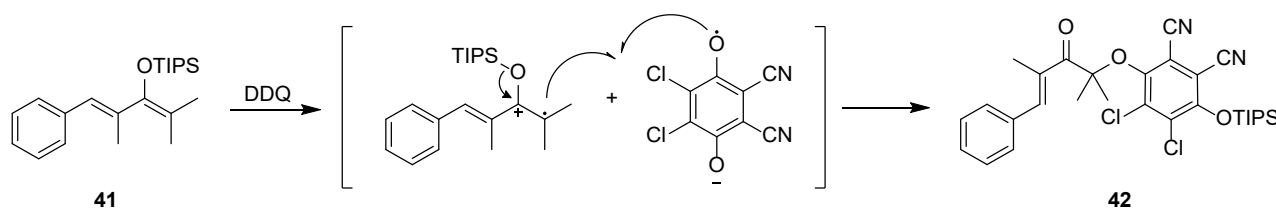
2.3 Results and discussion

The first targeted enol ether of type **35** was triisopropyl silyl enol ether **41**. A silyl enol ether was chosen due to its ease of preparation. TIPS was deemed the best choice as it is not as labile as other silyl groups, therefore would be more likely to withstand the oxidative reaction conditions. Formation of this compound was achieved by Grignard addition of isopropyl magnesium chloride to α -methyl trans cinnamaldehyde to give the resulting alcohol, which was oxidized with DMP and finally formation of the enol ether using TIPSOTf (Scheme 2.30).



Scheme 2.30 Synthesis of silyl enol ether **41**

The reaction conditions used for the initial trials were adopted from our previous oxidative cyclization study.¹² Compound **41** was reacted with 1.2 equivalents of DDQ in DCM at room temperature (Table 2.1, entry 1). The reaction was monitored by TLC and showed consumption of starting material after 24 hours. Characterization of the product formed revealed that the intended formation of the pentadienyl cation had not occurred. Instead, formation of DDQ adduct **42** was observed. A possible mechanistic sequence would involve radical recombination of the diene radical cation with the semiquinone radical anion and loss of TIPS to form the ketone (Scheme 2.31). This mechanism has been observed by Guo and Mayr in both cyclic and acyclic silyl enol ethers.⁹³ As per the observations of Guo and Mayr, the carbon radical of the substrate can either react via C or O-attack on DDQ. Characterization of the product indicates an O-attack, as only one characteristic carbonyl peak is seen in the ¹³C NMR spectrum. The adduct was formed within 24 h in a 51% yield.



Scheme 2.31 Proposed mechanism for the formation of product **42**

The incompatibility of DDQ with substrate **41** prompted the screening of another oxidizing agent. As discussed in Section 2.1.4.2 the use of carbocation oxidants has been observed with silyl enol ether reagents to yield enones via hydride abstraction.¹³² The hope was the intermediate carbocation formed by hydride abstraction would cyclize more quickly than the loss of the silyl group to form an enone, as was observed by Jung et al. When subjecting compound **41** to $\text{CPh}_3^+\text{BF}_4^-$ conditions, compound **40** was obtained in 34% yield (entry 2). The desilylation likely occurs from trace fluoride anion present in the BF_4^- counterion. Also observed was triphenylmethane in 51% yield. This suggested that the trityl cation is able to abstract a hydride from the starting material. Since no other significant products could be observed in the crude ¹H NMR spectrum, the oxidized compound likely decomposed after hydride abstraction. In an attempt to prevent desilylation of the starting material, collidine was added to the reaction mixture (entry 3). The crude ¹H NMR spectrum showed no ketone **40**, but significant amounts of starting material,

as well as triphenylmethane. When molecular sieves were added to the reaction, the starting material was consumed completely, indicating the presence of moisture in the reaction (entry 4). Without the presence of collidine, ketone **40** was present in 43% yield, as well as triphenylmethane, once again indicating that the substrate was being oxidized, but then rapidly decomposes. Bobbitt's salt was also tested, although the only product detected was ketone **40**, once again indicating the ready loss of the TIPS group via incidental fluoride.

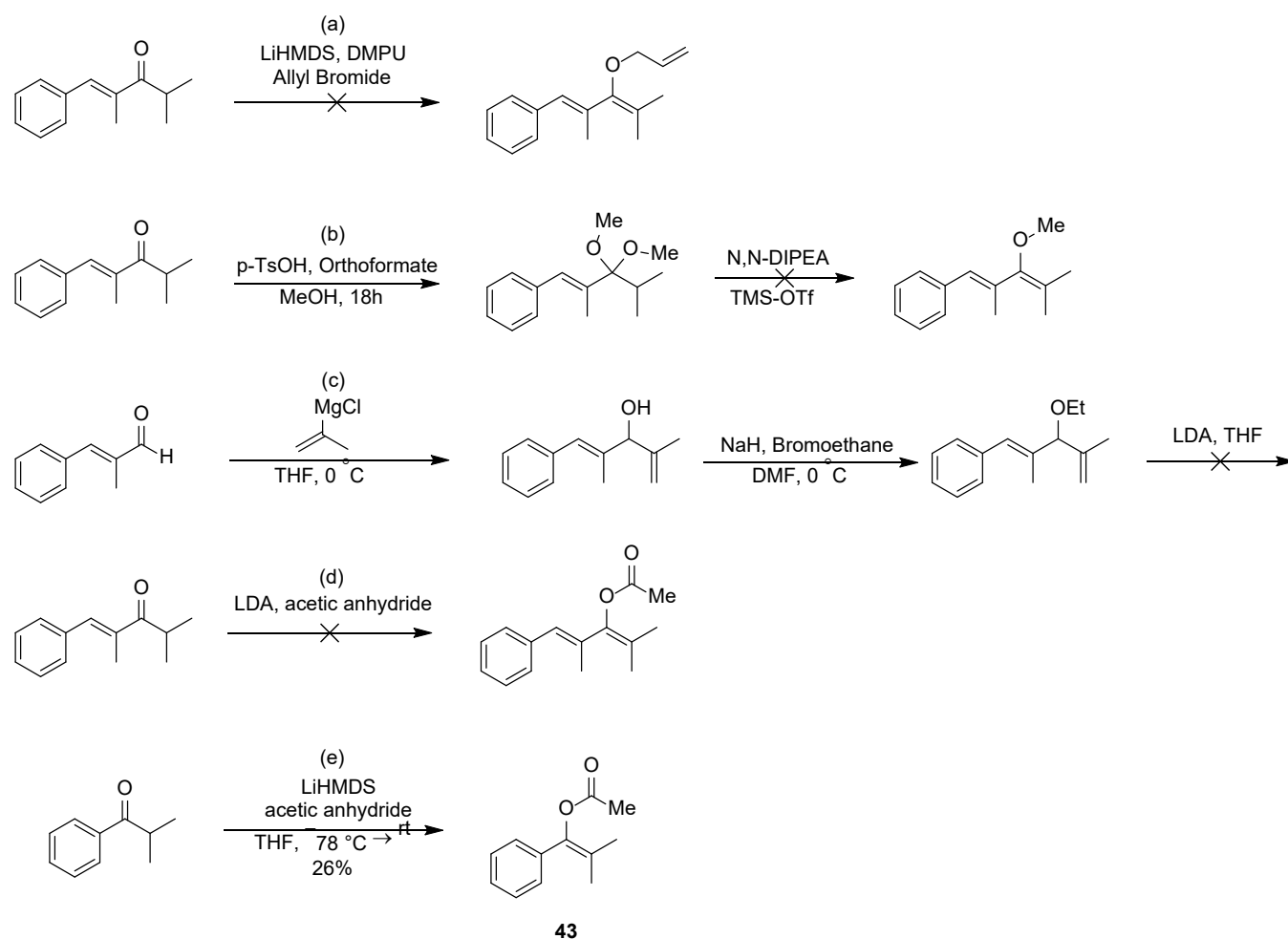
Table 2.1 Screening of oxidant conditions for compound **41**

Entry ^a	Oxidant (1.2 equiv.)	Additive	Products	Yield (%) ^b
1	DDQ	-	42	51
2	CPh ₃ ⁺	-	40	31
3	CPh ₃ ⁺	Collidine	-	- ^{c, d}
4	CPh ₃ ⁺	4 Å m.s.	40	43 ^{d, e}
5	Bobbitt's salt	-	40	20 ^c

^aConditions: Oxidant was added in one portion to a solution of **41** (0.2 mmol) in CH₂Cl₂ (0.1 M) at rt and was allowed to stir for 24 h. Reactions were quenched by elution through a short pad of silica, eluted with CH₂Cl₂. ^bYield determined by quantitative NMR spectroscopy by comparison to 1-bromo-3,5-bis(trifluoromethyl)benzene as internal standard. ^cStarting material present in crude ¹H NMR spectrum. ^dTLC showed intractable mixture. ^eCrude ¹H NMR spectrum showed consumption of starting material.

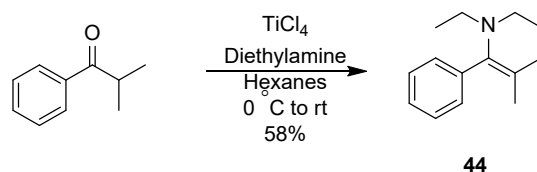
Various attempts were made to synthesize alkyl enol ethers, in hopes that the alkyl group would prove less labile, allowing the pentadienyl cation sufficient lifetime to undergo electrocyclization. Unfortunately, none of these attempts came to fruition. Scheme 2.32 details the attempted pathways towards various enol ether substrates. The first approach was a direct

alkylation following a report by Williams and coworkers.¹³⁴ DMPU was used in place of HMPA due to safety concerns. Unsurprisingly, the only product isolated was the C-alkylation product. A report by Gassman and coworkers described the transformation of cyclic and acyclic acetals to their corresponding enol ether using TMSOTf in the presence of *N,N*-DIPEA.¹³⁵ This reaction was attempted (Scheme 2.32b), but the acetal underwent complete cleavage to the corresponding ketone. Su and Willard described an LDA initiated conversion of allyl ethers to enol ethers.¹³⁶ Reaction of α -methyl trans cinnamaldehyde with isopropenyl magnesium chloride gave the corresponding alcohol, followed by alkylation to give the desired allyl ether (Scheme 2.32c). Reaction of this compound with LDA caused the substrate to decompose; no isomerization product was observed. Lastly, attempts to synthesize an enol acetate from the corresponding ketone were made (Scheme 2.32d). Surprisingly, no reaction occurred under a variety of conditions. As a model reaction, isobutyrophenone was subjected to the same reaction conditions, and did furnish an enol acetate **43** (Scheme 2.32e). This compound was subjected to DDQ oxidations under a variety of conditions, but ultimately only resulted in unreacted starting material, or decomposition of the substrate.



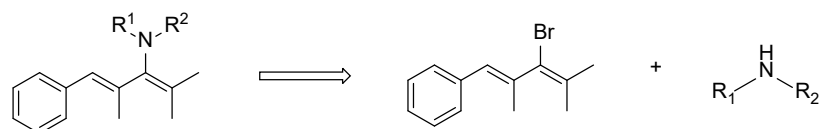
Scheme 2.32 Attempted synthesis of various enol ethers

From here the focus shifted to synthesizing 3-amino-1,3-dienes in an attempt to develop an oxidative imino-Nazarov cyclization reaction. The initial focus of their synthesis was by simple condensation with α,β -unsaturated carbonyl compounds. These efforts proved unsuccessful. This strategy was only successful when employed on an aromatic ketone to provide enamine **44** (Scheme 2.33). Attempts were made to cyclize this enamine product, but no reaction was observed, likely due to the high energetic barrier required for dearomatization that would be necessary for the reaction to proceed.



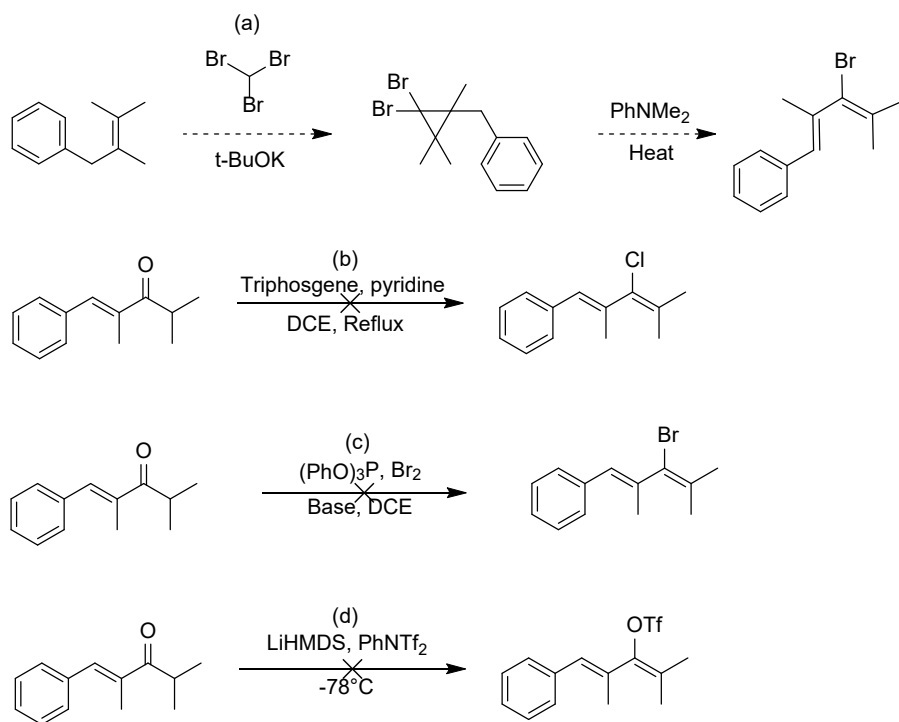
Scheme 2.33 Synthesis of enamine from aromatic ketone

Various alternative pathways towards the desired enamine compound were investigated, but ultimately none were successful. One such method was the cross coupling of alkenyl halides and amines, which was studied extensively by Barluenga (Scheme 2.34).^{137, 138, 139}



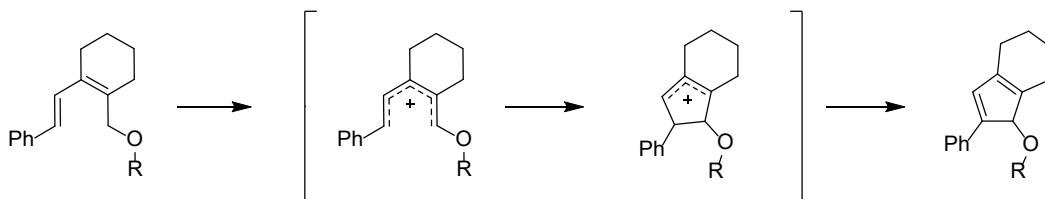
Scheme 2.34 Enamine synthesis via cross coupling of alkenyl halides

The required 3-halo-1,3-dienes required for this synthetic scheme proved more difficult to access than anticipated. Multiple methods were attempted to access these alkenyl halides/pseudo halides, including an electrocyclic ring opening pathway (Scheme 2.35a), but the alkene precursor could not be accessed.¹⁴⁰ Various methods from the corresponding ketone were explored, but none resulted in the desired product (Scheme 2.35b-d).^{141, 142}



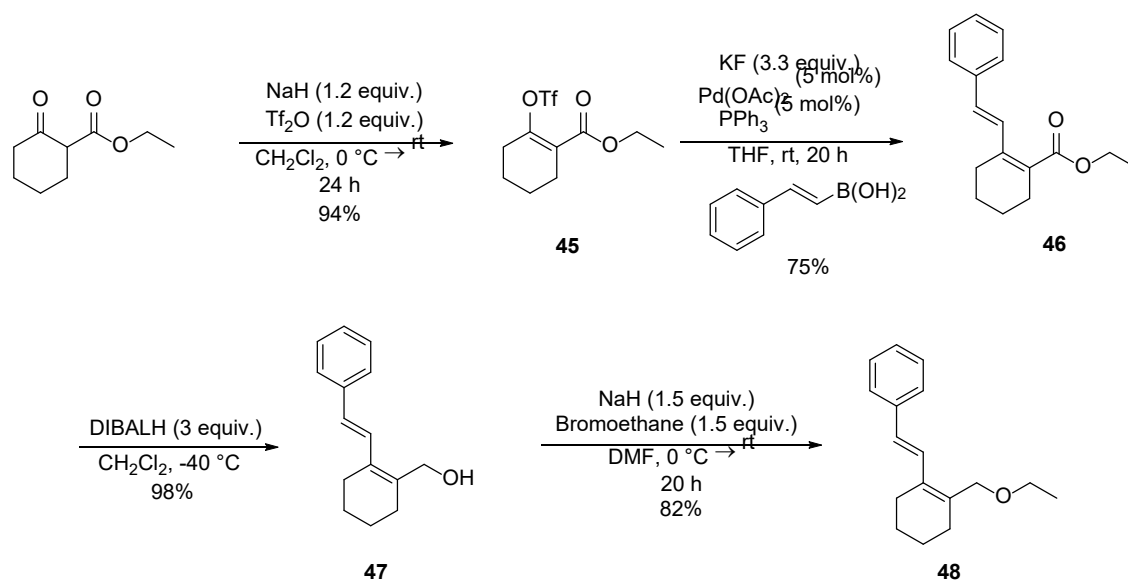
Scheme 2.35 Attempted synthesis of alkenyl halides/pseudo halides

From here, we shifted efforts to substrates that fall under the “iso-Nazarov” category, due to ease of preparation of the substrates. Scheme 2.36 shows the proposed mechanism of cyclization of these types of substrates.



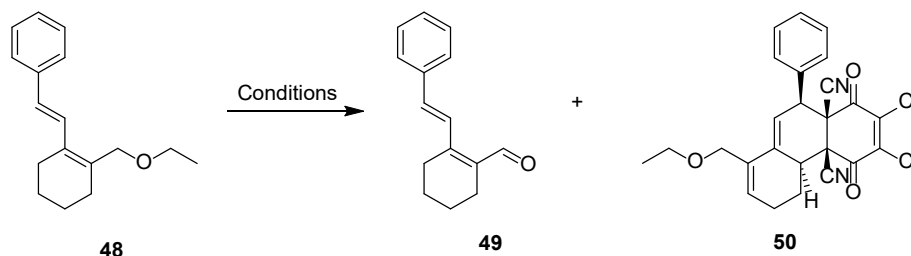
Scheme 2.36 Mechanism of iso-Nazarov cyclization with ethers

The general preparation of these compounds is shown in Scheme 2.37. Ethyl 2-oxocyclohexane-1-carboxylate was converted to vinyl triflate **45**, which was used in a Suzuki coupling to form compound **46**. Reduction of the ester gave compound **47** followed by alkylation of the alcohol leading to the desired starting material **48**.



Scheme 2.37 Preparation of iso-Nazarov substrates

With compound **48** in hand, oxidative conditions were explored (Table 2.2).

Table 2.2 Screening of oxidant conditions for compound **48**

Entry ^a	Oxidant (equiv.)	Solvent	Temperature	Additives (equiv.)	Product	Yield (%) ^b
1	DDQ (1.2)	CH ₂ Cl ₂	rt	-	50 ^c	10
2	DDQ (2.0)	CH ₂ Cl ₂	rt	-	50	15
3	DDQ (1.2)	DCE	80 °C	-	- ^c	-
4	DDQ (1.2)	CH ₂ Cl ₂	rt	LiClO ₄ (1.2)	50 ^c	9
5	CPh ₃ ⁺ (1.2)	CH ₂ Cl ₂	rt	-	- ^d	-
6	Bobbitt's salt (1.2)	CH ₂ Cl ₂	rt	-	49 ^c	28%
7	Bobbitt's salt (1.2)	CH ₂ Cl ₂	rt	4 Å m.s.	49 ^c	20%
8	DDQ (1.2)	CH ₂ Cl ₂	rt	In(OTf) ₃ (1.2)	-	- ^d
9	DDQ (1.2)	CH ₂ Cl ₂	rt	Cu(OTf) ₂ (1.2)	-	- ^d
10	DDQ (1.2)	CH ₂ Cl ₂	rt	FeCl ₃ (1.2)	-	- ^d

^aConditions: Oxidant was added in one portion to a solution of **48** (0.2 mmol) in solvent (0.1 M) and was allowed to stir for 24 h. Reactions were quenched by elution through a short pad of silica, eluted with CH₂Cl₂. ^bYield determined by quantitative NMR spectroscopy by comparison to 1-bromo-3,5-bis(trifluoromethyl)benzene as internal standard. ^cStarting material present in ¹H NMR spectrum. ^dStarting material consumed after 24 h, crude ¹H NMR spectrum showed intractable material.

Initial attempt to cyclize **48** under oxidative DDQ conditions showed the appearance of DDQ adduct **50** in 10% yield (entry 1). Key COSY and HMBC correlations were used to confirm the identity of DDQ adduct **50** (Figure 2.4).

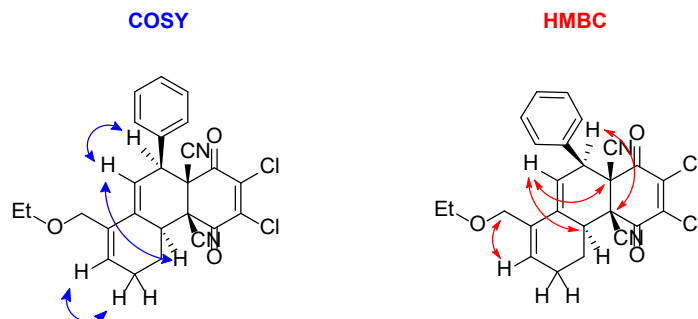
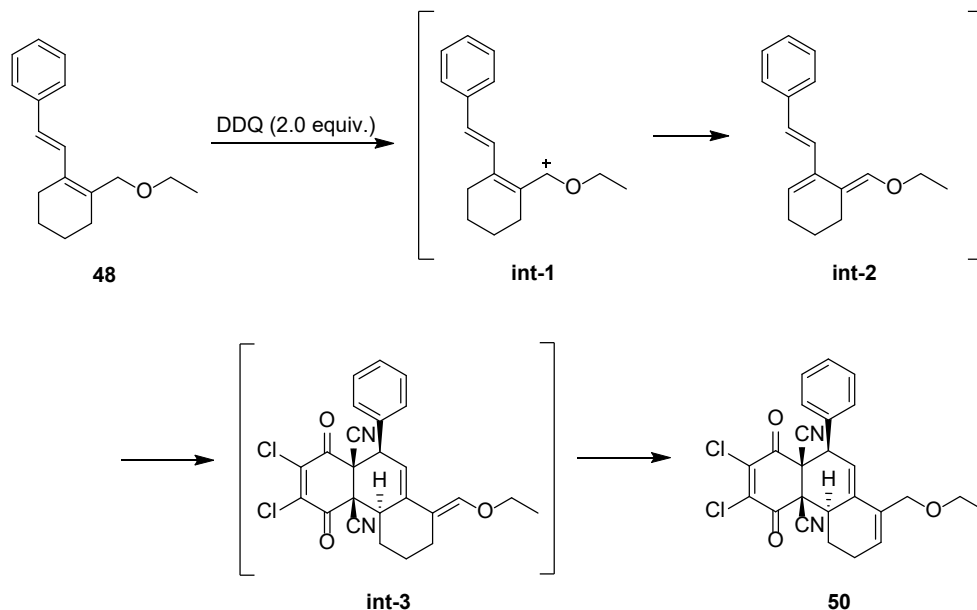


Figure 2.4 Key 2D NMR correlations for compound **50**

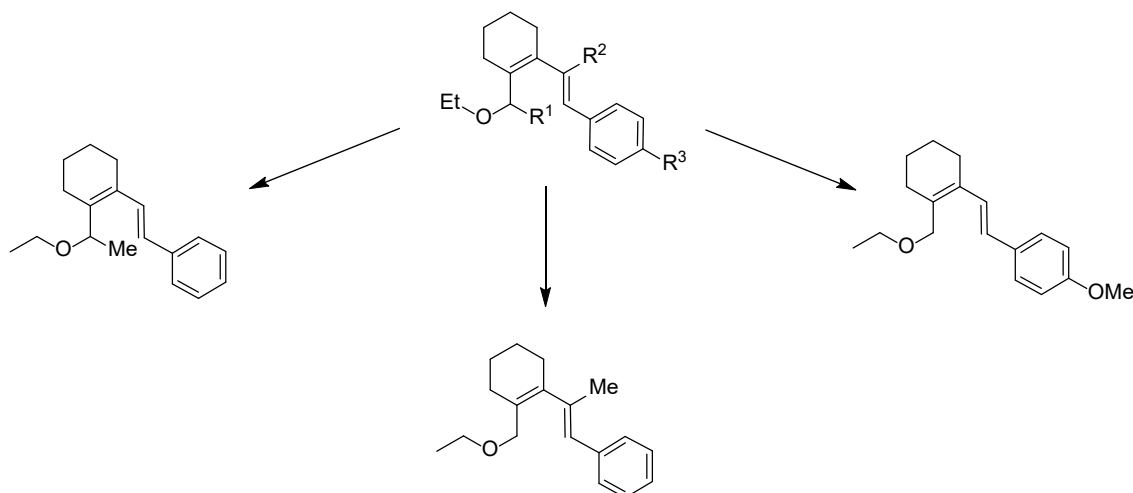
A plausible mechanistic proposal for the formation of compound **50** is presented in Scheme 2.38. Hydride abstraction from **48** generates **int 1**. Elimination by the partially reduced DDQH⁻ generates **int-2**, which then undergoes a Diels-Alder reaction with an additional equivalent of DDQ. Double bond rearrangement gives the product **50**. Other products were present in small amounts in the crude ¹H NMR spectrum. Unfortunately these products co-eluted with the unreacted starting material so could not be characterized. In an attempt to consume the starting material, 2.1 equivalents of DDQ was used (entry 2). The crude ¹H NMR spectrum showed consumption of starting material and a slight increase in the DDQ adduct product, at 15%. The TLC analysis of the reaction showed a large number of different products, indicating that the products formed may not be stable to oxidative conditions and are decomposing under excess DDQ conditions. Increasing the temperature to 80 °C inhibited the formation of compound **50**, possibly through a retro-Diels-Alder mechanism, although a significant amount of starting material remained (entry 3). The use LiClO₄ as an additive was also explored. LiClO₄ is often used in combination with DDQ, as it makes the carbocation more electrophilic, via counter ion exchange. When applied to substrate **48**, no appreciable difference was observed (entry 4). Other oxidants were also screened. When trityl cation was used, the only product observed in the crude ¹H NMR spectrum was triphenylmethane. This indicated that the oxidant is capable of oxidizing the substrate, but the products are not stable to the conditions, as no products or starting material were observed, indicating complete decomposition. When Bobbitt's salt was used as the oxidant, the

only compound observed apart from starting material was aldehyde **49** (entry 6). The addition of molecular sieves did not decrease the formation of this product appreciably (entry 7). Finally, the use of Lewis acids as additives was investigated. As discussed in section 2.1.3, using Lewis acids in conjunction with DDQ can provide favourable results by activating DDQ. When applied to substrate **48**, In(OTf)₃, Cu(OTf)₂ and FeCl₃ all resulted in complete decomposition, and no products or starting material were observed (entries 8-10).



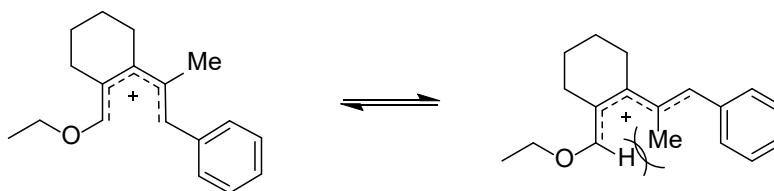
Scheme 2.38 Proposed mechanism for the formation of product **50**

The inability of substrate **48** to undergo the desired cyclization prompted us to investigate the design of the substrate (Scheme 2.39). Looking at the original substrate, there are three areas that can undergo modification that may provide more favourable electronic properties for hydride abstraction.



Scheme 2.39 Modification of iso-Nazarov substrates

Modifying R^1 by adding an electron donating group onto the carbon that will undergo hydride abstraction may provide favourable conditions by making the hydride more readily removed. While this makes that position more sterically encumbered, the hope was that the advantageous electronic properties would dominate. Adding a group to the R^2 position may provide favourable steric effects; increasing the steric bulk of the group at this position increases the population of the reactive U-conformer of the intermediate pentadienyl cation, thereby making the desired cyclization more likely (Scheme 2.40).

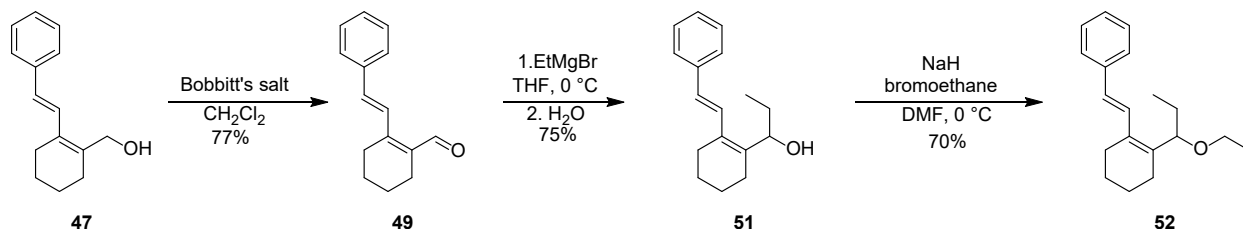


Scheme 2.40 Steric properties favouring the U-conformer

Adding an electron donating group in the R^3 position can also significantly increase the likelihood of hydride abstraction, by adding electron density into the π -system to stabilize the resulting cationic intermediate. Xu and coworkers explored the oxidative coupling of benzyl ethers with silyl nucleophiles. They demonstrated that in their system, DDQ was not strong enough to oxidize the benzylic substrate; an electron donating group was required on the aromatic ring to

facilitate the reaction.¹⁴³ With this in mind adding a *para*-methoxy group to the aromatic ring seemed to be a plausible method to promote hydride abstraction.

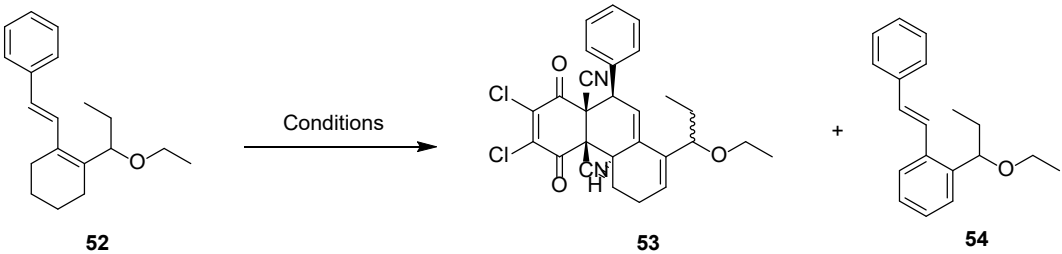
The synthesis of R¹ modified substrates began with the oxidation of alcohol **47**, followed by Grignard attack on **49** to give alcohol **51**. Lastly, alkylation gave compound **52** (Scheme 2.41).



Scheme 2.41 Synthesis of (*E*)-(2-(2-(1-ethoxypropyl)cyclohex-1-en-1-yl)vinyl)benzene

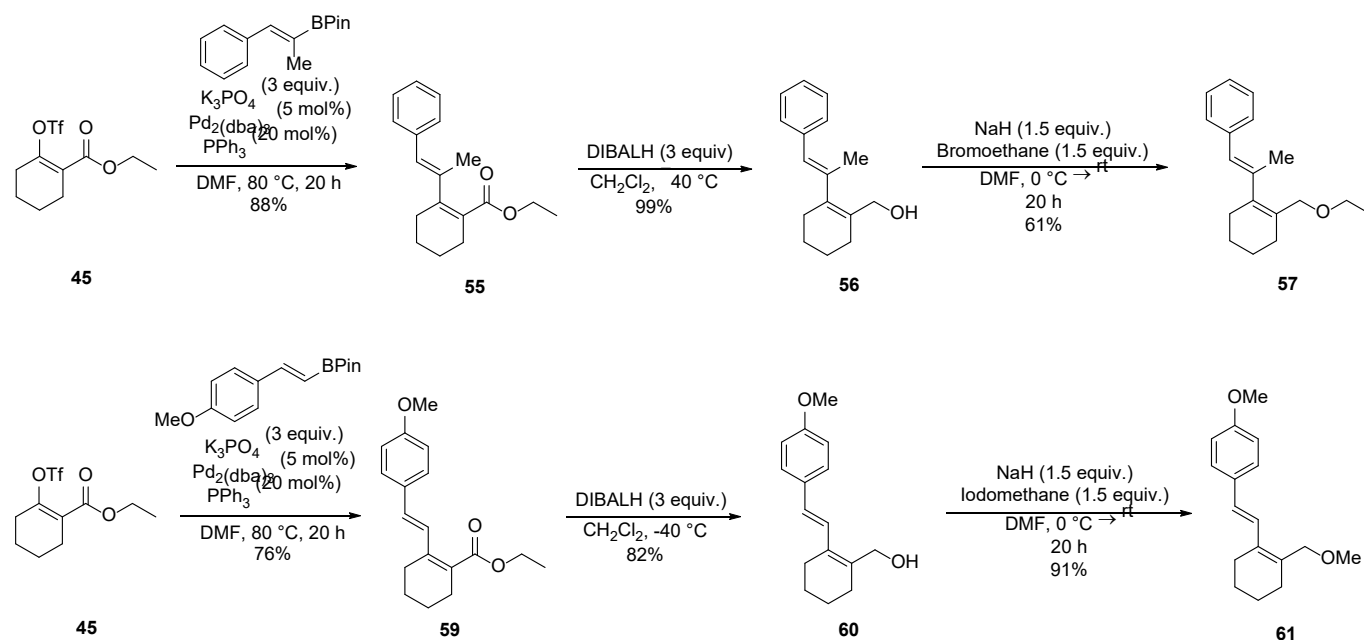
Compound **52** was subjected to oxidative conditions (Table 2.3). Two products were observed when compound **52** was subjected to 1.2 equivalents of DDQ. Compound **53** in 17% yield, which is formed in a similar manner to compound **50** and compound **54** in 28% yield, which is formed by two subsequent dehydrogenation steps, to fully aromatize the ring (entry 1). As both these compounds require 2 equivalents of DDQ to form, significant starting material remained. When the equivalents of DDQ was increased to 2.1, the starting material was fully consumed, and products **53** and **54** were isolated in 47% and 23% yield, respectively. Compound **53** was isolated as a mixture of inseparable diastereomers in a 3.8:1 ratio. When Bobbitt's salt was employed, mostly starting material was recovered, with a small amount of another product (entry 3). This product co-eluted with the starting material, so a large excess of oxidant was used in an attempt to consume the starting material (entry 4). Even when using 5 equivalents of the oxidant, a significant amount of starting material remained, so the product could not be characterized.

Table 2.3 Screening of oxidant conditions for compound **52**

 <p>Reaction scheme showing the oxidation of compound 52 to products 53 and 54 under 'Conditions'.</p>			
Entry ^a	Oxidant (equiv.)	Products	Yield (%)
1	DDQ (1.2)	53/54 ^b	17/28 ^c
2	DDQ (2.0)	53/54	47/23 ^d
3	Bobbitt's salt (1.2)	-	-
4	Bobbitt's salt (5.0)	-	-

^aConditions: Oxidant was added in one portion to a solution of **52** (0.2 mmol) in CH₂Cl₂ (0.1 M) at rt and was allowed to stir for 20 h. Reactions were quenched by elution through a short pad of silica, eluted with CH₂Cl₂. ^bStarting material present in crude ¹H NMR spectrum. ^cYield determined by quantitative NMR spectroscopy by comparison to 1-bromo-3,5-bis(trifluoromethyl)benzene as internal standard. ^dIsolated yield.

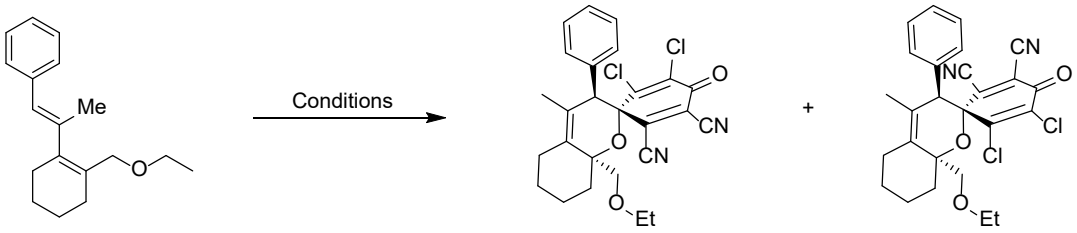
The syntheses of R² and R³ modified substrates were accomplished in a similar manner to that of compound **48**. Vinyl triflate **45** was reacted in a Suzuki reaction with 4,4,5,5-tetramethyl-2-[(1*Z*)-1-methyl-2-phenylethenyl]-1,3,2-dioxaborolane and 2-[(1*E*)-2-(4-methoxyphenyl)ethenyl]-4,4,5,5-tetramethyl-1,3,2-dioxaborolane to form compounds **55** and **59**, respectively. Reduction of the ester followed by alkylation gave compound **57** and **61** (Scheme 2.42).



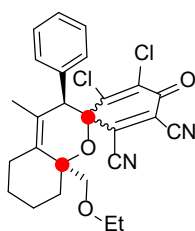
Scheme 2.42 Syntheses of compounds **57** and **61**

The effect of adding a methyl group in the R^2 position was examined (Table 2.4). Differing from the other substrates, **57** underwent an interesting hetero Diels-Alder reaction with the carbonyl of DDQ as the dienophile, resulting in spirocyclic compounds **58a** and **58b** (entry 1). The ^{13}C NMR spectrum was integral to the structural assignment of this compound. The appearance of two signals at 82.5 and 81.8 ppm (for the major diastereomer) are consistent with the proposed structure arising from a hetero Diels-Alder reaction. These two aliphatic carbons (indicated in red in Figure 2.5) appear farther downfield due to the proximity to one oxygen atom from DDQ. Additionally, there is only one signal observed in the carbonyl region, also consistent with the proposed structure.

Table 2.4 Screening of oxidant conditions for compound **57**

					
57			58a		58b
Entry ^a	Oxidant	Solvent	Temperature	Additives	Result
1	DDQ	CH ₂ Cl ₂	rt	-	58a+58b 73% d.r. 3.6:1
2	DDQ	CH ₂ Cl ₂	rt	In(OTf) ₃ (1.5 equiv.)	- ^b
3	DDQ	Toluene	110 °C	-	- ^c

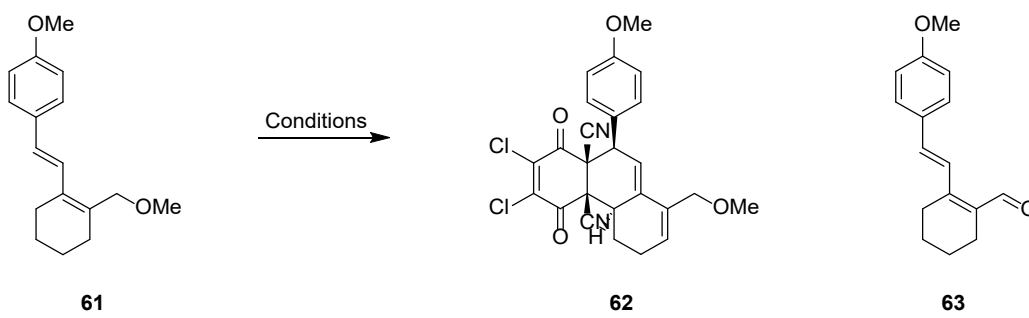
^aConditions: DDQ was added in one portion to a solution of **57** (0.2 mmol) in CH₂Cl₂ (0.1 M) at rt and was allowed to stir for 24 h. Reactions were quenched by elution through a short pad of silica, eluted with CH₂Cl₂. ^bStarting material consumed after 24 h, crude ¹H NMR spectrum showed intractable material. ^cOnly starting material observed by ¹H NMR analysis.

**Figure 2.5** Key carbon signals in compound **58**

The increased reactivity of this substrate to a Diels-Alder reaction over other substrates is likely due to the added electron donating methyl group on the diene. The effect of incorporating a Lewis acid was also examined with this substrate; In(OTf)₃ completely eroded the reactivity resulting in decomposition of the substrate. No starting material or product (desired product, or

Diels-Alder adduct product) was observed by ^1H NMR analysis. As mentioned in section 2.1.3.3, several groups have also observed competing Diels-Alder adduct formation with DDQ. This competitive pathway can be eliminated in some cases by increasing the temperature to force a retro Diels-Alder reaction to give back the substrate, which can hopefully then react via the desired pathway. When subjecting compound **57** to higher temperatures, no Diels-Alder product was observed. This indicates that the high temperature was able to invoke the retro-Diels alder reaction. No other products were observed at this temperature, meaning that even without the competitive Diels-Alder pathway, this substrate is not prone to hydride abstraction.

Table 2.5 Screening of oxidant conditions for compound **61**

				
Entry ^a	Oxidant	Additives	Product	Yield (%)
1	DDQ	-	62 ^b	19 ^c
2	Bobbitt's salt	-	63 ^b	10
3	Bobbitt's salt	4 Å m.s.	63 ^b	7
4	CPh ₃ ⁺	-	-	- ^d

^aConditions: Oxidant was added in one portion to a solution of **61** (0.2 mmol) in CH₂Cl₂ (0.1 M) at rt and was allowed to stir for 24 h. Reactions were quenched by elution through a short pad of silica, eluted with CH₂Cl₂. ^bStarting material present in crude ^1H NMR spectrum. ^cIsolated yield. ^dStarting material consumed after 24 h, crude ^1H NMR spectrum showed intractable material.

Finally, the effect of adding a *para*-methoxy group to the phenyl ring was examined (Table 2.5). When DDQ was employed, a DDQ adduct **62** was observed (entry 1). Changing the oxidant to Bobbitt's salt only afforded aldehyde **59** (entry 2). Adding molecular sieves to the reaction (entry

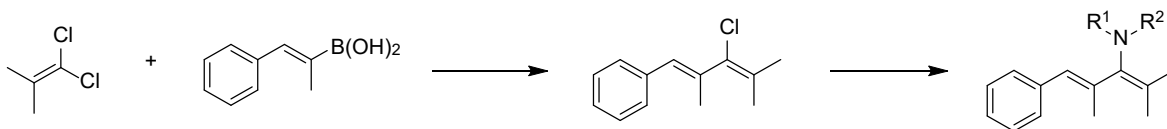
3) did not decrease the yield of aldehyde **59** appreciably. Trityl cation only resulted in decomposition, no products or starting material was observed on the crude ^1H NMR spectrum (entry 4).

2.4 Conclusion

In summary, this project has investigated employing oxidative conditions to a variety of substrates, towards the development of oxidative Nazarov reactions. While some of the substrates did undergo C–H bond oxidation to some extent, none of the substrates displayed the desired reactivity towards cyclization. Nonetheless, the reactivity of these substrates was probed, often resulting in interesting DDQ adduct structures.

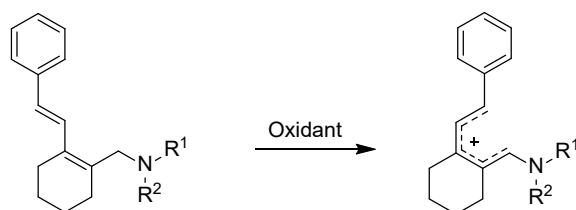
2.5 Future Directions

Many pathways were explored towards the synthesis of 3-amino-1,3-dienes. One method was the cross coupling of 3-halo-1,3-dienes, although the synthesis of these compounds also proved difficult. A method to synthesize 3-halo-1,3-dienes that was not explored was via palladium catalyzed cross coupling (Scheme 2.43). A similar reaction was reported by Barluenga and Valdés.¹⁴⁴



Scheme 2.43 Synthesis of 3-halo-1,3-dienes via palladium catalysis

Another subset of reactions that was not explored was the imino-iso Nazarov. The ease of preparation of the substrates and the advantages of incorporating nitrogen into the structure as was discussed in section 2.2 makes this an interesting avenue to explore (Scheme 2.44).



Scheme 2.44 Imino-iso-Nazarov substrates

Another avenue that could be explored is the use of photoredox catalysis to enable a formal hydride abstraction on the desired substrates. Several recent reports describe the generation of benzyl radicals from benzylic C-H bonds, oxidation of the radical to a benzylic carbocation, followed by reaction with a nucleophile.^{145, 146} One such report by the Yoon group describes the use of $[\text{Ir}(\text{dF}(\text{CF}_3)\text{ppy})_2(5,5'\text{-dCF}_3\text{bpy})]\text{PF}_6$ as the photocatalyst and a Cu^{II} species as the oxidant.¹⁴⁷ Reaction of the resulting carbocation with oxygen nucleophiles resulted in benzylic ethers in moderate to high yields. Applying these methods to the iso-Nazarov substrates may promote a formal hydride abstraction with a lower energetic barrier, resulting in a productive cyclization reaction.

2.6 Experimental

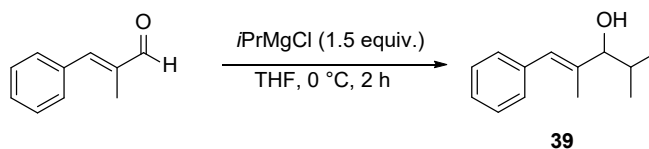
2.6.1 General information

All reactions were carried out under a nitrogen atmosphere in flame-dried glassware. Transfer of anhydrous solvents and reagents was accomplished with oven-dried syringes. Solvents (CH_2Cl_2 , THF and DMF) were dried using a LC Technology Solutions Inc. solvent purification system. Hexanes and DCE were distilled and dried over molecular sieves prior to use. Reagents were purchased from commercial sources and used without further purification. Column chromatography was performed using 230–400 mesh silica gel, and TLC analyses were completed on silica gel 60 F254 aluminium plates (Millipore-Sigma). ^1H NMR spectra were recorded at 500 MHz and coupling constants (J) are reported in Hertz (Hz). ^{13}C NMR spectra were recorded at 125 MHz. Chemical shifts are referenced to CDCl_3 (s, 7.26 ppm, ^1H ; t, 77.06 ppm, ^{13}C), and CD_2Cl_2 (t, 5.32 ppm, ^1H ; p, 53.8 ppm, ^{13}C) as internal standards and are reported on the δ scale (ppm). Observed multiplicities on ^1H NMR are described using the standard notation: broad (br), apparent

(app), multiplet (m), singlet (s), doublet (d), triplet (t), quartet (q), apparent triplet (app t). IR data were recorded using the Thermo Scientific Nicolet Summit LITE instrument. HRMS data were recorded using the Thermo Scientific Orbitrap Exploris 240 (DART/LIFDI), Agilent Technologies 6220 oaTOF (ESI), or the Kratos MS50G (EI).

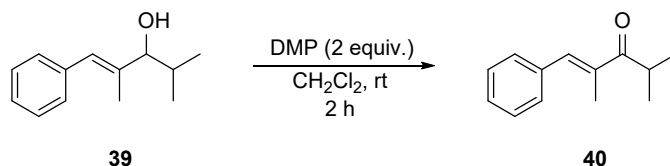
2.6.2 Characterization of compounds

(*E*)-2,4-Dimethyl-1-phenylpent-1-en-3-ol (39)



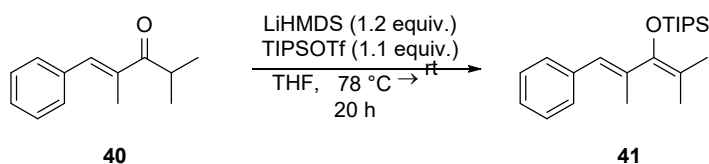
A solution of (*E*)-2-methylcinnamaldehyde (0.73 mL, 5.0 mmol) in THF (0.20 M, 25 mL) was cooled to 0 °C. A solution of *i*PrMgCl (2.0 M in THF) (3.8 mL, 7.5 mmol) was added dropwise. The reaction mixture was stirred at 0 °C for 2 h. The reaction mixture was quenched by the addition of a saturated aqueous solution of NH₄Cl. The aqueous phase was extracted 3x with ethyl acetate. The organic layers were combined and washed with water and brine, dried over magnesium sulfate, filtered and concentrated in vacuo. The crude mixture was purified by flash column chromatography (hexanes/EtOAc 9:1 → 3:2). The product was obtained as a yellow oil (672 mg, 3.53 mmol) in 72% yield. *R*_f 0.32 (hexanes/EtOAc 3:2); IR (neat) 3391 2958, 2870, 1728, 1599, 1491, 1448, 1378, 1294, 1248, 1172, 1117, 1008 cm⁻¹; ¹H NMR (500 MHz, CDCl₃) δ 7.37–7.31 (m, 2 H), 7.31–7.27 (m, 2 H), 7.24–7.29 (m, 1 H), 6.47 (s, 1 H), 3.80 (d, *J* = 8.0 Hz, 1 H), 1.94–1.85 (m, 4 H), 1.04 (d, *J* = 6.5 Hz, 3 H), 0.90 (d, *J* = 6.5 Hz, 3 H), (OH proton not detected); ¹³C NMR (125 MHz, CDCl₃) δ 139.7, 137.7, 129.0, 128.2, 126.9, 126.5, 84.2, 31.5, 19.6, 18.4, 13.3; HRMS (DART, [M-H₂O+H]⁺) for C₁₃H₁₇ calcd. 173.1325, found: *m/z* 173.1323.

(E)-2,4-Dimethyl-1-phenylpent-1-en-3-one (40)



(*E*)-2,4-Dimethyl-1-phenylpent-1-en-3-ol (**39**) (299 mg, 1.59 mmol) was added to a flask followed by DCM (0.10 M, 15 mL) and DMP (1.55 g, 3.65 mmol). The reaction was stirred at room temperature for 2 h. The reaction mixture was diluted with 25 mL ether and 10 mL 1.5 M NaOH and stirred for 10 minutes. The layers were separated, and the organic layer was extracted with 1.5 M NaOH, water and brine. The organic layers were dried over magnesium sulfate, filtered and concentrated in vacuo. The crude product was purified by flash column chromatography (hexanes/EtOAc 50:1 → 4:1). The crude product was obtained as a clear oil (221 mg, 1.17 mmol) in 75% yield. *R*_f 0.71 (hexanes/EtOAc 9:1); IR (neat) 2969, 2931, 2873, 1661, 1623, 1446, 1383, 1299, 1213 cm⁻¹; ¹H NMR (500 MHz, CDCl₃) δ 7.51 (s, 1 H), 7.44–7.39 (m, 4 H), 7.37–7.33 (m, 1 H), 3.48 (sept, *J* = 6.5 Hz, 1 H), 2.07 (d, *J* = 1.5 Hz, 3 H), 1.18 (d, *J* = 6.5 Hz, 6 H); ¹³C NMR (125 MHz, CDCl₃) δ 206.8, 137.9, 136.5, 136.2, 129.7, 128.5, 128.4, 34.2, 19.7, 13.6; HRMS (DART, [M+H]⁺) for C₁₃H₁₇O calcd. 189.1274, found: *m/z* 189.1272.

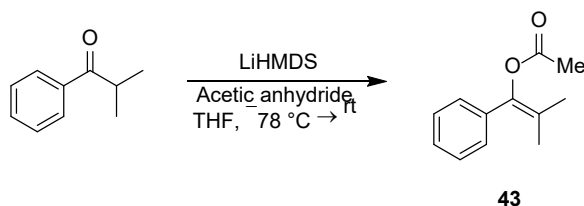
2,4-Dimethyl-1-phenyl-3-triisopropylsilyloxypenta-1,3-diene (41)



A solution of (*E*)-2,4-dimethyl-1-phenylpent-1-en-3-one (**40**) (146 mg, 0.775 mmol) in THF (0.15 M, 5.0 mL) was cooled to -78 °C. A 1 M solution of LiHMDS (0.93 mL, 0.93 mmol) was added at -78 °C and stirred for 30 minutes. TIPSOTf (0.23 mL, 0.85 mmol) was added dropwise at -78 °C, and solution was allowed to warm to room temperature while stirring for 20 h. The reaction mixture was quenched with a saturated aqueous solution of NH₄Cl. The aqueous layer was extracted 3x with ethyl acetate. The combined organic layers were washed with water, brine, dried over sodium sulfate, filtered and concentrated in vacuo. The crude product was purified by flash

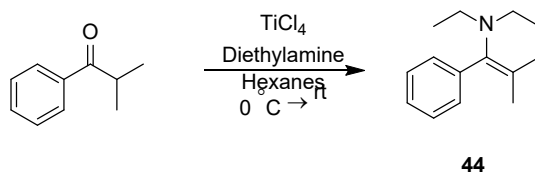
column chromatography (hexanes/EtOAc 20:1). The product was obtained as a clear liquid (226 mg, 0.655 mmol) in 85% yield. R_f 0.80 (hexanes/EtOAc 9:1); IR (neat) 2942, 2865, 1660, 1461, 1381, 1270, 1196, 1151 cm^{-1} ; ^1H NMR (500 MHz, CDCl_3) δ 7.38–7.33 (m, 2 H), 7.31–7.28 (m, 2 H), 7.25–7.20 (m, 1 H), 6.37 (s, 1 H), 1.99 (d, $J = 1.5$ Hz, 3 H), 1.74 (s, 3 H), 1.70 (s, 3 H), 1.21–1.24 (m, 3 H), 1.13–1.07 (m, 18 H); ^{13}C NMR (125 MHz, CDCl_3) δ 147.6, 137.8, 135.5, 130.1, 128.9, 128.2, 126.5, 110.3, 20.1, 18.2, 18.0, 17.4, 13.3; HRMS (ESI, $[\text{M}+\text{H}]^+$) for $\text{C}_{22}\text{H}_{37}\text{O}_5$ calcd. 345.2608, found: m/z 345.2608.

1-Acetoxy-2-methyl-1-phenylpropene (43)



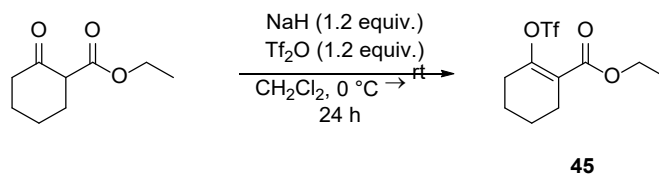
Isobutyrophenone (296 mg, 1.99 mmol) was added to a flask with THF (0.2 M, 10 mL) and cooled to -78°C . LiHMDS (1 M in THF) (2.4 mL, 2.0 mmol) was added and stirred for 30 minutes. Acetic anhydride (0.57 mL, 6.0 mmol) was added, and the reaction was allowed to warm to room temperature while stirring for 20 h. The reaction mixture was quenched with a saturated aqueous solution of NH_4Cl . The aqueous layer was extracted 3x with ethyl acetate. The combined organic layers were washed with water, brine, dried over sodium sulfate, filtered and concentrated in vacuo. The crude product was purified by flash column chromatography (hexanes/EtOAc 50:1 \rightarrow 20:1). The product was obtained as a clear liquid (99 mg, 0.52 mmol) in 26% yield. R_f 0.31 (hexanes/EtOAc 9:1); IR (neat) 2991, 2918, 1748, 1491, 1442, 1369, 1206 cm^{-1} ; ^1H NMR (500 MHz, CDCl_3) δ 7.38–7.30 (m, 4 H), 7.29–7.26 (m, 1 H), 2.15 (s, 3 H), 1.80 (s, 3 H), 1.75 (s, 3 H); ^{13}C NMR (125 MHz, CDCl_3) δ 169.3, 141.2, 135.9, 128.9, 128.0, 127.8, 121.9, 20.8, 19.8, 18.4; HRMS (DART, $[\text{M}+\text{NH}_4]^+$) for $\text{C}_{12}\text{H}_{18}\text{NO}_2$ calcd. 208.1332, found: m/z 208.1331.

N,N-diethyl-2-methyl-1-phenylprop-1-en-1-amine (44)



Isobutyrophenone (74 mg, 0.50 mmol) and diethylamine (0.30 mL, 3.0 mmol) were added to a flask with hexanes (0.20 M, 2.5 mL) and cooled to 0 °C. TiCl₄ (0.03 mL, 0.3 mmol) was added dropwise at 0 °C. The reaction was allowed to come to room temperature while stirring for 20 h. Diethyl ether was added to the reaction mixture and filtered, then concentrated in vacuo. The crude product was dissolved in toluene, extracted into aqueous HCl (x3). The acidic fractions were basified with 2M NaOH until pH 10–12. The product was extracted into ethyl acetate (x3), then the organic fractions were washed with brine, dried over MgSO₄, filtered and concentrated in vacuo. The product was obtained as a brown oil (59 mg, 0.29 mmol) in 58% yield. *R*_f 0.41(hexanes/EtOAc 9:1); IR (neat) 2969, 2922, 2821, 1444, 1374, 1303, 1289, 1215 cm⁻¹; ¹H NMR (500 MHz, CDCl₃) δ 7.33–7.28 (m, 2 H), 7.27–7.20 (m, 1 H), 7.10 (d, *J* = 7.5 Hz, 2 H), 2.62 (q, *J* = 7.5 Hz, 4 H), 1.87 (s, 3 H), 1.52 (s, 3 H), 1.03 (t, *J* = 7.0 Hz, 6 H); ¹³C NMR (125 MHz, CDCl₃) δ 141.0, 138.2, 130.1, 127.6, 126.7, 126.3, 47.1, 21.1, 20.0, 14.2; HRMS (DART, [M+H]⁺) for C₁₄H₂₂N calcd. 204.1747, found: *m/z* 204.1746.

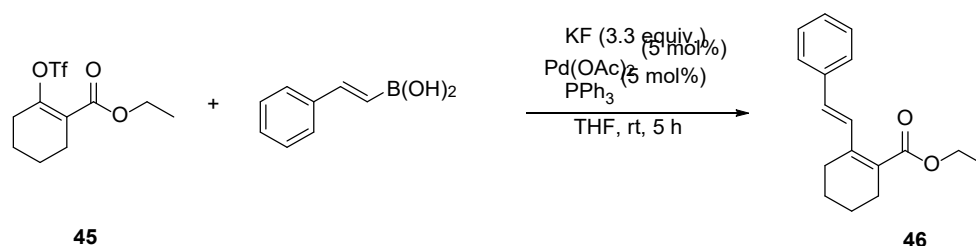
Ethyl 2-(((trifluoromethyl)sulfonyl)oxy)cyclohex-1-ene-1-carboxylate (45)



NaH (959 mg, 24.0 mmol) was added to a flask with DCM (0.2 M, 100 mL) and cooled to 0 °C. Ethyl 2-oxocyclohexane-1-carboxylate (3.2 mL, 20 mmol) dissolved in DCM (1 M, 20 mL) was added dropwise and stirred for 15 minutes. Tf₂O (4.0 mL, 24 mmol) was added dropwise, and reaction was allowed to come to room temperature while stirring over 24 hours. The reaction was quenched with a saturated aqueous solution of Na₂CO₃. The aqueous phase was extracted with

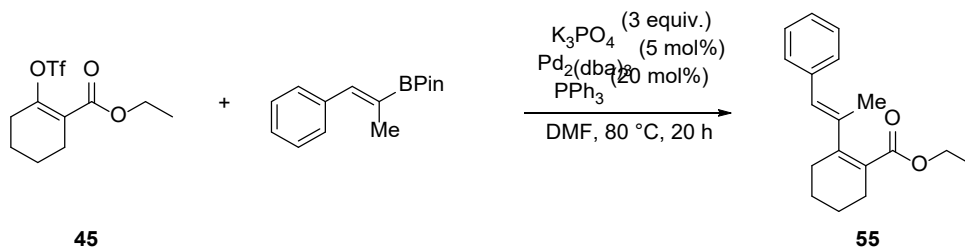
DCM (3x). The combined organic phases were washed with water and brine, dried over Na₂SO₄, filtered, and concentrated in vacuo. The crude mixture was purified by flash column chromatography (hexanes/EtOAc 20:1). The product was obtained as a colourless oil (5.68 g, 18.8 mmol) in 94% yield. *R*_f 0.59 (hexanes/EtOAc 9:1); IR (neat) 2947, 1721, 1420, 1283, 1242, 1202 cm⁻¹; ¹H NMR (500 MHz, CDCl₃) δ 4.28 (q, *J* = 7.5 Hz, 2 H), 2.51–2.45 (m, 2 H), 2.43–2.37 (m, 2 H), 1.82–1.75 (m, 2 H), 1.71–1.64 (m, 2 H), 1.33 (t, *J* = 7.0 Hz, 3 H); ¹³C NMR (125 MHz, CDCl₃) δ 164.8, 151.3, 123.3, 118.4 (q, *J* = 321 Hz), 61.6, 28.5, 26.2, 22.3, 21.1, 14.0; HRMS (ESI, [M+H]⁺) for C₁₀H₁₄F₃O₅S calcd. 303.0509, found: *m/z* 303.0507.

Ethyl (*E*)-2-styrylcyclohex-1-ene-1-carboxylate (**46**)



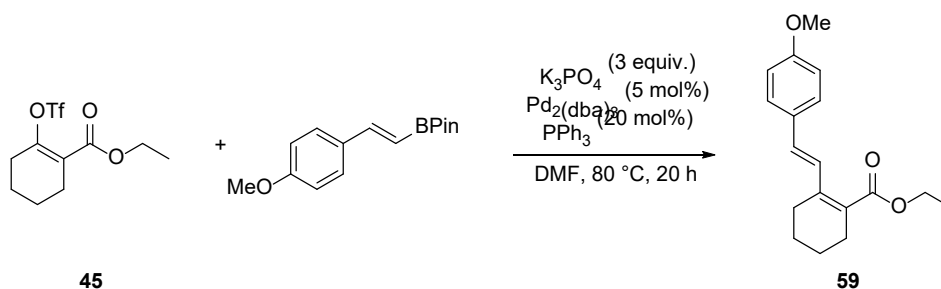
KF (1.54g, 26.4 mmol) was flame dried in a flask for 10 minutes. After cooling, ethyl 2-(((trifluoromethyl)sulfonyl)oxy)cyclohex-1-ene-1-carboxylate (**45**) (2.41 g, 7.97 mmol), (*E*)-styrylboronic acid (1.32 g, 8.92 mmol), and Pd(OAc)₂ (93 mg, 0.40 mmol) were added to flask. THF (0.2 M, 40 mL) was added and stirred for 5 minutes. PPh₃ (106 mg, 0.404 mmol) in THF (0.25 M, 1.6 mL) was added, and reaction was stirred at room temperature for 5 h. The reaction was quenched by filtration through celite eluted with DCM, followed by concentration in vacuo. The crude product was purified by flash column chromatography (hexanes/EtOAc 50:1 → 20:1). The product was obtained as a yellow oil (1.54 g, 6.07 mmol) in 75% yield. *R*_f 0.46 (hexanes/EtOAc 9:1); IR (neat) 2931, 1698, 1587, 1446, 1369, 1198 cm⁻¹; ¹H NMR (500 MHz, CDCl₃) δ 7.76 (d, *J* = 16.5 Hz, 1 H), 7.46–7.43 (m, 2 H), 7.34–7.29 (m, 2 H), 7.25–7.21 (m, 1 H), 6.74 (d, *J* = 16.5 Hz, 1 H), 4.28 (q, *J* = 7.0 Hz, 2 H), 2.51–2.42 (m, 4 H), 1.76–1.64 (m, 4 H), 1.35 (t, *J* = 7.0 Hz, 3 H); ¹³C NMR (125 MHz, CDCl₃) δ 169.3, 141.1 137.6, 130.0, 129.2, 128.7, 128.0, 127.8, 126.8, 60.5, 27.7, 26.3, 22.2, 22.1, 14.5; HRMS (ESI [M+H]⁺) for C₁₇H₂₁O₂ calcd. 257.1536, found: *m/z* 257.1537.

Ethyl (*E*)-2-(1-phenylprop-1-en-2-yl)cyclohex-1-ene-1-carboxylate (**55**)



4,4,5,5-Tetramethyl-2-[(1*Z*)-1-methyl-2-phenylethenyl]-1,3,2-dioxaborolane was prepared via a known literature procedure.¹⁴⁸ A mixture of Pd₂(dba)₃ (350 mg, 0.38 mmol), PPh₃ (350 mg, 1.3 mmol) and K₃PO₄ (4.41 g, 20.8 mmol) was added to a flask followed by DMF (0.1 M, 70 mL), and stirred for 10 minutes. 4,4,5,5-Tetramethyl-2-[(1*Z*)-1-methyl-2-phenylethenyl]-1,3,2-dioxaborolane (1.67 g, 6.90 mmol) and ethyl 2-(((trifluoromethyl)sulfonyl)oxy)cyclohex-1-ene-1-carboxylate (**45**) (2.96 g, 9.79 mmol) were added to a flask, and the reaction mixture was heated to 80 °C for 20 h. The reaction was quenched by filtration through celite eluted with DCM, then concentration in vacuo. The crude product was purified by flash column chromatography (hexanes/EtOAc 50:1 → 20:1). The product was obtained as a yellow oil (1.63 g, 6.03 mmol) in 88% yield. *R*_f 0.63 (hexanes/EtOAc 9:1); IR (neat) 2931, 2860, 1706, 1443, 1368, 1227 cm⁻¹; ¹H NMR (500 MHz, CD₂Cl₂) δ 7.35–7.30 (m, 2 H), 7.27–7.24 (m, 2 H), 7.22–7.17 (m, 1 H), 6.13 (s, 1 H), 4.06 (q, *J* = 7.0 Hz, 2 H), 2.36–2.29 (m, 2 H), 2.28–2.22 (m, 2 H), 2.00 (d, *J* = 1.0 Hz, 3 H), 1.71–1.64 (m, 4 H), 1.17 (t, *J* = 7.0 Hz, 3 H); ¹³C NMR (125 MHz, CD₂Cl₂) δ 169.8, 150.2, 141.6, 138.4, 129.1, 128.4, 126.5, 126.0, 125.1, 60.3, 30.4, 26.5, 22.7, 22.5, 17.5, 14.4; HRMS (ESI, [M+H]⁺) for C₁₈H₂₃O₂ calcd. 271.1693, found: *m/z* 271.1694.

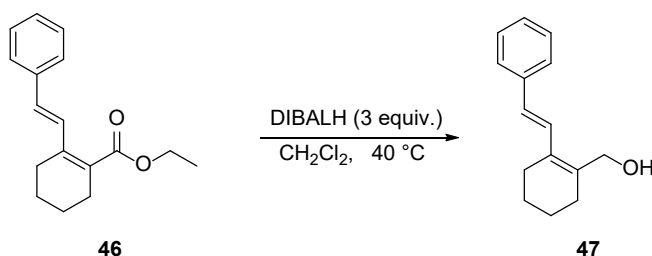
Ethyl (*E*)-2-(4-methoxystyryl)cyclohex-1-ene-1-carboxylate (**59**)



2-[(1*E*)-2-(4-Methoxyphenyl)ethenyl]-4,4,5,5-tetramethyl-1,3,2-dioxaborolane was prepared via a known literature procedure.¹⁴⁹ A mixture of Pd₂(dba)₃ (182 mg, 0.199 mmol), PPh₃ (192 mg, 0.732 mmol) and K₃PO₄ (2.40 g, 11.1 mmol) was added to a flask followed by DMF (0.1 M, 50 mL), and stirred for 10 minutes. 2-[(1*E*)-2-(4-Methoxyphenyl)ethenyl]-4,4,5,5-tetramethyl-1,3,2-dioxaborolane (905 mg, 3.70 mmol) and ethyl 2-(((trifluoromethyl)sulfonyl)oxy)cyclohex-1-ene-1-carboxylate (**45**) (1.58 g, 5.22 mmol) were added to flask, and the reaction mixture was heated to 80 °C for 20 h. The reaction was quenched by filtration through celite eluted with DCM, then concentration in vacuo. The crude product was purified by flash column chromatography (hexanes/EtOAc 20:1 → 9:1). The product was obtained as a yellow oil (811 mg, 2.83 mmol) in 76% yield. *R*_f 0.53 (hexanes/EtOAc 9:1); IR (neat) 2931, 2361, 1692, 1602, 1508, 1447, 1218 cm⁻¹; ¹H NMR (500 MHz, CDCl₃) δ 7.66 (d, *J* = 16.0 Hz, 1 H), 7.39 (d, *J* = 9.0 Hz, 2 H), 6.86 (d, *J* = 9.0 Hz, 2 H), 6.70 (d, *J* = 16.5 Hz, 1 H), 4.27 (q, *J* = 7.0 Hz, 2 H), 3.81, (s, 3 H), 2.50–2.41 (m, 4 H), 1.75–1.63 (m, 4 H), 1.35 (t, *J* = 7.0 Hz, 3 H); ¹³C NMR (125 MHz, CDCl₃) δ 169.3, 159.5, 141.6, 130.4, 129.7, 128.1, 128.0, 126.0, 114.1, 60.4, 55.4, 27.6, 26.3, 22.3, 22.1, 14.5; HRMS (DART, [M+H]⁺) for C₁₈H₂₃O₃ calcd. 287.1642, found: *m/z* 287.1641.

Representative Procedure A for the Reduction of Esters

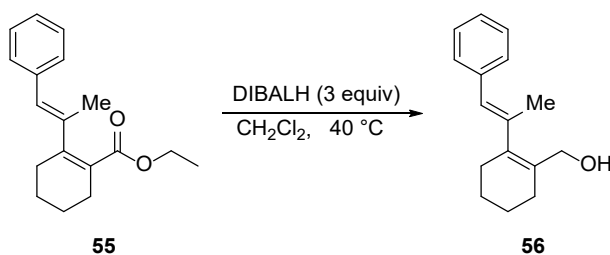
(*E*)-(2-Styrylcyclohex-1-en-1-yl)methanol (**47**)



A solution of ethyl (*E*)-2-styrylcyclohex-1-ene-1-carboxylate (**46**) (288 mg, 1.12 mmol) and DCM (0.1 M, 10 mL) was cooled to −40 °C. A 1 M solution of DIBALH (2.85 mL, 2.85 M) was added dropwise. The reaction mixture was allowed to warm to room temperature while stirring over 2 h. After the 2 h, the reaction mixture was cooled to 0 °C. The reaction mixture was slowly quenched with EtOAc, and a half saturated aqueous solution of potassium sodium tartrate was added, and stirred for 30 minutes. The layers were separated, and the aqueous layer was extracted 3x with

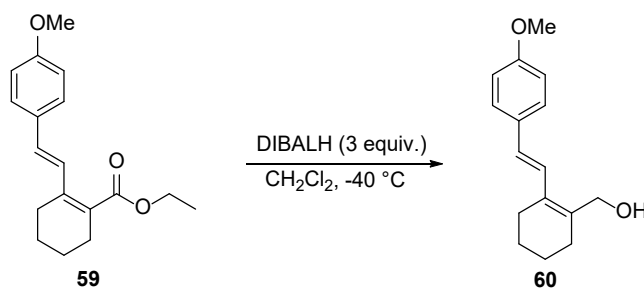
ethyl acetate. The combined organic layers were washed with water and brine, dried over magnesium sulfate, filtered and concentrated in vacuo. The crude product was purified by flash column chromatography (hexanes/EtOAc 9:1 \rightarrow 3:2). The product was obtained as a yellow oil (237 mg, 1.1 mmol) in 98% yield. R_f 0.29 (hexanes/EtOAc 4:1); IR (neat) 3312, 3043, 2924, 2858, 1595, 1443 cm^{-1} ; ^1H NMR (700 MHz, CDCl_3) δ 7.43 (d, J = 7.7 Hz, 2 H), 7.33–7.28 (m, 3 H), 7.22 (t, J = 8.4 Hz, 1 H), 6.59 (d, J = 16.1 Hz, 1 H), 4.36 (s, 2 H), 2.39–2.29 (m, 4 H), 2.75–2.65 (m, 4 H), (OH proton not detected); ^{13}C NMR (125 MHz, CDCl_3) δ 138.0, 136.8, 132.0, 128.7, 127.33, 127.29, 126.4, 126.2, 62.7, 29.3, 25.8, 22.7, 22.6; HRMS (DART, $[\text{M}-\text{H}_2\text{O}+\text{H}]^+$) for $\text{C}_{15}\text{H}_{17}$ calcd. 197.1325, found: m/z 197.1322.

(*E*)-(2-(1-Phenylprop-1-en-2-yl)cyclohex-1-en-1-yl)methanol (56**)**



The reaction was performed under general procedure A, and purified by flash column chromatography (hexanes/EtOAc 9:1 \rightarrow 3:2). The product was obtained as a yellow oil (23 mg, 0.10 mmol) in 99% yield from ethyl (*E*)-2-(1-phenylprop-1-en-2-yl)cyclohex-1-ene-1-carboxylate (**55**) (28 mg, 0.110 mmol). R_f 0.77 (hexanes/EtOAc 3:2); IR (neat) 3314, 2924, 2857, 2361, 1634, 1598, 1440, 1374, 1001 cm^{-1} ; ^1H NMR (500 MHz, CDCl_3) δ 7.36–7.31 (m, 2 H), 7.30–7.27 (m, 2 H), 7.24–7.19 (m, 1 H), 6.21 (s, 1 H), 4.15 (s, 2 H), 2.23–2.13 (m, 4 H), 1.95 (d, J = 1.5 Hz, 3 H), 1.72–1.63 (m, 4 H), (OH proton not detected); ^{13}C NMR (125 MHz, CDCl_3) δ 140.6, 139.7, 137.9, 130.3, 128.9, 128.2, 126.8, 126.3, 64.3, 29.3, 26.7, 23.0, 22.8, 18.1; HRMS (DART, $[\text{M}-\text{H}_2\text{O}+\text{H}]^+$) for $\text{C}_{16}\text{H}_{19}$ calcd. 211.1481, found: m/z 211.1478.

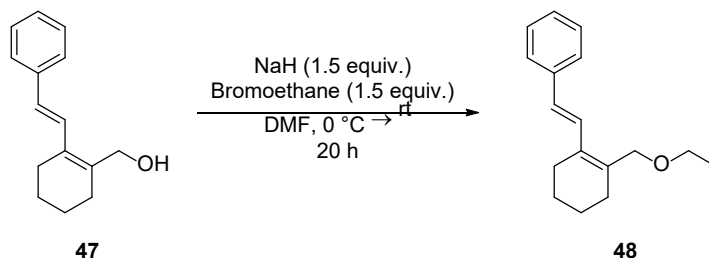
(*E*)-(2-(4-methoxystyryl)cyclohex-1-en-1-yl)methanol (60**)**



The reaction was performed under general procedure A, and purified by flash column chromatography (hexanes/EtOAc 9:1 → 3:2). The product was obtained as a white solid in 82% yield (495 mg, 2.03 mmol) from ethyl (*E*)-2-(4-methoxystyryl)cyclohex-1-ene-1-carboxylate (**59**) (705 mg, 2.5 mmol). *R*_f 0.47 (hexanes/EtOAc 3:2); IR (neat) 3273, 2931, 2831, 2361, 1602, 1507, 1459, 1222 cm⁻¹; ¹H NMR (500 MHz, CDCl₃) δ 7.36 (d, *J* = 8.5 Hz, 2 H), 7.17 (d, *J* = 16 Hz, 1 H), 6.86 (d, *J* = 9.0 Hz, 2 H), 6.54 (d, *J* = 16.0 Hz, 1 H), 4.34 (s, 2 H), 3.81 (s, 3 H), 2.37–2.27 (m, 4 H), 1.74–1.63 (m, 4 H), 1.32 (br s, 1 H); ¹³C NMR (125 MHz, CDCl₃) δ 159.1, 135.7, 132.1, 130.8, 127.5, 126.8, 124.2, 114.1, 62.7, 55.3, 29.2, 25.8, 22.71, 22.65; HRMS (LIFDI, M⁺) for C₁₆H₂₀O₂ calcd. 244.1458, found: *m/z* 244.1461.

General Procedure B for the Preparation of Allylic Ethers

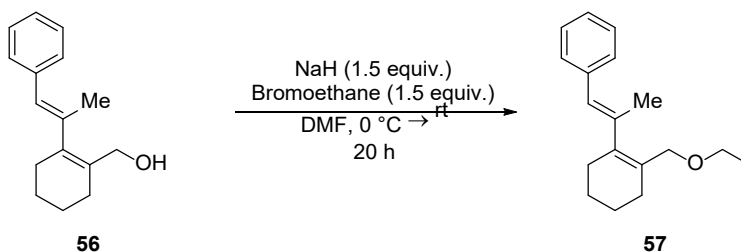
(*E*)-(2-(2-(Ethoxymethyl)cyclohex-1-en-1-yl)vinyl)benzene (48**)**



A solution of (*E*)-(2-styrylcyclohex-1-en-1-yl)methanol (**47**) (455 mg, 2.12 mmol) in DMF (0.25 M, 8.5 mL) was cooled to 0 °C. NaH (148 mg, 3.70 mmol) was added in one portion, followed by bromoethane (0.25 mL, 3.2 mmol) dropwise. The reaction mixture was allowed to warm to room

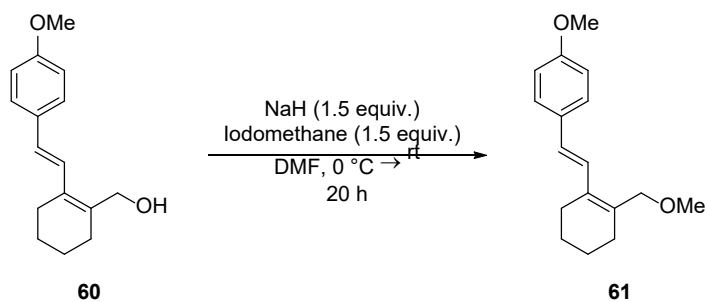
temperature while stirring over 20 h. The reaction mixture was quenched with a saturated aqueous solution of NH_4Cl . The layers were separated, and the aqueous layer was extracted 3x with ethyl acetate. The combined organic layers were washed with water, brine, dried over sodium sulfate, filtered and concentrated in vacuo. The crude product was purified by flash column chromatography (hexanes/EtOAc 50:1 \rightarrow 9:1). The product was obtained as a clear oil (410 mg, 1.69 mmol) in 82% yield. R_f 0.56 (hexanes/EtOAc 9:1); IR (neat) 3044, 2971, 2925, 1858, 1597, 1491, 1445, 1350, 1272, 1089 cm^{-1} ; ^1H NMR (500 MHz, CDCl_3) δ 7.47–7.41 (m, 2 H), 7.38–7.31 (m, 3 H), 7.26–7.21 (m, 1 H), 6.59 (d, J = 16.0 Hz, 1 H), 4.21 (s, 2 H), 3.54 (q, J = 7.0 Hz, 2 H), 2.40–2.35 (m, 2 H), 2.32–2.26 (m, 2 H), 1.77–1.65 (m, 4 H), 1.27 (t, J = 7.0 Hz, 3 H); ^{13}C NMR (125 MHz, CDCl_3) δ 138.3, 134.8, 132.4, 128.6, 127.1, 126.8, 126.7, 126.4, 70.1, 65.6, 29.5, 25.9, 22.7, 22.6, 15.4; HRMS (ESI, $[\text{M}+\text{Na}]^+$) for $\text{C}_{17}\text{H}_{22}\text{NaO}$ calcd. 265.1563, found: m/z 265.1565.

(*E*)-(2-(2-(Ethoxymethyl)cyclohex-1-en-1-yl)prop-1-en-1-yl)benzene (57)



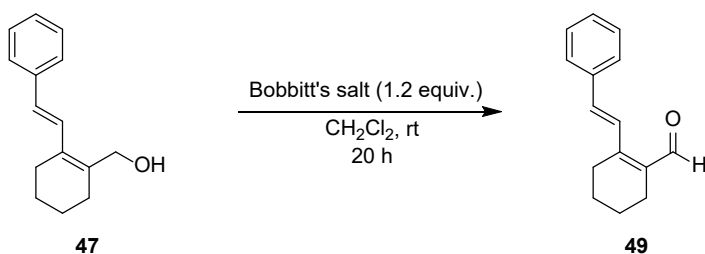
The reaction was performed under general procedure B, and purified by flash column chromatography (hexanes/EtOAc 50:1 \rightarrow 9:1). The product was obtained as a clear liquid (468 mg, 1.82 mmol) in 61% yield from (*E*)-(2-(1-phenylprop-1-en-2-yl)cyclohex-1-en-1-yl)methanol (**56**) (681 mg, 2.98 mmol) and bromoethane (0.33 mL, 4.5 mmol). R_f 0.71 (hexanes/EtOAc 9:1); IR (neat) 2972, 2925, 2857, 1599, 1490, 1441, 1373, 1271, 1087 cm^{-1} ; ^1H NMR (500 MHz, CDCl_3) δ 7.36–7.31 (m, 2 H), 7.31–7.27 (m, 2 H), 7.23–7.19 (m, 1 H), 6.21 (s, 1 H), 3.99 (s, 2 H), 3.42 (q, J = 7.0 Hz, 2 H), 2.19–2.13 (m, 4 H), 1.94 (d, J = 1.5 Hz, 3 H), 1.71–1.64 (m, 4 H), 1.19 (t, J = 7.0 Hz, 3 H); ^{13}C NMR (125 MHz, CDCl_3) δ 141.0, 139.5, 138.2, 128.9, 128.2, 128.1, 126.9, 126.2, 71.5, 65.2, 29.3, 26.9, 23.0, 22.8, 18.0, 15.4; HRMS (ESI, $[\text{M}+\text{Na}]^+$) for $\text{C}_{18}\text{H}_{24}\text{NaO}$ calcd. 279.1719, found: m/z 279.1721.

(*E*)-1-Methoxy-4-(2-(2-(methoxymethyl)cyclohex-1-en-1-yl)vinyl)benzene (61)



The reaction was performed under general procedure B, and purified by flash column chromatography (hexanes/EtOAc 50:1 → 9:1). The product was obtained as a yellow oil in 91% yield (412 mg, 1.59 mmol) from (*E*)-2-(4-methoxystyryl)cyclohex-1-en-1-ylmethanol (**60**) (427 mg, 0.175 mmol) and iodomethane (0.16 mL, 0.26 mmol). R_f 0.72 (hexanes/EtOAc 3:2); IR (neat) 2925, 2832, 1603, 1508, 1453, 1243 cm^{-1} ; ^1H NMR (500 MHz, CDCl_3) δ 7.36 (d, J = 8.5 Hz, 2 H), 7.16 (d, J = 16.5 Hz, 1 H), 6.86 (d, J = 9.0 Hz, 2 H), 6.53 (d, J = 16.0 Hz, 1 H), 4.12 (s, 2 H), 3.81 (s, 3 H), 3.36 (s, 3 H), 2.37–2.31 (m, 2 H), 2.27–2.21 (m, 2 H), 1.74–1.62 (m, 4 H); ^{13}C NMR (125 MHz, CDCl_3) δ 159.0, 133.3, 132.8, 131.0, 127.5, 126.5, 124.7, 114.1, 72.0, 58.0, 55.3, 29.4, 25.9, 22.69, 22.68; HRMS (LIFDI, $[\text{M}^+]$) for $\text{C}_{17}\text{H}_{22}\text{O}_2$ calcd. 258.1614, found: m/z 258.1614.

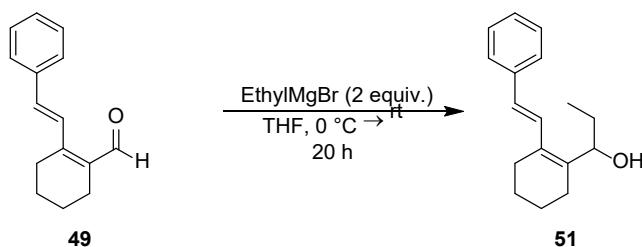
(*E*)-2-Styrylcyclohex-1-ene-1-carbaldehyde (49)



(*E*)-2-(2-((benzyloxy)methyl)cyclohex-1-en-1-yl)vinylbenzene (**47**) (104 mg, 0.485 mmol) was added to a flask followed by DCM (0.1 M, 5 mL) and Bobbitt's salt (183 mg, 0.610 mmol). The reaction was stirred at room temperature for 20 h. The reaction was quenched by filtration through a silica gel plug, eluted with CH_2Cl_2 . The crude reaction mixture was purified by column chromatography (hexanes/EtOAc 50:1 → 9:1). The product was obtained as a yellow oil (79 mg, 0.37 mmol) in 77% yield. R_f 0.52 (hexanes/EtOAc 9:1); IR (neat) 3027, 2931, 2864, 1702, 1652,

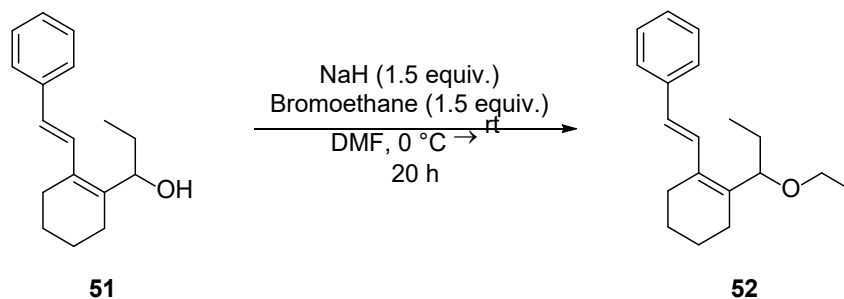
1612, 1449, 1146 cm^{-1} ; ^1H NMR (500 MHz, CDCl_3) δ 10.47 (s, 1 H), 7.76 (d, $J = 16.0$ Hz, 1 H), 7.50–7.46 (m, 2 H), 7.40–7.35 (m, 2 H), 7.33–7.28 (m, 1 H), 6.87 (d, $J = 16.0$ Hz, 1 H), 2.60–2.55 (m, 2 H), 2.39–2.34 (m, 2 H), 1.77–1.71 (m, 2 H), 1.70–1.63 (m, 2 H); ^{13}C NMR (125 MHz, CDCl_3) δ 190.5, 151.6, 136.7, 135.8, 133.5, 128.9, 128.7, 127.0, 123.5, 27.6, 23.4, 22.1, 21.6; HRMS (DART, $[\text{M}+\text{H}]^+$) for $\text{C}_{15}\text{H}_{17}\text{O}$ calcd. 213.1274, found: m/z 213.1270.

(*E*)-1-(2-Styrylcyclohex-1-en-1-yl)propan-1-ol (51)



A solution of (*E*)-2-styrylcyclohex-1-ene-1-carbaldehyde (**49**) (278 mg, 1.31 mmol) and THF (0.2 M, 6.5 mL) were cooled to 0 °C. A solution of EtMgBr (3 M in diethyl ether) (0.87 mL, 2.6 mmol) was added dropwise. The reaction mixture was stirred at 0 °C for 2 h, then allowed to warm to rt overnight. The reaction mixture was quenched by the addition of a saturated aqueous solution of NH_4Cl . The aqueous phase was extracted 3x with ethyl acetate. The organic layers were combined and washed with water and brine, dried over magnesium sulfate, filtered and concentrated in vacuo. The crude mixture was purified by flash column chromatography (hexanes/EtOAc 9:1 \rightarrow 3:2). The product was obtained as a yellow oil in 75% yield (240 mg, 0.990 mmol). R_f 0.23 (hexanes/EtOAc 9:1); IR (neat) 3353, 2967, 2939, 1703, 1454, 1375, 1303 cm^{-1} ; ^1H NMR (500 MHz, CDCl_3) δ 7.42 (d, $J = 7.5$ Hz, 2 H), 7.37–7.29 (m, 3 H), 7.22 (app t, $J = 7.0$ Hz, 1 H), 6.57 (d, $J = 16.0$ Hz, 1 H), 4.90 (t, $J = 7.0$ Hz, 1 H), 2.46–2.26 (m, 3 H), 2.16–2.06 (m, 1 H), 1.80–1.54 (m, 7 H), 0.93 (t, $J = 7.5$ Hz, 3 H); ^{13}C NMR (125 MHz, CDCl_3) δ 139.2, 138.2, 130.3, 128.6, 127.1, 126.8, 126.3, 126.2, 71.6, 28.2, 26.2, 24.0, 22.7, 22.6, 10.5; HRMS (LIFDI, M^+) for $\text{C}_{17}\text{H}_{22}\text{O}$ calcd. 242.1669, found: m/z 242.1665.

(*E*)-(2-(2-(1-Ethoxypropyl)cyclohex-1-en-1-yl)vinyl)benzene (52)

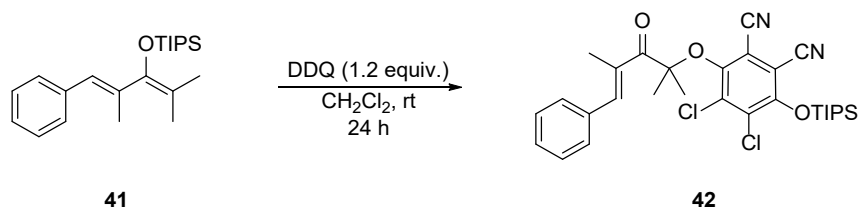


The reaction was performed under general procedure B, and purified by flash column chromatography (hexanes/EtOAc 50:1 → 9:1). The product was obtained as a clear oil in 70% yield (182 mg, 0.673 mmol) from (*E*)-1-(2-styrylcyclohex-1-en-1-yl)propan-1-ol (**51**) (235 mg, 0.969 mmol). R_f 0.76 (hexanes/EtOAc 9:1); IR (neat) 2926, 2866, 1597, 1447, 1371, 1274, 1081 cm^{-1} ; ^1H NMR (500 MHz, CDCl_3) δ 7.45–7.32 (m, 5 H), 7.21 (app t, J = 7.5 Hz, 1 H), 6.55 (d, J = 16.5 Hz, 1 H), 4.46 (t, J = 7.0 Hz, 1 H), 3.46–3.38 (m, 1 H), 3.34–3.28 (m, 1 H), 2.45–2.28 (m, 2 H), 2.24–2.02 (m, 2 H), 1.79–1.48 (6 H), 1.19 (t, J = 7.0 Hz, 3 H), 0.90 (t, J = 7.5 Hz, 3 H); ^{13}C NMR (125 MHz, CDCl_3) δ 138.42, 138.40, 131.5, 128.7, 127.1, 126.4, 126.33, 126.27, 78.8, 63.6, 27.1, 26.2, 24.3, 22.9, 22.7, 15.5, 10.6; HRMS (LIFDI, M^+) for $\text{C}_{19}\text{H}_{26}\text{O}$ calcd. 270.1978, found: m/z 270.1976.

General procedure C for DDQ mediated reactions

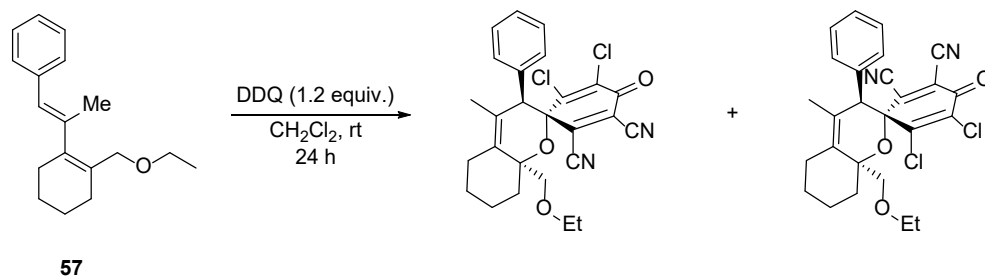
Substrate (0.2 mmol) was added to flask followed by DCM (0.1 M). DDQ was added in one portion, and reaction was monitored for consumption of starting material. Reaction was quenched by filtration through silica gel plug eluted with DCM. Solvent was evaporated in vacuo. The crude reaction mixture was purified by column chromatography.

(*E*)-4,5-dichloro-3-((2,4-dimethyl-3-oxo-5-phenylpent-4-en-2-yl)oxy)-6-((triisopropylsilyl)oxy)phthalonitrile (42)



The reaction was performed under general procedure C, and purified by flash column chromatography (hexanes/EtOAc 50:1 → 9:1). The product was obtained as a white solid (57 mg, 0.099 mmol) in 51% yield from (*E*)-((2,4-dimethyl-1-phenylpenta-1,3-dien-3-yl)oxy)triisopropylsilane (**41**) (68 mg, 0.20 mmol) and DDQ (55 mg, 0.24 mmol). *R*_f 0.52 (hexanes/EtOAc 9:1); IR (neat) 2948, 2868, 2233, 1660, 1623, 1551, 1421, 1387, 1239 cm⁻¹; ¹H NMR (500 MHz, CDCl₃) δ 8.08 (s, 1 H), 7.47–7.38 (m, 4 H), 7.37–7.31 (m, 1 H), 2.17 (d, *J* = 1.0 Hz, 3 H), 1.72 (s, 6 H), 1.50 (sept, *J* = 8.0 Hz, 3 H), 1.15 (d, *J* = 8.0 Hz, 18 H); ¹³C NMR (125 MHz, CDCl₃) δ 200.9, 153.4, 149.9, 142.0, 136.9, 136.1, 134.1, 132.6, 129.9, 128.5, 128.4, 113.3, 112.9, 111.8, 106.3, 92.5, 27.0, 17.8, 14.8, 14.2; HRMS (DART, [M+NH₄]⁺ for C₃₀H₄₀³⁵Cl₂N₃O₃Si calcd. 588.2211, found: *m/z* 588.2205.

(2*R,3*R**,8*aS**)-2',3'-Dichloro-8*a*-(ethoxymethyl)-4-methyl-4'-oxo-3-phenyl-3,5,6,7,8,8*a*-hexahydrospiro[chromene-2,1'-cyclohexane]-2',5'-diene-5',6'-dicarbonitrile and (2*S**,3*R**,8*aS**)-2',3'-Dichloro-8*a*-(ethoxymethyl)-4-methyl-4'-oxo-3-phenyl-3,5,6,7,8,8*a*-hexahydrospiro[chromene-2,1'-cyclohexane]-2',5'-diene-5',6'-dicarbonitrile**

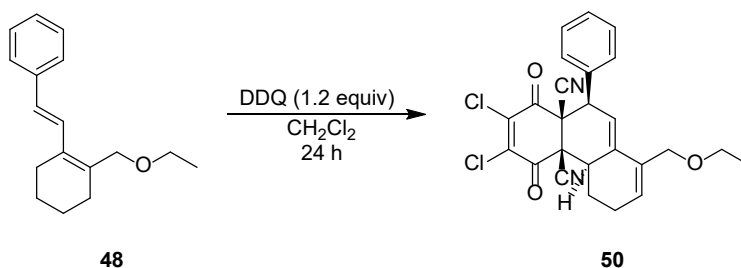


The reaction was performed under general procedure C, and purified by flash column chromatography (hexanes/EtOAc 50:1 → 9:1). The major product was obtained as a yellow solid

(27 mg, 0.055 mmol) in 56% yield from (*E*)-(2-(2-(ethoxymethyl)cyclohex-1-en-1-yl)prop-1-en-1-yl)benzene (**57**) (26 mg, 0.10 mmol) and DDQ (27 mg, 0.12 mmol). R_f 0.42 (hexanes/EtOAc 9:1); IR (neat) 2931, 2866, 1686, 1607, 1574, 1450, 1333, 1292, 1158, 1105 cm^{-1} ; ^1H NMR (500 MHz, CDCl_3) δ 7.35 (ddd, $J = 7.5, 7.5, 1.5$ Hz, 1 H), 7.29 (dddd, $J = 7.5, 7.5, 1.0, 1.0$ Hz, 1 H), 7.25 (ddd, $J = 7.5, 7.5, 1.5$ Hz, 1 H), 7.08–7.04 (m, 1 H), 6.98–6.94 (m, 1 H), 4.57 (dd, $J = 4.0, 1.5$ Hz, 1 H), 3.71 (d, $J = 10.5$ Hz, 1 H), 3.61 (d, $J = 10.5$ Hz, 1 H), 3.59–3.52 (m, 2 H), 2.97–2.90 (m, 1 H), 2.24–2.18 (m, 1 H), 2.02–1.93 (m, 2 H), 1.92–1.85 (m, 1 H), 1.84–1.76 (m, 1 H), 1.76–1.64 (m, 4 H), 1.52–1.42 (m, 1 H), 1.25 (t, $J = 7.0$ Hz, 3 H); ^{13}C NMR (125 MHz, CDCl_3) δ 168.4, 154.2, 142.1, 134.4, 133.4, 131.7, 131.3, 129.7, 129.1, 129.0, 128.0, 124.0, 123.2, 114.7, 110.2, 82.5, 81.8, 74.3, 66.8, 53.2, 34.9, 28.4, 24.0, 23.9, 18.0, 15.3; HRMS (DART, $[\text{M}+\text{H}]^+$) for $\text{C}_{26}\text{H}_{25}^{35}\text{Cl}_2\text{N}_2\text{O}_3$ calcd. 483.1237, found: m/z 483.1234.

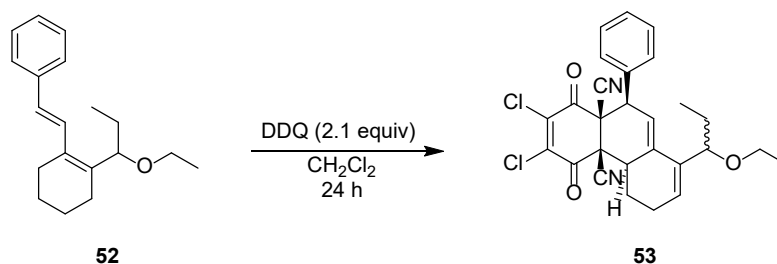
The minor product was obtained as a yellow solid (7 mg, 0.02 mmol) in 15% yield from (*E*)-(2-(2-(ethoxymethyl)cyclohex-1-en-1-yl)prop-1-en-1-yl)benzene (**57**) (26 mg, 0.10 mmol) and DDQ (27 mg, 0.12 mmol). R_f 0.45 (hexanes/EtOAc 9:1); IR (neat) 2931, 2867, 1686, 1608, 1574, 1451, 1378 1334, 1291, 1157, 1103 cm^{-1} ; ^1H NMR (500 MHz, CDCl_3) δ 7.31–7.27 (m, 3 H), 6.99–6.95 (m, 1 H), 6.91–6.88 (m, 1 H), 4.46 (d, $J = 2.0$ Hz, 1 H), 3.74 (d, $J = 10.5$ Hz, 1 H), 3.65–3.58 (m, 2 H), 3.57–3.50 (m, 1 H), 2.88 (d, $J = 15.5$ Hz, 1 H), 2.19–2.09 (m, 1 H), 2.04–1.92 (m, 2 H), 1.88–1.82 (m, 2 H), 1.62 (s, 3 H), 1.52–1.38 (m, 2 H), 1.29 (t, $J = 7.0$ Hz, 3 H); ^{13}C NMR (125 MHz, CDCl_3) δ 168.2, 154.0, 144.0, 133.2, 133.1, 132.2, 131.9, 129.7, 129.1, 128.9, 128.0 122.1, 122.08, 112.5, 110.0, 83.2, 82.0, 74.7, 66.4, 54.5, 34.3, 28.1, 24.9, 24.0, 17.7, 15.2; HRMS (LIFDI, $[\text{M}]^+$) for $\text{C}_{26}\text{H}_{24}^{35}\text{Cl}_2\text{N}_2\text{O}_3$ calcd. 482.1158, found: m/z 482.1156.

2,3-Dichloro-8-(ethoxymethyl)-1,4-dioxo-10-phenyl-1,4,4b,5,6,10-hexahydrophenanthrene-4a,10a-dicarbonitrile (50)



The reaction was performed under general procedure C, and purified by flash column chromatography (hexanes/EtOAc 50:1 → 9:1). The product was obtained as a yellow solid (16 mg, 0.034 mmol) in 7% yield from (*E*)-2-(2-(ethoxymethyl)cyclohex-1-en-1-yl)vinylbenzene (**48**) (121 mg, 0.499 mmol) and DDQ (136 mg, 0.599 mmol) as a single diastereomer. R_f 0.14 (hexanes/EtOAc 9:1); IR (neat) 2930, 2859, 1710, 1557, 1451, 1423, 1395, 1240, 1198, 1144, 1098 cm^{-1} ; ^1H NMR (500 MHz, CD_2Cl_2) δ 7.32–7.25 (m, 3 H), 6.86–6.80 (m, 2 H), 6.24 (d, J = 6.5 Hz, 1 H), 5.95 (dd, J = 3.5, 3.5 Hz, 1 H), 4.61 (s, 1 H), 4.24 (d, J = 12.0 Hz, 1 H), 4.08 (d, J = 12.5 Hz, 1 H), 3.56–3.46 (m, 1 H), 3.44–3.36 (m, 1 H), 3.33–3.26 (m, 1 H), 2.72–2.62 (m, 1 H), 2.56–2.46 (m, 1 H), 2.42–2.31 (m, 1 H), 2.23–2.16 (m, 1 H), 1.15 (t, J = 7.5 Hz, 3 H); ^{13}C NMR (125 MHz, CD_2Cl_2) δ 180.5, 177.1, 145.5, 144.5, 135.2, 133.3, 133.1, 132.4, 130.07, 130.06, 129.8, 117.2, 115.6, 115.4, 72.0, 65.5, 60.2, 52.5, 49.2, 40.3, 25.7, 23.4, 15.4; HRMS (DART, $[\text{M}+\text{NH}_4]^+$) for $\text{C}_{25}\text{H}_{24}^{35}\text{Cl}_2\text{N}_3\text{O}_3$ calcd. 484.1189, found: m/z 484.1190.

2,3-Dichloro-8-(1-ethoxypropyl)-1,4-dioxo-10-phenyl-1,4,4b,5,6,10-hexahydrophenanthrene-4a,10a-dicarbonitrile (53)

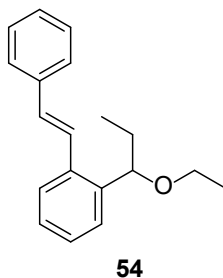


The reaction was performed under general procedure C, and purified by flash column chromatography (hexanes/EtOAc 50:1 → 9:1). The product was obtained as a yellow solid (35 mg, 0.070 mmol) in 23% yield from (*E*)-(2-(2-(1-ethoxypropyl)cyclohex-1-en-1-yl)vinyl)benzene (**52**) (80 mg, 0.30 mmol) and DDQ (143 mg, 0.630 mmol) as an inseparable mixture of diastereomers (3.7:1 ratio). Diastereomeric ratio was determined using ^1H NMR resonances of the alkene protons. R_f 0.27 (hexanes/EtOAc 9:1); IR (neat) 2965, 2929, 2869, 1709, 1553, 1451, 1378, 1241, 1192, 1143, 1103 cm^{-1} .

Major Diastereomer: ^1H NMR (500 MHz, CDCl_3) δ 7.30–7.27 (m, 3 H), 6.81–6.76 (m, 2 H), 6.20–6.14 (2 H), 4.59–4.53 (m, 1 H), 3.89 (t, $J = 7.0$ Hz, 1 H), 3.61–3.43 (m, 1 H), 3.37–3.29 (m, 1 H), 3.29–3.22 (m, 1 H), 2.73–2.56 (m, 1 H), 2.56–2.46 (m, 1 H), 2.42–2.32 (m, 1 H), 2.23–2.15 (m, 1 H), 1.78–1.64 (m, 2 H), 1.18 (t, $J = 7.0$ Hz, 3 H), 0.90 (t, $J = 7.5$ Hz, 3 H); ^{13}C NMR (125 MHz, CDCl_3) δ 179.7, 176.9, 145.0, 144.3, 134.7, 134.4, 132.2, 131.5, 129.69, 129.66, 129.5, 116.6, 115.1, 115.0, 84.1, 64.1, 59.4, 52.3, 48.9, 40.1, 28.0, 25.3, 23.2, 15.3, 10.9; HRMS (DART, $[\text{M}+\text{NH}_4]^+$) for $\text{C}_{27}\text{H}_{28}^{35}\text{Cl}_2\text{N}_3\text{O}_3$ calcd. 512.1502, found: m/z 512.1503.

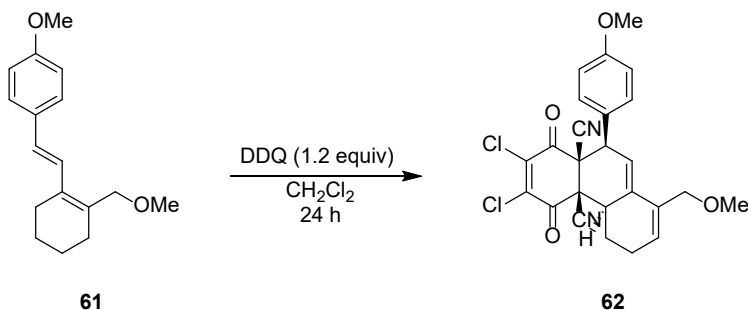
Minor Diastereomer: ^1H NMR (500 MHz, CDCl_3) δ 7.30–7.27 (m, 3 H), 6.81–6.76 (m, 2 H), 6.27–6.74 (2 H), 4.59–4.53 (m, 1 H), 3.89 (t, $J = 7.0$ Hz, 1 H), 3.61–3.43 (m, 1 H), 3.37–3.29 (m, 1 H), 3.29–3.22 (m, 1 H), 2.73–2.56 (m, 1 H), 2.56–2.46 (m, 1 H), 2.42–2.32 (m, 1 H), 2.23–2.15 (m, 1 H), 1.78–1.64 (m, 2 H), 1.16 (t, $J = 7.0$ Hz, 3 H), 0.95 (t, $J = 7.5$ Hz, 3 H); ^{13}C NMR (125 MHz, CDCl_3) δ 179.7, 176.9, 145.0, 144.3, 134.8, 134.6, 132.2, 132.0, 129.8, 129.7, 129.5, 116.6, 115.2, 115.0, 83.6, 63.6, 59.5, 52.3, 49.0, 40.2, 28.4, 25.5, 23.4, 15.5, 11.0; HRMS (DART, $[\text{M}+\text{NH}_4]^+$) for $\text{C}_{27}\text{H}_{28}^{35}\text{Cl}_2\text{N}_3\text{O}_3$ calcd. 512.1502, found: m/z 512.1503.

(*E*)-1-(1-Ethoxypropyl)-2-styrylbenzene (54)



The product was obtained as a yellow oil (75 mg, 0.14 mmol) in 47% yield from (*E*)-(2-(2-(1-ethoxypropyl)cyclohex-1-en-1-yl)vinyl)benzene (**52**) (80 mg, 0.30 mmol) and DDQ (143 mg, 0.630 mmol). R_f 0.57 (hexanes/EtOAc 9:1); IR (neat) 2967, 2929, 2870, 1710, 1599, 1553, 1492, 1449 cm^{-1} ; ^1H NMR (500 MHz, CDCl_3) δ 7.62–7.58 (m, 1 H), 7.55–7.50 (m, 3 H), 7.43–7.36 (m, 3 H), 7.32–7.26 (m, 3 H), 6.96 (d, $J = 16.5$ Hz, 1 H), 4.55 (dd, $J = 7.0, 6.0$ Hz, 1 H), 3.46–3.39 (m, 1 H), 3.39–3.31 (m, 1 H), 1.85–1.70 (m, 2 H), 1.20 (t, $J = 7.0$ Hz, 3 H), 0.94 (t, $J = 7.0$ Hz, 3 H); ^{13}C NMR (125 MHz, CDCl_3) δ 140.5, 137.7, 136.0, 130.6, 128.7, 127.67, 127.66, 127.3, 126.8, 126.6, 126.04, 126.02, 80.8, 64.2, 30.7, 15.4, 10.6; HRMS (DART, $[\text{M}+\text{NH}_4]^+$) for $\text{C}_{19}\text{H}_{26}\text{NO}$ calcd. 284.2009, found: m/z 284.2007.

2,3-Dichloro-8-(methoxymethyl)-10-(4-methoxyphenyl)-1,4-dioxo-1,4,4b,5,6,10-hexahydrophenanthrene-4a,10a-dicarbonitrile (62)



The reaction was performed under general procedure C, and purified by flash column chromatography (hexanes/EtOAc 20:1 \rightarrow 3:2). The product was obtained as a yellow solid (17 mg, 0.035 mmol) in 19% yield from (*E*)-1-methoxy-4-(2-(2-(methoxymethyl)cyclohex-1-en-1-

yl)vinyl)benzene (**61**) (52 mg, 0.20 mmol) and DDQ (54 mg, 0.24 mmol). *R*_f 0.19 (hexanes/EtOAc 4:1) as a single diastereomer; IR (neat) 2933, 1693, 1605, 1509, 1455, 1292, 1242 cm⁻¹; ¹H NMR (500 MHz, CDCl₃) δ 6.77, (d, *J* = 8.5 Hz, 2 H), 6.71 (d, *J* = 9.0 Hz, 2 H), 6.23 (d, *J* = 6.0 Hz, 1 H), 5.90 (dd, *J* = 2.5, 2.5 Hz, 1 H), 4.55–4.51 (m, 1 H), 4.18 (d, *J* = 12.0 Hz, 1 H), 4.05 (d, *J* = 12.0 Hz, 1 H), 3.76 (s, 3 H), 3.31 (s, 3 H), 3.29–3.22 (m, 1 H), 2.75–2.64 (m, 1 H), 2.56–2.47 (m, 1 H), 2.42–2.32 (m, 1 H), 2.23–2.16 (m, 1 H); ¹³C NMR (125 MHz, CDCl₃) δ 179.9, 176.8, 160.3, 145.1, 144.3, 133.4, 132.5, 131.6, 131.0, 126.3, 117.2, 115.12, 115.09, 115.02, 73.7, 59.7, 57.5, 55.5, 52.0, 48.5, 40.0, 25.4, 23.0; HRMS (ESI, [M+H]⁺) for C₂₅H₂₁³⁵Cl₂N₂O₄ calcd. 482.0803, found: *m/z* 482.0875.

Chapter 3: Development of a Catalytic Method for the Synthesis of Cyclobutanes via a Formal [2+2] Cycloaddition of o-Styrenyl Chalcones

3.1 Introduction

In recent years cyclobutane and cyclobutane derivatives have become increasingly popular to synthetic chemists, both for the synthetic challenge of synthesizing cyclobutane compounds, as well as the biological activity displayed by some compounds of this class.

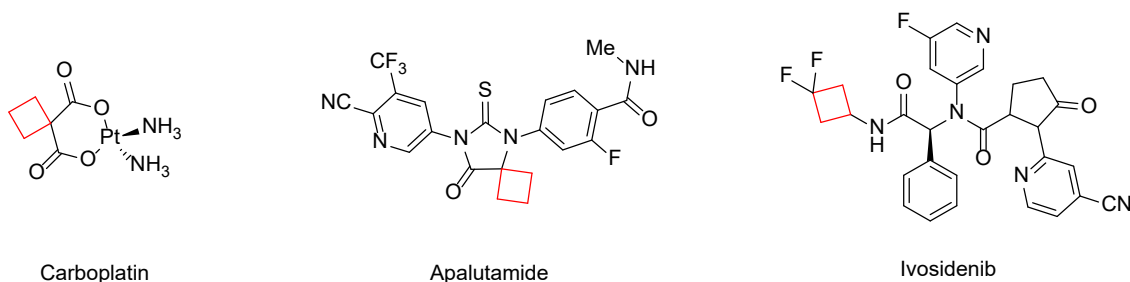


Figure 3.1 FDA approved cyclobutane containing drugs

3.1.1 Applications of cyclobutane compounds in medicinal chemistry

There have been numerous examples in which using cyclobutane as an isostere has imparted favourable properties onto a drug molecule. These properties arise from conformational restriction, which can be beneficial for binding. It can also improve metabolic stability, prevent *cis/trans* isomerization of alkenes, reduce planarity when replacing a phenyl group, or fill a hydrophobic pocket. Savage and coworkers demonstrated that replacing a methylene group in compound **1** with a cyclobutane moiety in compound **2** resulted in increased inhibition of the target AKT proteins (Figure 3.2).¹⁵⁰ The increase in inhibition is a result of improved binding, as the cyclobutane moiety resides in a hydrophobic pocket. Zhou et al. found that a MDM2 inhibitor (compound **3**) suffered from low metabolic stability, resulting from the 1,2-diol moiety.¹⁵¹ Replacing the diol moiety with a cyclobutanol (compound **4**) resulted in higher metabolic stability by blocking the metabolic oxidative site, as a result of the reduced conformational flexibility. Compound **5** is a natural product that has been shown to have anti-tumour activity. The *cis*-conformation is important for its activity; the compound is prone to undergo *cis/trans*

isomerization under physiological conditions. Rinner and coworkers utilized a cyclobutene ring to lock the double bond in the active *cis* conformation.¹⁵²

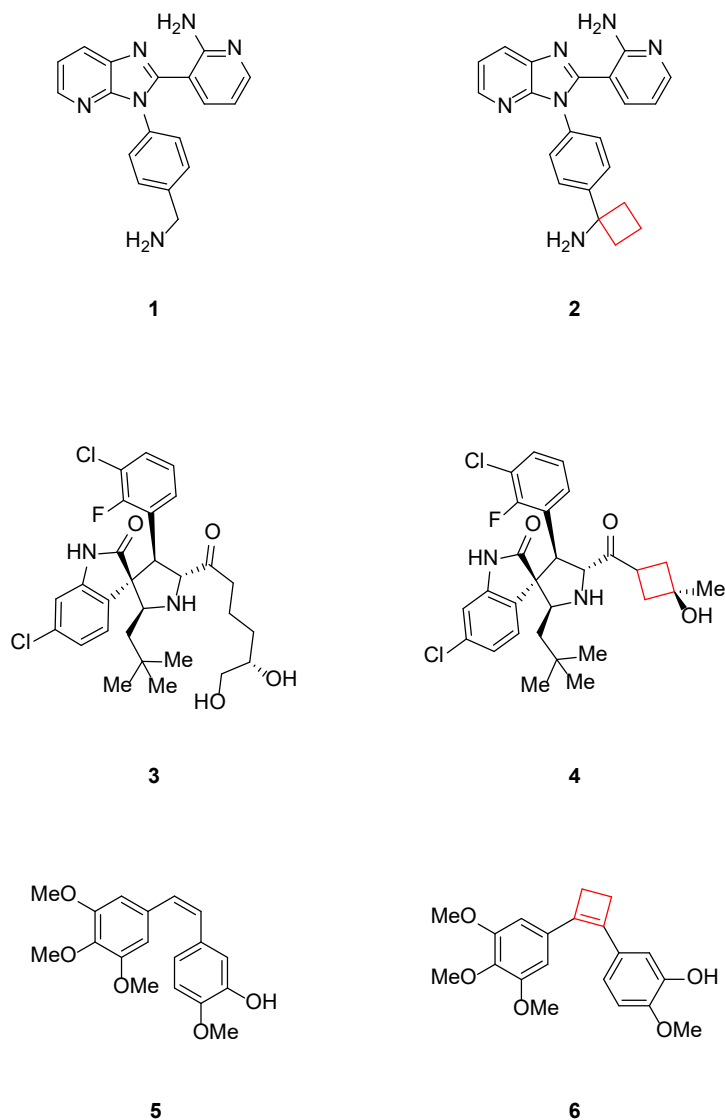


Figure 3.2 Examples of cyclobutanes as isosteres

The demonstrated utility of cyclobutane containing compounds in the field of medicinal chemistry demands that robust methodologies exist for their synthesis. Another reason why the construction of cyclobutane moieties is of value is their ability to act as key synthetic intermediates that can undergo subsequent transformations. This is mainly due to the ring strain (26.7 kcal/mol),

which allows for selective bond cleavage in a ring opening process. The main synthetic transformations are ring opening, ring expansion and ring contraction processes. Over the last few decades synthetic chemists have drastically expanded the knowledge in the area of cyclobutane synthesis. Historic examples and recent progress in the field will be discussed in subsequent sections.

3.1.2 Mechanistic considerations of [2+2] photocycloadditions

The most widely used method for the preparation of cyclobutane compounds is the [2+2] photocycloaddition. A [2+2] cycloaddition entails the formation of two new σ -bonds from the existing π -bonds of the reactants. Interaction of the HOMO and LUMO in a thermal reaction cannot result in suprafacial overlap, disallowing the reaction from occurring. Promotion of one electron to an excited state, and therefore promoting the HOMO to what was formerly the LUMO, results in constructive overlap of the involved orbitals, and therefore a productive reaction (Figure 3.3).

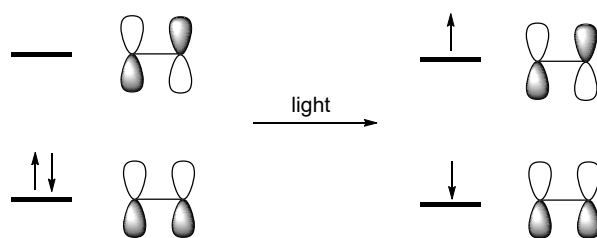
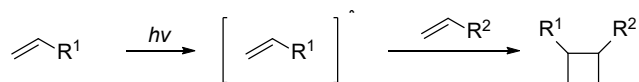


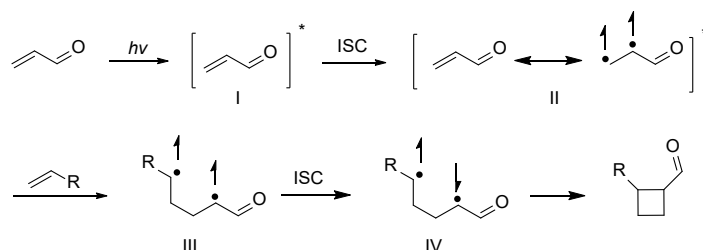
Figure 3.3 Molecular orbitals involved in a [2+2] photocycloaddition

There are multiple modes of excitation that can be utilized to promote a [2+2] photocycloaddition. The most straightforward of the methods involves the direct excitation of one olefin from its ground state (S_0) to its first excited state S_1 , which then reacts with another olefin, or with another molecule of itself (Scheme 3.1).



Scheme 3.1 [2+2] Photocycloaddition via direct excitation

While straightforward, this method is only feasible for conjugated olefins, as the first excited state (S_1) for non-conjugated olefins is typically too high energy above S_0 for an electron to be promoted using commercial irradiation sources. Additionally, fluorescence and internal conversion are often competitive pathways, decreasing the efficiency of the desired reaction. Salomon and Kochi demonstrated that copper(I) salts can catalyse the [2+2] photodimerization of non-conjugated alkenes via metal-to-ligand charge transfer, or ligand-to-metal charge transfer which lowers the energy of the S_1 state, making the transformation feasible.^{153, 154} Photocycloadditions can also occur via their first excited triplet state (T_1), accessed via intersystem crossing (ISC) from the first excited singlet state (S_1) to the lower energy triplet state (Scheme 3.2). ISC is typically rapid with enone substrates. The triplet excited state (T_1) is a long-lived species from which photochemical reactions can occur. Direct excitation of an enone to its first excited singlet state (intermediate I), followed by ISC to its first excited triplet state (intermediate II) and addition to another alkene gives diradical intermediate III. This intermediate undergoes intersystem crossing to intermediate IV, followed by radical recombination to close the 4-membered ring.



Scheme 3.2 [2+2] Photocycloaddition via its triplet state (T_1)

To increase the population of the triplet state, triplet sensitizer molecules are often employed. This is advantageous as longer wavelength light can be used, since sensitizers typically have a low lying S_1 state. The sensitizer molecule absorbs energy, promotes an electron to the S_1 state, followed by ISC to its triplet state T_1 . Once in its triplet state, it can transfer its energy to an olefin, promoting an electron from the olefin's ground state to the triplet state (Figure 3.4). In order for this to be an efficient process, the triplet energy of the olefin must be lower than the triplet energy of the sensitizer. The sensitizer must also show a high ISC rate.

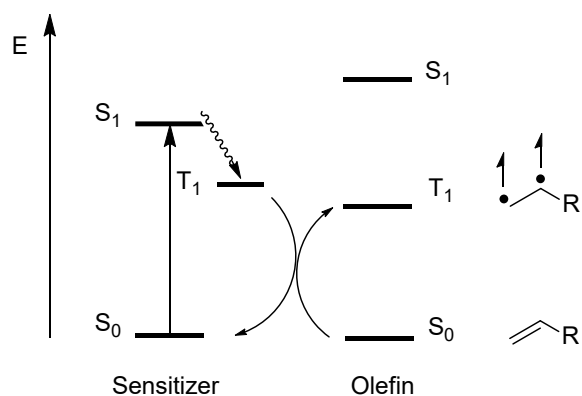


Figure 3.4 Excitation mechanism via triplet energy transfer from sensitizer

The last mechanism by which [2+2] photocycloadditions can be initiated is by photoredox catalysis (Figure 3.5). A photocatalyst can be excited by light, then undergo ISC to its triplet state. This long-lived state can then participate in single electron transfer (SET) events with the substrate. The photocatalyst can either act as an oxidant or a reductant, depending on the substrate. In an oxidative quenching cycle, the photocatalyst acts as a reductant, reducing the substrate to a radical anion intermediate, which can then add to another olefin, then undergo another SET event to give a diradical intermediate which can cyclize to the product. Alternatively, in a reductive quenching cycle, the photocatalyst acts as an oxidant, removing an electron from the substrate resulting in a radical cation. This intermediate can add to another olefin, then undergo single electron transfer from the reduced photocatalyst to form a diradical that can cyclize to the product. Often an additional electron transfer agent is employed as a co-catalyst.

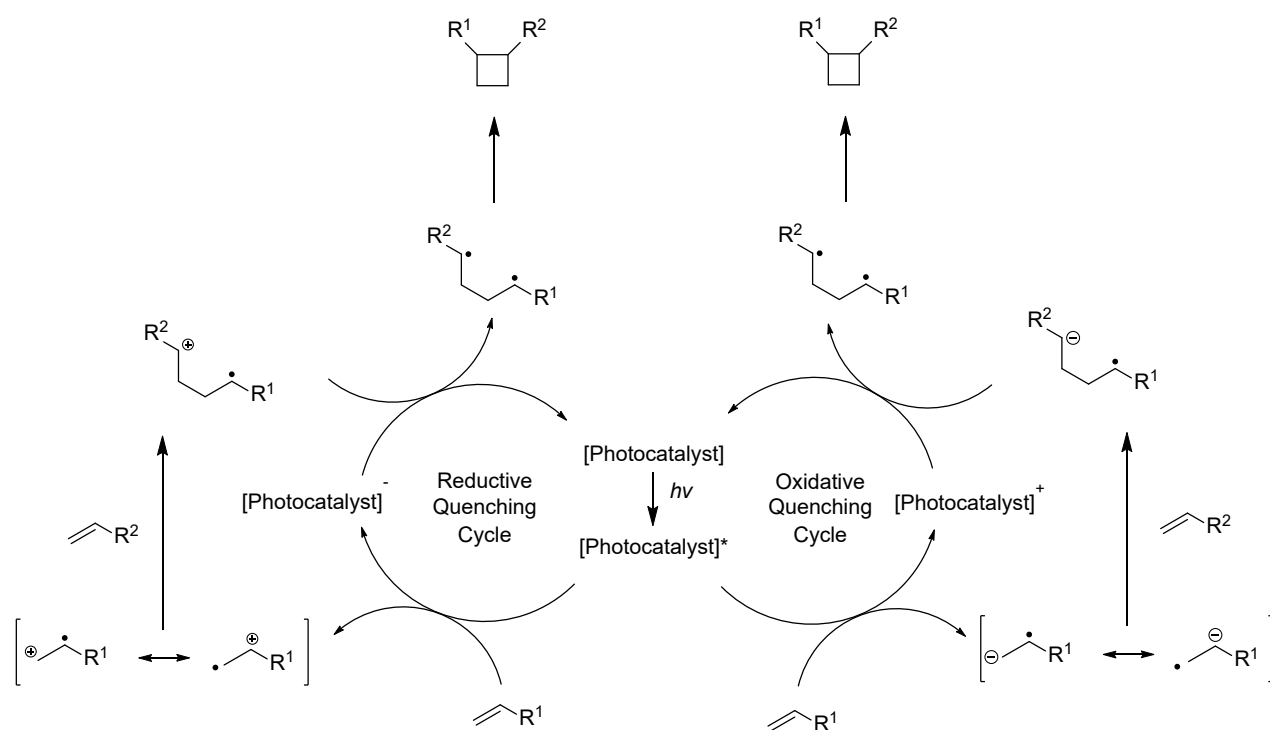


Figure 3.5 [2+2] photocycloaddition via photoredox catalysis

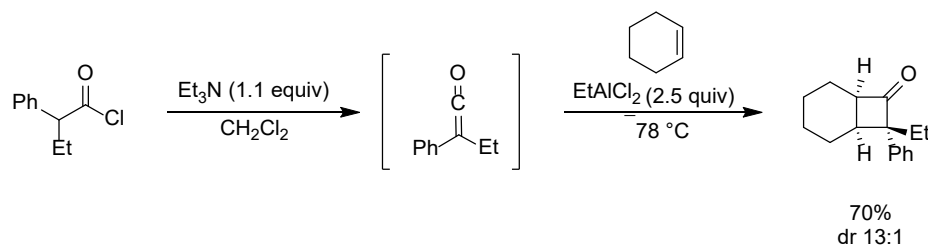
3.1.3 Thermal [2+2] cycloadditions

There is a plethora of literature on photochemical mediated synthesis of cyclobutane containing compounds.^{155, 156, 157} The thermal equivalent, though, has seen much less attention. As mentioned in section 3.1.2, suprafacial thermal [2+2] cycloadditions are forbidden according to the Woodward-Hoffman rules of conservation of orbital symmetry. Therefore, these reactions must proceed in a stepwise manner. The disadvantage to this is that long-lived intermediates are generated, and undesired side reactions can take place.

3.1.3.1 Thermal [2+2] cycloaddition of ketenes and allenes

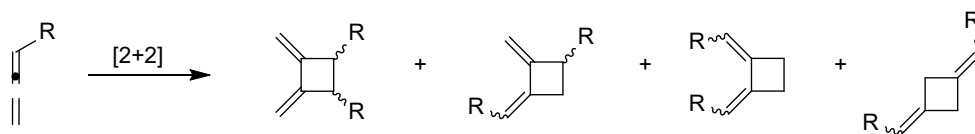
Ketenes are a commonly encountered reaction partners when discussing thermal [2+2] cycloadditions. They can undergo [2+2] cycloadditions with alkenes via antarafacial overlap of orbitals, yielding cyclobutanones. Unfortunately, these reactions are plagued with several problems, including the need for reactive olefins as coupling partners, low yield and

diastereoselectivity, and the dimerization of unsubstituted ketenes.¹⁵⁸ Several strategies have been realized to overcome these issues, such as employing chloro or thio substituted ketenes, or the use of ketene iminium salts. Utilizing these ketene surrogates allows for the coupling with less activated olefins.^{159, 160, 161} More recently, Brown has introduced a strategy to overcome some of these issues by introducing a Lewis acid into the reaction (Scheme 3.3).¹⁶² Interaction of the Lewis acid and the ketene lowered the LUMO energy of the ketene, making it more electrophilic.



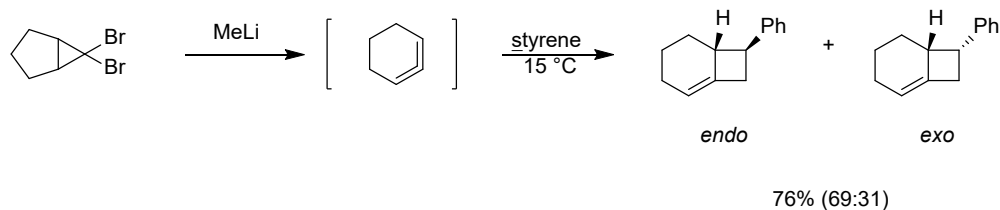
Scheme 3.3 Lewis acid assisted [2+2] cyclization of ketenes

Allenes are also common substrates employed in thermal [2+2] cycloadditions. While some studies point to a concerted mechanism (via $[\pi_{2a} + \pi_{2s}]$ interaction), most examples are understood to proceed via diradical intermediates.¹⁶³ The dimerization of allenes to substituted cyclobutanes has been studied extensively.^{164, 165, 166} These reactions can be problematic, as unsymmetrically substituted allenes can produce multiple regioisomers (Scheme 3.4).



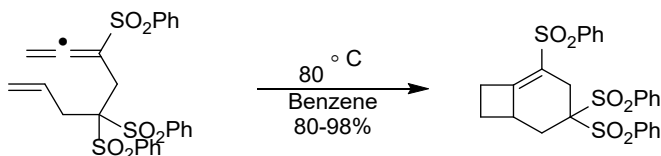
Scheme 3.4 Regioisomers in a [2+2] dimerization of allenes

Intermolecular [2+2] reactions between allenes and olefins often require either the olefin partner or the allene itself to be electron deficient in nature. Alternatively, in situ generated cyclic allenes can react with a variety of coupling partners, due to the strain energy associated with having the allene moiety contained within a ring (Scheme 3.5). This can be accomplished both intra- and intermolecularly.^{167, 168, 169}



Scheme 3.5 Formal [2+2] cycloaddition of in situ generated cyclic allenes

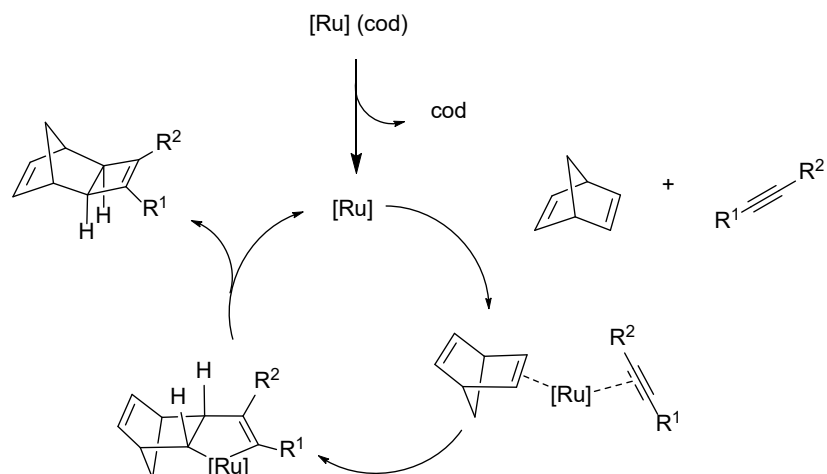
Intramolecular [2+2] reactions of allenes are useful for synthesizing bicyclic compounds. These reactions can also suffer from regioselectivity issues, as either the internal or external double bond of the allene can react, giving either the proximal or distal adduct, respectively. Padwa and coworkers found that introducing a sulfonyl group to the α position resulted in exclusive formation of the distal adduct (Scheme 3.6).¹⁷⁰ Other research groups have employed other activators, such as carboxylates, difluoroallenes, and β -lactams.^{171, 172, 173}



Scheme 3.6 [2+2] Cycloaddition of sulphonyl-substituted allenes

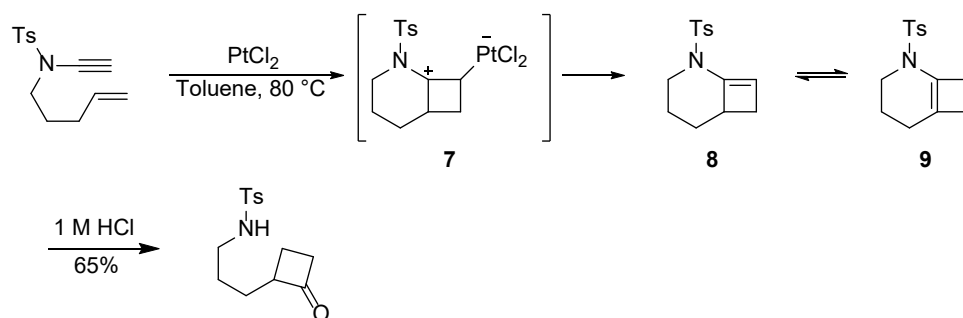
3.1.3.2 Metal catalyzed [2+2] cycloadditions of alkenes

Some early examples of non-photochemically promoted [2+2] reactions are the metal catalyzed reactions. Watanabe and coworkers described the [2+2] cycloaddition of norbornenes with alkynes, catalyzed by $[\text{Cp}^*\text{RuCl}(\text{cod})]$ (Scheme 3.7).¹⁷⁴ Coordination of the alkene and norbornene to ruthenium in an *exo* fashion, followed by oxidative cyclization and successive reductive elimination gave the cyclobutene product. A similar report was published by Riddell et al., instead using ynamides as the coupling partners with norbornene.¹⁷⁵



Scheme 3.7 Ruthenium catalyzed [2+2] cycloaddition of norbornene

Malacria and coworkers utilized platinum to enable the cyclization of ene-ynamides to form bicyclic nitrogenated heterocycles (Scheme 3.8).¹⁷⁶ Initial π -complexation of platinum to the alkyne moiety facilitated ring closure to intermediate **7**, followed by metal elimination to give **8**. Isomerization of **8** resulted in product **9**. The authors mentioned that the products **9** were prone to decomposition (as illustrated by the isolation of product **9** in only 34% yield), so the crude cycloisomerized products were hydrolyzed to the more stable cyclobutanones. A similar study by Cossy and coworkers demonstrated the cycloisomerization of ene-ynamides, using AuCl.¹⁷⁷

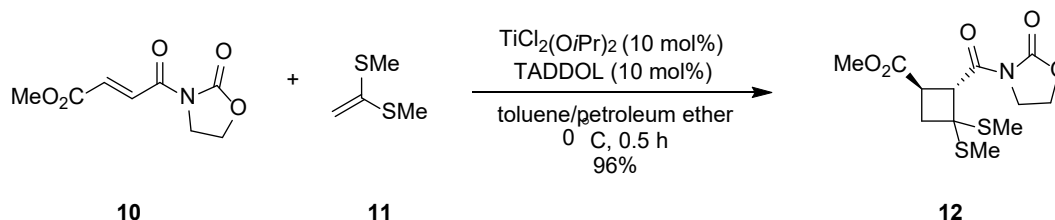


Scheme 3.8 Platinum catalyzed [2+2] reaction of ene-ynamides

Transition metal catalyzed transformations have also become very popular in the [2+2+2] reaction of alkenes and alkynes for the construction of 6-membered carbocycles and heterocycles.¹⁷⁸

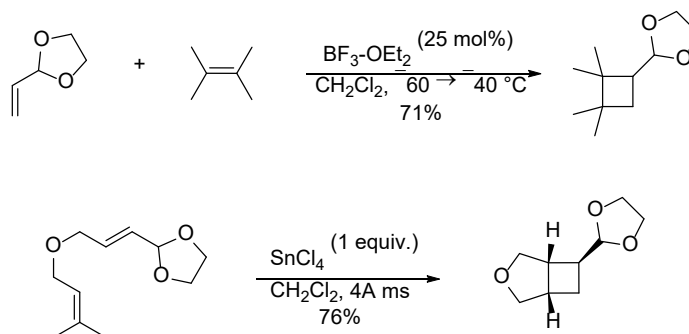
3.1.3.3 Lewis acid mediated [2+2] cycloadditions

Another class of formal [2+2] reactions are Lewis acid mediated ring closures. These reactions often proceed by Michael-aldol mechanism, through a zwitterionic intermediate. In 1992 Narasaka and coworkers reported an asymmetric [2+2] cycloaddition between unsaturated oxazolidinone **10** and alkenyl sulfide **11** (Scheme 3.9).¹⁷⁹ This reaction, catalyzed by a TADDOL-titanium reagent, proceeded in a stepwise manner through a Michael-aldol type mechanism.



Scheme 3.9 Ti(IV) catalyzed asymmetric [2+2] cycloaddition

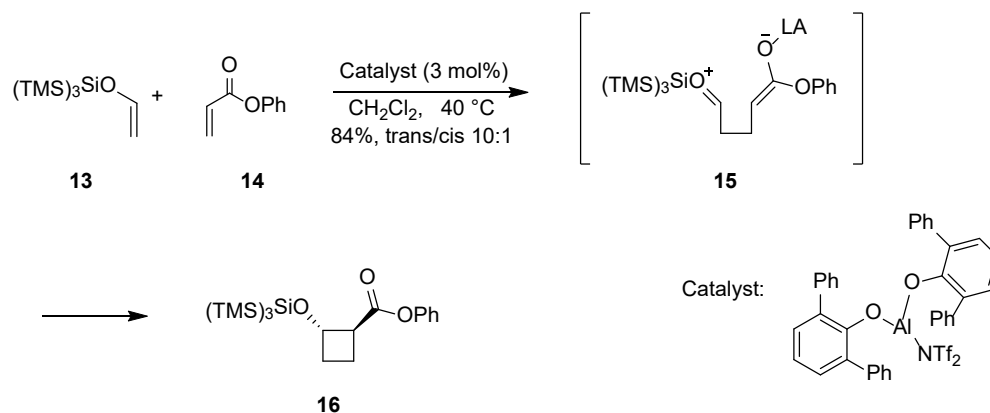
Another early report comes from Gassman and Lottes, who described the Lewis-acid mediated opening of cyclic acetals to generate an allyl cation intermediate.¹⁸⁰ This intermediate was then attacked by an unactivated olefin, followed by ring closure and reformation of the acetal. Following this report, Hsung and coworkers described an intramolecular version of this reaction, towards the total synthesis of *epi*-raikovenal (Scheme 3.10).¹⁸¹



Scheme 3.10 [2+2] cycloadditions of vinyl acetals

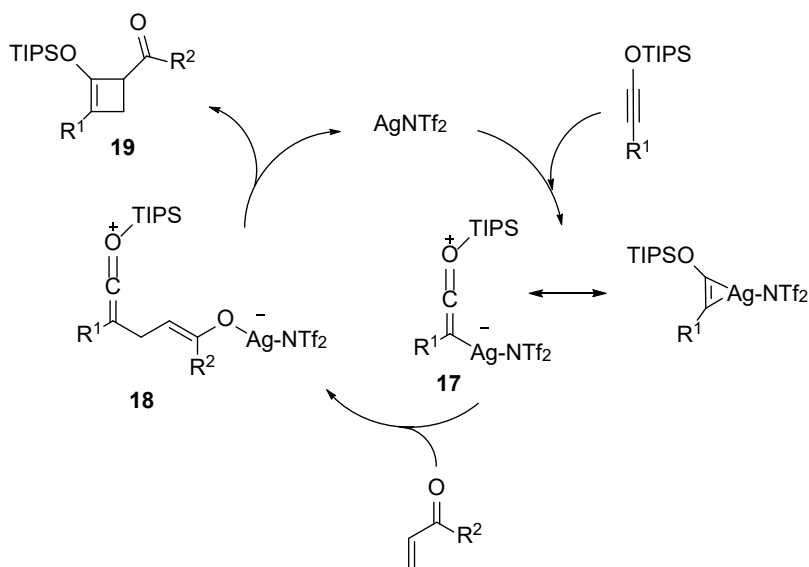
Later, Boxer and Yamamoto reported a diastereoselective formal [2+2] reaction between silyl enol ethers **13** and acrylates **14**, catalyzed by an aluminum triflimide catalyst.¹⁸² Important to this reaction was the tris(trimethylsilyl)silyl group providing increased stabilization to the intermediate oxocarbenium cation **15** via hyperconjugation. Simple silyl enol ethers did not yield

any desired cyclobutane product. The bulky aluminum catalyst was chosen to provide a steric environment that would enforce diastereoselectivity in the ring closing step. The products **16** were obtained in high yield and diastereoselectivity.



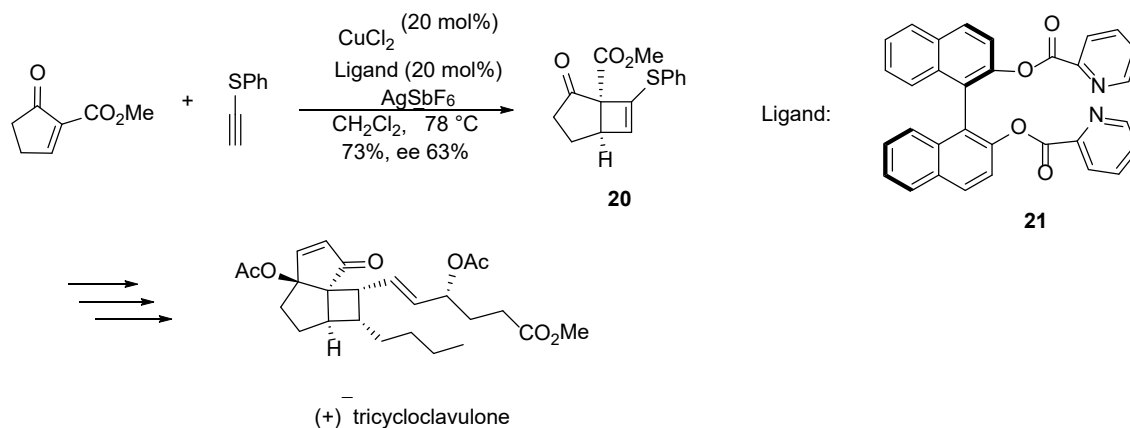
Scheme 3.11 [2+2] cyclization of silyl enol ethers and acrylates

Kozmin and coworkers demonstrated the aptitude of siloxy alkynes towards [2+2] cycloaddition using Ag(I) as the catalyst (Scheme 3.12).¹⁸³ The mechanism of this reaction is presumed to occur via silver activation of the siloxy alkyne forming ketenium ion **17**, followed by 1,4- addition to the enone resulting in intermediate **18** and ring closure to form the cyclobutene product **19**. The authors mentioned the possibility of the reaction occurring via Lewis acid activation of the enone first, but deemed this pathway less likely.



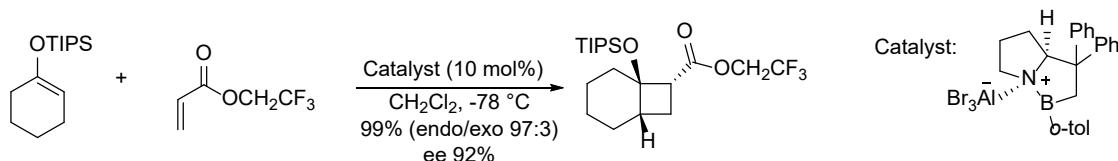
Scheme 3.12 Silver(I) catalyzed cycloaddition of siloxy alkynes to enones

More recent examples of Lewis acid catalyzed [2+2] cycloaddition reactions have focused on obtaining enantioselective transformations. Iguchi and coworkers developed an enantioselective [2+2] cycloaddition, employing a chiral bipyridine ligand, towards enantioselective total synthesis of (+)-tricycloclavulone (Scheme 3.13).¹⁸⁴ The reaction between phenylthioacetylene and 2-methoxycarbonyl-2-cyclopenten-1-one in the presence of ligand **21** and copper salts resulted in cyclobutene **20** in 67% yield and 73% ee. The authors mentioned that previously used chiral catalysts for similar transformations (such as the Ti-TADDOL system, described by Narasaka) gave inferior results, so this novel catalytic system was developed.



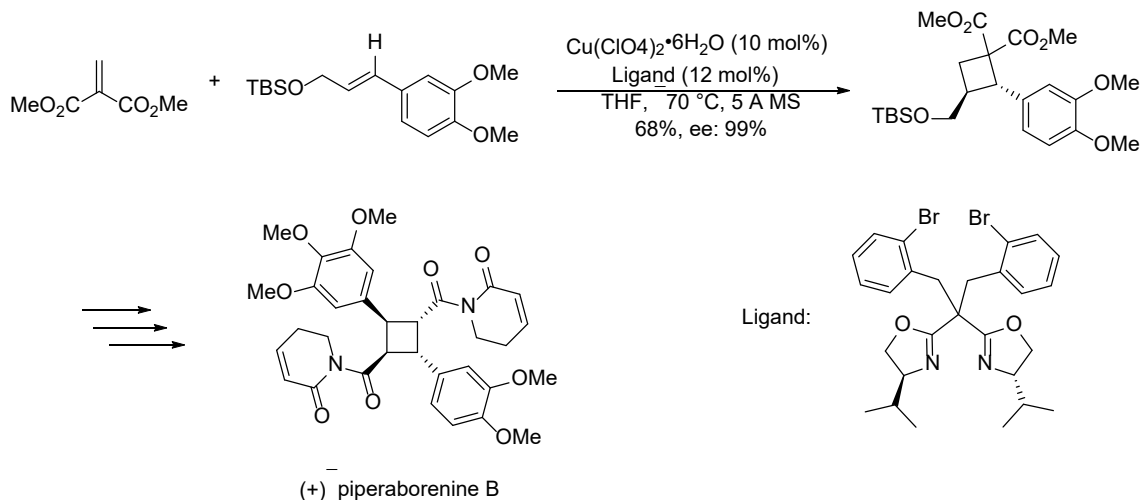
Scheme 3.13 Total synthesis of (+)-tricycloclavulone

Canales and Corey described the enantioselective cycloaddition of silyl enol ethers and an α,β -unsaturated ester using a chiral aluminum bromide complex (Scheme 3.14).¹⁸⁵ While the diastereoselectivities and enantiomeric excesses were quite high for all substrates, there was a limited substrate scope as the only ester used was the highly reactive trifluoroethyl acrylate.



Scheme 3.14 Chiral aluminum complex-catalyzed [2+2] cycloaddition

Recently, Tang and coworkers accomplished the total synthesis of (+)-piperarborenine B, leveraging an enantioselective [2+2] cycloaddition between methylidenemalonate and styrenes (Scheme 3.15).¹⁸⁶ The developed methodology utilized a Cu(II)/bisoxazoline system to obtain cyclobutane products in moderate to high yields, and high enantioselectivities. The newly developed method was applied to the total synthesis of (+)-piperarborenine B, with the key cyclobutane forming step occurring in 68% yield and 99% ee.

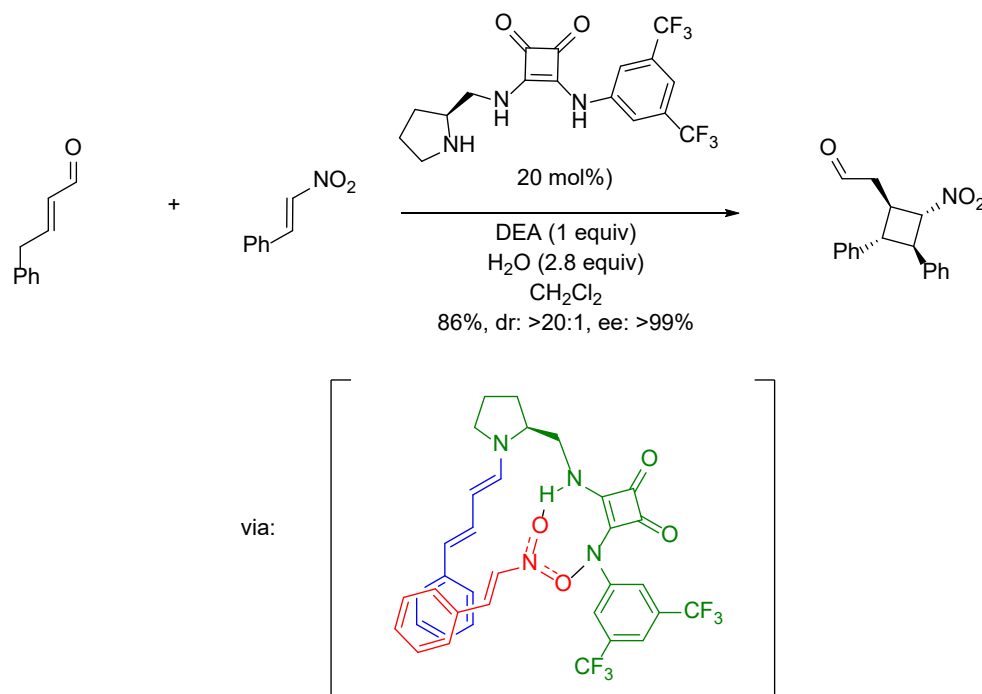


Scheme 3.15 Total synthesis of (+)-piperarborenine B

3.1.3.4 Organocatalytic formal [2+2] cycloadditions

Several groups have also turned to organocatalysis to realize enantioselective formal [2+2] cyclizations. The Jørgensen group utilized an organocatalyst that activated both reaction partners

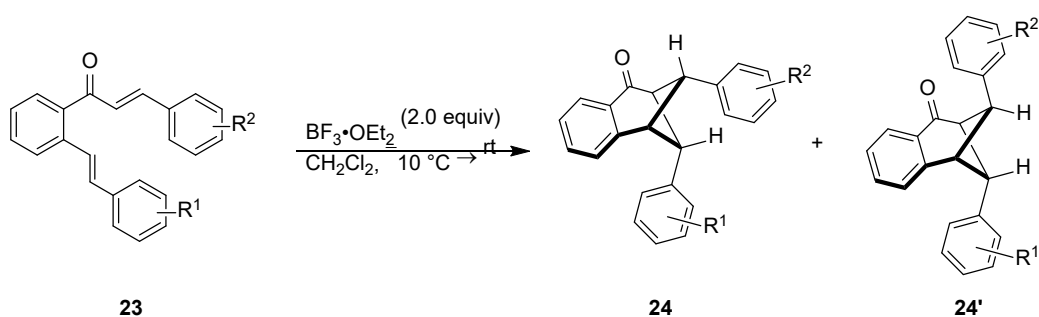
simultaneously (Scheme 3.16).¹⁸⁷ The squaramide-based amino catalyst activated the α,β -unsaturated aldehyde via formation of a dienamine, and activated the nitroolefin by hydrogen-bonding catalysis. The products of this reaction were cyclobutanes bearing four contiguous stereocenters; this was accomplished in high yields and exceptional enantioselectivity (greater than 99% ee for all substrates).



Scheme 3.16 Organocatalytic [2+2] cycloaddition via cooperative diamine/H-bond directing catalysis

3.2 Background

As part of the continuous program of our group to develop Nazarov electrocyclizations and similar transformations, the treatment of *o*-styrenyl chalcones with Lewis acid was investigated; the hope was that these substrates would undergo electrocyclization leading to 7-membered ring systems. This study, conducted by Dr. Shorena Gelozia as part of her PhD thesis, revealed that treatment of substrates **23** with $\text{BF}_3 \cdot \text{OEt}_2$ led to two diastereomeric products **24** and **24'** through a formal crossed [2+2] cycloaddition (Scheme 3.17).¹⁸⁸ The X-ray crystal structure shown in Figure 3.6 was crucial to the initial structural and stereochemical assignment of product **24a**.



Scheme 3.17 Formal crossed [2+2] cycloaddition of *o*-styrenyl chalcones

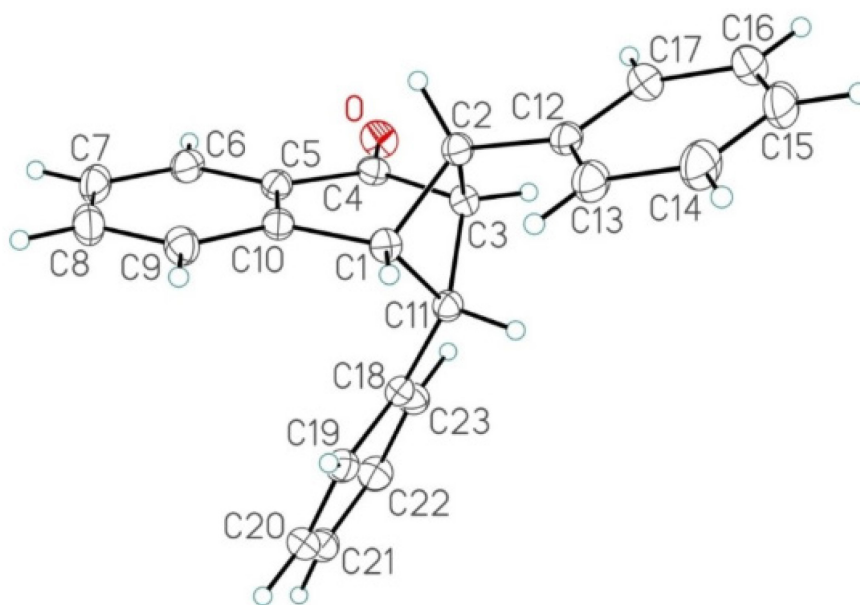
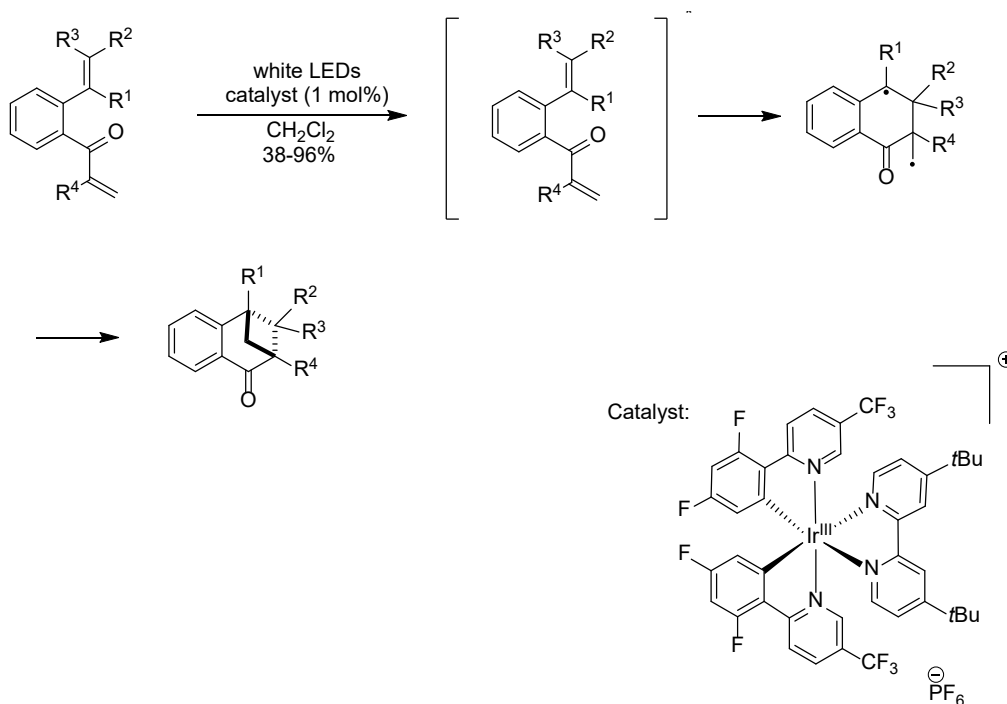


Figure 3.6 X-Ray crystal structure of **24a**

A report by Kwon in 2017 demonstrated the photocycloaddition of similar substrates, using visible light, and a polypyridyl Ir(III) catalyst as a triplet photosensitizer (Scheme 3.18).¹⁸⁹ This method proceeds via energy transfer from the sensitizer to the enone, exciting the enone to its triplet excited state. Cyclization to form a biradical, followed by radical recombination gave the bridged bicyclic products. High yields and excellent regioselectivity for the crossed product were observed. Computational studies rationalized the regiocontrol; the observed diradical was thermodynamically favoured over other possible intermediates and led to the crossed products.



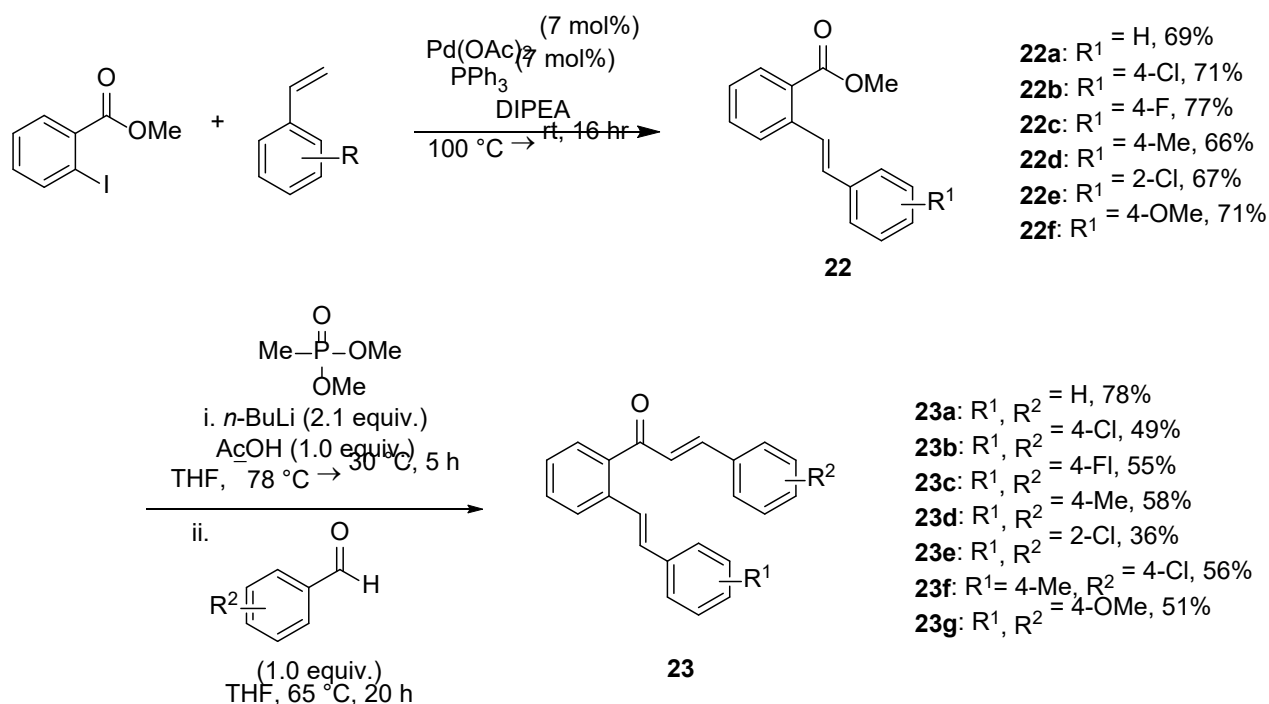
Scheme 3.18 Crossed [2+2] photocycloaddition via triplet energy transfer

The facile conversion of *o*-styrenyl chalcones to interesting bicyclic scaffolds inspired us to investigate whether this transformation could be carried out catalytically, and possibly enantioselectively.

3.3 Results and discussion

3.3.1 Development of a catalytic formal [2+2] cycloaddition

The substrates were synthesized in a two-step procedure; a Heck coupling between methyl 2-iodobenzoate and substituted styrenes gave products **22**.³⁹ Reaction of dimethyl (lithiomethyl)phosphonate with **22**, followed by Horner-Wadsworth-Emmons reaction with substituted benzaldehydes gave substrates **23** (Scheme 3.19).

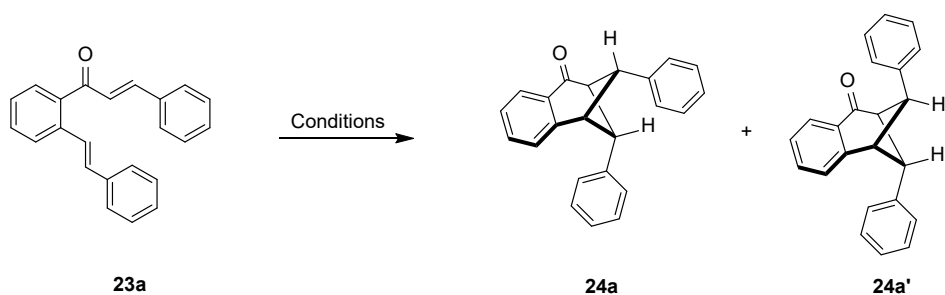


Scheme 3.19 Preparation of *o*-styrenyl chalcones

To investigate the catalytic transformation of *o*-styrenyl chalcones, compound **23a** was chosen as the model substrate (Table 3.1). Several Lewis acids were screened for their ability to transform compound **23a** to **24a** and **24a'**, typically in a loading of 20 mol% (entries 1-6). Early studies indicated that Lewis acids at room temperature would not allow the reaction to proceed to completion, so temperatures above room temperature were screened. It was found that copper triflate at 50 °C yielded the desired products **24a** and **24a'** in 31% and 10% yield (entry 1). FeCl₃ and Zn(OTf)₂ gave no conversion or nonselective decomposition (entries 2-3). Titanium (IV) chloride gave 32% yield of **24a** with only trace amounts of **24a'** being observed in the crude ¹H NMR spectrum (entry 4). Scandium (III) triflate only gave 11% of product **24a**, and no signals for **24a'** were observed in the crude ¹H NMR spectrum (entry 5). Promising results were observed with indium (III) triflate at 60 °C; compounds **24a** and **24a'** were obtained in 51% and 12% yield, respectively (entry 6). As some starting material was observed in the crude ¹H NMR spectrum the temperature was increased to 80 °C, which resulted in decomposition (entry 7). When the Lewis acid was switched to indium (III) chloride at 80 °C no decomposition was observed, although the yield was the same as entry 6, with inferior diastereoselectivity (entry 8). At this point, the use of additives was explored. Sodium tetrakis[3,5-bis(trifluoromethyl)phenyl]borate (NaBARF) was

chosen, as it can act as a non-coordinating anion; this makes the Lewis acid metal center more cationic, and thus potentially better able to activate the enone carbonyl in the [2+2] cycloaddition. It was found that when using 60 mol% NaBARF (3 equiv. relative to the Lewis acid) with 20 mol% indium (III) triflate, the reaction proceeded resulting in 49% and 12% of **24a** and **24a'** respectively, at room temperature (entry 9). This result was exciting, as the eventual goal for this project is to develop enantioselective conditions, so having reactions conditions at or below room temperature is desirable to maximize selectivity involving transition states with small energetic differences. Decreasing the amount of NaBARF used to 40 mol% resulted in the same overall yield, but increased diastereoselectivity for **24a** over **24a'** (entry 10). This result was interesting; it suggested that the increased Lewis acidity observed when using more equivalents of the non-coordinating anion may facilitate equilibration between the two diastereomeric cycloadducts (Scheme 3.21). Encouraged by the ability of NaBARF to help facilitate product formation, scandium (III) triflate was revisited as a Lewis acid, using NaBARF as an additive (entry 11). Comparing the two Lewis acids ($\text{Sc}(\text{OTf})_3$ and $\text{In}(\text{OTf})_3$), the yields and diastereoselectivity were essentially identical. Scandium (III) triflate was chosen as the optimal catalyst to move forward with for two reasons. First, while the price per gram of $\text{Sc}(\text{OTf})_3$ and $\text{In}(\text{OTf})_3$ is very similar, $\text{Sc}(\text{OTf})_3$ has a much lower molecular weight. Second, thinking of the eventual development of an enantioselective version of this reaction, there is more precedent in the literature using chiral ligands in scandium complexes than with indium. Next, the solvent was investigated, and it was found that when the reaction was performed in acetonitrile, no product was formed (entry 12). When the reaction was performed in toluene, no difference was observed in yield or diastereoselectivity from dichloromethane (entry 13). There was no appreciable difference in the reaction when using 40 mol% NaBARF over 20 mol% (entry 14). An attempt was made to decrease the catalyst loading of $\text{Sc}(\text{OTf})_3$, but with only 10 mol% the reaction did not go to completion and only 30% of **24a** and 4% of **24a'** were obtained. Finally, when the reaction time was increased to 24 h, the yield of the reaction increased slightly to 58% **24a** and 5% **24a'** (entry 16). These were taken as the optimized conditions to be used when evaluating the substrate scope.

Table 3.1 Screening of catalytic conditions for the formal [2+2] cycloaddition of **23a**

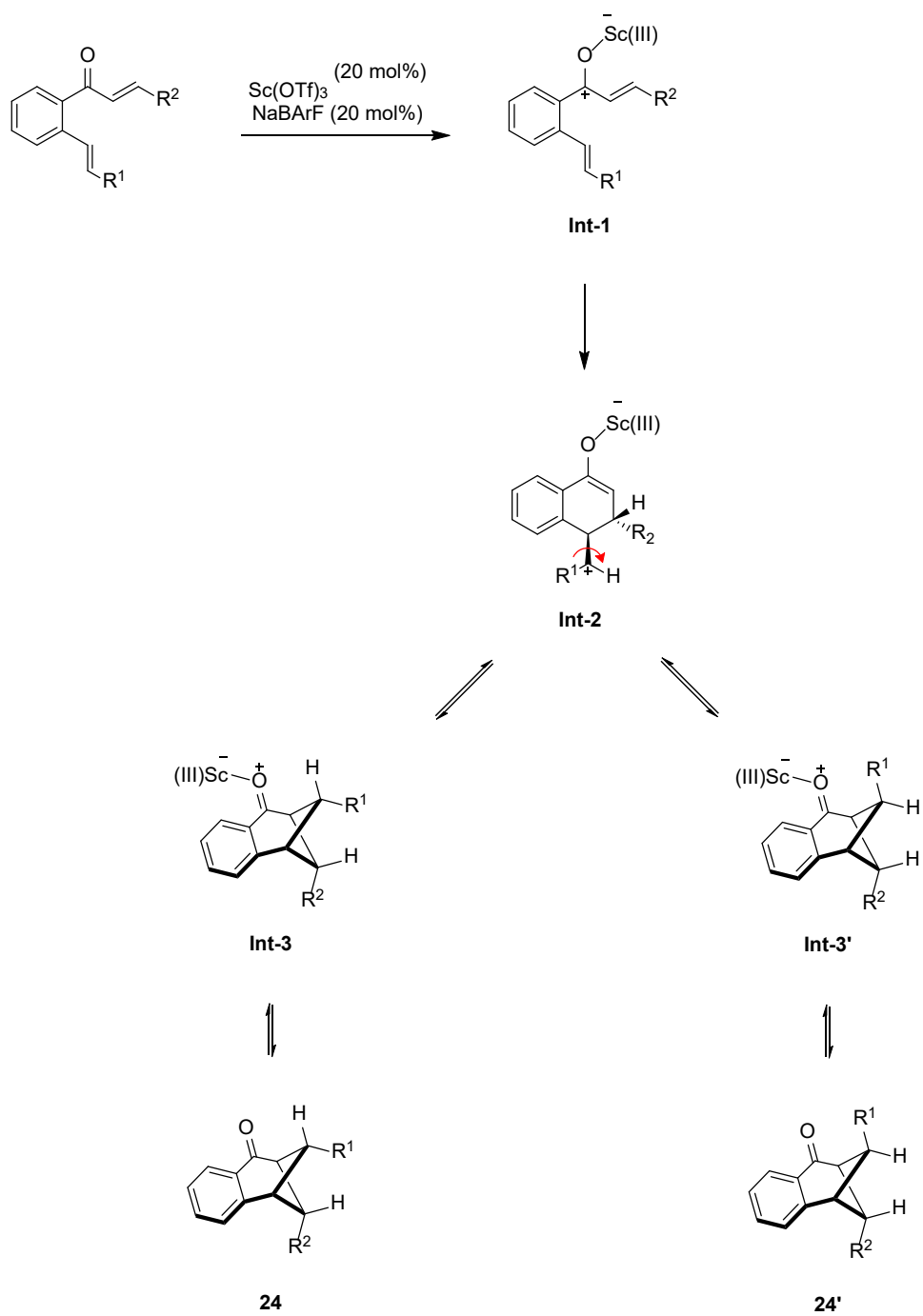


Entry	Lewis Acid (mol %)	Solvent	Temperature	Additive	Time	Yield 24a ^b	Yield 24a' ^b
1	Cu(OTf) ₂ (20 mol%)	DCE	rt → 50 °C	-	16 h	31	10
2	FeCl ₃ (20 mol%)	CH ₂ Cl ₂	rt → 40 °C	-	20 h	- ^c	-
3	Zn(OTf) ₂ (20 mol%)	DCE	rt → 50 °C	-	16 h	- ^d	-
4	TiCl ₄ (20 mol%)	CH ₂ Cl ₂	-10 °C → rt	-	16 h	32	trace
5	Sc(OTf) ₃ (20 mol%)	DCE	rt → 80 °C	-	16 h	11	-
6	In(OTf) ₃ (20 mol%)	DCE	rt → 60 °C	-	20 h	51	12
7	In(OTf) ₃ (20 mol%)	DCE	rt → 80 °C	-	20 h	- ^c	-
8	InCl ₃ (20 mol%)	DCE	rt → 80 °C	-	20 h	40	24
9	In(OTf) ₃ (20 mol%)	CH ₂ Cl ₂	rt	NaBArF (60 mol%)	20 h	48	12
10	In(OTf) ₃ (20 mol%)	CH ₂ Cl ₂	rt	NaBArF (40 mol%)	20 h	55	4
11	Sc(OTf) ₃ (20 mol%)	CH ₂ Cl ₂	rt	NaBArF (40 mol%)	20 h	54	5
12	Sc(OTf) ₃ (20 mol%)	ACN	rt	NaBArF (40 mol%)	20 h	- ^d	-
13	Sc(OTf) ₃ (20 mol%)	Toluene	rt	NaBArF (40 mol%)	20 h	55	4
14	Sc(OTf) ₃ (20 mol%)	CH ₂ Cl ₂	rt	NaBArF (20 mol%)	20 h	50	4
15	Sc(OTf) ₃ (10 mol%)	CH ₂ Cl ₂	rt	NaBArF (20 mol%)	20 h	30	4

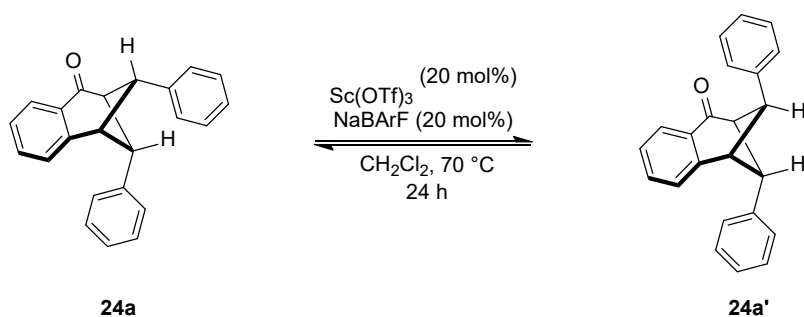
16	Sc(OTf) ₃ (20 mol%)	CH ₂ Cl ₂	rt	NaBArF (20 mol%)	24 h	58	5
----	--------------------------------	---------------------------------	----	---------------------	------	----	---

^aConditions: Lewis acid was dissolved in solvent (2 mL), **23a** (0.3 mmol) dissolved in same solvent (3 mL) was added, and was allowed to stir for designated time. Reactions were quenched by elution through a short pad of silica, eluted with CH₂Cl₂. ^bYield determined by quantitative NMR spectroscopy by comparison of average of aliphatic protons to 1-bromo-3,5-bis(trifluoromethyl)benzene as internal standard. ^cDecomposition of the substrate observed in crude ¹H NMR spectrum. ^dOnly starting material observed in crude ¹H NMR spectrum.

The proposed mechanism for the formation of products **24** and **24'** is illustrated in Scheme 3.20. Lewis acid activation of the enone by scandium(III) complex gives **int-1**. Michael-type addition of the styrenyl double bond onto the enone double bond results in benzylic cation **int-2**. Rotation around the indicated C–C single bond, followed by enolate attack onto the benzylic cation from either face gives **int-3** and **int-3'**. Release of the Lewis acid gives products **24** and **24'**. The ability for cycloadducts **24** and **24'** to interconvert via cyclobutane ring opening was confirmed with two control studies. Products **24a** and **24a'** were separately subjected to the optimized reaction conditions; no interconversion was observed at room temperature, but increasing the temperature to 70 °C showed nearly 1:1 equilibration of products (Scheme 3.21).

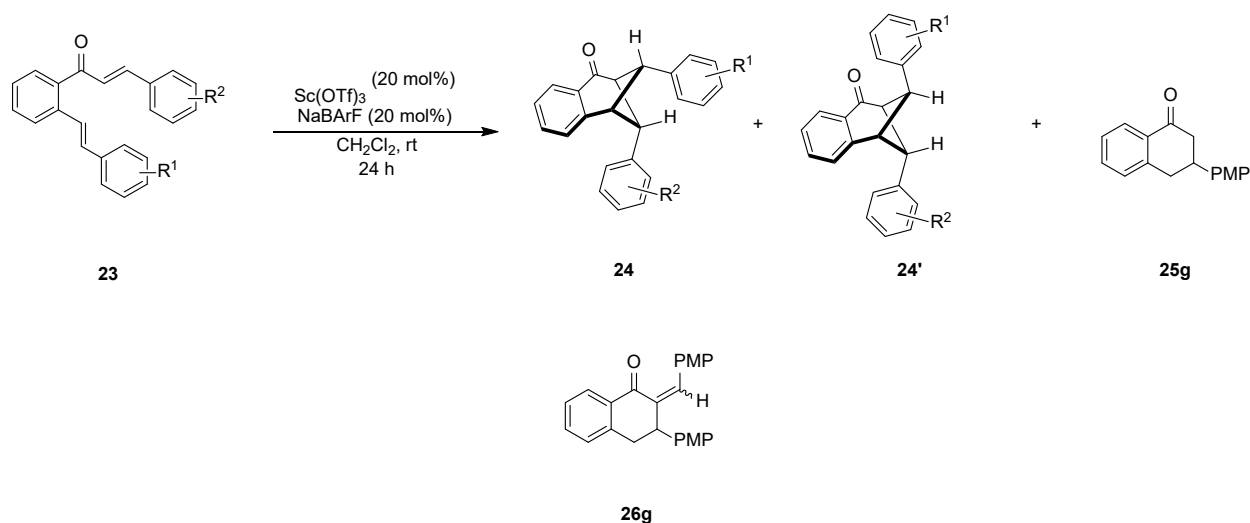


Scheme 3.20 Proposed mechanism for the formation of products **24** and **24'**



Scheme 3.21 Equilibration of diastereomers via cyclobutane ring opening

With optimized conditions in hand, the generality of the reaction was investigated. Six additional substrates were chosen from Dr. Gelozia's initial study, to examine if any improvements in yield or diastereoselectivity were observed between the two methods (Table 3.2).

Table 3.2 Generality of the catalytic formal [2+2] cycloaddition

Entry ^a	Substrate	R ¹ /R ²	Products	Yield (%) ^b	dr (24:24') ^c
1	23a	H/H	24a/24a'	63	11.6:1
2	23b	4-Cl/4-Cl	24b/24b'	70	6.7:1
3	23c	4-F/4-F	24c/24c'	75	4.8:1
4	23d	4-Me/4-Me	24d/24d'	77	2.3:1
5 ^c	23e	2-Cl/2-Cl	24e/24e'	75	11.5:1
6	23f	4-Me/4-Cl	24f/24f'	78	1.2:1
7 ^d	23g	4-OMe/4-OMe	24g/24g'/25g/26g	24g/24g' : 31 25g : 14 26g : 5	1:1.2

^aConditions: Sc(OTf)₃ (20 mol%) and NaBARF (20 mol%) were stirred under N₂ in CH₂Cl₂ (2 mL) for 2 h. A solution of *o*-styrenyl chalcone **23** (0.3 mmol) in CH₂Cl₂ (3 mL) was added, and the reaction was left to stir for 24 h. The reaction was quenched by filtration through a short pad of silica, eluted with CH₂Cl₂. ^bYields are based on isolated products after column chromatography. ^cRequired 40 mol% catalyst for starting material to be consumed. ^dCompounds **24g** and **26g** were isolated as an inseparable mixture, yield of each compound was determined by comparison of key peaks in the ¹H NMR spectrum to 1-bromo-3,5-bis(trifluoromethyl)benzene as internal standard.

First, the effect of adding an electron withdrawing group was examined (entries 2-3). Both *para*-chloro and fluoro groups furnished the products in comparable yields, and moderate diastereoselectivity with preference for **24** over **24'**. Next, an electron donating group was examined (entry 4). The presence of a *para*-methyl group permitted the formation of the desired products, albeit with significantly reduced diastereoselectivity (entry 4). This is possibly due to the added stabilization provided to the benzylic cation intermediate as compared with the other examined substrates, resulting in a longer-lived **int-2** species, allowing for more rotation of the single bond to erode the diastereoselectivity. Next, the effect of sterics of substitution on the phenyl ring was examined (entry 5). Adding a chloro group to the *ortho*-position of the aromatic ring hindered the reaction significantly. Under the normal reaction conditions, the starting material was not fully consumed; the catalytic loading had to be increased to 40% to see full consumption of starting material. A substrate bearing non-identical phenyl group substitution was examined next (entry 6). This substrate showed high yield, and still only two diastereomers, although the ratio of **24f** to **24f'** was nearly even, for similar reasons to that of entry 4. Lastly, substitution of *para*-methoxy groups on both the aryl units was examined, and in this case competing reactivity pathways became significant (entry 7). The desired compounds were formed in 31% yield, with a 1:1.2 diastereomeric ratio. Product **26g** was formed in 5% yield. This compound co-eluted with **24g** during column chromatography, so the yields of these two products was determined by integration of distinct aliphatic peaks in the ¹H NMR spectrum of the mixture in comparison to 1-bromo-3,5-bis(trifluoromethyl)benzene as the internal standard. This product likely formed from cyclobutane ring opening, followed by proton elimination adjacent to the benzylic cation. Another product was also observed with this substrate, and it proved to be compound **25g**, which was formed in 14% yield. A likely mechanistic pathway for the formation of this product involves ring opening of the product, attack of water on the benzylic cation, followed by an acid catalyzed retro-aldol reaction to afford product **25g**. This mechanism operates on the basis of trace water being present in the reaction; this was confirmed by adding 4 Å molecular sieves to the reaction, which suppressed the formation of this product almost entirely.

In general, results from both stoichiometric BF₃·Et₂O and catalytic Sc(OTf)₃ methods were comparable. The stoichiometric method gave slightly higher yields for all substrates, with one

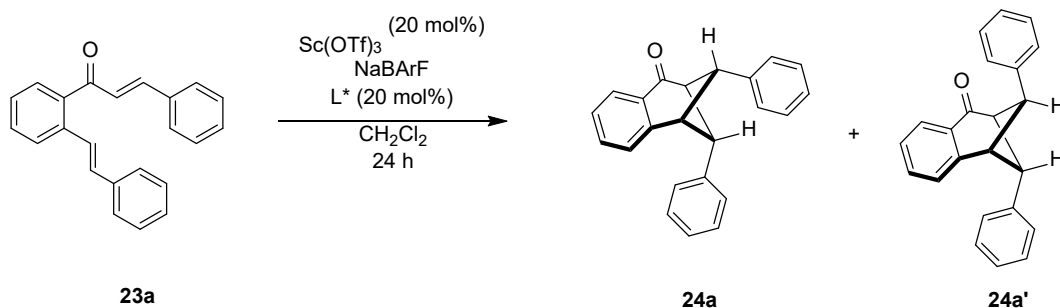
exception being the 4-Me/4-Cl derivative; my catalytic method showed higher combined yield of **24f** and **24f'**, and furnished only two diastereomers. Using the stoichiometric method, another diastereomer was observed, although in a low yield (4%). Diastereomeric ratios were generally higher using the catalytic Sc(OTf)₃ method for substrates bearing electron withdrawing groups or H (**23a-c, e**). The diastereomeric ratio for substrates with electron donating groups on the phenyl ring were very similar, showing little preference for one diastereomer over the other. The advantages for utilizing the catalytic method described in this study are an improvement on diastereomeric ratio for some substrates, ability to use sub-stoichiometric amounts of promoter, and the potential to develop an enantioselective variant of the reaction. Scandium complexes in conjunction with chiral ligands have been used extensively for various enantioselective transformations.¹⁹⁰ The following section will describe some preliminary efforts towards the development of an enantioselective formal [2+2] cyclization of *o*-styrenyl chalcones.

3.3.2 Preliminary investigations into an enantioselective transformation

Substrate **23a** was chosen as the model substrate to conduct a ligand screen (Table 3.3). A variety of ligand classes were evaluated, including pybox, pyox, bisoxazoline, and *N,N*-dioxide ligands (Figure 3.7). The first ligand chosen was a pybox ligand, as these type of ligands are frequently employed with Sc(OTf)₃. Interestingly, when chiral ligand **27a** was introduced to the reaction, it completely suppressed the reaction (entry 1). Increasing the temperature did not show any product formation (entry 2). With the thought that the ligand may be decreasing the Lewis acidity of the metal, the equivalents of NaBArF was increased from 20 to 40 mol%. (entry 3). This only resulted in trace formation of product. Pyox ligand **27b** showed no improvement in the reaction (entry 4). Moving away from pyridine-based ligands, bisoxazoline ligand **27c** was employed, and provided 15% yield of **24a**, when using 20 mol% of NaBArF (entry 5). When the loading of NaBArF was increased to 40 mol%, full consumption of starting material was observed, with a yield of 63 and 5% for **24a** and **24a'**, respectively (entry 6). Unfortunately, no enantiomeric excess was observed by chiral HPLC analysis. Bisoxazoline ligands **27d** and **27e** were screened; both showed full consumption of starting material, but no enantiomeric excess (entries 7-8). The last ligand screened was an *N,N*-dioxide ligand **27f** (entries 9-11). This ligand also completely

suppressed the reaction, in the presence of 20 and 40 mol% of NaBARF. Increasing the temperature to 40 °C yielded 15% **24a**, although unsurprisingly did not show any enantiomeric excess.

Table 3.3 Screening of chiral ligands for the formal [2+2] cycloaddition of **23a**



Entry ^a	Ligand	Equiv. NaBARf	Temperature	Yield (24a/24a') ^b	e.e. ^c
1	27a	20 mol%	rt	0 ^d	-
2	27a	20 mol%	40 °C	0 ^d	-
3	27a	40 mol%	rt	trace	-
4	27b	20 mol%	rt	0 ^d	-
5	27c	20 mol%	rt	15/0	-
6	27c	40 mol%	rt	63/5	-
7	27d	40 mol%	rt	63/6	-
8	27e	40 mol%	rt	56/7	-
9	27f	20 mol%	rt	0 ^d	-
10	27f	40 mol%	rt	0 ^d	-
11	27f	20 mol%	40 °C	15/0	-

^aConditions: Sc(OTf)₃ (20 mol%) and NaBARf (indicated amount), and chiral ligand (20 mol%) were stirred under N₂ in CH₂Cl₂ (0.5 mL) for 2 h. A solution of *o*-styrenyl chalcone **23a** (0.1 mmol) in CH₂Cl₂ (0.5 mL) was added, and the reaction was left to stir for 24 h. The reaction was quenched by filtration through a short pad of silica, eluted with CH₂Cl₂. ^bYield determined by quantitative NMR spectroscopy by comparison of average of aliphatic protons to 1-bromo-3,5-bis(trifluoromethyl)benzene as internal standard. ^cEnantiomeric excess was determined by HPLC

analysis using Chiralpak AS-H column. ^dOnly starting material observed by ¹H NMR spectroscopy.

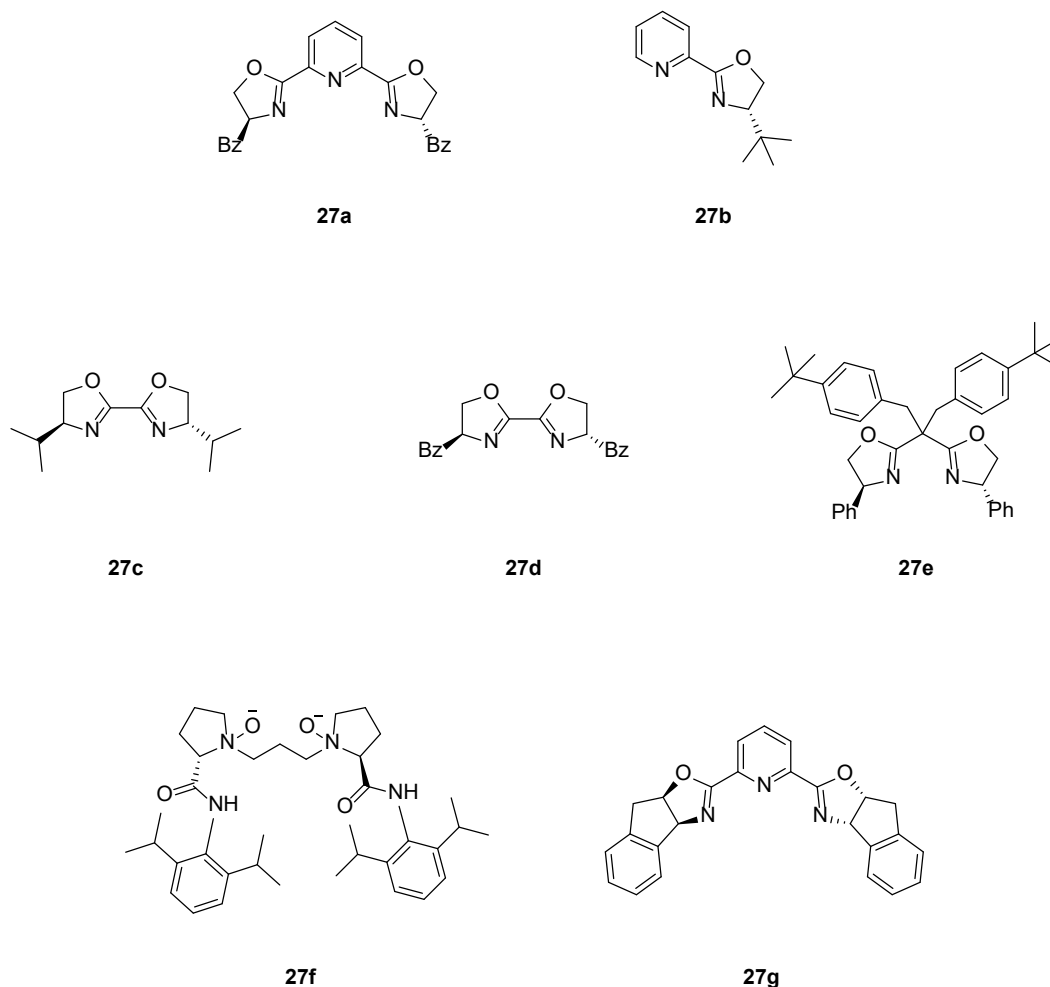
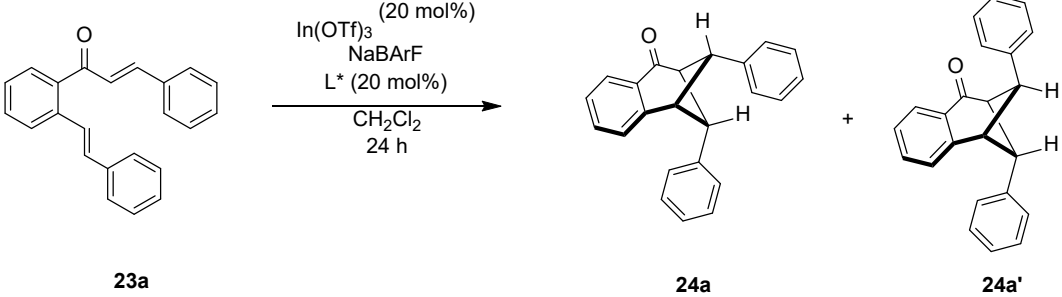


Figure 3.7 Chiral ligands used in formal [2+2] cycloaddition screening study

Bearing in mind that $\text{In}(\text{OTf})_3$ provided very similar results in the racemic reaction condition screening, a short study was conducted using this metal and a select few chiral ligands, to see if the Lewis acid has any effect on the ability to induce an enantioselective transformation (Table 3.4). First, ligand **27d** was screened, and showed 70% and 9% of **24a** and **24a'**, respectively (entry 1). Next, **27e** was screened and yielded 66% and 8% of the desired products (entry 2). N,N-dioxide ligand **27f** was able to give a small amount of product **24a** (10%) at room temperature with

In(OTf)₃ (entry 3). Lastly, a bulky pybox ligand **27g** was screened, but only gave 16% **24a**. Unfortunately, none of the chiral ligands screened with In(OTf)₃ gave any enantiomeric excess.

Table 3.4 Screening of chiral ligands using In(OTf)₃ for the formal [2+2] cycloaddition of **23a**

					
Entry ^a	Ligand	Equiv. NaBARF	Temperature	Yield (24a/24a') ^b	e.e. ^c
1	27d	2	rt	70/9	-
2	27e	2	rt	66/8	-
3	27f	1	rt	10/trace	-
4	27g	2	rt	16/0	-

^aConditions: Sc(OTf)₃ (20 mol%) and NaBARF (indicated amount), and chiral ligand (20 mol%) were stirred under N₂ in CH₂Cl₂ (0.5 mL) for 2 h. A solution of *o*-styrenyl chalcone **23a** (0.1 mmol) in CH₂Cl₂ (0.5 mL) was added, and the reaction was left to stir for 24 h. The reaction was quenched by filtration through a short pad of silica, eluted with CH₂Cl₂. ^bYield determined by quantitative NMR spectroscopy by comparison of average of aliphatic protons to 1-bromo-3,5-bis(trifluoromethyl)benzene as internal standard. ^cEnantiomeric excess was determined by HPLC analysis using Chiralpak AS-H column.

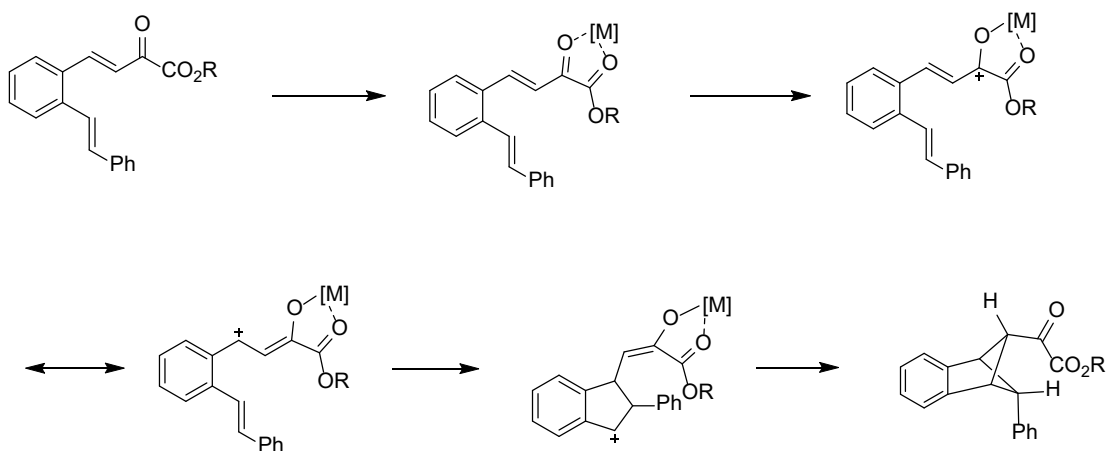
3.4 Conclusion

This study has presented a method to furnish formal [2+2] cycloaddition products from *o*-styrenyl chalcones using sub-stoichiometric amounts of Sc(OTf)₃ as the promoter. The chosen Lewis acid is cheap, readily available, and environmentally benign.¹⁹¹ Preliminary studies

investigating a potential catalytic asymmetric transformation was presented, but did not yield any enantioselectivity.

3.5 Future Directions

The immediate direction for this project would be to continue developing the enantioselective version of the reaction. A strategy that wasn't fully investigated was the use of chiral Brønsted acids. While the typical BINOL-derived phosphoric acids are not strong enough to catalyze this reaction, N-triflyl phosphoramidate catalysts are significantly more acidic and have been shown to activate less electrophilic substrates such as ketones.¹⁹² Additionally, after the initial protonation of the ketone, the chiral counterion would form an ion pair with the cationic intermediate. Having the chiral moiety in close proximity during the carbon-carbon bond forming steps may provide more enantiocontrol. Another avenue to explore would be to modify the substrate to allow for an additional coordination site to the catalyst (Scheme 3.22). Coordination to the catalyst through only one Lewis basic site on the substrate may provide too much conformational flexibility to induce an enantioselective transformation.



Scheme 3.22 Incorporation of another coordination site

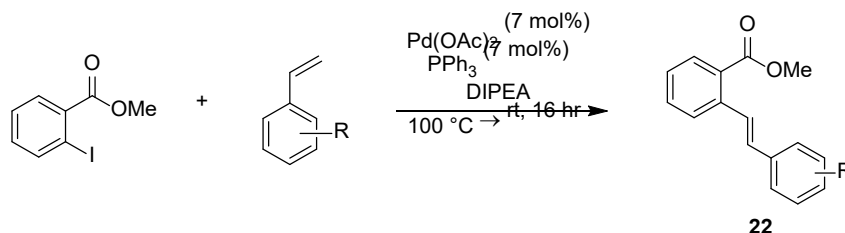
3.6 Experimental

3.6.1 General information

All reactions were carried out under a nitrogen atmosphere in flame-dried glassware. Transfer of anhydrous solvents and reagents was accomplished with oven-dried syringes. Solvents (CH_2Cl_2 , THF) were dried using a LC Technology Solutions Inc. solvent purification system. DIPEA and DCE were dried over molecular sieves prior to use. Reagents were purchased from commercial sources and used without further purification. Column chromatography was performed using 230–400 mesh silica gel, and TLC analyses were completed on silica gel 60 F254 aluminium plates (Millipore-Sigma). ^1H NMR spectra were recorded at 500 MHz and coupling constants (J) are reported in Hertz (Hz). ^{13}C NMR spectra were recorded at 125 MHz. Chemical shifts are referenced to CDCl_3 (s, 7.26 ppm, ^1H ; t, 77.06 ppm, ^{13}C), and CD_2Cl_2 (t, 5.32 ppm, ^1H ; p, 53.8 ppm, ^{13}C) as internal standards and are reported on the δ scale (ppm). Observed multiplicities on ^1H NMR are described using the standard notation: broad (br), apparent (app), multiplet (m), singlet (s), doublet (d), triplet (t), quartet (q), apparent triplet (app t). IR data were recorded using the Thermo Scientific Nicolet Summit LITE instrument. HRMS data were recorded using the Thermo Scientific Orbitrap Exploris 240 (DART) or the Kratos MS50G (EI).

3.6.2 Characterization of compounds

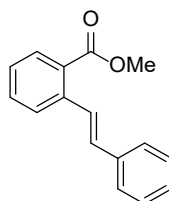
General Procedure 1 for the preparation of 2-Substituted Benzoates (**22**)



2-Substituted benzoates (22**) were prepared via modified literature procedure:**¹⁹³ A mixture of methyl 2-iodo benzoate (1.0 equiv.), styrene (1.2 equiv), palladium acetate (7 mol%), triphenylphosphine (7 mol%) and *N,N*-diisopropylamine (3.0 equiv) was heated to $100\text{ }^\circ\text{C}$ for 5 hours, then stirred at room temperature for 16 hours. The reaction was quenched by filtration through celite eluted with DCM. The organic layer was washed with a 2 M solution of HCl, water

and brine, dried over MgSO_4 , and concentrated in vacuo. The crude reaction mixture was purified by flash column chromatography.

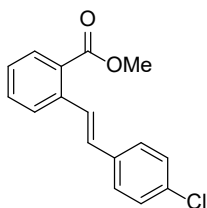
Methyl (*E*)-2-styrylbenzoate (**22a**)



22a

The product was obtained as a brown oil (1.65 g, 6.92 mmol) in 69% yield from methyl 2-iodobenzoate (1.47 mL, 10.0 mmol) and styrene (1.37 mL, 12.0 mmol). R_f 0.38 (hexanes/EtOAc 4:1); IR (neat) 3016, 2952, 1708, 1564, 1509, 1469, 1433, 1244 cm^{-1} ; ^1H NMR (500 MHz, CDCl_3) δ 7.99 (d, $J = 16.5$ Hz, 1 H), 7.94 (dd, $J = 7.5, 1.0$ Hz, 1 H), 7.73 (d, $J = 8.5$ Hz, 1 H), 7.58–7.54 (m, 2 H), 7.52 (ddd, $J = 7.5, 7.5, 1.0$ Hz, 1 H), 7.39–7.35 (m, 2 H), 7.33 (ddd, $J = 8.0, 8.0, 1.0$ Hz, 1 H), 7.30–7.26 (m, 1 H), 7.01 (d, $J = 16.0$ Hz, 1 H), 3.93 (s, 3 H); ^{13}C NMR (125 MHz, CDCl_3) δ 167.9, 139.3, 137.4, 132.2, 131.5, 130.7, 128.7, 128.6, 127.9, 127.5, 127.2, 127.0, 126.9, 52.2; HRMS (DART, $[\text{M}+\text{H}]^+$) for $\text{C}_{16}\text{H}_{15}\text{O}_2$ calcd. 239.1067, found: m/z 239.1064

Methyl (*E*)-2-(4-chlorostyryl)benzoate (**22b**)

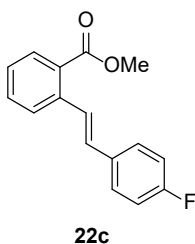


22b

The product was obtained as a white solid (1.93 g, 7.07 mmol) in 71% yield, from methyl 2-iodobenzoate (1.47 mL, 10.0 mmol), and 4-chlorostyrene (1.53 mL, 12.0 mmol). R_f 0.50 (hexanes/EtOAc 4:1); IR (neat) 2996, 2945, 1709, 1564, 1485, 1432, 1402, 1246 cm^{-1} ; ^1H NMR (500 MHz, CDCl_3) δ 7.98 (d, $J = 16.5$ Hz, 1 H), 7.95 (dd, $J = 7.5, 1.0$ Hz, 1 H), 7.70 (d, $J = 8.0$

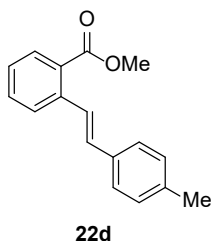
Hz, 1 H), 7.52 (ddd, $J = 7.5, 7.5, 1.0$ Hz, 1 H), 7.49–7.45 (m, 2 H), 7.35–7.31 (m, 3 H), 6.95 (d, $J = 16.5$ Hz, 1 H), 3.93 (s, 3 H); ^{13}C NMR (125 MHz, CDCl_3) δ 167.8, 139.1, 136.0, 133.5, 132.3, 130.8, 130.1, 128.9, 128.6, 128.2, 128.1, 127.4, 127.0, 52.2; HRMS (DART, $[\text{M}+\text{H}]^+$) for $\text{C}_{16}\text{H}_{14}^{35}\text{ClO}_2$ calcd. 273.0677, found: m/z 273.0675.

Methyl (*E*)-2-(4-fluorostyryl)benzoate (22c)



The product was obtained as a pale yellow solid (1.30 g, 5.07 mmol) in 77% yield from methyl 2-iodobenzoate (0.79 mL, 6.6 mmol). and 4-fluorostyrene (0.94 mL, 7.9 mmol). R_f 0.56 (hexanes/EtOAc 9:1); IR (neat) 3070, 2948, 1714, 1593, 1566, 1503, 1434, 1223 cm^{-1} ; ^1H NMR (500 MHz, CDCl_3) δ 7.96–7.89 (m, 2 H), 7.70 (d, $J = 8.0$ Hz, 1 H), 7.54–7.49 (m, 3 H), 7.33 (dd, $J = 7.5$ Hz, 7.5 Hz, 1 H), 7.08–7.02 (m, 2 H), 6.97 (d, $J = 16$ Hz, 1 H), 3.93 (s, 3 H); ^{13}C NMR (125 MHz, CDCl_3) δ 167.9, 162.5 (d, $J = 246.1$ Hz), 139.2, 133.6 (d, $J = 3.4$ Hz), 132.3, 130.7, 130.2, 128.4 (d, $J = 8.3$ Hz), 127.34, 127.32, 127.2, 127.0, 115.6 (d, $J = 21.8$ Hz), 52.2; HRMS (DART, $[\text{M}+\text{H}]^+$) for $\text{C}_{16}\text{H}_{14}\text{FO}_2$ calcd. 257.0972, found: m/z 257.0969.

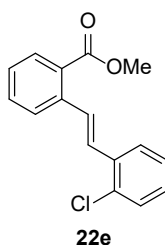
Methyl (*E*)-2-(4-methylstyryl)benzoate (22d)



The product was obtained as a white solid (1.67 g, 6.62 mmol) in 66% yield from methyl 2-iodobenzoate (1.47 mL, 10.0 mmol) and 4-methylstyrene (1.58 mL, 12.0 mmol). R_f 0.48

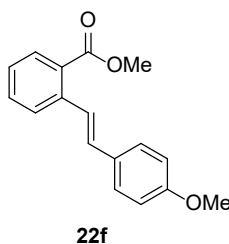
(hexanes/EtOAc 9:1); IR (neat) 3023, 2949, 1714, 1597, 1491, 1434, 1270, 1243 cm^{-1} ; ^1H NMR (500 MHz, CDCl_3) δ 7.96–7.90 (m, 2 H), 7.72 (d, $J = 7.5$ Hz, 1 H), 7.50 (ddd, 8.0, 8.0, 0.5 Hz, 1 H), 7.47–7.43 (m, 2 H), 7.31 (ddd, $J = 7.5, 7.5, 1.0$ Hz, 1 H), 7.19–7.16 (m, 2 H), 7.00 (d, $J = 16.0$ Hz, 1 H), 3.93 (s, 3 H), 2.37 (s, 3 H); ^{13}C NMR (125 MHz, CDCl_3) δ 168.0, 139.4, 137.8, 134.7, 132.1, 131.5, 130.7, 129.4, 128.5, 127.0, 126.9, 126.8, 126.4, 52.1, 21.3; HRMS (DART, $[\text{M}+\text{H}]^+$) for $\text{C}_{17}\text{H}_{17}\text{O}_2$ calcd. 253.1223, found: m/z 253.1220.

Methyl (*E*)-2-(2-chlorostyryl)benzoate (**22e**)



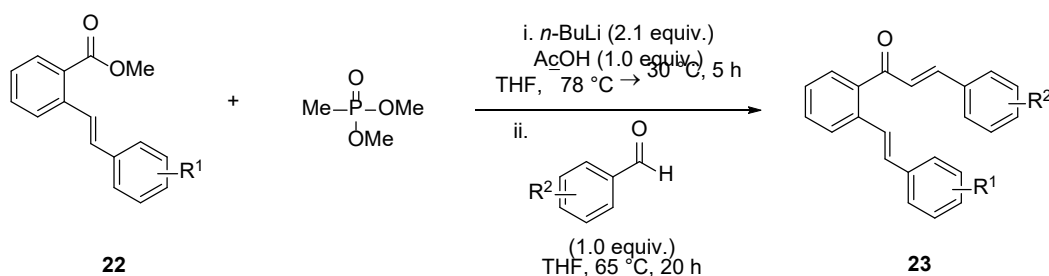
The product was obtained as a yellow solid (1.83 g, 6.71 mmol) in 67% yield from methyl 2-iodobenzoate (1.47 mL, 10.0 mmol) and 2-chlorostyrene (1.53 mL, 12.0 mmol). R_f 0.39 (hexanes/EtOAc 9:1); IR (neat) 3058, 2950, 2361 1717, 1595, 1584, 1478, 1430, 1243 cm^{-1} ; ^1H NMR (500 MHz, CDCl_3) δ 8.02–7.94 (m, 2 H), 7.79–7.76 (m, 2 H), 7.55 (ddd, $J = 7.5, 7.5, 1.0$ Hz, 1 H), 7.43–7.32 (m, 3 H), 7.28 (ddd, $J = 7.5, 7.5, 1.0$ Hz, 1 H), 7.21 (ddd, $J = 8.0, 8.0, 2.0$ Hz, 1H), 3.93 (s, 3 H); ^{13}C NMR (125 MHz, CDCl_3) δ 167.8, 139.2, 135.5, 133.6, 132.4, 130.7, 130.1, 129.8, 128.8, 128.6, 127.6, 127.5, 127.4, 127.1, 127.0, 52.2; HRMS (DART, $[\text{M}+\text{H}]^+$) for $\text{C}_{16}\text{H}_{14}^{35}\text{ClO}_2$ calcd. 273.0677, found: m/z 273.0675.

Methyl (*E*)-2-(4-methoxystyryl)benzoate (**22f**)



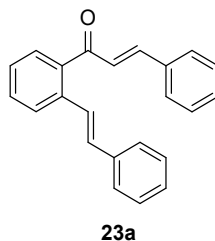
The product was obtained as an orange solid (1.92 g, 7.16 mmol) in 71% yield from methyl 2-iodobenzoate (1.47 mL, 10.0 mmol) and 4-vinylnisole (1.61 mL, 12.0 mmol). R_f 0.35 (hexanes/EtOAc 9:1); IR (neat) 3063, 2993, 2945, 2837, 1713, 1596, 1563, 1506, 1435, 1245 cm^{-1} ; ^1H NMR (500 MHz, CDCl_3) δ 7.92 (dd, J = 8.0, 1.5 Hz, 1 H), 7.87 (d, J = 16.0 Hz, 1 H), 7.71 (d, J = 8.0 Hz, 1 H), 7.52–7.47 (m, 3 H), 7.29 (ddd, J = 7.5, 7.5, 1.0 Hz, 1 H), 6.98 (d, J = 16.5 Hz, 1 H), 6.93–6.89 (m, 2 H), 3.93 (s, 3 H), 3.83 (s, 3 H); ^{13}C NMR (125 MHz, CDCl_3) δ 168.0, 159.5, 139.5, 132.1, 131.0, 130.7, 130.3, 128.4, 128.1, 126.8, 126.7, 125.2, 114.1, 55.35, 52.1; HRMS (DART, $[\text{M}+\text{H}]^+$) for $\text{C}_{17}\text{H}_{17}\text{O}_3$ calcd. 269.1172, found: m/z 269.1169.

General Procedure 2 for the Preparation of *o*-Styrenyl Chalcones (**23**)



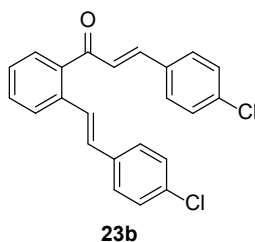
o-Styrenyl chalcones were prepared via a modified literature procedure:¹⁹⁴ A 2.5 M hexane solution of $n\text{-BuLi}$ (2.1 equiv.) was added dropwise to a stirred solution of dimethyl methylphosphonate (2.1 equiv.) in THF (0.4 M solution) at -78°C under nitrogen and stirred for 30 min. 2-Substituted benzoate (**22**) (1.0 equiv.) in THF (1.7 M solution) was added slowly and stirred at -78°C for 30 min. Then, the reaction was allowed to warm to -42°C and stirred for 3 h. After the addition of glacial acetic acid (1.0 equiv.) at -42°C , the mixture was allowed to reach room temperature with continued stirring over 2 h. Aldehyde (1.0 equiv.) was added to the reaction mixture and stirred at 65°C for 20 h. The reaction was quenched by another portion of glacial acetic acid (1.0 equiv.). The solvent was evaporated, and the residue was dissolved in DCM. The organic phase was washed with a 5% ammonium hydroxide solution (4 mL per 1 mmol of benzoate), water and brine, dried over MgSO_4 , and concentrated in vacuo. The crude reaction mixture was purified by column chromatography.

(*E*)-3-Phenyl-1-(2-((*E*)-styryl)phenyl)prop-2-en-1-one (23a)



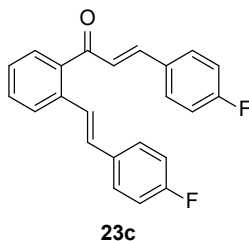
The product was obtained as a yellow solid (1.54 g, 4.96 mmol) in 78% yield from **22a** (1.51 g, 6.34 mmol) and benzaldehyde (0.64 mL, 6.3 mmol). R_f 0.41 (hexanes/EtOAc 9:1); IR (neat) 3057, 1655, 1591, 1490, 1455 cm^{-1} ; ^1H NMR (500 MHz, CDCl_3) δ 7.79 (d, $J = 8.0$ Hz, 1 H), 7.59–7.46 (m, 7 H), 7.44 (d, $J = 16.0$ Hz, 1 H), 7.41–7.34 (m, 4 H), 7.34–7.29 (m, 2 H), 7.26–7.22 (m, 1 H), 7.19 (d, $J = 16.0$ Hz, 1 H), 7.08 (d, $J = 16.5$ Hz, 1 H); ^{13}C NMR (125 MHz, CDCl_3) δ 196.1, 146.1, 138.6, 137.2, 136.6, 134.6, 131.5, 130.9, 130.8, 129.0, 128.7, 128.6, 128.5, 128.0, 127.2, 126.9, 126.8, 126.4, 125.3; HRMS (DART, $[\text{M}+\text{H}]^+$) for $\text{C}_{23}\text{H}_{19}\text{O}$ calcd. 311.1430, found: m/z 311.1428.

(*E*)-3-(4-Chlorophenyl)-1-(2-((*E*)-4-chlorostyryl)phenyl)prop-2-en-1-one (23b)



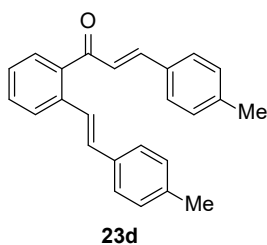
The product was obtained as a yellow solid (1.22 g, 3.21 mmol) in 49% yield from **22b** (1.77 g, 6.48 mmol) and 4-chlorobenzaldehyde (930 mg, 6.5 mmol). R_f 0.31 (hexanes/EtOAc 9:1); IR (neat) 3055, 1663, 1596, 1485, 1401 cm^{-1} ; ^1H NMR (500 MHz, CDCl_3) δ 7.76 (d, $J = 8.0$ Hz, 1 H), 7.57 (dd, $J = 7.5, 1.0$ Hz, 1 H), 7.55–7.45 (m, 4 H), 7.44–7.32 (m, 6 H), 7.30–7.27 (m, 2 H), 7.15 (d, $J = 16$ Hz, 1 H), 7.01 (d, $J = 16.5$ Hz, 1 H); ^{13}C NMR (125 MHz, CDCl_3) δ 195.5, 144.5, 138.4, 136.8, 136.5, 135.7, 133.7, 133.1, 131.1, 130.3, 129.6, 129.4, 128.9, 128.7, 128.0, 127.4, 127.1, 127.0, 126.6; HRMS (DART, $[\text{M}+\text{H}]^+$) for $\text{C}_{23}\text{H}_{17}^{35}\text{Cl}_2\text{O}$ calcd. 379.0651, found: m/z 379.0651.

(E)-3-(4-Fluorophenyl)-1-(2-((E)-4-fluorostyryl)phenyl)prop-2-en-1-one (23c)



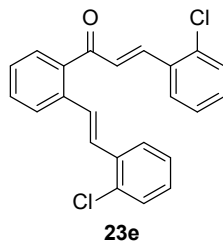
The product was obtained as a yellow solid (874 mg, 2.52 mmol) in 55% yield from **22c** (1.18 g, 4.60 mmol) and 4-fluorobenzaldehyde (0.49 mL, 4.6 mmol). R_f 0.33 (hexanes/EtOAc 9:1); IR (neat) 3052, 1663, 1589, 1499, 1409 cm^{-1} ; ^1H NMR (500 MHz, CDCl_3) δ 7.76 (d, J = 8.0 Hz, 1 H), 7.60–7.48 (m, 5 H), 7.47–7.41 (m, 2 H), 7.40–7.31 (m, 2 H), 7.14–6.97 (m, 6 H); ^{13}C NMR (125 MHz, CDCl_3) δ 195.7, 164.4 (d, $J_{\text{C-F}}$ = 208.6 Hz), 162.4 (d, $J_{\text{C-F}}$ = 204.3 Hz), 144.7, 138.4, 136.5, 133.4 (d, $J_{\text{C-F}}$ = 3.3 Hz), 131.0, 130.8 (d, $J_{\text{C-F}}$ = 3.4 Hz), 130.4 (d, $J_{\text{C-F}}$ = 8.8 Hz), 130.3 (d, $J_{\text{C-F}}$ = 1.0 Hz), 128.6, 128.3 (d, $J_{\text{C-F}}$ = 7.9 Hz), 127.2, 126.5 (d, $J_{\text{C-F}}$ = 2.4 Hz), 126.47, 126.2 (d, $J_{\text{C-F}}$ = 2.3 Hz), 116.2 (d, $J_{\text{C-F}}$ = 21.8 Hz), 115.6 (d, $J_{\text{C-F}}$ = 21.3 Hz); HRMS (DART, $[\text{M}+\text{H}]^+$) for $\text{C}_{23}\text{H}_{17}\text{F}_2\text{O}$ calcd. 347.1242, found: m/z 347.1242.

(E)-1-(2-((E)-4-Methylstyryl)phenyl)-3-(p-tolyl)prop-2-en-1-one (23d)



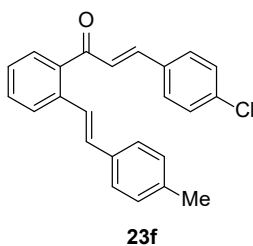
The product was obtained as a yellow solid (1.17 g, 3.46 mmol) in 58% yield from **22d** (1.50 g, 5.95 mmol) and *p*-tolualdehyde (0.70 mL, 6.0 mmol). R_f 0.39 (hexanes/EtOAc 9:1); IR (neat) 3017, 2915, 1657, 1587, 1509, 1444, 1411 cm^{-1} ; ^1H NMR (500 MHz, CDCl_3) δ 7.77 (d, J = 8.0 Hz, 1 H), 7.55–7.43 (m, 5 H), 7.40–7.31 (m, 4 H), 7.20–7.10 (m, 5 H), 7.06 (d, J = 16.0 Hz, 1 H), 2.37 (s, 3 H), 2.33 (s, 3 H); ^{13}C NMR (125 MHz, CDCl_3) δ 196.4, 146.2, 141.3, 138.7, 137.9, 136.6, 134.4, 131.9, 131.3, 130.6, 129.7, 129.4, 128.52, 128.46, 126.9, 126.7, 126.2, 126.1, 125.3, 21.6, 21.3; (DART, $[\text{M}+\text{H}]^+$) for $\text{C}_{25}\text{H}_{23}\text{O}$ calcd. 339.1743, found: m/z 339.1743.

(E)-3-(2-Chlorophenyl)-1-(2-((E)-2-chlorostyryl)phenyl)prop-2-en-1-one (23e)



The product was obtained as a yellow solid (869 mg, 2.29 mmol) in 36% yield from **22e** (1.73 g, 6.34 mmol) and 2-chlorobenzaldehyde (0.71 mL, 6.3 mmol). R_f 0.32 (hexanes/EtOAc 9:1); IR (neat) 3062, 1659, 1591, 1473, 1436 cm^{-1} ; ^1H NMR (500 MHz, CD_2Cl_2) δ 7.94 (d, J = 16.0 Hz, 1 H), 7.84 (d, J = 8.0 Hz, 1 H), 7.71 (dd, J = 7.5, 1.5 Hz, 1 H), 7.65 (dd, J = 8.0, 2.5 Hz, 1 H), 7.63 (dd, J = 8.0, 1.5 Hz, 1 H), 7.57 (ddd, J = 7.5, 7.5, 1.0 Hz, 1 H), 7.50–7.41 (m, 4 H), 7.39 (dd, J = 8.0, 2.0 Hz, 1 H), 7.34 (ddd, J = 7.5, 7.5, 2.0 Hz, 1 H), 7.30 (ddd, J = 8.0, 8.0, 1.5 Hz, 1 H), 7.27–7.16 (m, 3 H); ^{13}C NMR (125 MHz, CD_2Cl_2) δ 195.4, 141.7, 138.8, 136.8, 135.6, 133.8, 133.3, 131.8, 131.5, 130.5, 130.1, 129.6, 129.4, 129.3, 129.1, 128.2, 128.0, 127.7, 127.6, 127.4, 127.3, 127.2 (two signals, overlapping); HRMS (DART, $[\text{M}+\text{H}]^+$) for $\text{C}_{23}\text{H}_{17}^{35}\text{Cl}_2\text{O}$ calcd. 379.0651, found: m/z 379.0652.

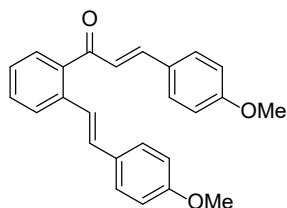
(E)-3-(4-Chlorophenyl)-1-(2-((E)-4-methylstyryl)phenyl)prop-2-en-1-one (23f)



The product was obtained as a yellow solid (1.19, 3.32 mmol), in 56% yield from **22d** (1.50, 5.94 mmol) and 4-chlorobenzaldehyde (0.85 mL, 6.0 mmol). R_f 0.38 (hexanes/EtOAc 9:1); IR (neat) 3020, 2915, 1638, 1590, 1484, 1443, 1404 cm^{-1} ; ^1H NMR (500 MHz, CDCl_3) δ 7.77 (d, J = 8.0 Hz, 1 H), 7.55 (dd, J = 7.5, 1.0 Hz, 1 H), 7.53–7.45 (m, 4 H), 7.39–7.32 (m, 6 H), 7.17–7.11 (m, 3 H), 7.05 (d, J = 16.5 Hz, 1 H), 2.34 (s, 3 H); ^{13}C NMR (125 MHz, CDCl_3) δ 195.7, 144.2, 138.3, 138.0, 136.8, 136.6, 134.3, 133.1, 131.7, 131.0, 129.6, 129.4, 129.3, 128.5, 127.3, 127.0, 126.7,

126.4, 125.2, 21.3; HRMS (DART, $[M+H]^+$) for $C_{24}H_{20}^{35}ClO$ calcd. 359.1197, found: m/z 359.1195.

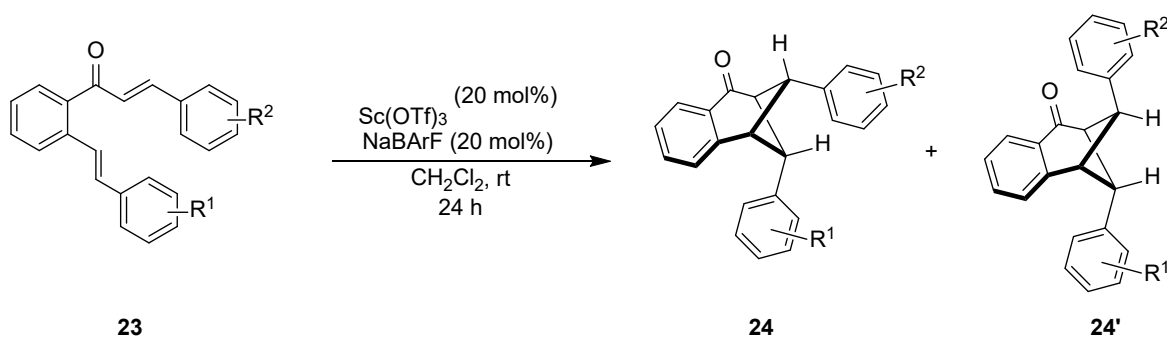
(*E*)-3-(4-Methoxyphenyl)-1-(2-((*E*)-4-methoxystyryl)phenyl)prop-2-en-1-one (23g)



23g

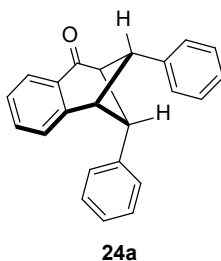
The product was obtained as a yellow solid (1.08 g, 2.92 mmol), in 51% yield from **22f** (1.53, 5.70 mmol), and *p*-anisaldehyde (0.70 mL, 5.7 mmol). R_f 0.27 (hexanes/EtOAc 4:1); IR (neat) 2935, 2836, 1653, 1590, 1505, 1422, 1294, 1246, 1171 cm^{-1} ; 1H NMR (500 MHz, CD_2Cl_2) δ 7.77 (d, J = 8.0 Hz, 1 H), 7.76–7.44 (m, 5 H), 7.44–7.39 (m, 2 H), 7.34 (ddd, J = 7.5, 7.5, 1.0 Hz, 1 H), 7.25 (d, J = 16.5 Hz, 1 H), 7.07 (d, J = 4.0 Hz, 1 H), 7.04 (d, J = 5.0 Hz, 1 H), 6.93–6.89 (m, 2 H), 6.88–6.84 (m, 2 H), 3.83 (s, 3 H), 3.80 (s, 3 H); ^{13}C NMR (125 MHz, CD_2Cl_2) δ 196.3, 162.3, 160.0, 146.0, 139.3, 136.9, 130.9, 130.8, 130.6, 130.3, 128.7, 128.3, 127.7, 127.1, 126.3, 125.2, 124.5, 114.8, 114.3, 55.8, 55.6; HRMS (DART, $[M+H]^+$) for $C_{25}H_{23}O_3$ calcd. 371.1642, found: m/z 371.2637.

General Procedure (4) for the Preparation of Formal [2+2] Cycloadducts (24 and 24')



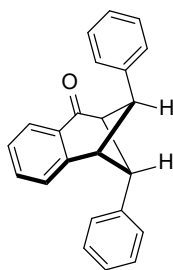
A flask was charged with Sc(OTf)₃ (0.2 equiv), and NaBARF (0.2 equiv.) followed by DCM (2 mL), and stirred for 2 hours. *o*-Styrenyl chalcone (**23**) dissolved in DCM (3 mL) was added dropwise. The reaction mixture was stirred at room temperature for 24 h. The reaction mixture was then filtered through a silica gel plug, eluted with CH₂Cl₂ (50 mL). The filtrate was concentrated, and the crude product was purified by flash column chromatography.

(1R*,2S*,3R*,9S*)-2,9-Diphenyl-2,3-dihydro-1,3-methanonaphthalen-4(1H)-one (24a)



The product was obtained as a white solid in 58% yield (54 mg, 0.17 mmol) from **23a** (93 mg, 0.30 mmol). *R*_f 0.38 (hexanes/EtOAc 9:1); IR (neat) 3033, 2968, 1688, 1600, 1467, 1458, 1380, 1188.33 cm⁻¹; ¹H NMR (500 MHz, CDCl₃) δ 7.79 (d, *J* = 8.0 Hz, 1 H), 7.54 (d, *J* = 7.5 Hz, 2 H), 7.46 (app t, *J* = 7.5 Hz, 2 H), 7.43–7.36 (m, 2 H), 7.33 (app t, *J* = 7.5 Hz, 1 H), 7.21 (ddd, *J* = 7.0, 7.0, 1.0 Hz, 1 H), 7.06 (app t, *J* = 7.0 Hz, 2 H), 6.97 (app t, *J* = 7.0 Hz, 1 H), 6.85 (d, *J* = 8.0 Hz, 2 H), 4.67 (app t, *J* = 6.0 Hz, 1 H), 4.10 (app t, *J* = 6.0 Hz, 1 H), 3.98 (app t, *J* = 6.0 Hz, 1 H), 3.91 (s, 1 H); ¹³C NMR (125 MHz, CDCl₃) δ 199.6, 147.9, 140.1, 139.2, 133.5, 130.3, 128.9, 128.1, 127.3, 127.1, 127.0, 126.64, 126.60, 126.2, 125.8, 57.3, 55.9, 52.6, 48.1; HRMS (EI, M⁺) for C₂₃H₁₈O calcd. 310.1358, found: *m/z* 310.1361.

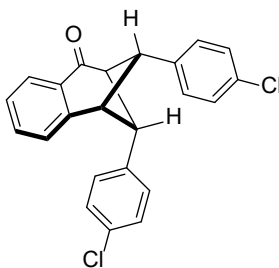
(1R*,2R*,3S*,9S*)-2,9-Diphenyl-2,3-dihydro-1,3-methanonaphthalen-4(1H)-one (24a')



24a'

The product was obtained as a white solid in 5% yield (5 mg, 0.02 mmol) from **23a** (93 mg, 0.30 mmol). R_f 0.28 (hexanes/EtOAc 9:1); IR (neat) 3023, 2895, 1683, 1602, 1445, 1297 cm^{-1} ; ^1H NMR (500 MHz, CDCl_3) δ 7.41 (d, $J = 7.5$ Hz, 1 H), 7.30–7.24 (m, 2 H), 7.10 (app t, $J = 7.0$ Hz, 4 H), 7.03–6.93 (m, 7 H), 4.49 (app t, $J = 5.5$ Hz, 2 H), 4.34 (app q, $J = 5.5$ Hz, 1 H), 4.20 (app q, $J = 6.0$ Hz, 1 H); ^{13}C NMR (125 MHz, CDCl_3) δ 198.9, 143.9, 138.4, 133.5, 130.7, 128.1, 127.9, 127.1, 126.9, 125.9, 125.1, 56.8, 53.1, 47.9; HRMS (EI, M^+) for $\text{C}_{23}\text{H}_{18}\text{O}$ calcd. 310.1358, found: m/z 310.1354.

(1R*,2S*,3R*,9S*)-2,9-Bis(4-chlorophenyl)-2,3-dihydro-1,3-methanonaphthalen-4(1H)-one (24b)

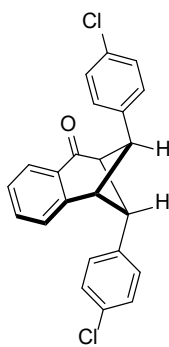


24b

The product was obtained as a yellow solid in 61% yield (70 mg, 0.18 mmol) from **23b** (114 mg, 0.300 mmol). R_f 0.31 (hexanes/EtOAc 9:1); IR (neat) 3022, 2896, 1685, 1602, 1487, 1445, 1297 cm^{-1} ; ^1H NMR (500 MHz, CDCl_3) δ 7.80 (d, $J = 7.5$ Hz, 1 H), 7.48–7.40 (m, 5 H), 7.36 (d, $J = 7.0$ Hz, 1 H), 7.25 (ddd, $J = 7.5, 7.5, 1.5$ Hz, 1 H), 7.03 (d, $J = 8.5$ Hz, 2 H), 6.77 (d, $J = 8.0$ Hz, 2 H), 4.55 (app t, $J = 6.0$ Hz, 1 H), 4.03 (app t, $J = 6.0$ Hz, 1 H), 3.89 (app t, $J = 6.0$ Hz, 1 H), 3.85 (s, 1

H); ^{13}C NMR (125 MHz, CDCl_3) δ 198.9, 147.2, 138.3, 137.5, 133.8, 133.0, 131.9, 130.1, 129.1, 128.5, 128.4, 128.0, 127.7, 126.6, 126.5, 57.2, 55.2, 52.0, 48.0; HRMS (EI, M^+) for $\text{C}_{23}\text{H}_{16}^{35}\text{Cl}_2\text{O}$ calcd. 378.0578, found: m/z 378.0581.

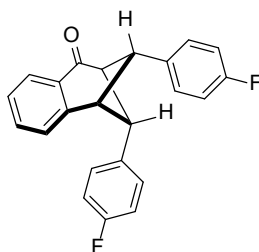
(1R*,2R*,3S*,9S*)-2,9-Bis(4-chlorophenyl)-2,3-dihydro-1,3-methanonaphthalen-4(1H)-one (24b')



24b'

The product was obtained as a yellow solid in 10% yield (12 mg, 0.031 mmol) from **23b** (114 mg, 0.300 mmol). R_f 0.24 (hexanes/EtOAc 9:1); IR (neat) 3022, 2898, 1685, 1604, 1487, 1444, 1297 cm^{-1} ; ^1H NMR (500 MHz, CDCl_3) δ 7.43 (d, $J = 8.0$ Hz, 1 H), 7.29 (ddd, $J = 7.0, 7.0, 1.0$ Hz, 1 H), 7.28–7.24 (m, 1 H), 7.06 (d, $J = 8.5$ Hz, 4 H), 7.01 (ddd, $J = 8.0, 8.0, 1.5$ Hz, 1 H), 6.87 (d, $J = 8.5$ Hz, 4 H), 4.42 (app t, $J = 5.5$ Hz, 2 H), 4.29 (app q, $J = 5.5$ Hz, 1 H), 4.14 (app q, $J = 5.5$ Hz, 1 H); ^{13}C NMR (125 MHz, CDCl_3) δ 198.3, 143.2, 136.7, 133.9, 132.0, 130.5, 128.6, 128.5, 128.4, 127.8, 127.4, 125.4, 56.7, 52.3, 47.6; HRMS (EI, M^+) for $\text{C}_{23}\text{H}_{16}^{35}\text{Cl}_2\text{O}$ calcd. 378.0578, found: m/z 378.0580.

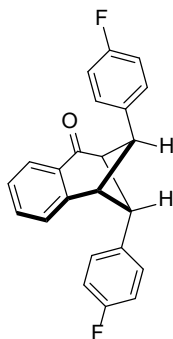
(1R*,2S*,3R*,9S*)-2,9-Bis(4-fluorophenyl)-2,3-dihydro-1,3-methanonaphthalen-4(1H)-one (24c)



24c

The product was obtained as a white solid in 62% yield (64 mg, 0.19 mmol) from **23c** (104 mg, 0.300 mmol). R_f 0.34 (hexanes/EtOAc 9:1); IR (neat) 3052, 2898, 1687, 1603, 1507, 1297, 1220 cm^{-1} ; ^1H NMR (500 MHz, CDCl_3) δ 7.80 (d, $J = 7.5$ Hz, 1 H), 7.52–7.46 (m, 2 H), 7.43 (ddd, $J = 7.5, 7.5, 1.0$ Hz, 1 H), 7.36 (d, $J = 7.0$ Hz, 1 H), 7.24 (ddd, $J = 7.5, 7.5, 1.0$ Hz, 1 H), 7.17–7.11, (m, 2 H), 6.83–6.78 (m, 2 H), 6.78–6.72 (m, 2 H), 4.58 (app t, $J = 5.5$ Hz, 1 H), 4.03 (app t, $J = 6.0$ Hz, 1 H), 3.89 (app t, $J = 6.0$ Hz, 1 H), 3.86 (s, 1 H); ^{13}C NMR (125 MHz, CDCl_3) δ 199.2, 161.8 (d, $J_{\text{C-F}} = 244.9$ Hz), 161.0 (d, $J_{\text{C-F}} = 243.4$ Hz), 147.4, 135.5 (d, $J_{\text{C-F}} = 3.3$ Hz), 134.7 (d, $J_{\text{C-F}} = 3.0$ Hz), 133.7, 130.2, 128.7 (d, $J_{\text{C-F}} = 7.9$ Hz), 128.2 (d, $J_{\text{C-F}} = 7.8$ Hz), 127.5, 126.6, 126.3, 115.8 (d, $J_{\text{C-F}} = 21.3$ Hz), 115.1 (d, $J_{\text{C-F}} = 21.4$ Hz), 57.4, 55.1, 51.9, 48.1; HRMS (DART, $[\text{M}+\text{H}]^+$) for $\text{C}_{23}\text{H}_{17}\text{F}_2\text{O}$ calcd. 347.1242, found: m/z 347.1244.

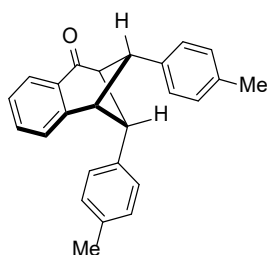
(1R*,2R*,3S*,9S*)-2,9-Bis(4-fluorophenyl)-2,3-dihydro-1,3-methanonaphthalen-4(1H)-one (24c')



24c'

The product was obtained as an off-white solid in 13% yield (13 mg, 0.038 mmol) from **23c** (104 mg, 0.300 mmol). R_f 0.24 (hexanes/EtOAc 9:1); IR (neat) 3049, 2898, 1688, 1604, 1507, 1297, 1217 cm^{-1} ; ^1H NMR (500 MHz, CDCl_3) δ 7.43 (d, $J = 7.5$ Hz, 1 H), 7.31–7.26 (m, 2 H), 7.00 (ddd, $J = 7.0, 7.0, 1.0$ Hz, 1 H), 6.93–6.87 (m, 4 H), 6.81–6.74 (m, 4 H), 4.43 (app t, $J = 5.5$ Hz, 2 H), 4.29 (app q, $J = 5.5$ Hz, 1 H), 4.13 (app q, $J = 5.5$ Hz, 1 H); ^{13}C NMR (125 MHz, CDCl_3) δ 198.6, 161.1 (d, $J_{\text{C-F}} = 243.6$ Hz), 143.5, 133.9 (d, $J_{\text{C-F}} = 3.3$ Hz), 133.8, 130.7, 128.6 (d, $J_{\text{C-F}} = 7.9$ Hz), 127.8, 127.2, 125.2, 115.1 (d, $J_{\text{C-F}} = 21.4$ Hz), 56.8, 52.3, 47.8; HRMS (DART, $[\text{M}+\text{H}]^+$) for $\text{C}_{23}\text{H}_{17}\text{F}_2\text{O}$ calcd. 347.1242, found: m/z 347.1242.

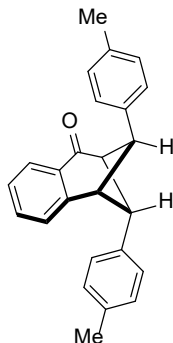
(1R*,2S*,3R*,9S*)-2,9-Di-*p*-tolyl-2,3-dihydro-1,3-methanonaphthalen-4(1H)-one (24d)



24d

The product was obtained as an off white solid in 54% yield (55 mg, 0.16 mmol) from **23d** (101 mg, 0.298 mmol). R_f 0.54 (hexanes/EtOAc 9:1); IR (neat) 3004, 2898, 1688, 1604, 1509, 1296, 1218 cm^{-1} ; ^1H NMR (500 MHz, CDCl_3) δ 7.80 (d, $J = 7.5$ Hz, 1 H), 7.45–7.34 (m, 4 H), 7.26 (d, $J = 7.5$ Hz, 2 H), 7.22 (app t, $J = 7.5$, 1 H), 6.86 (d, $J = 7.5$ Hz, 2 H), 6.73 (d, $J = 7.5$ Hz, 2 H), 4.63 (app t, $J = 6.0$ Hz, 1 H), 4.04 (app t, $J = 6.0$ Hz, 1 H), 3.92 (app t, $J = 6.0$ Hz, 1 H), 3.86 (s, 1 H), 2.39 (s, 3 H), 2.14 (s, 3 H); ^{13}C NMR (125 MHz, CD_2Cl_2) δ 199.9, 148.1, 137.1, 136.6, 136.2, 135.2, 133.4, 130.4, 129.5, 128.8, 127.2, 127.0, 126.6, 126.5, 126.2, 57.5, 55.8, 52.4, 48.1, 21.1, 21.0; HRMS (DART, $[\text{M}+\text{H}]^+$) for $\text{C}_{25}\text{H}_{23}\text{O}$ calcd. 339.1743, found: m/z 339.1744.

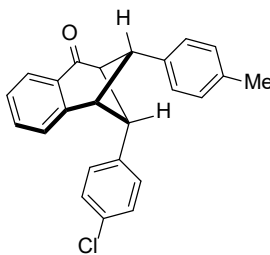
(1R*,2R*,3S*,9S*)-2,9-Di-*p*-tolyl-2,3-dihydro-1,3-methanonaphthalen-4(1H)-one (24d')



24d'

The product was obtained as an off-white solid in 23% yield (24 mg, 0.070 mmol), from **23d** (101 mg, 0.298 mmol). R_f 0.38 (hexanes/EtOAc 9:1); IR (neat) 3016, 2893, 1687, 1604, 1509, 1296, 1217 cm^{-1} ; ^1H NMR (500 MHz, CDCl_3) δ 7.45 (d, $J = 7.5$ Hz, 1 H), 7.27 (d, $J = 4.5$ Hz, 2 H), 6.99–6.94 (m, 1 H), 6.89 (d, $J = 8.0$ Hz, 4 H), 6.84 (d, $J = 8.0$ Hz, 4 H), 4.44 (app t, $J = 5.5$ Hz, 2 H), 4.29 (app q, $J = 5.5$ Hz, 1 H), 4.15 (app q, $J = 5.5$ Hz, 1 H), 2.16 (s, 6 H); ^{13}C NMR (125 MHz, CDCl_3) δ 199.1, 144.1, 135.4, 135.3, 133.4, 130.9, 128.8, 127.9, 127.0, 126.8, 125.0, 56.9, 53.0, 47.7, 21.0; HRMS (DART, $[\text{M}+\text{H}]^+$) for $\text{C}_{25}\text{H}_{23}\text{O}$ calcd. 339.1743, found: m/z 339.1743.

(1S*,2S*,3R*,9S*)-2-(4-Chlorophenyl)-9-(*p*-tolyl)-2,3-dihydro-1,3-methanonaphthalen-4(1H)-one (24e)

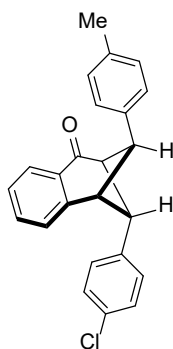


24e

The product was obtained as a white solid in 43% yield (46 mg, 0.13 mmol), from **23f** (107 mg, 0.282 mmol). R_f 0.40 (hexanes/EtOAc 9:1); IR (neat) 3049, 2898, 1688, 1604, 1509, 1296, 1218 cm^{-1} ; ^1H NMR (500 MHz, CDCl_3) δ 7.71 (d, $J = 7.0$ Hz, 1 H), 7.44–7.39 (m, 3 H), 7.36 (d, $J = 7.0$ Hz, 1 H), 7.26 (d, $J = 8.5$ Hz, 2 H), 7.25–7.21 (m, 1 H), 7.02 (d, $J = 8.5$ Hz, 2 H), 6.77 (d, $J = 8.5$

Hz, 2 H), 4.59 (app t, $J = 5.5$ Hz, 1 H), 4.04 (app t, $J = 5.5$ Hz, 1 H), 3.91 (app t, $J = 5.5$ Hz, 1 H), 3.87 (s, 1 H), 2.39 (s, 3 H); ^{13}C NMR (125 MHz, CDCl_3) δ 199.4, 147.6, 137.9, 136.79, 136.77, 133.6, 131.7, 130.2, 129.6, 128.3, 128.1, 127.5, 127.0, 126.6, 126.3, 57.4, 55.6, 52.1, 48.0, 21.1; HRMS (EI, M^+) for $\text{C}_{24}\text{H}_{19}^{35}\text{ClO}$ calcd. 358.1125, found: m/z 358.1120

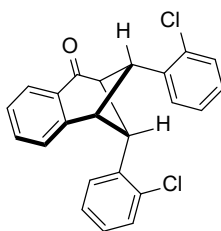
(1R*,2R*,3S*,9S*)-2-(4-Chlorophenyl)-9-(*p*-tolyl)-2,3-dihydro-1,3-methanonaphthalen-4(1H)-one (24e')



24e'

The product was obtained as a white solid in 35% yield (38 mg, 0.10 mmol) from **23f** (107 mg, 0.282 mmol). R_f 0.20 (hexanes/EtOAc 9:1); IR (neat) 2936, 1688, 1605, 1509, 1460, 1291, 1212 cm^{-1} ; ^1H NMR (500 MHz, CDCl_3) δ 7.43 (d, $J = 7.5$ Hz, 1 H), 7.31–7.27 (m, 2 H), 7.05 (d, $J = 8.5$ Hz, 2 H), 6.99 (ddd, $J = 6.5, 6.5, 2$ Hz, 1 H), 6.91–6.86 (m, 4 H), 6.83 (d, $J = 8.0$ Hz, 2 H), 4.45 (app t, $J = 5.5$ Hz, 1 H), 4.41 (app t, $J = 5.5$ Hz, 1 H), 4.29 (app q, $J = 5.5$ Hz, 1 H), 4.14 (app q, $J = 5.5$ Hz, 1 H), 2.16 (s, 3 H); ^{13}C NMR (125 MHz, CDCl_3) δ 198.7, 143.7, 137.0, 135.5, 134.9, 133.6, 131.8, 130.7, 128.9, 128.5, 128.3, 127.8, 127.1, 126.9, 125.2, 56.8, 52.8, 52.5, 47.7, 21.0; HRMS (EI, M^+) for $\text{C}_{24}\text{H}_{19}^{35}\text{ClO}$ calcd. 358.1125, found: m/z 358.1123.

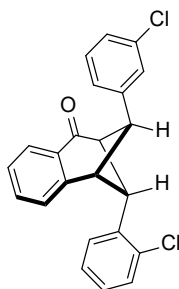
(1R*,2S*,3R*,9S*)-2,9-Bis(2-chlorophenyl)-2,3-dihydro-1,3-methanonaphthalen-4(1H)-one (24f)



24f

The product was obtained as a white solid in 69% yield (78 mg, 0.21 mmol) from **23e** (113 mg, 0.298 mmol). R_f 0.32 (hexanes/EtOAc 9:1); IR (neat) 2987, 1687, 1602, 1470, 1455, 1283 cm^{-1} ; ^1H NMR (500 MHz, CDCl_3) δ 7.86 (d, $J = 7.5$ Hz, 1 H), 7.71 (d, $J = 7.5$ Hz, 1 H), 7.49 (dd, $J = 8.0, 1.5$ Hz, 1 H), 7.44–7.37 (m, 3 H), 7.32 (ddd, $J = 7.5, 7.5, 1.5$ Hz, 1 H), 7.26–7.23 (m, 1 H), 7.14–7.10 (m, 1 H), 7.01–6.92 (m, 3 H), 4.63 (app t, $J = 5.5$ Hz, 1 H), 4.33 (app t, $J = 6.0$ Hz, 1 H), 4.03 (app t, $J = 6.0$ Hz, 1 H), 3.94 (s, 1 H); ^{13}C NMR (125 MHz, CDCl_3) δ 199.3, 147.1, 137.1, 136.5, 135.4, 133.6, 133.1, 130.2, 129.9, 129.5, 129.2, 128.6, 128.0, 127.5, 127.2, 127.1, 126.7, 126.4, 126.1, 55.4, 55.0, 51.9, 48.1; HRMS (EI, M^+) for $\text{C}_{23}\text{H}_{16}^{35}\text{Cl}_2\text{O}$ calcd. 378.0578, found: m/z 378.0580.

(1R*,2R*,3S*,9S*)-2,9-Bis(2-chlorophenyl)-2,3-dihydro-1,3-methanonaphthalen-4(1H)-one (24f')

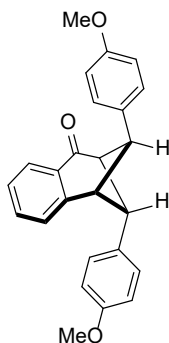


24f'

The product was obtained as a yellow solid in 6% yield (7 mg, 0.02 mmol), from **23f** (113 mg, 0.298 mmol). R_f 0.44 (hexanes/EtOAc 9:1); IR (neat) 2915, 1686, 1600, 1469, 1435, 1282 cm^{-1} ;

^1H NMR (500 MHz, CDCl_3) δ 8.19 (d, $J = 7.5$ Hz, 1 H), 7.57 (ddd, $J = 7.5, 7.5, 1.0$ Hz, 1 H), 7.53–7.47 (m, 2 H), 7.34 (dd, $J = 8.0, 1.0$ Hz, 2 H), 7.04 (ddd, $J = 8.0, 8.0, 1.5$ Hz, 2 H), 6.75 (ddd, $J = 7.5, 7.5, 1.0$ Hz, 2 H), 6.69 (dd, $J = 8.0, 0.5$ Hz, 2 H), 4.25 (d, $J = 6.5$ Hz, 1 H), 4.15 (d, $J = 6.5$ Hz, 1 H), 3.88 (s, 2 H); ^{13}C NMR (125 MHz, CDCl_3) δ 199.7, 152.2, 137.0, 134.2, 133.4, 129.7, 129.5, 128.4, 127.9, 127.82, 127.78, 125.7, 125.2, 56.5, 54.3, 46.0; HRMS (EI, M^+) for $\text{C}_{23}\text{H}_{16}^{35}\text{Cl}_2\text{O}$ calcd. 378.0578, found: m/z 378.0585.

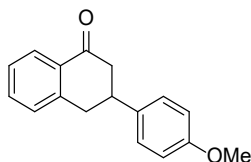
(1R*,2R*,3S*,9S*)-2,9-Bis(4-methoxyphenyl)-2,3-dihydro-1,3-methanonaphthalen-4(1H)-one (24g')



24g'

The product was obtained as an off-white solid in 14% yield (15 mg, 0.041 mmol), from **23g** (111 mg, 0.300 mmol). R_f 0.17 (hexanes/EtOAc 4:1); IR (neat) 2949, 1692, 1605, 1509, 1458, 1293, 1240 cm^{-1} ; ^1H NMR (500 MHz, CDCl_3) δ 7.43 (d, $J = 7.0$ Hz, 1 H), 7.29–7.23 (m, 2 H), 7.01–6.94 (m, 1 H), 6.86 (d, $J = 8.5$ Hz, 4 H), 6.62 (d, $J = 8.5$ Hz, 4 H), 4.42 (app t, $J = 6.0$ Hz, 2 H), 4.26 (app q, $J = 6.0$ Hz, 1 H), 4.11 (app q, $J = 6.0$ Hz, 1 H), 3.66 (s, 6 H); ^{13}C NMR (125 MHz, CDCl_3) δ 199.3, 157.6, 144.0, 133.5, 130.9, 130.4, 128.1, 127.8, 126.9, 125.0, 113.9, 113.6, 56.9, 55.1, 5.6, 47.9; HRMS (DART, $[\text{M}+\text{H}]^+$) for $\text{C}_{25}\text{H}_{23}\text{O}_3$ calcd. 371.1642, found: m/z 371.1643.

3-(4-Methoxyphenyl)-3,4-dihydronaphthalen-1(2H)-one (25g)



25g

The product was obtained as a white solid in 14% yield (11 mg, 0.043 mmol) from **23g** (111 mg, 0.300 mmol). R_f 0.50 (hexanes/EtOAc 4:1); IR (neat) 2930, 1674, 1599, 1509, 1446, 1284, 1246 cm^{-1} ; ^1H NMR (500 MHz, CDCl_3) δ 8.08 (d, $J = 8.5$ Hz, 1 H), 7.51 (app t, $J = 7.5$ Hz, 1 H), 7.35 (app t, $J = 7.5$ Hz, 1 H), 7.28 (d, $J = 7.0$ Hz, 1 H), 7.23 (d, $J = 9.5$ Hz, 2 H), 6.91 (d, $J = 9.0$ Hz, 2 H), 3.82 (s, 3 H), 3.47–3.37 (m, 1 H), 3.20–3.13 (m, 2 H), 2.95 (dd, $J = 16.5, 3.5$ Hz, 1 H), 2.81 (dd, $J = 17.0, 13.5$ Hz, 1 H); ^{13}C NMR (125 MHz, CDCl_3) δ 198.0, 158.6, 143.5, 135.7, 133.8, 132.2, 128.9, 127.7, 127.2, 127.0, 114.2, 55.4, 46.3, 40.4, 38.0; HRMS (DART, $[\text{M}+\text{H}]^+$) for $\text{C}_{17}\text{H}_{17}\text{O}_2$ calcd. 253.1223, found: m/z 253.1223.

Compounds **24g** and **26g** could not be separated using column chromatography. Yields were determined using quantitative ^1H NMR, by comparison of aliphatic protons in the crude mixture to 1-bromo-3,5-bis(trifluoromethyl)benzene as internal standard. ^1H NMR resonances agreed with previously reported compounds.³⁹

References

- (1) Vorländer, D.; Schroedter, M. Einwirkung von Schwefelsäure Und Essigsäureanhydrid Auf Dibenzalacetone. *Berichte Dtsch. Chem. Ges.* **1903**, 36 (2), 1490–1497. <https://doi.org/10.1002/cber.19030360227>.
- (2) Allen, C. F. H.; VanAllan, J. A.; Tinker, J. F. The Structure of Certain Substituted Diphenylcyclopentenones. *J. Org. Chem.* **1955**, 20 (10), 1387–1391. <https://doi.org/10.1021/jo01127a016>.
- (3) Braude, E. A.; Coles, J. A. 261. Syntheses of Polycyclic Systems. Part III. Some Hydroindanones and Hydrofluorenones. The Mechanism of the Nazarov Cyclisation Reaction. *J. Chem. Soc.* **1952**, 1430–1433. <https://doi.org/10.1039/JR9520001430>.
- (4) Que, Y.; Shao, H.; He, H.; Gao, S. Total Synthesis of Farnesin through an Excited-State Nazarov Reaction. *Angew. Chem. Int. Ed.* **2020**, 59 (19), 7444–7449. <https://doi.org/10.1002/anie.202001350>.
- (5) Zhou, Z.; Tius, M. A. Synthesis of Each Enantiomer of Rocaglamide by Means of a Palladium(0)-Catalyzed Nazarov-Type Cyclization. *Angew. Chem. Int. Ed.* **2015**, 54 (20), 6037–6040. <https://doi.org/10.1002/anie.201501374>.
- (6) Li, W.-D. Z.; Duo, W.-G.; Zhuang, C.-H. Concise Total Synthesis of (±)-Cephalotaxine via a Transannulation Strategy: Development of a Facile Reductive Oxy-Nazarov Cyclization. *Org. Lett.* **2011**, 13 (13), 3538–3541. <https://doi.org/10.1021/ol201390r>.
- (7) Douelle, F.; Tal, L.; Greaney, M. F. Reagent-Free Nazarov Cyclisations. *Chem. Commun.* **2005**, 660–662. <https://doi.org/10.1039/B415463K>.
- (8) Miao, M.; Xu, H.; Luo, Y.; Jin, M.; Chen, Z.; Xu, J.; Ren, H. Catalyst-Free Regioselective Nazarov Cyclization of Aryl Allenyl Ketones. *Synthesis* **2018**, 50 (2), 349–360. <https://doi.org/10.1055/s-0036-1591487>.
- (9) Smith, A. B.; Agosta, W. C. Photochemical Reactions of 1-Cyclopentenyl and 1-Cyclohexenyl Ketones. *J. Am. Chem. Soc.* **1973**, 95 (6), 1961–1968. <https://doi.org/10.1021/ja00787a041>.
- (10) Leitich, J.; Heise, I.; Werner, S.; Krüger, C.; Schaffner, K. The Photo-Nazarov Cyclization of 1-Cyclohexenyl Phenyl Ketone Revisited. Observation of Intermediates. *J. Photochem. Photobiol. Chem.* **1991**, 57 (1), 127–151. [https://doi.org/10.1016/1010-6030\(91\)85011-5](https://doi.org/10.1016/1010-6030(91)85011-5).
- (11) Churrua, F.; Foustieris, M.; Ishikawa, Y.; von Wantoch Rekowski, M.; Hounsou, C.; Surrey, T.; Giannis, A. A Novel Approach to Indoloditerpenes by Nazarov Photocyclization: Synthesis and Biological Investigations of Terpendole E Analogues. *Org. Lett.* **2010**, 12 (9), 2096–2099. <https://doi.org/10.1021/ol100579w>.
- (12) Fradette, R. J.; Kang, M.; West, F. G. Oxidation-Initiated Cyclizations of Pentadienyl Ethers: An Alternative Entry to the Nazarov Reaction. *Angew. Chem. Int. Ed.* **2017**, 56 (22), 6335–6338. <https://doi.org/10.1002/anie.201701748>.
- (13) Terraneo, G.; Resnati, G.; Metrangolo, P. Iodine and Halogen Bonding. In *Iodine Chemistry and Applications*; John Wiley & Sons, Ltd, 2014; pp 159–194. <https://doi.org/10.1002/9781118909911.ch8>.
- (14) Dreger, A.; Wonner, P.; Engelage, E.; Walter, S. M.; Stoll, R.; Huber, S. M. A Halogen-Bonding-Catalysed Nazarov Cyclisation Reaction. *Chem. Commun.* **2019**, 55 (57), 8262–8265. <https://doi.org/10.1039/C9CC02816A>.
- (15) Matsuzaki, K.; Uno, H.; Tokunaga, E.; Shibata, N. Fluorobissulfonylmethyl Iodides: An Efficient Scaffold for Halogen Bonding Catalysts with an sp^3 -Hybridized Carbon–Iodine Moiety. *ACS Catal.* **2018**, 8 (7), 6601–6605. <https://doi.org/10.1021/acscatal.8b01330>.

- (16) Heiden, D. von der; Detmar, E.; Kuchta, R.; Breugst, M. Activation of Michael Acceptors by Halogen-Bond Donors. *Synlett* **2018**, 29 (10), 1307–1313. <https://doi.org/10.1055/s-0036-1591841>.
- (17) Gliese, J.-P.; H. Jungbauer, S.; M. Huber, S. A Halogen-Bonding-Catalyzed Michael Addition Reaction. *Chem. Commun.* **2017**, 53 (88), 12052–12055. <https://doi.org/10.1039/C7CC07175B>.
- (18) Koenig, J. J.; Arndt, T.; Gildemeister, N.; Neudörfl, J.-M.; Breugst, M. Iodine-Catalyzed Nazarov Cyclizations. *J. Org. Chem.* **2019**, 84 (12), 7587–7605. <https://doi.org/10.1021/acs.joc.9b01083>.
- (19) Stephan, D. W. A Tale of Two Elements: The Lewis Acidity/Basicity Umpolung of Boron and Phosphorus. *Angew. Chem. Int. Ed.* **2017**, 56 (22), 5984–5992. <https://doi.org/10.1002/anie.201700721>.
- (20) Vogler, M.; Süsse, L.; LaFortune, J. H. W.; Stephan, D. W.; Oestreich, M. Electrophilic Phosphonium Cations as Lewis Acid Catalysts in Diels–Alder Reactions and Nazarov Cyclizations. *Organometallics* **2018**, 37 (19), 3303–3313. <https://doi.org/10.1021/acs.organomet.8b00496>.
- (21) Rej, S.; Klare, H. F. T.; Oestreich, M. The [3]Dendralene Motif as an Entry into Nazarov Cyclizations by Silylium-Ion Initiation. *Org. Lett.* **2023**, 25 (2), 426–431. <https://doi.org/10.1021/acs.orglett.2c04166>.
- (22) Bee, C.; Leclerc, E.; Tius, M. A. The Palladium(II)-Catalyzed Nazarov Reaction. *Org. Lett.* **2003**, 5 (26), 4927–4930. <https://doi.org/10.1021/ol036017e>.
- (23) Shimada, N.; Stewart, C.; Bow, W. F.; Jolit, A.; Wong, K.; Zhou, Z.; Tius, M. A. Neutral Nazarov-Type Cyclization Catalyzed by Palladium(0). *Angew. Chem. Int. Ed.* **2012**, 51 (23), 5727–5729. <https://doi.org/10.1002/anie.201201724>.
- (24) Kitamura, K.; Shimada, N.; Stewart, C.; Atesin, A. C.; Ateşin, T. A.; Tius, M. A. Enantioselective Palladium(0)-Catalyzed Nazarov-Type Cyclization. *Angew. Chem. Int. Ed.* **2015**, 54 (21), 6288–6291. <https://doi.org/10.1002/anie.201500881>.
- (25) Bharadwaj, S. K.; Bankar, S. K.; Ramasastry, S. S. V. Facile Access to Cyclopentadienes via Catalytic Intramolecular Palladium-Ene Reaction of 2,4-Pentadienyl Acetates. *Synlett* **2018**, 29 (19), 2456–2460. <https://doi.org/10.1055/s-0037-1610552>.
- (26) Singh, B.; Bankar, S. K.; Kumar, K.; Ramasastry, S. S. V. Palladium-Catalysed 5-Endo-Trig Allylic (Hetero)Arylation. *Chem. Sci.* **2020**, 11 (19), 4948–4953. <https://doi.org/10.1039/D0SC01932A>.
- (27) Occhiato, E. G.; Prandi, C.; Ferrali, A.; Guarna, A.; Venturello, P. New Synthetic Approach to Cyclopenta-Fused Heterocycles Based upon a Mild Nazarov Reaction. *J. Org. Chem.* **2003**, 68 (25), 9728–9741. <https://doi.org/10.1021/jo034939p>.
- (28) Prandi, C.; Ferrali, A.; Guarna, A.; Venturello, P.; Occhiato, E. G. New Synthetic Approach to Cyclopenta-Fused Heterocycles Based upon a Mild Nazarov Reaction. 2. Further Studies on the Torquoselectivity. *J. Org. Chem.* **2004**, 69 (22), 7705–7709. <https://doi.org/10.1021/jo0489263>.
- (29) Barluenga, J.; Barrio, P.; Vicente, R.; López, L. A.; Tomás, M. Copper-Catalyzed Dimerization of Chromium Fischer Carbene Complexes: Synthesis of Dialkoxytrienes and Their Nazarov-Type Cyclization to 2-Alkoxy-2-Cyclopentenones. *J. Organomet. Chem.* **2004**, 689 (23), 3793–3799. <https://doi.org/10.1016/j.jorganchem.2004.07.005>.
- (30) Stephen, A.; Hashmi, K.; Bats, J. W.; Choi, J.-H.; Schwarz, L. Isomerizations on Silica Gel: Synthesis of Allenyl Ketones and the First Nazarov Cyclizations of Vinyl Allenyl Ketones.

- Tetrahedron Lett.* **1998**, 39 (41), 7491–7494. [https://doi.org/10.1016/S0040-4039\(98\)01619-0](https://doi.org/10.1016/S0040-4039(98)01619-0).
- (31) Banaag, A. R.; Tius, M. A. Design of Chiral Auxiliaries for the Allene Ether Nazarov Cyclization. *J. Am. Chem. Soc.* **2007**, 129 (17), 5328–5329. <https://doi.org/10.1021/ja069342g>.
 - (32) Harrington, P. E.; Murai, T.; Chu, C.; Tius, M. A. Asymmetric Cyclopentannulation: Camphor-Derived Auxiliary. *J. Am. Chem. Soc.* **2002**, 124 (34), 10091–10100. <https://doi.org/10.1021/ja020591o>.
 - (33) Schultz-Fademrecht, C.; Tius, M. A.; Grimme, S.; Wibbeling, B.; Hoppe, D. Synthesis of Enantioenriched 5-Alkylidene-2-Cyclopentenones from Chiral Allenyl Carbamates: Generation of a Chiral Lithium Allenolate and Allylic Activation for a Conrotatory 4π -Electrocyclization. *Angew. Chem. Int. Ed.* **2002**, 41 (9), 1532–1535. [https://doi.org/10.1002/1521-3773\(20020503\)41:9<1532::AID-ANIE1532>3.0.CO;2-J](https://doi.org/10.1002/1521-3773(20020503)41:9<1532::AID-ANIE1532>3.0.CO;2-J).
 - (34) Teske, J.; Plietker, B. Fe-Catalyzed Cycloisomerization of Aryl Allenyl Ketones: Access to 3-Arylidene-Indan-1-Ones. *Org. Lett.* **2018**, 20 (8), 2257–2260. <https://doi.org/10.1021/acs.orglett.8b00612>.
 - (35) Miao, M.; Jin, M.; Chen, P.; Wang, L.; Zhang, S.; Ren, H. Iron(III)-Mediated Bicyclization of 1,2-Allenyl Aryl Ketones: Assembly of Indanone-Fused Polycyclic Scaffolds and Dibenzo[a,e]Pentalene Derivatives. *Org. Lett.* **2019**, 21 (15), 5957–5961. <https://doi.org/10.1021/acs.orglett.9b02079>.
 - (36) Muxfeldt, H.; Weigele, M.; Rheenen, V. V. Magnesium Methoxide Cyclization of Biacetyl Derivatives. *J. Org. Chem.* **1965**, 30 (10), 3573–3574. <https://doi.org/10.1021/jo01021a511>.
 - (37) Batson, W. A.; Sethumadhavan, D.; Tius, M. A. α -Hydroxy Cyclopentenones from α -Diketones. *Org. Lett.* **2005**, 7 (13), 2771–2774. <https://doi.org/10.1021/ol050970x>.
 - (38) Basak, A. K.; Shimada, N.; Bow, W. F.; Vicic, D. A.; Tius, M. A. An Organocatalytic Asymmetric Nazarov Cyclization. *J. Am. Chem. Soc.* **2010**, 132 (24), 8266–8267. <https://doi.org/10.1021/ja103028r>.
 - (39) Jacob, S. D.; Brooks, J. L.; Frontier, A. J. No Acid Required: 4π and 6π Electrocyclization Reactions of Dienyl Diketones for the Synthesis of Cyclopentenones and 2H-Pyrans. *J. Org. Chem.* **2014**, 79 (21), 10296–10302. <https://doi.org/10.1021/jo501914w>.
 - (40) Huang, Y.-W.; Frontier, A. J. Nazarov Cyclization/Internal Redox Cyclization Sequence for the Synthesis of N-Heterocyclic Bridged Ring Systems. *Org. Lett.* **2016**, 18 (19), 4896–4899. <https://doi.org/10.1021/acs.orglett.6b02369>.
 - (41) Sudhakar, G.; Satish, K. Nazarov Cyclization of Divinyl and Arylvinyl Epoxides: Application in the Synthesis of Resveratrol-Based Natural Products. *Chem. Eur. J.* **2015**, 21 (17), 6475–6480. <https://doi.org/10.1002/chem.201500362>.
 - (42) Malona, J. A.; Cariou, K.; Spencer, W. T. I.; Frontier, A. J. Total Synthesis of (\pm)-Rocaglamide via Oxidation-Initiated Nazarov Cyclization. *J. Org. Chem.* **2012**, 77 (4), 1891–1908. <https://doi.org/10.1021/jo202366c>.
 - (43) Sudhakar, G.; Reddy, K. J.; Nanubolu, J. B. Nazarov Cyclization of Dienylaziridines: Synthesis of Cyclopentadienyl/Hydrindienyl/Indenyl Glycines. *Org. Biomol. Chem.* **2015**, 13 (33), 8875–8885. <https://doi.org/10.1039/C5OB01219H>.
 - (44) Smith, D. A.; Ulmer, C. W. Effects of Substituents in the 3-Position on the [2 + 2] Pentadienyl Cation Electrocyclization. *J. Org. Chem.* **1997**, 62 (15), 5110–5115. <https://doi.org/10.1021/jo9703313>.

- (45) Bonderoff, S. A.; Grant, T. N.; West, F. G.; Tremblay, M. Nazarov Reactions of Vinyl Cyclopropylamines: An Approach to the Imino-Nazarov Problem. *Org. Lett.* **2013**, *15* (11), 2888–2891. <https://doi.org/10.1021/ol4012663>.
- (46) Grant, T. N.; West, F. G. Interrupted Nazarov Reactions Using Dichlorocyclopropanes: A Novel Mode of Arene Trapping. *Org. Lett.* **2007**, *9* (19), 3789–3792. <https://doi.org/10.1021/ol7015669>.
- (47) Tsuge, O.; Kanemasa, S.; Otsuka, T.; Suzuki, T. Synthesis and Acid-Catalyzed Ring Opening of 1-Alkenyl Cyclopropyl Ketones. *Bull. Chem. Soc. Jpn.* **1988**, *61* (8), 2897–2908. <https://doi.org/10.1246/bcsj.61.2897>.
- (48) De Simone, F.; Andr  s, J.; Torosantucci, R.; Waser, J. Catalytic Formal Homo-Nazarov Cyclization. *Org. Lett.* **2009**, *11* (4), 1023–1026. <https://doi.org/10.1021/ol802970g>.
- (49) Patil, D. V.; Cavitt, M. A.; Grzybowski, P.; France, S. An Efficient Synthesis of Hydropyrido[1,2-a]Indole-6(7H)-Ones via an In(III)-Catalyzed Tandem Cyclopropane Ring-Opening/Friedel–Crafts Alkylation Sequence. *Chem. Commun.* **2011**, *47* (37), 10278–10280. <https://doi.org/10.1039/C1CC14131G>.
- (50) Cavitt, M.; France, S. Aluminum(III)-Catalyzed, Formal Homo-Nazarov-Type Ring-Opening Cyclizations toward the Synthesis of Functionalized Tetrahydroindolizines. *Synthesis* **2016**, *48* (12), 1910–1919. <https://doi.org/10.1055/s-0035-1561621>.
- (51) Aponte-Guzm  n, J.; Taylor, J. E. Jr.; Tillman, E.; France, S. Catalytic, Formal Homo-Nazarov-Type Cyclizations of Alkylidene Cyclopropane-1,1-Ketoesters: Access to Functionalized Arenes and Heteroaromatics. *Org. Lett.* **2014**, *16* (14), 3788–3791. <https://doi.org/10.1021/ol501676q>.
- (52) De Simone, F.; Saget, T.; Benfatti, F.; Almeida, S.; Waser, J. Formal Homo-Nazarov and Other Cyclization Reactions of Activated Cyclopropanes. *Chem. Eur. J.* **2011**, *17* (51), 14527–14538. <https://doi.org/10.1002/chem.201102583>.
- (53) Tius, M. A.; Chu, C. C.; Nieves-Colberg, R. An Imino Nazarov Cyclization. *Tetrahedron Lett.* **2001**, *42* (13), 2419–2422. [https://doi.org/10.1016/S0040-4039\(01\)00201-5](https://doi.org/10.1016/S0040-4039(01)00201-5).
- (54) Yu, K.-Y.; Deng, Y.-H.; Ge, X.-M.; An, X.-T.; Shu, P.-F.; Cao, Y.-X.; Zhao, X.-H.; Fan, C.-A. Tandem (2 + 2) Annulation/Retro-4 π Electrocyclization/Imino-Nazarov Cyclization Reaction of p-Quinone Methides with Ynamides: Expeditious Construction of Functionalized Aminoindenes. *Org. Lett.* **2021**, *23* (15), 5885–5890. <https://doi.org/10.1021/acs.orglett.1c02003>.
- (55) Ma, Z.-X.; He, S.; Song, W.; Hsung, R. P. α -Aryl-Substituted Allenamides in an Imino-Nazarov Cyclization Cascade Catalyzed by Au(I). *Org. Lett.* **2012**, *14* (22), 5736–5739. <https://doi.org/10.1021/ol302743k>.
- (56) Fan, T.; Wang, A.; Li, J.-Q.; Ye, J.-L.; Zheng, X.; Huang, P.-Q. Versatile One-Pot Synthesis of Polysubstituted Cyclopent-2-Enimines from α,β -Unsaturated Amides: Imino-Nazarov Reaction. *Angew. Chem. Int. Ed.* **2018**, *57* (32), 10352–10356. <https://doi.org/10.1002/anie.201805641>.
- (57) Alachouzos, G.; Frontier, A. J. Diastereoselective Construction of Densely Functionalized 1-Halocyclopentenenes Using an Alkynyl Halo-Prins/Halo-Nazarov Cyclization Strategy. *Angew. Chem. Int. Ed.* **2017**, *56* (47), 15030–15034. <https://doi.org/10.1002/anie.201709482>.
- (58) Alachouzos, G.; Frontier, A. J. Cationic Cascade for Building Complex Polycyclic Molecules from Simple Precursors: Diastereoselective Installation of Three Contiguous

- Stereogenic Centers in a One-Pot Process. *J. Am. Chem. Soc.* **2019**, *141* (1), 118–122. <https://doi.org/10.1021/jacs.8b11713>.
- (59) Holt, C.; Alachouzos, G.; Frontier, A. J. Leveraging the Halo-Nazarov Cyclization for the Chemodivergent Assembly of Functionalized Haloindenes and Indanones. *J. Am. Chem. Soc.* **2019**, *141* (13), 5461–5469. <https://doi.org/10.1021/jacs.9b00198>.
- (60) Sultana, S.; Lee, Y. R. Construction of Halofunctionalized Indenes via a Cascade Prins-Nazarov Cyclization Promoted by Dual Roles of BX₃. *Adv. Synth. Catal.* **2020**, *362* (4), 927–941. <https://doi.org/10.1002/adsc.201901266>.
- (61) Kumari, A.; Fernandes, R. BX₃-Mediated Intermolecular Formation of Functionalized 3-Halo-1H-Indenes via Cascade Halo-Nazarov-Type Cyclization. *Synthesis* **2020**, *52*, 2245–2258. <https://doi.org/10.1055/s-0039-1690881>.
- (62) Zheng, H.; Lejkowski, M.; Hall, D. G. Mild Boronic Acid Catalyzed Nazarov Cyclization of Divinyl Alcohols in Tandem with Diels–Alder Cycloaddition. *Tetrahedron Lett.* **2013**, *54* (1), 91–94. <https://doi.org/10.1016/j.tetlet.2012.10.100>.
- (63) Jin, J.; Zhao, Y.; Gouranourimi, A.; Ariaferd, A.; Hong Chan, P. W. Chiral Brønsted Acid Catalyzed Enantioselective Dehydrative Nazarov-Type Electrocyclization of Aryl and 2-Thienyl Vinyl Alcohols. *J. Am. Chem. Soc.* **2018**, *140* (17), 5834–5841. <https://doi.org/10.1021/jacs.8b02339>.
- (64) Lempenauer, L.; Duñach, E.; Lemièrre, G. Catalytic Rearrangement of 2-Alkoxy Diallyl Alcohols: Access to Polysubstituted Cyclopentenones. *Org. Lett.* **2016**, *18* (6), 1326–1329. <https://doi.org/10.1021/acs.orglett.6b00270>.
- (65) Nair, V.; Bindu, S.; Sreekumar, V.; Chiaroni, A. A Novel Approach to the Synthesis of Bicyclic Lactones via an Interrupted Nazarov Reaction of Gem-Divinyl Dihydrofurans. *Org. Lett.* **2002**, *4* (17), 2821–2823. <https://doi.org/10.1021/ol026010h>.
- (66) Komatsuki, K.; Sadamitsu, Y.; Sekine, K.; Saito, K.; Yamada, T. Stereospecific Decarboxylative Nazarov Cyclization Mediated by Carbon Dioxide for the Preparation of Highly Substituted 2-Cyclopentenones. *Angew. Chem. Int. Ed.* **2017**, *56* (38), 11594–11598. <https://doi.org/10.1002/anie.201705909>.
- (67) Ciufolini, M. A.; Roschangar, F. Practical Total Synthesis of (+)-Camptothecin: The Full Story. *Tetrahedron* **1997**, *53* (32), 11049–11060. [https://doi.org/10.1016/S0040-4020\(97\)00365-7](https://doi.org/10.1016/S0040-4020(97)00365-7).
- (68) Klumpp, D. A.; Zhang, Y.; O'Connor, M. J.; Esteves, P. M.; de Almeida, L. S. Aza-Nazarov Reaction and the Role of Superelectrophiles. *Org. Lett.* **2007**, *9* (16), 3085–3088. <https://doi.org/10.1021/ol0711570>.
- (69) Liu, Z.; Liu, X.; Yang, S.; Miao, X.; Li, D.; Wang, D. Titanium-Mediated Aza-Nazarov Annulation for the Synthesis of N-Fused Tricycles: A General Method to Access Lamellarin Analogues. *J. Org. Chem.* **2022**, *87* (15), 10319–10332. <https://doi.org/10.1021/acs.joc.2c01379>.
- (70) Ji, W.; Liu, Y. A.; Liao, X. Transition-Metal-Free Synthesis of N-Hydroxy Oxindoles by an Aza-Nazarov-Type Reaction Involving Azaoxyallyl Cations. *Angew. Chem. Int. Ed.* **2016**, *55* (42), 13286–13289. <https://doi.org/10.1002/anie.201607177>.
- (71) Aegurla, B.; Peddinti, R. K. The Diaza-Nazarov Cyclization Involving a 2,3-Diaza-Pentadienyl Cation for the Synthesis of Polysubstituted Pyrazoles. *Org. Biomol. Chem.* **2017**, *15* (45), 9643–9652. <https://doi.org/10.1039/C7OB01949A>.

- (72) Chen, T.; Gong, F.; Nagaraju, S.; Liu, J.; Yang, S.; Chen, X.; Fang, X. Oxa-Nazarov Cyclization-Michael Addition Sequence for the Rapid Construction of Dihydrofuranones. *Org. Lett.* **2022**, *24* (48), 8837–8842. <https://doi.org/10.1021/acs.orglett.2c03601>.
- (73) Tian, Y.; Tang, M.; Lian, C.; Song, R.; Yang, D.; Lv, J. Asymmetric Binary-Acid Catalysis: A Diastereo- and Enantioselective Oxa-Nazarov Cyclization-Michael Addition of Conjugated 1,2-Diketones. *Org. Chem. Front.* **2023**, *10* (12), 3039–3044. <https://doi.org/10.1039/D3QO00558E>.
- (74) Miller, A. K.; Banghart, M. R.; Beaudry, C. M.; Suh, J. M.; Trauner, D. Development of Novel Lewis Acid Catalyzed Cycloisomerizations: Synthesis of Bicyclo[3.1.0]Hexenes and Cyclopentenones. *Tetrahedron* **2003**, *59* (45), 8919–8930. <https://doi.org/10.1016/j.tet.2003.04.006>.
- (75) Denmark, S. E.; Hite, G. A. Silicon-Directed Nazarov Cyclizations. Part VI. The Anomalous Cyclization of Vinyl Dienyl Ketones. *Helv. Chim. Acta* **1988**, *71* (1), 195–208. <https://doi.org/10.1002/hlca.19880710121>.
- (76) Marsili, L. A.; Pergomet, J. L.; Gandon, V.; Riveira, M. J. Iodine-Catalyzed Iso-Nazarov Cyclization of Conjugated Dienals for the Synthesis of 2-Cyclopentenones. *Org. Lett.* **2018**, *20* (22), 7298–7303. <https://doi.org/10.1021/acs.orglett.8b03229>.
- (77) Marques, A.-S.; Coeffard, V.; Chataigner, I.; Vincent, G.; Moreau, X. Iron-Mediated Domino Interrupted Iso-Nazarov/Dearomative (3 + 2)-Cycloaddition of Electrophilic Indoles. *Org. Lett.* **2016**, *18* (20), 5296–5299. <https://doi.org/10.1021/acs.orglett.6b02613>.
- (78) Rieder, C. J.; Winberg, K. J.; West, F. G. Cyclization of Cross-Conjugated Trienes: The Vinylogous Nazarov Reaction. *J. Am. Chem. Soc.* **2009**, *131* (22), 7504–7505. <https://doi.org/10.1021/ja9023226>.
- (79) Riveira, M. J.; Mischne, M. P. An Interrupted Vinylogous Iso-Nazarov Reaction: Cycloisomerization of Conjugated Trienones to Cyclopenta[b]Furan Derivatives. *J. Org. Chem.* **2014**, *79* (17), 8244–8254. <https://doi.org/10.1021/jo501453b>.
- (80) Dethe, D. H.; Boda, R.; Murhade, G. M. Lewis Acid Catalyzed Nazarov Type Cyclization for the Synthesis of a Substituted Indane Framework: Total Synthesis of (±)-Mutisianthol. *Org. Chem. Front.* **2015**, *2* (6), 645–648. <https://doi.org/10.1039/C5QO00005J>.
- (81) Zhang, L.; Wang, S. Efficient Synthesis of Cyclopentenones from Enynyl Acetates via Tandem Au(I)-Catalyzed 3,3-Rearrangement and the Nazarov Reaction. *J. Am. Chem. Soc.* **2006**, *128* (5), 1442–1443. <https://doi.org/10.1021/ja057327q>.
- (82) Zi, W.; Wu, H.; Toste, F. D. Gold(I)-Catalyzed Dearomative Rautenstrauch Rearrangement: Enantioselective Access to Cyclopenta[b]Indoles. *J. Am. Chem. Soc.* **2015**, *137* (9), 3225–3228. <https://doi.org/10.1021/jacs.5b00613>.
- (83) Shu, C.; Wang, Y.-H.; Shen, C.-H.; Ruan, P.-P.; Lu, X.; Ye, L.-W. Gold-Catalyzed Intermolecular Ynamide Amination-Initiated Aza-Nazarov Cyclization: Access to Functionalized 2-Aminopyrroles. *Org. Lett.* **2016**, *18* (13), 3254–3257. <https://doi.org/10.1021/acs.orglett.6b01503>.
- (84) Braude, E. A.; Jackman, L. M.; Linstead, R. P.; Lowe, G. 624. Hydrogen Transfer. Part XII. Dehydrogenation of “Blocked” Hydroaromatic Compounds by Quinones. *J. Chem. Soc.* **1960**, 3123–3132. <https://doi.org/10.1039/JR9600003123>.
- (85) Creighton, A. M.; Jackman, L. M. 626. Hydrogen Transfer. Part XIV. The Quinone Cyclodehydrogenation of Acids and Alcohols. *J. Chem. Soc.* **1960**, 3138. <https://doi.org/10.1039/jr9600003138>.

- (86) Horita, K.; Yoshioka, T.; Tanaka, T.; Oikawa, Y.; Yonemitsu, O. On the Selectivity of Deprotection of Benzyl, Mpm (4-Methoxybenzyl) and Dmpm (3,4-Dimethoxybenzyl) Protecting Groups for Hydroxy Functions. *Tetrahedron* **1986**, *42* (11), 3021–3028. [https://doi.org/10.1016/S0040-4020\(01\)90593-9](https://doi.org/10.1016/S0040-4020(01)90593-9).
- (87) Yamamoto, S.; Sakurai, T.; Yingjin, L.; Sueishi, Y. Mechanism of Hydride Transfer Reaction from 4-(Dimethylamino)Phenyl Methane Derivatives to 2,3-Dichloro-5,6-Dicyano-p-Benzoquinone. *Phys. Chem. Chem. Phys.* **1999**, *1* (5), 833–837. <https://doi.org/10.1039/a809358j>.
- (88) Fukuzumi, S.; Ohkubo, K.; Tokuda, Y.; Suenobu, T. Hydride Transfer from 9-Substituted 10-Methyl-9,10-Dihydroacridines to Hydride Acceptors via Charge-Transfer Complexes and Sequential Electron–Proton–Electron Transfer. A Negative Temperature Dependence of the Rates. *J. Am. Chem. Soc.* **2000**, *122* (18), 4286–4294. <https://doi.org/10.1021/ja9941375>.
- (89) Zaman, K. M.; Yamamoto, S.; Nishimura, N.; Maruta, J.; Fukuzumi, S. Charge-Transfer Complexes Acting as Real Intermediates in Hydride Transfer from Michler’s Hydride to 2,3-Dichloro-5,6-Dicyano-p-Benzoquinone via Electron Transfer. *J. Am. Chem. Soc.* **1994**, *116* (26), 12099–12100. <https://doi.org/10.1021/ja00105a079>.
- (90) Luca, O. R.; Wang, T.; Konezny, S. J.; Batista, V. S.; Crabtree, R. H. DDQ as an Electrocatalyst for Amine Dehydrogenation, a Model System for Virtual Hydrogen Storage. *New J. Chem.* **2011**, *35* (5), 998–999. <https://doi.org/10.1039/c0nj01011a>.
- (91) Tsang, A. S.-K.; Hashmi, A. S. K.; Comba, P.; Kerscher, M.; Chan, B.; Todd, M. H. N-Aryl Groups Are Ubiquitous in Cross-Dehydrogenative Couplings Because They Stabilize Reactive Intermediates. *Chem. Eur. J.* **2017**, *23* (39), 9313–9318. <https://doi.org/10.1002/chem.201700430>.
- (92) Yamabe, S.; Yamazaki, S.; Sakaki, S. A DFT Study of Hydride Transfers to the Carbonyl Oxygen of DDQ. *Int. J. Quantum Chem.* **2015**, *115* (21), 1533–1542. <https://doi.org/10.1002/qua.24967>.
- (93) Guo, X.; Mayr, H. Manifestation of Polar Reaction Pathways of 2,3-Dichloro-5,6-Dicyano-p-Benzoquinone. *J. Am. Chem. Soc.* **2013**, *135* (33), 12377–12387. <https://doi.org/10.1021/ja405890d>.
- (94) Batista, V. S.; Crabtree, R. H.; Konezny, S. J.; Luca, O. R.; Praetorius, J. M. Oxidative Functionalization of Benzylic C–H Bonds by DDQ. *New J. Chem.* **2012**, *36* (5), 1141. <https://doi.org/10.1039/c2nj40021a>.
- (95) Morales-Rivera, C. A.; Floreancig, P. E.; Liu, P. Predictive Model for Oxidative C–H Bond Functionalization Reactivity with 2,3-Dichloro-5,6-Dicyano-1,4-Benzoquinone. *J. Am. Chem. Soc.* **2017**, *139* (49), 17935–17944. <https://doi.org/10.1021/jacs.7b08902>.
- (96) Höfler, C.; Rüchardt, C. Bimolecular Formation of Radicals by Hydrogen Transfer, 10. On the Mechanism of Quinone Dehydrogenations. *Liebigs Ann.* **1996**, *1996* (2), 183–188. <https://doi.org/10.1002/jlac.199619960206>.
- (97) Pratt, D. A.; Wright, J. S.; Ingold, K. U. Theoretical Study of Carbon–Halogen Bond Dissociation Enthalpies of Substituted Benzyl Halides. How Important Are Polar Effects? *J. Am. Chem. Soc.* **1999**, *121* (20), 4877–4882. <https://doi.org/10.1021/ja982866z>.
- (98) Wu, Y.-D.; Wong, C.-L.; Chan, K. W. K.; Ji, G.-Z.; Jiang, X.-K. Substituent Effects on the C–H Bond Dissociation Energy of Toluene. A Density Functional Study. *J. Org. Chem.* **1996**, *61* (2), 746–750. <https://doi.org/10.1021/jo951212v>.

- (99) Braude, E. A.; Linstead, R. P.; Wooldridge, K. R. 593. Hydrogen Transfer. Part IX. The Selective Dehydrogenation of Unsaturated Alcohols by High-Potential Quinones. *J. Chem. Soc.* **1956**, 3070–3074. <https://doi.org/10.1039/jr9560003070>.
- (100) Guo, X.; Zipse, H.; Mayr, H. Mechanisms of Hydride Abstractions by Quinones. *J. Am. Chem. Soc.* **2014**, *136* (39), 13863–13873. <https://doi.org/10.1021/ja507598y>.
- (101) Tu, W.; Liu, L.; Floreancig, P. E. Diastereoselective Tetrahydropyrone Synthesis through Transition-Metal-Free Oxidative Carbon–Hydrogen Bond Activation. *Angew. Chem. Int. Ed.* **2008**, *47* (22), 4184–4187. <https://doi.org/10.1002/anie.200706002>.
- (102) Hayashi, Y.; Mukaiyama, T. New Method for Oxidative Carbon-Carbon Bond Formation by the Reaction of Allyl Ethers, 2,3-Dichloro-5,6-Dicyano-p-Benzoquinone(DDQ) and Silyl Carbon Nucleophiles. *Chem. Lett.* **1987**, *16* (9), 1811–1814. <https://doi.org/10.1246/cl.1987.1811>.
- (103) Muramatsu, W.; Nakano, K. Organocatalytic Approach for C(Sp³)–H Bond Arylation, Alkylation, and Amidation of Isochromans under Facile Conditions. *Org. Lett.* **2014**, *16* (7), 2042–2045. <https://doi.org/10.1021/ol5006399>.
- (104) Cheng, D.; Bao, W. Highly Efficient Metal-Free Cross-Coupling by C–H Activation between Allylic and Active Methylenic Compounds Promoted by DDQ. *Adv. Synth. Catal.* **2008**, *350* (9), 1263–1266. <https://doi.org/10.1002/adsc.200800085>.
- (105) Grenning, A. J.; Snyder, J. K.; Porco, J. A. Remodeling of Fumagillol: Discovery of an Oxygen-Directed Oxidative Mannich Reaction. *Org. Lett.* **2014**, *16* (3), 792–795. <https://doi.org/10.1021/ol4035269>.
- (106) Liu, L.; Floreancig, P. E. Cyclization Reactions through DDQ-Mediated Vinyl Oxazolidinone Oxidation. *Org. Lett.* **2009**, *11* (14), 3152–3155. <https://doi.org/10.1021/ol901188q>.
- (107) Liu, L.; Floreancig, P. E. Structurally and Stereochemically Diverse Tetrahydropyran Synthesis through Oxidative C–H Bond Activation. *Angew. Chem. Int. Ed.* **2010**, *49* (17), 3069–3072. <https://doi.org/10.1002/anie.201000033>.
- (108) Brizgys, G. J.; Jung, H. H.; Floreancig, P. E. Stereoselective Piperidine Synthesis through Oxidative Carbon–Hydrogen Bond Functionalizations of Enamides. *Chem. Sci.* **2012**, *3* (2), 438–442. <https://doi.org/10.1039/C1SC00670C>.
- (109) Cui, Y.; Floreancig, P. E. Synthesis of Sulfur-Containing Heterocycles through Oxidative Carbon–Hydrogen Bond Functionalization. *Org. Lett.* **2012**, *14* (7), 1720–1723. <https://doi.org/10.1021/ol3002877>.
- (110) Peh, G.; Floreancig, P. E. Cyclopropane Compatibility with Oxidative Carbocation Formation: Total Synthesis of Clavosolide A. *Org. Lett.* **2012**, *14* (21), 5614–5617. <https://doi.org/10.1021/ol302744t>.
- (111) Peh, G.; Floreancig, P. E. Convergent One-Pot Oxidative [n + 1] Approaches to Spiroacetal Synthesis. *Org. Lett.* **2015**, *17* (15), 3750–3753. <https://doi.org/10.1021/acs.orglett.5b01736>.
- (112) Reddy, B. V. S.; Borkar, P.; S. Yadav, J.; Reddy, P. P.; C. Kunwar, A.; Sridhar, B.; Grée, R. Oxidative Prins and Prins/Friedel–Crafts Cyclizations for the Stereoselective Synthesis of Dioxabicycles and Hexahydro-1 H -Benzo[f]Isochromenes via the Benzylic C–H Activation. *Org. Biomol. Chem.* **2012**, *10* (7), 1349–1358. <https://doi.org/10.1039/C1OB06489D>.
- (113) Jiao, Z.-W.; Tu, Y.-Q.; Zhang, Q.; Liu, W.-X.; Zhang, S.-Y.; Wang, S.-H.; Zhang, F.-M.; Jiang, S. Tandem C–H Oxidation/Cyclization/Rearrangement and Its Application to

- Asymmetric Syntheses of (–)-Brussonol and (–)-Przewalskine E. *Nat. Commun.* **2015**, *6* (1). <https://doi.org/10.1038/ncomms8332>.
- (114) Yu, B.; Jiang, T.; Li, J.; Su, Y.; Pan, X.; She, X. A Novel Prins Cyclization through Benzylic/Allylic C–H Activation. *Org. Lett.* **2009**, *11* (15), 3442–3445. <https://doi.org/10.1021/ol901291w>.
- (115) Kar, A.; Chakraborty, B.; Kundal, S.; Rana, G.; Jana, U. DDQ/FeCl₃-Mediated Tandem Oxidative Carbon–Carbon Bond Formation for the Synthesis of Indole–Fluorene Hybrid Molecules. *Org. Biomol. Chem.* **2021**, *19* (4), 906–910. <https://doi.org/10.1039/D0OB00413H>.
- (116) Qi, C.; Cong, H.; Cahill, K. J.; Müller, P.; Johnson, R. P.; Porco, J. A. Biomimetic Dehydrogenative Diels–Alder Cycloadditions: Total Syntheses of Brosimones A and B. *Angew. Chem. Int. Ed.* **2013**, *52* (32), 8345–8348. <https://doi.org/10.1002/anie.201302847>.
- (117) Xu, W.-L.; Zhang, H.; Hu, Y.-L.; Yang, H.; Chen, J.; Zhou, L. Metal-Free Dehydrogenative Diels–Alder Reactions of Prenyl Derivatives with Dienophiles via a Thermal Reversible Process. *Org. Lett.* **2018**, *20* (18), 5774–5778. <https://doi.org/10.1021/acs.orglett.8b02469>.
- (118) Chandrasekhar, S.; Sumithra, G.; Yadav, J. S. Deprotection of Mono and Dimethoxy Phenyl Methyl Ethers Using Catalytic Amounts of DDQ. *Tetrahedron Lett.* **1996**, *37* (10), 1645–1646. [https://doi.org/10.1016/0040-4039\(96\)00081-0](https://doi.org/10.1016/0040-4039(96)00081-0).
- (119) Sharma, G. V. M.; Lavanya, B.; Mahalingam, A. K.; Krishna, P. R. Mn(OAc)₃—an Efficient Oxidant for Regeneration of DDQ: Deprotection of *p*-Methoxy Benzyl Ethers. *Tetrahedron Lett.* **2000**, *41* (52), 10323–10326. [https://doi.org/10.1016/S0040-4039\(00\)01855-4](https://doi.org/10.1016/S0040-4039(00)01855-4).
- (120) Shen, Z.; Dai, J.; Xiong, J.; He, X.; Mo, W.; Hu, B.; Sun, N.; Hu, X. 2,3-Dichloro-5,6-Dicyano-1,4-Benzoquinone (DDQ)/Tert-Butyl Nitrite/Oxygen: A Versatile Catalytic Oxidation System. *Adv. Synth. Catal.* **2011**, *353* (16), 3031–3038. <https://doi.org/10.1002/adsc.201100429>.
- (121) Liu, L.; Floreancig, P. E. 2,3-Dichloro-5,6-Dicyano-1,4-Benzoquinone-Catalyzed Reactions Employing MnO₂ as a Stoichiometric Oxidant. *Org. Lett.* **2010**, *12* (20), 4686–4689. <https://doi.org/10.1021/ol102078v>.
- (122) Cheng, D.; Yuan, K.; Xu, X.; Yan, J. The Oxidative Coupling of Benzylic Compounds Catalyzed by 2,3-Dichloro-5,6-Dicyano-Benzoquinone and Sodium Nitrite Using Molecular Oxygen as a Co-Oxidant. *Tetrahedron Lett.* **2015**, *56* (13), 1641–1644. <https://doi.org/10.1016/j.tetlet.2015.02.018>.
- (123) Rozantsev, E. G.; Sholle, V. D. Synthesis and Reactions of Stable Nitroxyl Radicals II. Reactions I. *Synthesis* **1971**, *1971* (8), 401–414. <https://doi.org/10.1055/s-1971-21749>.
- (124) Pradhan, P. P.; Bobbitt, J. M.; Bailey, W. F. Oxidative Cleavage of Benzylic and Related Ethers, Using an Oxoammonium Salt. *J. Org. Chem.* **2009**, *74* (24), 9524–9527. <https://doi.org/10.1021/jo902144b>.
- (125) Miller, J. L.; Zhou, L.; Liu, P.; Floreancig, P. E. Mechanism-Based Approach to Reagent Selection for Oxidative Carbon–Hydrogen Bond Cleavage Reactions. *Chem. Eur. J.* **2022**, *28* (1). <https://doi.org/10.1002/chem.202103078>.
- (126) Richter, H.; García Mancheño, O. Dehydrogenative Functionalization of C(Sp³)–H Bonds Adjacent to a Heteroatom Mediated by Oxoammonium Salts. *Eur. J. Org. Chem.* **2010**, *2010* (23), 4460–4467. <https://doi.org/10.1002/ejoc.201000548>.

- (127) Wang, G.; Mao, Y.; Liu, L. Diastereoselectively Complementary C–H Functionalization Enables Access to Structurally and Stereochemically Diverse 2,6-Substituted Piperidines. *Org. Lett.* **2016**, *18* (24), 6476–6479. <https://doi.org/10.1021/acs.orglett.6b03372>.
- (128) Liu, L.; Cheng, H.-L.; Ma, W.-Q.; Hou, S.-H.; Tu, Y.-Q.; Zhang, F.-M.; Zhang, X.-M.; Wang, S.-H. Improved Synthesis of 8-Oxabicyclo[3.2.1]Octanes via Tandem C–H Oxidation/Oxa-[3,3] Cope Rearrangement/Aldol Cyclization. *Chem. Commun.* **2018**, *54* (2), 196–199. <https://doi.org/10.1039/C7CC08511G>.
- (129) Barton, D. H. R.; Magnus, P. D.; Smith, G.; Zurr, D. Oxidation of Ketone Acetals by Hydride Transfer. *J. Chem. Soc. Chem. Commun.* **1971**, 861–863. <https://doi.org/10.1039/C29710000861>.
- (130) R. Barton, D. H.; D. Magnus, P.; Streckert, G.; Zurr, D. Deprotection of Masked Steroidal Alcohols by Hydride Transfer. *J. Chem. Soc. Chem. Commun.* **1971**, (18), 1109–1111. <https://doi.org/10.1039/C29710001109>.
- (131) Barton, D. H. R.; Magnus, P. D.; Smith, G.; Streckert, G.; Zurr, D. Experiments on the Synthesis of Tetracycline. Part XI. Oxidation of Ketone Acetals and Ethers by Hydride Transfer. *J. Chem. Soc. Perkin I* **1972**, 542–552. <https://doi.org/10.1039/P19720000542>.
- (132) Jung, M. E.; Pan, Y.-G.; Rathke, M. W.; Sullivan, D. F.; Woodbury, R. P. Oxidation of Trialkylsilyl Enol Ethers via Hydride Abstraction: A New Procedure for Ketone to Enone Conversion. *J. Org. Chem.* **1977**, *42* (24), 3961–3963. <https://doi.org/10.1021/jo00444a040>.
- (133) Wan, M.; Meng, Z.; Lou, H.; Liu, L. Practical and Highly Selective C–H Functionalization of Structurally Diverse Ethers. *Angew. Chem. Int. Ed.* **2014**, *53* (50), 13845–13849. <https://doi.org/10.1002/anie.201407083>.
- (134) Schwartz, B. D.; Denton, J. R.; Lian, Y.; Davies, H. M. L.; Williams, C. M. Asymmetric [4 + 3] Cycloadditions between Vinylcarbenoids and Dienes: Application to the Total Synthesis of the Natural Product (–)-5- *Epi* -Vibsanin E. *J. Am. Chem. Soc.* **2009**, *131* (23), 8329–8332. <https://doi.org/10.1021/ja9019484>.
- (135) Gassman, P. G.; Burns, S. J.; Pfister, K. B. Synthesis of Cyclic and Acyclic Enol Ethers (Vinyl Ethers). *J. Org. Chem.* **1993**, *58* (6), 1449–1457. <https://doi.org/10.1021/jo00058a027>.
- (136) Su, C.; Williard, P. G. Isomerization of Allyl Ethers Initiated by Lithium Diisopropylamide. *Org. Lett.* **2010**, *12* (23), 5378–5381. <https://doi.org/10.1021/ol102029u>.
- (137) Barluenga, J.; Fernández, M. A.; Aznar, F.; Valdés, C. Palladium-Catalyzed Cross-Coupling Reactions of Amines with Alkenyl Bromides: A New Method for the Synthesis of Enamines and Imines. *Chem. Eur. J.* **2004**, *10* (2), 494–507. <https://doi.org/10.1002/chem.200305406>.
- (138) Barluenga, J.; Fernández, M. A.; Aznar, F.; Valdés, C. Novel Method for the Synthesis of Enamines by Palladium Catalyzed Amination of Alkenyl Bromides. *Chem Commun* **2002**, 2362–2363. <https://doi.org/10.1039/B207524E>.
- (139) Barluenga, J.; Fernández, M. A.; Aznar, F.; Valdés, C. Palladium Catalyzed Amination of Vinyl Chlorides: A New Entry to Imines, Enamines and 2-Amino-1,3-Butadienes. *Chem Commun* **2004**, 1400–1401. <https://doi.org/10.1039/B403655G>.
- (140) Halton, B.; Harvey, J. Electrocyclic Ring-Opening Reactions of Gem-Dibromocyclopropanes in the Synthesis of Natural Products and Related Compounds. *Synlett* **2006**, *2006* (13), 1975–2000. <https://doi.org/10.1055/s-2006-948193>.

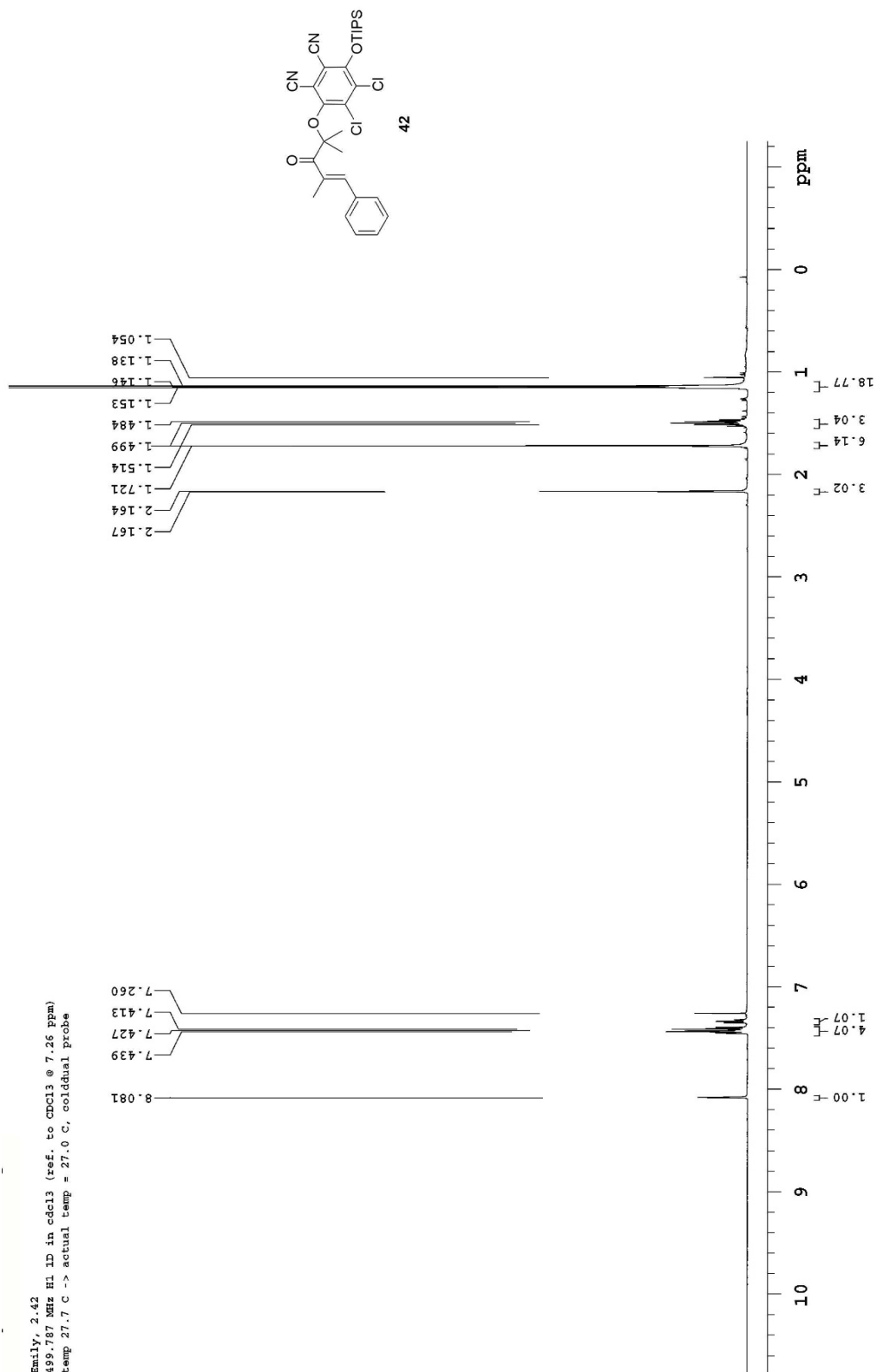
- (141) Saputra, M. A.; Ngo, L.; Kartika, R. Synthesis of Vinyl Chlorides via Triphosgene–Pyridine Activation of Ketones. *J. Org. Chem.* **2015**, *80* (17), 8815–8820. <https://doi.org/10.1021/acs.joc.5b01137>.
- (142) Spaggiari, A.; Vaccari, D.; Davoli, P.; Torre, G.; Prati, F. A Mild Synthesis of Vinyl Halides and Gem-Dihalides Using Triphenyl Phosphite–Halogen-Based Reagents. *J. Org. Chem.* **2007**, *72* (6), 2216–2219. <https://doi.org/10.1021/jo061346g>.
- (143) Ying, B.-P.; Trogden, B. G.; Kohlman, D. T.; Liang, S. X.; Xu, Y.-C. Oxidative C–C Bond-Forming Reaction of Electron-Rich Alkylbenzyl Ether with Trimethylvinylloxysilane. *Org. Lett.* **2004**, *6* (10), 1523–1526. <https://doi.org/10.1021/ol036314j>.
- (144) Barluenga, J.; Moriel, P.; Aznar, F.; Valdés, C. A Very Simple Synthesis of Chloroalkenes and Chlorodienes by Selective Suzuki Couplings of 1,1- and 1,2-Dichloroethylene. *Adv. Synth. Catal.* **2006**, *348* (3), 347–353. <https://doi.org/10.1002/adsc.200505302>.
- (145) Zhang, Y.; Fitzpatrick, N.A.; Das, M.; Bedre, I. P.; Yayla, H. G.; Lall, M. S.; Musacchio, P. Z. A Photoredox-Catalyzed Approach for Formal Hydride Abstraction to Enable Csp³–H Functionalization with Nucleophilic Partners (F, C, O, N, and Br/Cl). *Chem Catal.* **2022**, *2* (2), 292–308. <https://doi.org/10.1016/j.checat.2021.12.010>.
- (146) Dong, M.; Jia, Y.; Zhou, W.; Gao, J.; Lv, X.; Luo, F.; Zhang, Y.; Liu, S. A Photoredox/Nickel Dual-Catalytic Strategy for Benzylic C–H Alkoxylation. *Org. Chem. Front.* **2021**, *8* (24), 6881–6887. <https://doi.org/10.1039/D1QO01421H>.
- (147) Lee, B. J.; DeGlopper, K. S.; Yoon, T. P. Site-Selective Alkoxylation of Benzylic C–H Bonds by Photoredox Catalysis. *Angew. Chem. Int. Ed.* **2020**, *59* (1), 197–202. <https://doi.org/10.1002/anie.201910602>.
- (148) Yan, Q.; Shen, X.; Zi, G.; Hou, G. Rh-Catalyzed Asymmetric Hydrogenation of α,β - and β,β -Disubstituted Unsaturated Boronate Esters. *Chem. Eur. J.* **2020**, *26* (27), 5961–5964. <https://doi.org/10.1002/chem.202000703>.
- (149) Yang, C.; Gao, Y.; Bai, S.; Jiang, C.; Qi, X. Chemoselective Cross-Coupling of Gem-Borazirconocene Alkanes with Aryl Halides. *J. Am. Chem. Soc.* **2020**, *142* (26), 11506–11513. <https://doi.org/10.1021/jacs.0c03821>.
- (150) Yu, Y.; Savage, R. E.; Eathiraj, S.; Meade, J.; Wick, M. J.; Hall, T.; Abbadessa, G.; Schwartz, B. Targeting AKT1-E17K and the PI3K/AKT Pathway with an Allosteric AKT Inhibitor, ARQ 092. *PLOS ONE* **2015**, *10* (10). <https://doi.org/10.1371/journal.pone.0140479>.
- (151) Zhao, Y.; Yu, S.; Sun, W.; Liu, L.; Lu, J.; McEachern, D.; Shargary, S.; Bernard, D.; Li, X.; Zhao, T.; Zou, P.; Sun, D.; Wang, S. A Potent Small-Molecule Inhibitor of the MDM2–P53 Interaction (MI-888) Achieved Complete and Durable Tumor Regression in Mice. *J. Med. Chem.* **2013**, *56* (13), 5553–5561. <https://doi.org/10.1021/jm4005708>.
- (152) Nowikow, C.; Fuerst, R.; Kauderer, M.; Dank, C.; Schmid, W.; Hajduch, M.; Rehulka, J.; Gurska, S.; Mokshyna, O.; Polishchuk, P.; Zupkó, I.; Dzubak, P.; Rinner, U. Synthesis and Biological Evaluation of *Cis*-Restrained Carbocyclic Combretastatin A-4 Analogs: Influence of the Ring Size and Saturation on Cytotoxic Properties. *Bioorg. Med. Chem.* **2019**, *27* (19), 115032. <https://doi.org/10.1016/j.bmc.2019.07.048>.
- (153) Salomon, R. G.; Kochi, J. K. Copper(I) Catalysis in Photocycloadditions. I. Norbornene. *J. Am. Chem. Soc.* **1974**, *96* (4), 1137–1144. <https://doi.org/10.1021/ja00811a030>.
- (154) Salomon, R. G.; Folting, K.; Streib, W. E.; Kochi, J. K. Copper(I) Catalysis in Photocycloadditions. II. Cyclopentene, Cyclohexene, and Cycloheptene. *J. Am. Chem. Soc.* **1974**, *96* (4), 1145–1152. <https://doi.org/10.1021/ja00811a031>.

- (155) Poplata, S.; Tröster, A.; Zou, Y.-Q.; Bach, T. Recent Advances in the Synthesis of Cyclobutanes by Olefin [2 + 2] Photocycloaddition Reactions. *Chem. Rev.* **2016**, *116* (17), 9748–9815. <https://doi.org/10.1021/acs.chemrev.5b00723>.
- (156) Lee-Ruff, E.; Mladenova, G. Enantiomerically Pure Cyclobutane Derivatives and Their Use in Organic Synthesis. *Chem. Rev.* **2003**, *103* (4), 1449–1484. <https://doi.org/10.1021/cr010013a>.
- (157) Sarkar, D.; Bera, N.; Ghosh, S. [2+2] Photochemical Cycloaddition in Organic Synthesis. *Eur. J. Org. Chem.* **2020**, *2020* (10), 1310–1326. <https://doi.org/10.1002/ejoc.201901143>.
- (158) Rasik, C. M.; Brown, M. K. Intermolecular Ketene-Alkene [2+2] Cycloadditions: The Significance of Lewis Acid Promoted Variants. *Synlett* **2014**, *25* (6), 760–765. <https://doi.org/10.1055/2-0033-1340626>.
- (159) Ghosez, L.; Montaigne, R.; Roussel, A.; Vanlierde, H.; Mollet, P. Cycloadditions of Dichloroketene to Olefins and Dienes. *Tetrahedron* **1971**, *27* (3), 615–633. [https://doi.org/10.1016/S0040-4020\(01\)90730-6](https://doi.org/10.1016/S0040-4020(01)90730-6).
- (160) Lawlor, M. D.; Lee, T. W.; Danheiser, R. L. Rhodium-Catalyzed Rearrangement of α -Diazo Thiol Esters to Thio-Substituted Ketenes. Application in the Synthesis of Cyclobutanones, Cyclobutenones, and β -Lactams. *J. Org. Chem.* **2000**, *65* (14), 4375–4384. <https://doi.org/10.1021/jo000227c>.
- (161) Marchand-Brynaert, J.; Ghosez, L. Cycloadditions of Keteneimmonium Cations to Olefins and Dienes. New Synthesis of Four-Membered Rings. *J. Am. Chem. Soc.* **1972**, *94* (8), 2870–2872. <https://doi.org/10.1021/ja00763a062>.
- (162) Rasik, C. M.; Brown, M. K. Lewis Acid-Promoted Ketene–Alkene [2 + 2] Cycloadditions. *J. Am. Chem. Soc.* **2013**, *135* (5), 1673–1676. <https://doi.org/10.1021/ja3103007>.
- (163) Alcaide, B.; Almendros, P.; Aragoncillo, C. Exploiting [2+2] Cycloaddition Chemistry: Achievements with Allenes. *Chem Soc Rev* **2010**, *39* (2), 783–816. <https://doi.org/10.1039/B913749A>.
- (164) Blomquist, A. T.; Verdol, J. A. Thermal Dimerization of Allene to 1,2-Dimethylenecyclobutane. *J. Am. Chem. Soc.* **1956**, *78* (1), 109–112. <https://doi.org/10.1021/ja01582a033>.
- (165) Brattesani, A. J.; Maverick, E.; Muscio, O. J.; Jacobs, T. L. Dimerization of Substituted 1,3-Diarylallenes. *J. Org. Chem.* **1992**, *57* (26), 7346–7349. <https://doi.org/10.1021/jo00052a063>.
- (166) Gajewski, J. J.; Shih, C. N. Characterization of the Dimethyl-1,2-Dimethylenecyclobutanes from the Methylallene Thermal Dimerization. *J. Org. Chem.* **1972**, *37* (1), 64–68. <https://doi.org/10.1021/jo00966a018>.
- (167) Moore, W. R.; Moser, W. R. Reaction of 6,6-Dibromobicyclo[3.1.0]Hexane with Methylolithium. Efficient Trapping of 1,2-Cyclohexadiene by Styrene. *J. Org. Chem.* **1970**, *35* (4), 908–912. <https://doi.org/10.1021/jo00829a008>.
- (168) McIntosh, K. Investigation of Strain-Activated Trapping Reactions of 1,2-Cyclohexadiene: Intramolecular Capture by Pendent Furans and Styrenes. PhD Dissertation, University of Alberta, 2020.
- (169) Jankovic, Christian. L.; West, F. G. 2 + 2 Trapping of Acyloxy-1,2-Cyclohexadienes with Styrenes and Electron-Deficient Olefins. *Org. Lett.* **2022**, *24* (51), 9497–9501. <https://doi.org/10.1021/acs.orglett.2c03978>.

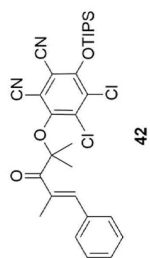
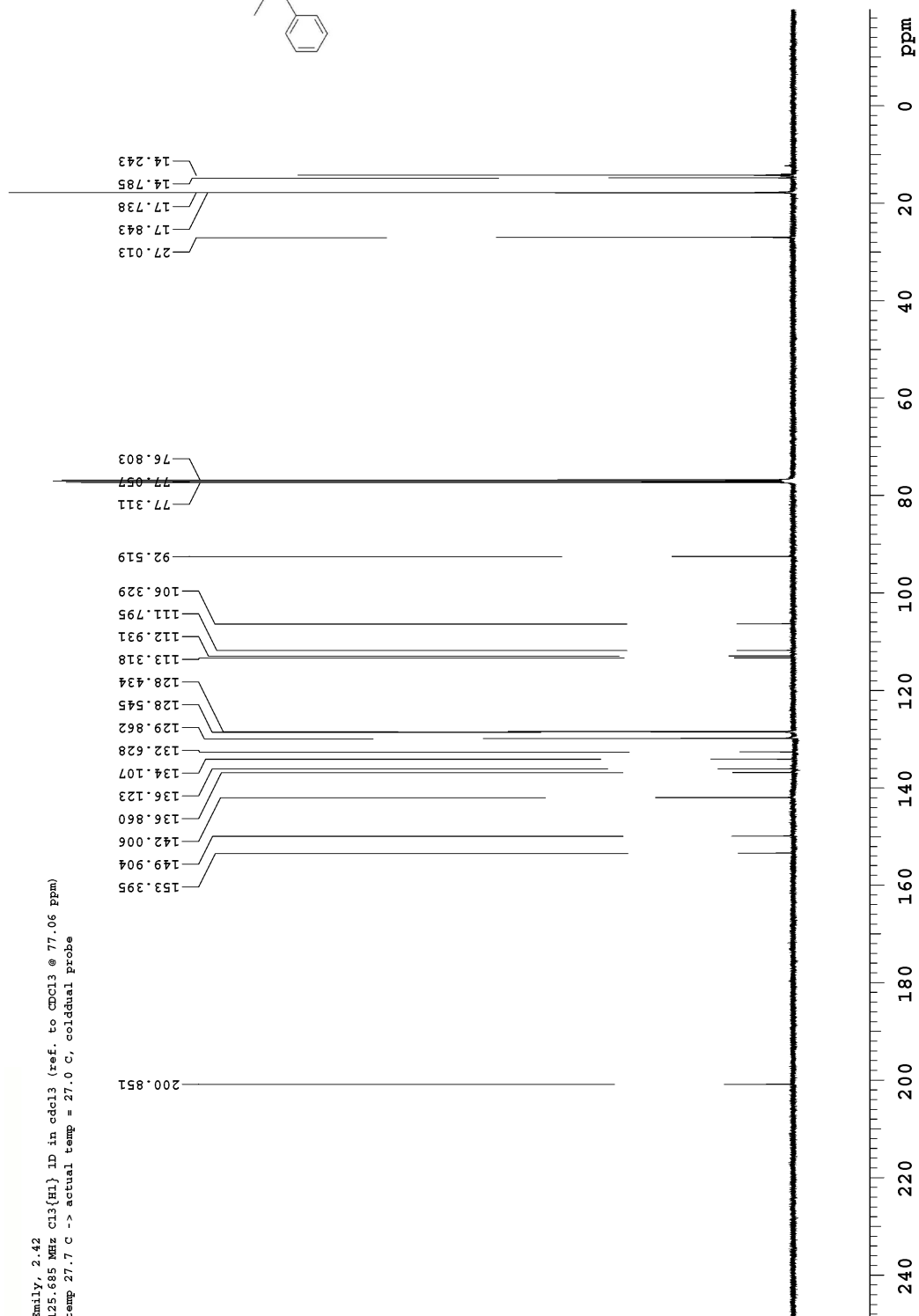
- (170) Padwa, A.; Filipkowski, M. A.; Meske, M.; Watterson, S. H.; Ni, Z. Peri and Stereoselectivity Effects in the Intramolecular [2+2]-Cycloaddition Reaction of Phenylsulfonyl-Substituted Allenes. *J. Am. Chem. Soc.* **1993**, *115* (9), 3776–3777. <https://doi.org/10.1021/ja00062a054>.
- (171) Yoshida, Mitsutaka.; Hidaka, Yukari.; Nawata, Yoshiharu.; Rudzinski, J. M.; Osawa, Eiji.; Kanematsu, Ken. Periselective Intramolecular Cycloaddition of Allene-1,3-Dicarboxylates. Unusual Structural Feature of [2 + 2] Cycloadducts. *J. Am. Chem. Soc.* **1988**, *110* (4), 1232–1238. <https://doi.org/10.1021/ja00212a036>.
- (172) Shen, Q.; Hammond, G. B. Regiospecific Synthesis of Bicyclo- and Heterobicyclo-Gem-Difluorocyclobutenes Using Functionalized Fluoroallenes and a Novel Mo-Catalyzed Intramolecular [2 + 2] Cycloaddition Reaction. *J. Am. Chem. Soc.* **2002**, *124* (23), 6534–6535. <https://doi.org/10.1021/ja0263893>.
- (173) Alcaide, B.; Almendros, P.; Aragoncillo, C. Structurally Novel Bi- and Tricyclic β -Lactams via [2 + 2] Cycloaddition or Radical Reactions in 2-Azetidinone-Tethered Enallenes and Allenynes. *Org. Lett.* **2003**, *5* (21), 3795–3798. <https://doi.org/10.1021/ol034995c>.
- (174) Mitsudo, T.; Naruse, H.; Kondo, T.; Ozaki, Y.; Watanabe, Y. [2 + 2]Cycloaddition of Norbornenes with Alkynes Catalyzed by Ruthenium Complexes. *Angew. Chem. Int. Ed.* **1994**, *33* (5), 580–581. <https://doi.org/10.1002/anie.199405801>.
- (175) Riddell, N.; Villeneuve, K.; Tam, W. Ruthenium-Catalyzed [2 + 2] Cycloadditions of Ynamides. *Org. Lett.* **2005**, *7* (17), 3681–3684. <https://doi.org/10.1021/ol0512841>.
- (176) Marion, F.; Coulomb, J.; Courillon, C.; Fensterbank, L.; Malacria, M. Platinum Dichloride-Catalyzed Cycloisomerization of Ene-Ynamides. *Org. Lett.* **2004**, *6* (9), 1509–1511. <https://doi.org/10.1021/ol049530g>.
- (177) Couty, S.; Meyer, C.; Cossy, J. Diastereoselective Gold-Catalyzed Cycloisomerizations of Ene-Ynamides. *Angew. Chem. Int. Ed.* **2006**, *45* (40), 6726–6730. <https://doi.org/10.1002/anie.200602270>.
- (178) Roglans, A.; Pla-Quintana, A.; Solà, M. Mechanistic Studies of Transition-Metal-Catalyzed [2 + 2 + 2] Cycloaddition Reactions. *Chem. Rev.* **2021**, *121* (3), 1894–1979. <https://doi.org/10.1021/acs.chemrev.0c00062>.
- (179) Narasaka, K.; Hayashi, Y.; Shimadzu, H.; Niihata, S. Asymmetric [2 + 2] Cycloaddition Reaction Catalyzed by a Chiral Titanium Reagent. *J. Am. Chem. Soc.* **1992**, *114* (23), 8869–8885. <https://doi.org/10.1021/ja00049a020>.
- (180) Gassman, P. G.; Lottes, A. C. Cyclobutane Formation in the $2\pi + 2\pi$ Cycloaddition of Allyl and Related Cations to Unactivated Olefins. Evidence for the Second Step in the Proposed Mechanism of the Ionic Diels-Alder Reaction. *Tetrahedron Lett.* **1992**, *33* (2), 157–160. [https://doi.org/10.1016/0040-4039\(92\)88038-7](https://doi.org/10.1016/0040-4039(92)88038-7).
- (181) Ko, C.; Feltenberger, J. B.; Ghosh, S. K.; Hsung, R. P. Gassman's Intramolecular [2 + 2] Cationic Cycloaddition. Formal Total Syntheses of Raikovenal and Epi-Raikovenal. *Org. Lett.* **2008**, *10* (10), 1971–1974. <https://doi.org/10.1021/ol8004968>.
- (182) Boxer, M. B.; Yamamoto, H. Remarkable Tris(Trimethylsilyl)Silyl Group for Diastereoselective [2 + 2] Cyclizations. *Org. Lett.* **2005**, *7* (14), 3127–3129. <https://doi.org/10.1021/ol0512334>.
- (183) Sweis, R. F.; Schramm, M. P.; Kozmin, S. A. Silver-Catalyzed [2 + 2] Cycloadditions of Siloxy Alkynes. *J. Am. Chem. Soc.* **2004**, *126* (24), 7442–7443. <https://doi.org/10.1021/ja048251l>.

- (184) Ito, H.; Hasegawa, M.; Takenaka, Y.; Kobayashi, T.; Iguchi, K. Enantioselective Total Synthesis of (+)-Tricycloclovulone. *J. Am. Chem. Soc.* **2004**, *126* (14), 4520–4521. <https://doi.org/10.1021/ja049750p>.
- (185) Canales, E.; Corey, E. J. Highly Enantioselective [2+2]-Cycloaddition Reactions Catalyzed by a Chiral Aluminum Bromide Complex. *J. Am. Chem. Soc.* **2007**, *129* (42), 12686–12687. <https://doi.org/10.1021/ja0765262>.
- (186) Hu, J.-L.; Feng, L.-W.; Wang, L.; Xie, Z.; Tang, Y.; Li, X. Enantioselective Construction of Cyclobutanes: A New and Concise Approach to the Total Synthesis of (+)-Piperarborenine B. *J. Am. Chem. Soc.* **2016**, *138* (40), 13151–13154. <https://doi.org/10.1021/jacs.6b08279>.
- (187) Albrecht, L.; Dickmeiss, G.; Acosta, F. C.; Rodríguez-Escrich, C.; Davis, R. L.; Jørgensen, K. A. Asymmetric Organocatalytic Formal [2 + 2]-Cycloadditions via Bifunctional H-Bond Directing Dienamine Catalysis. *J. Am. Chem. Soc.* **2012**, *134* (5), 2543–2546. <https://doi.org/10.1021/ja211878x>.
- (188) Gelozia, S. Lewis Acid Mediated Approaches for the Generation of 4- and 5-Membered Ring Systems. PhD Dissertation, University of Alberta, 2018.
- (189) Zhao, J.; Brosmer, J. L.; Tang, Q.; Yang, Z.; Houk, K. N.; Diaconescu, P. L.; Kwon, O. Intramolecular Crossed [2+2] Photocycloaddition through Visible Light-Induced Energy Transfer. *J. Am. Chem. Soc.* **2017**, *139* (29), 9807–9810. <https://doi.org/10.1021/jacs.7b05277>.
- (190) Pellissier, H. Recent Developments in Enantioselective Scandium-Catalyzed Transformations. *Chemistry* **2024**, *6* (1), 98–152. <https://doi.org/10.3390/chemistry6010007>.
- (191) Kobayashi, S.; Sugiura, M.; Kitagawa, H.; Lam, W. W.-L. Rare-Earth Metal Triflates in Organic Synthesis. *Chem. Rev.* **2002**, *102* (6), 2227–2302. <https://doi.org/10.1021/cr010289i>.
- (192) Nakashima, D.; Yamamoto, H. Design of Chiral N-Triflyl Phosphoramidate as a Strong Chiral Brønsted Acid and Its Application to Asymmetric Diels–Alder Reaction. *J. Am. Chem. Soc.* **2006**, *128* (30), 9626–9627. <https://doi.org/10.1021/ja062508t>.
- (193) Shahzad, S. A.; Vivant, C.; Wirth, T. Selenium-Mediated Synthesis of Biaryls through Rearrangement. *Org. Lett.* **2010**, *12* (6), 1364–1367. <https://doi.org/10.1021/ol100274e>.
- (194) Wenkert, E.; Schorp, M. K. A Synthesis of 3-Alkenylcycloalkenones. *J. Org. Chem.* **1994**, *59* (7), 1943–1944. <https://doi.org/10.1021/jo00086a063>.

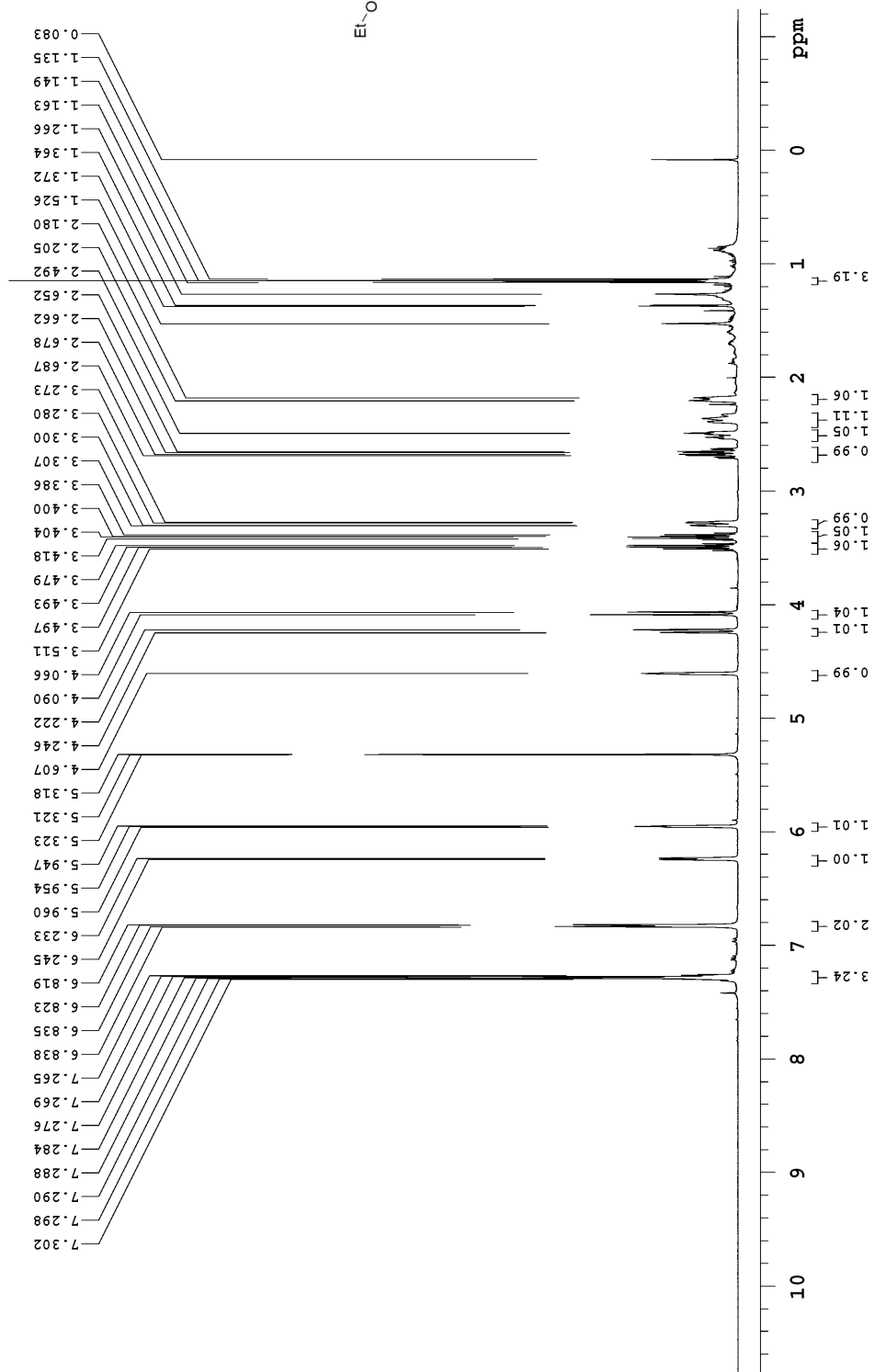
Appendix I: Selected NMR Spectra
(Chapter 2)

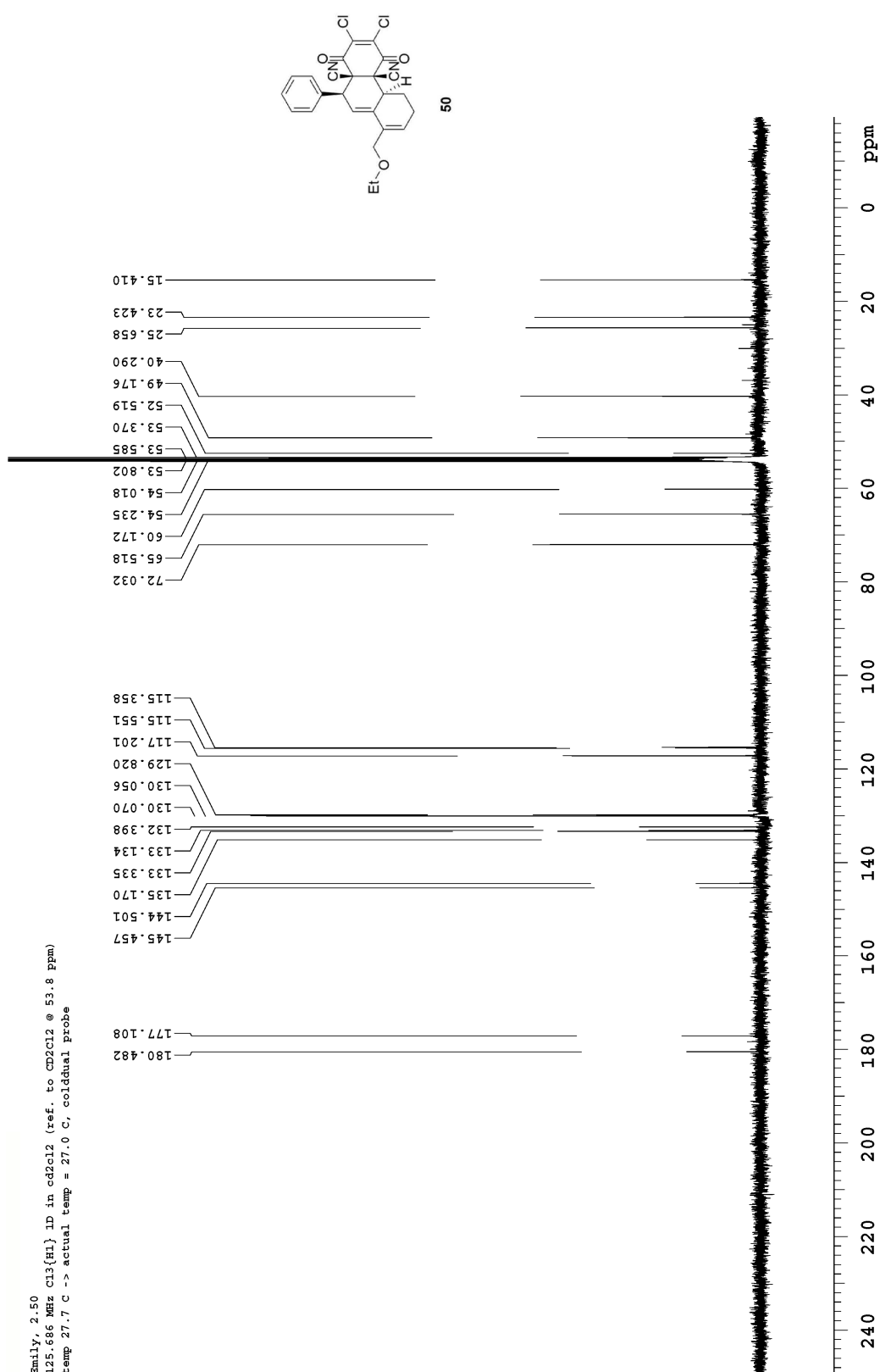


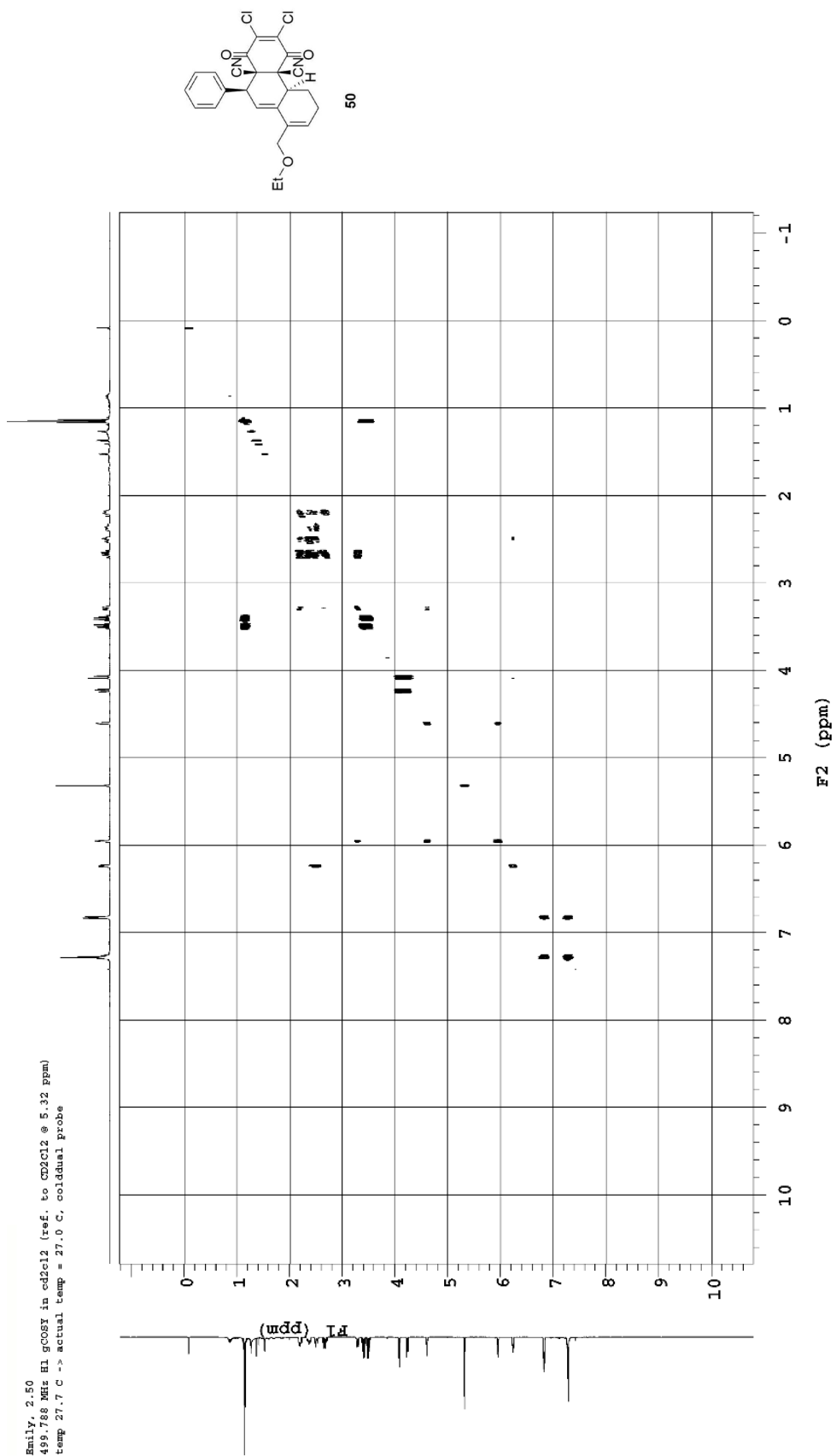
Emily, 2.42
 125.685 MHz C13{H1} ID in cdcl3 (ref. to CDCl3 @ 77.06 ppm)
 temp 27.7 C -> actual temp = 27.0 C, solidual probe

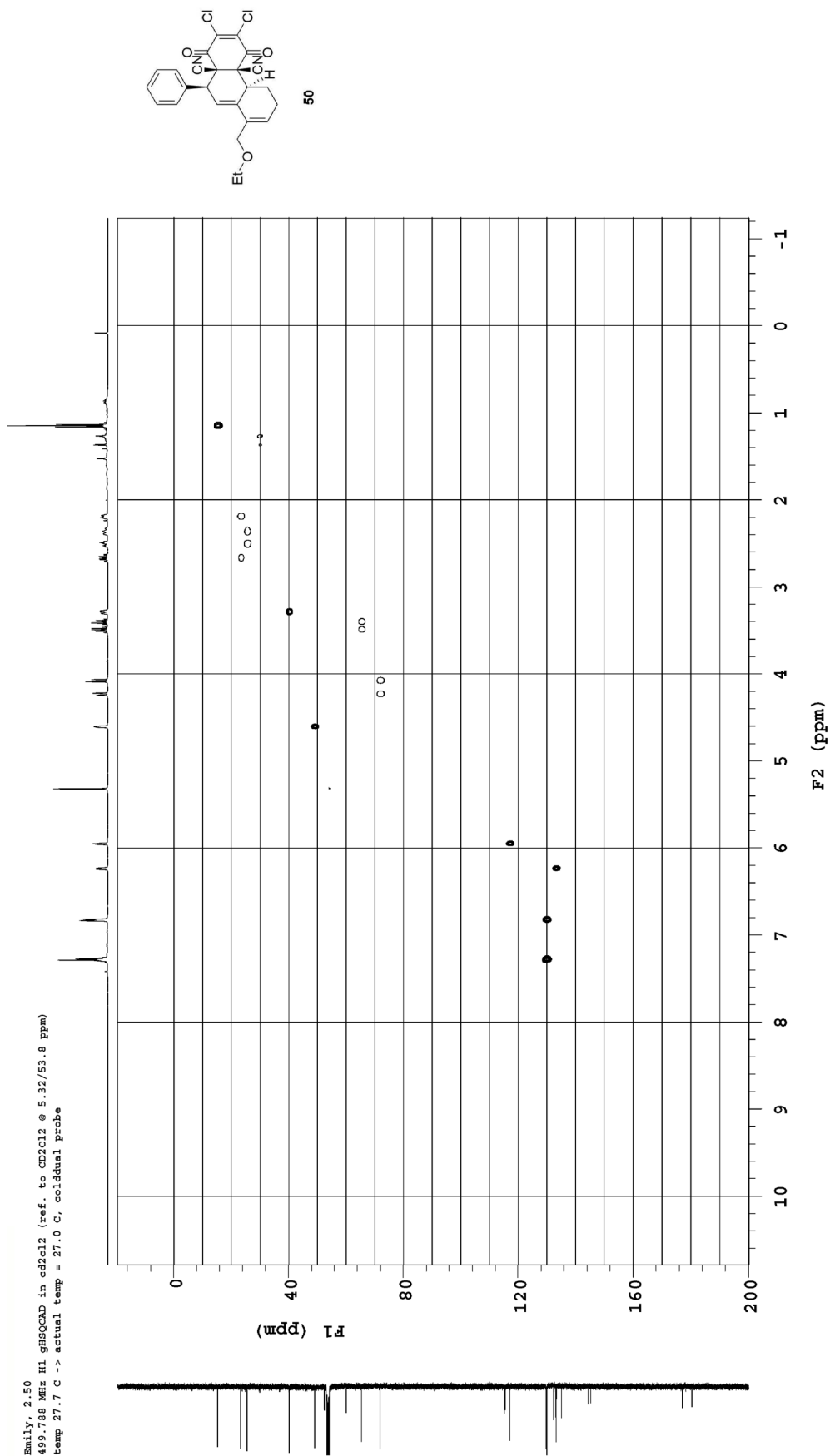


Emily, 2.50
 499.788 MHz ¹H 1D in cd2cl2 (ref. to CD2Cl2 @ 5.32 ppm)
 temp 27.7 C --> actual temp = 27.0 C, coldlual probe

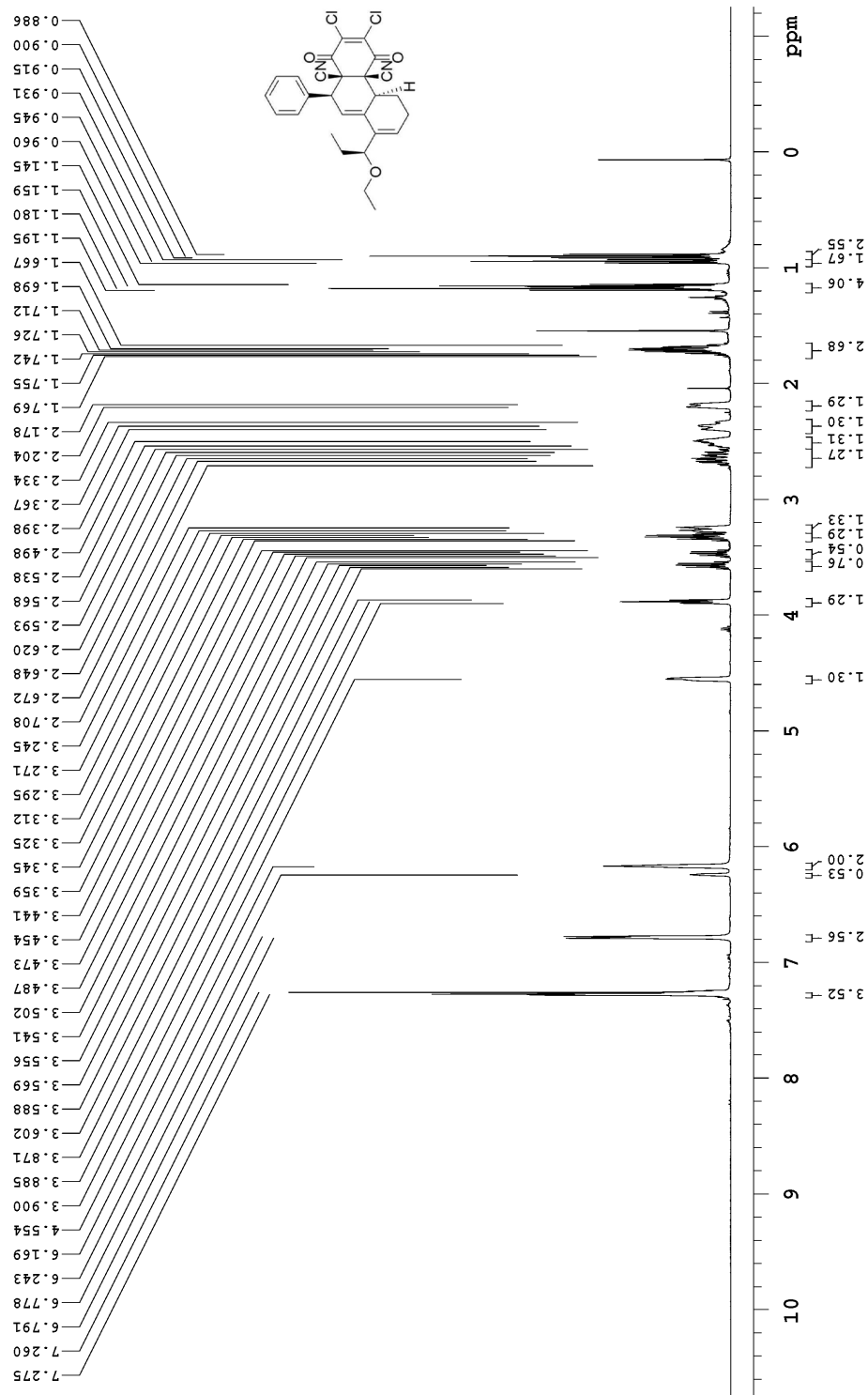


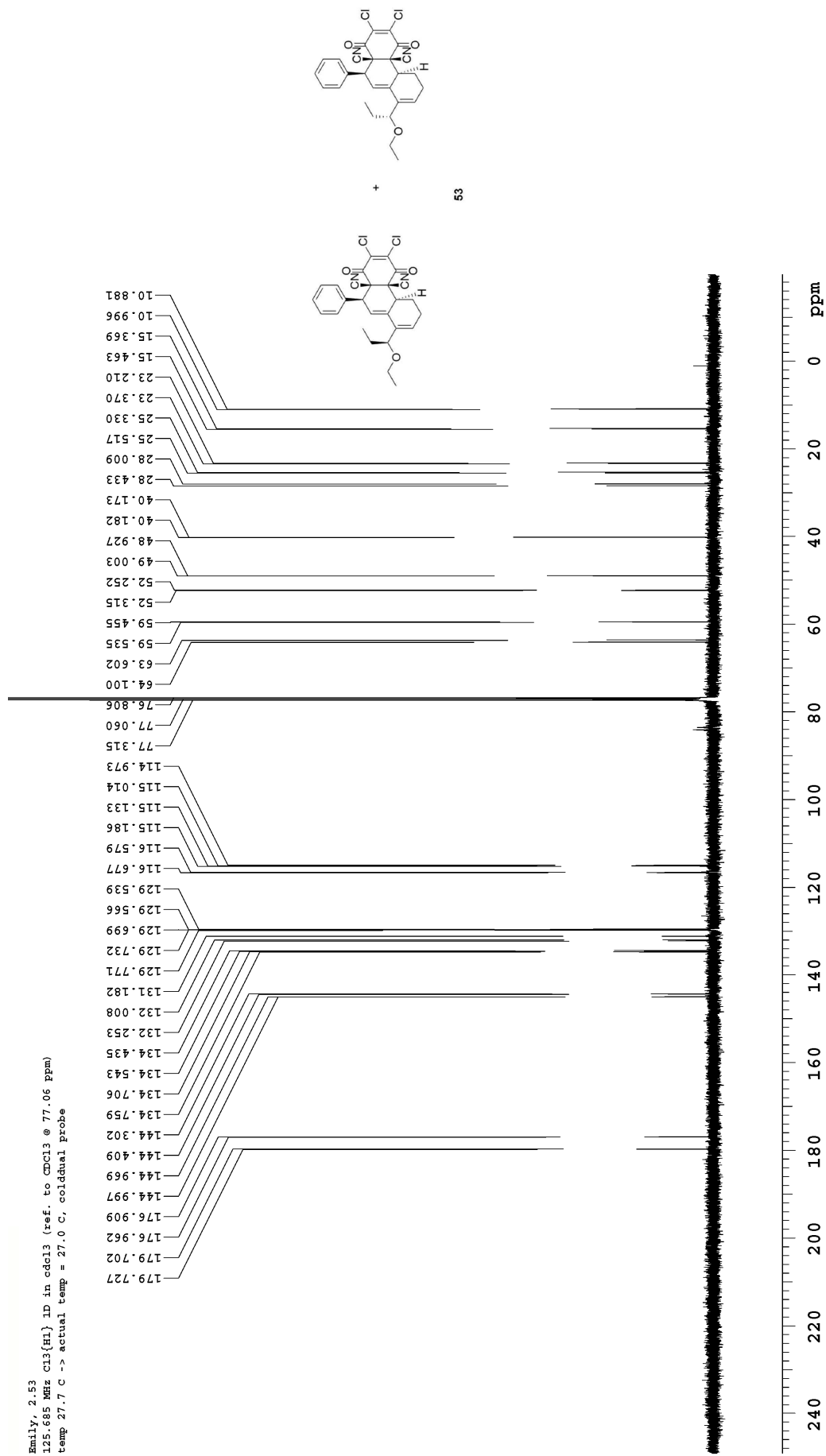




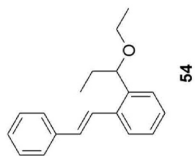
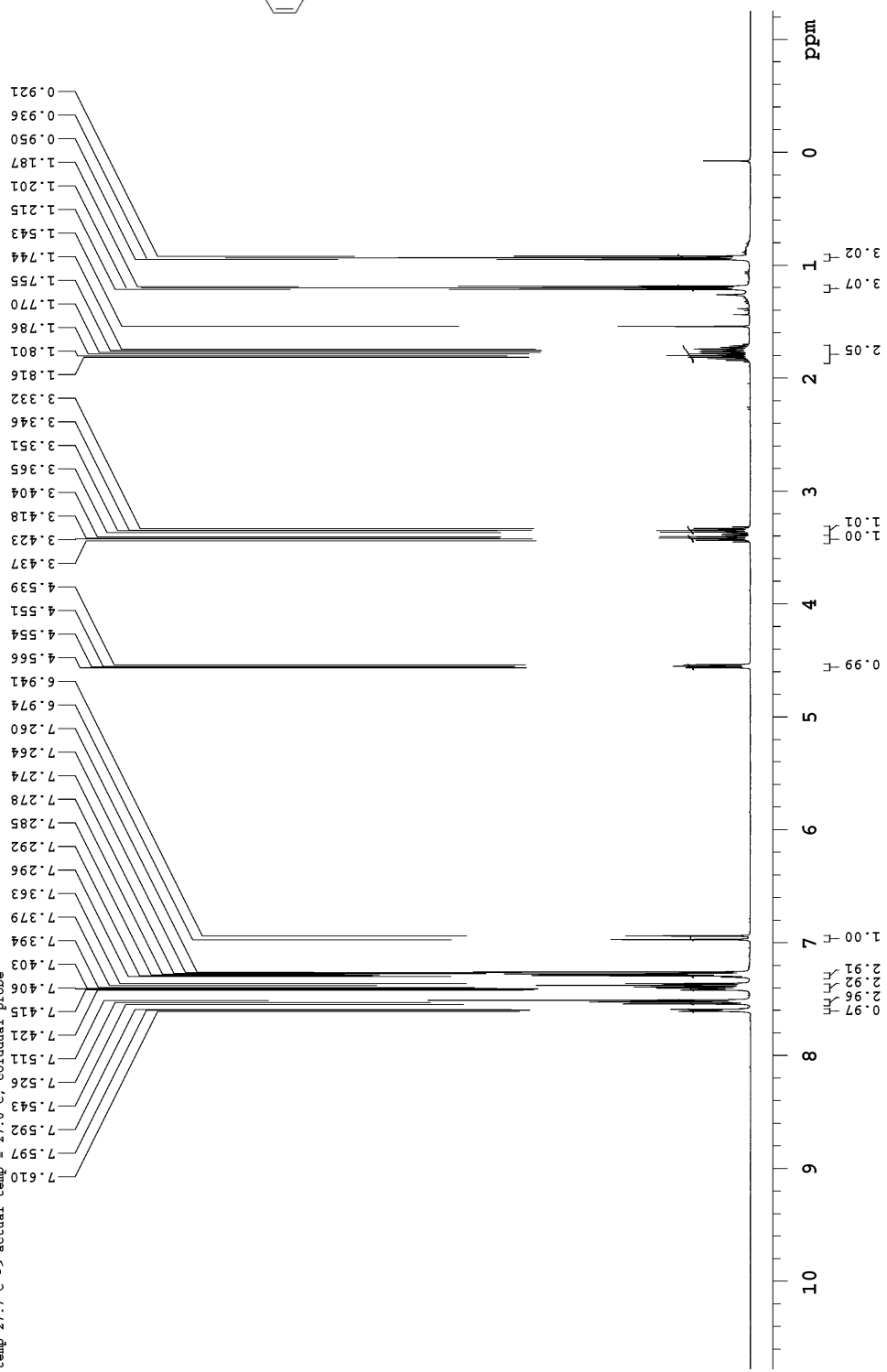


Emily, 2.53
 499.787 MHz H1 1D in cdcl3 (ref. to CDCl3 @ 7.26 ppm)
 temp 27.7 C -> actual temp = 27.0 C, coldlual probe

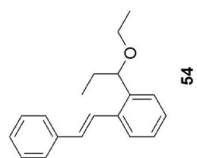
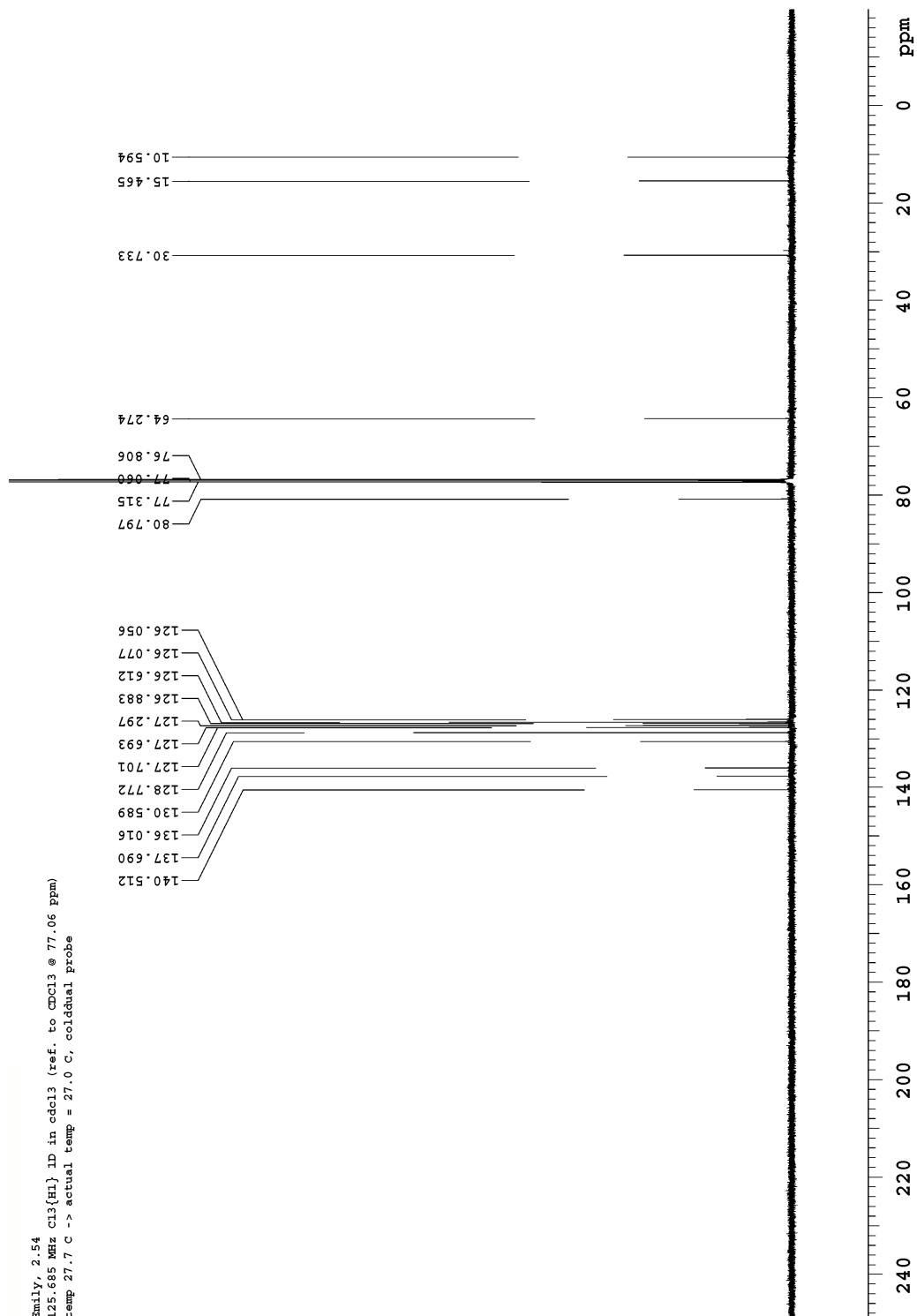


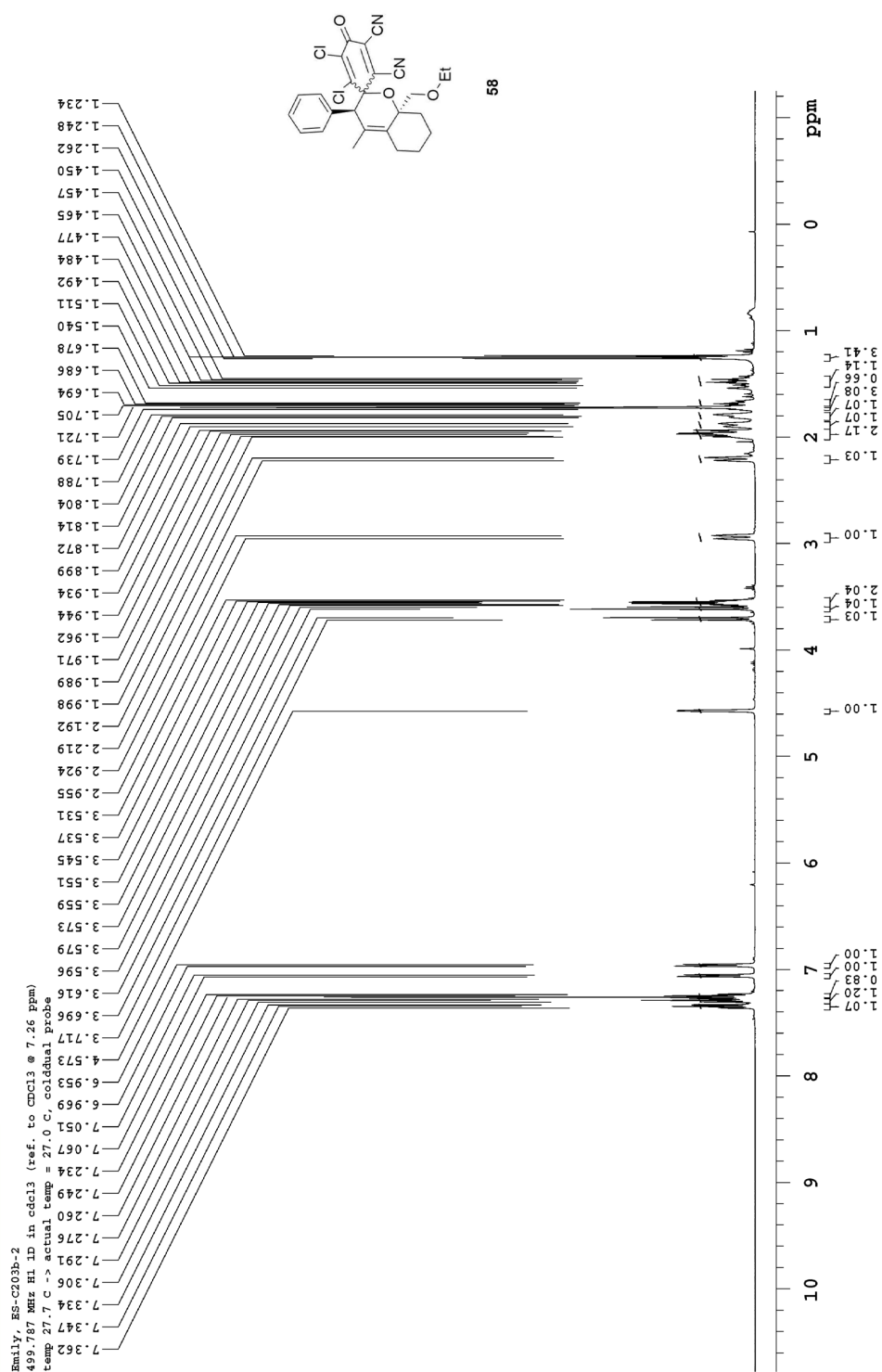


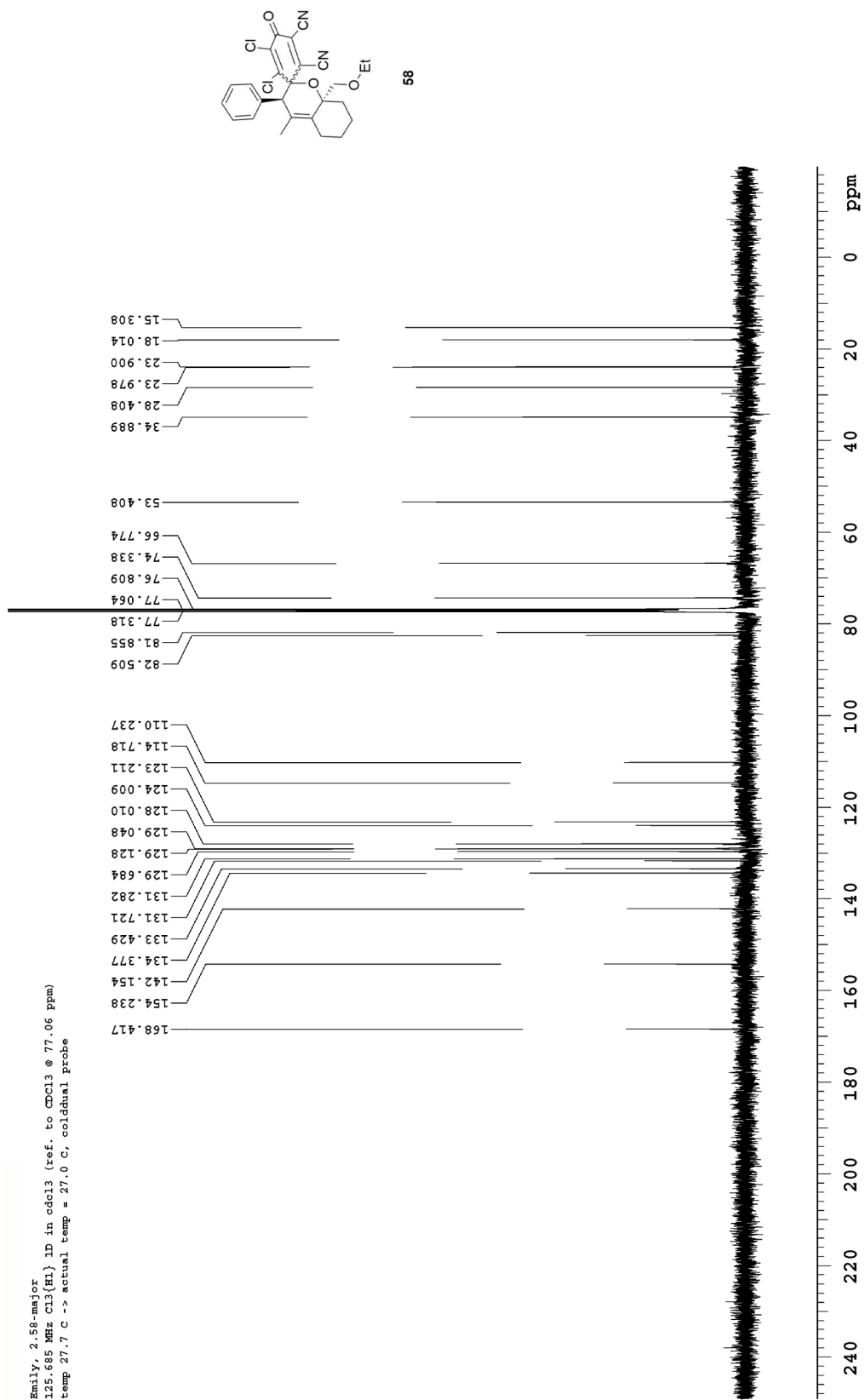
Emily, 2.54
 499.787 MHz ¹H 1D in cdcl3 (ref. to CDCl3 @ 7.26 ppm)
 temp 27.7 C -> actual temp = 27.0 C, coldchual probe

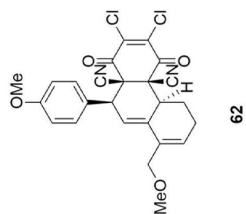
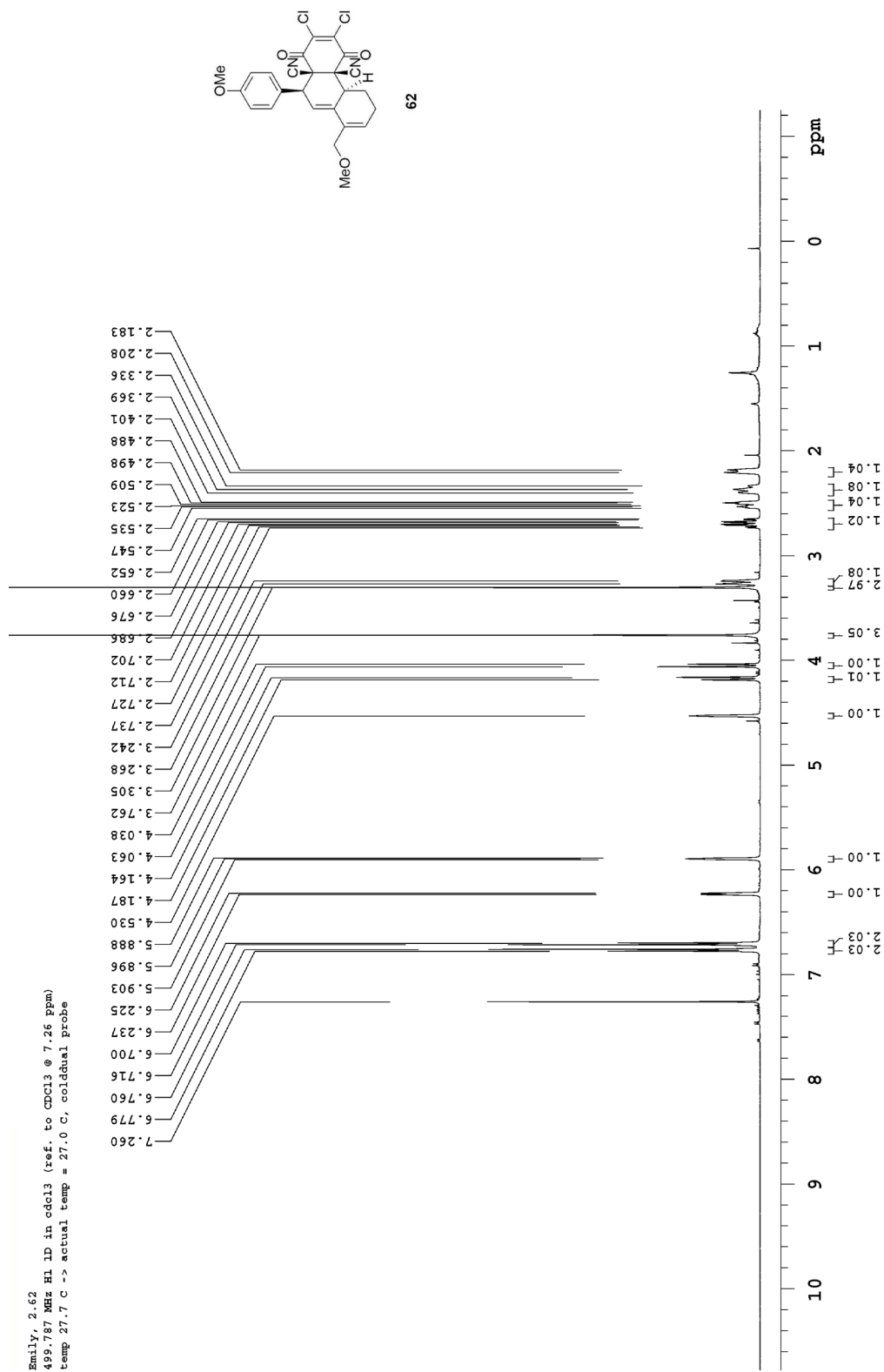


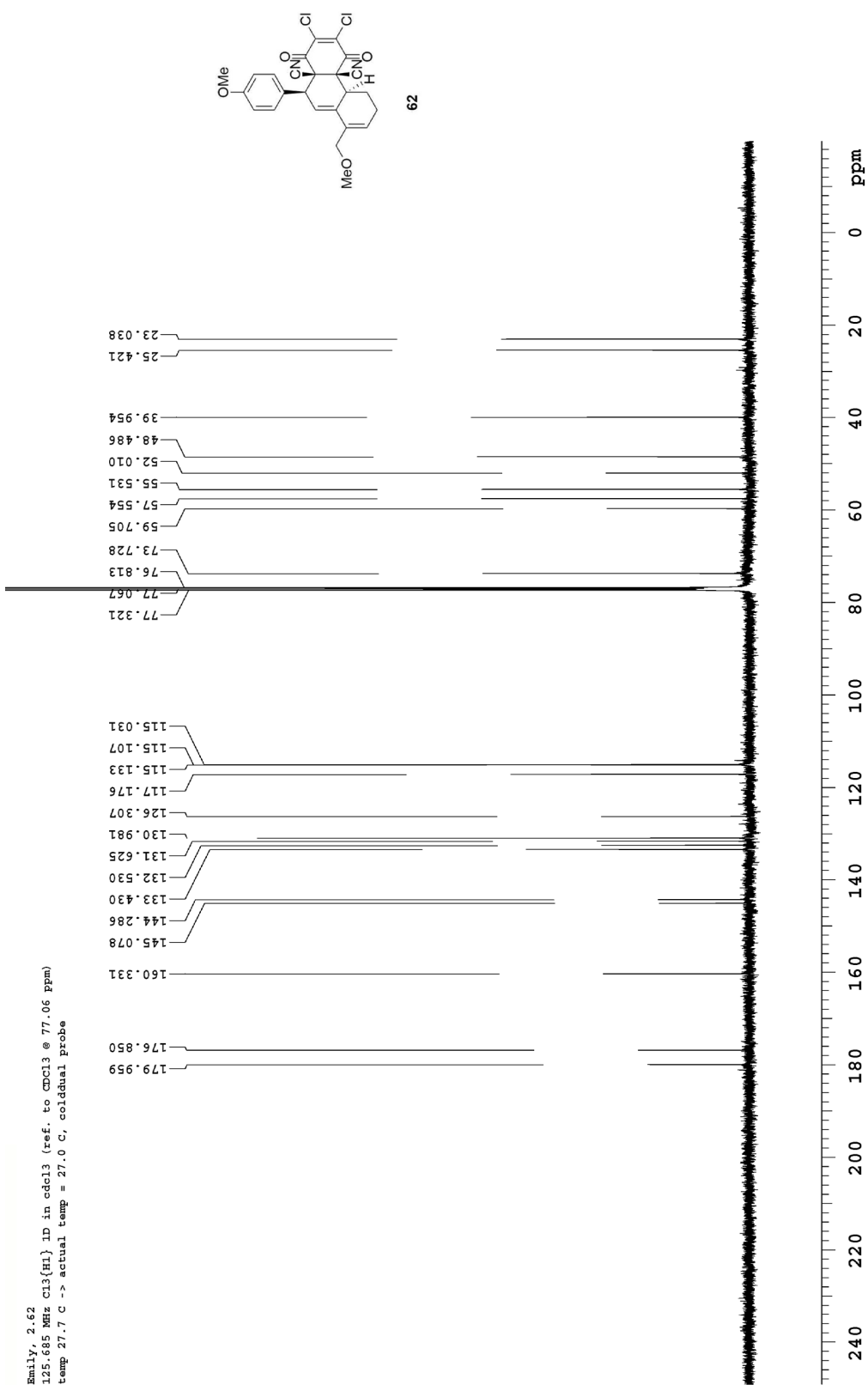
Emily, 2.54
 125.685 MHz Cl3{H1} 1D in cdcl3 (ref. to CDCl3 @ 77.06 ppm)
 temp 27.7 C -> actual temp = 27.0 C, coldlual probe



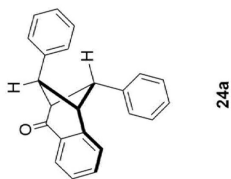
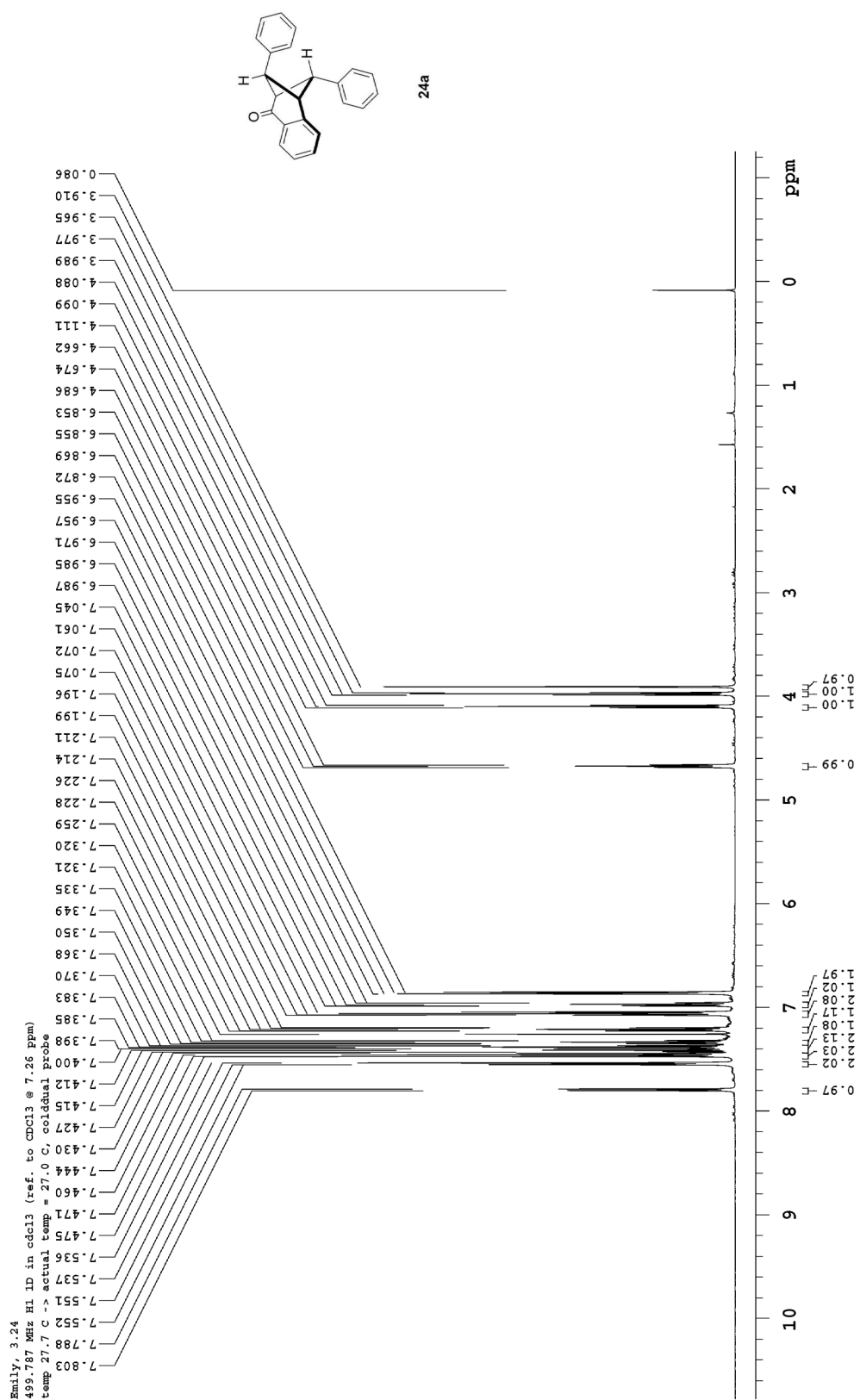




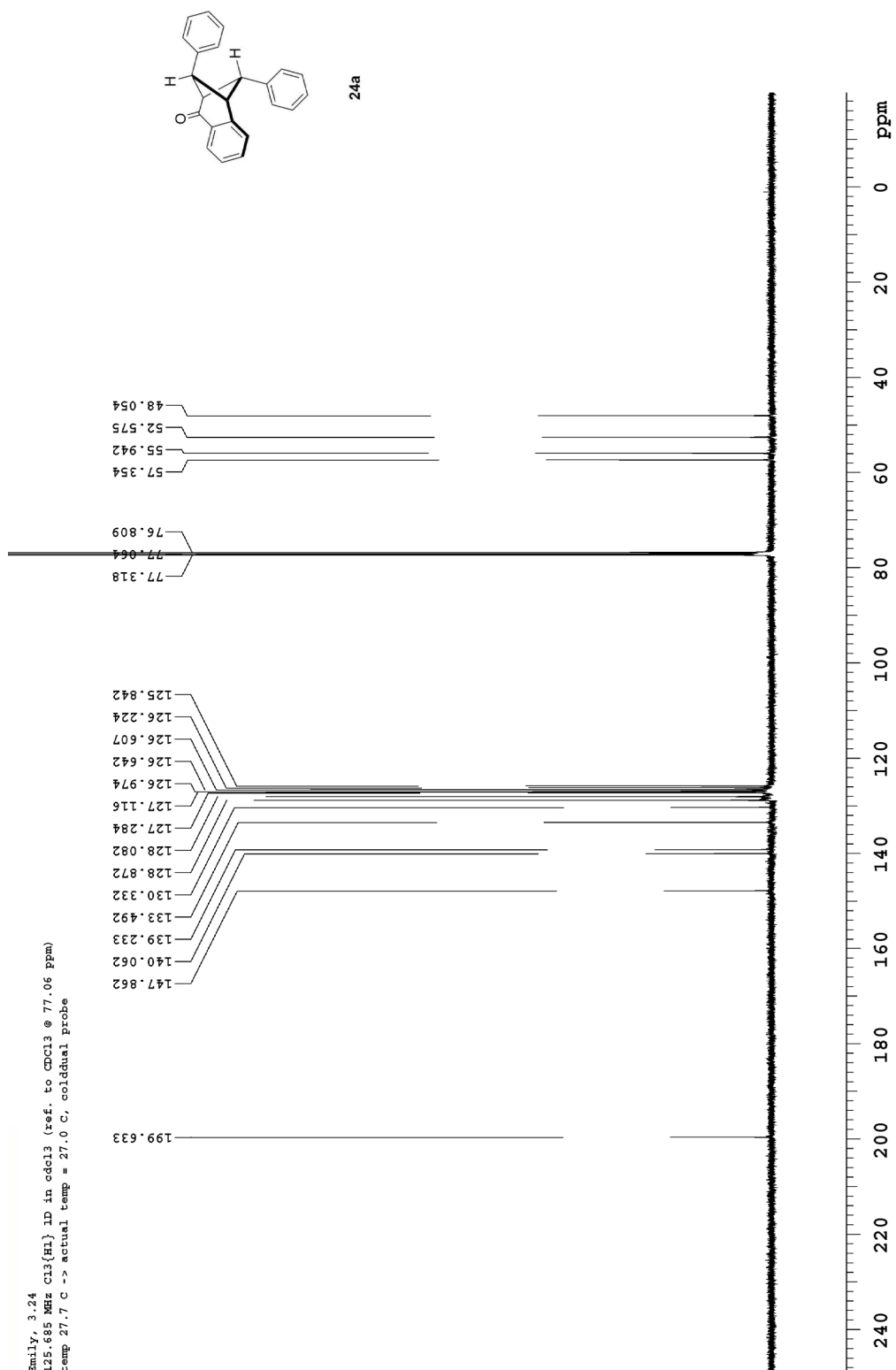


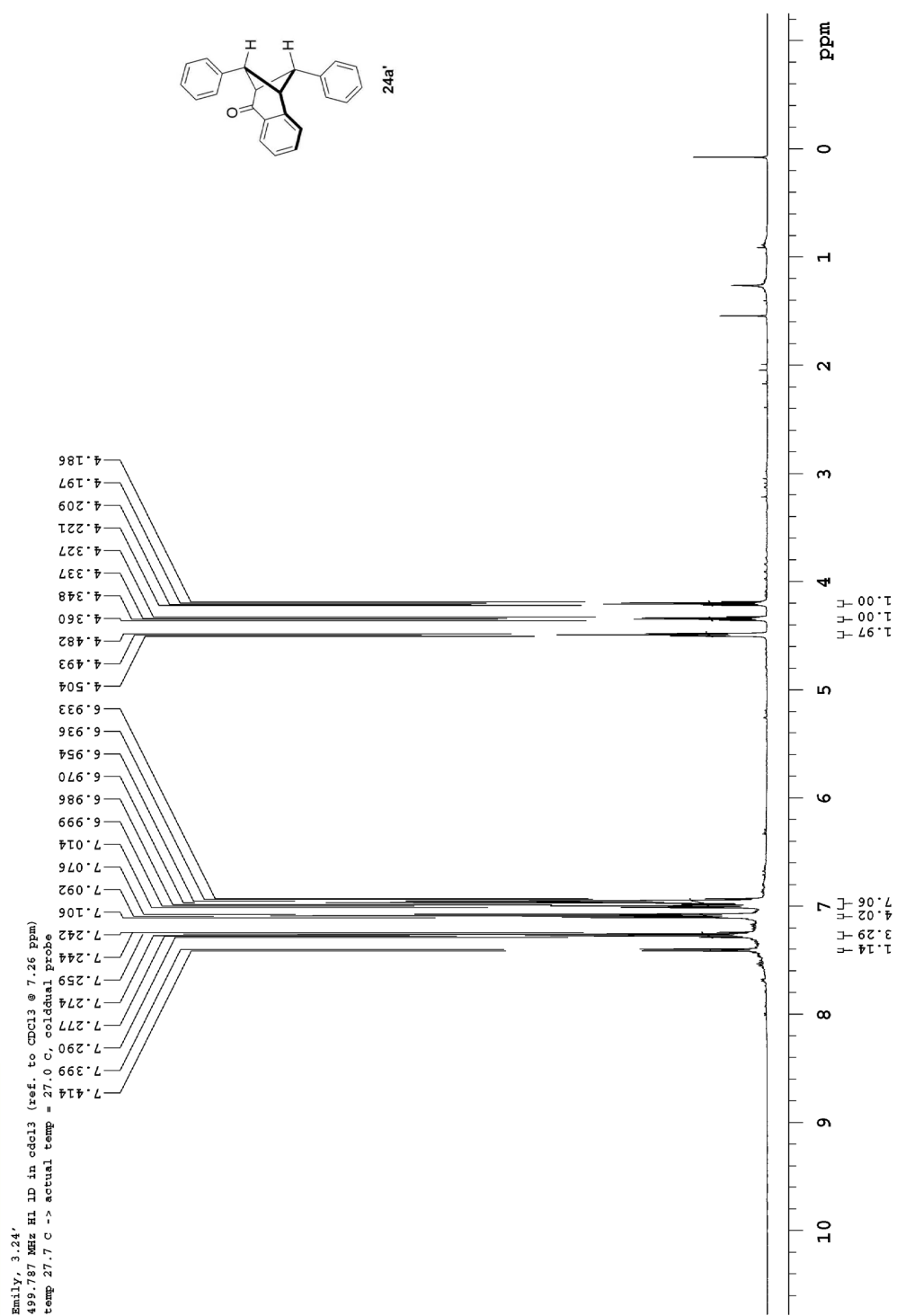


Appendix II: Selected NMR Spectra
(Chapter 3)

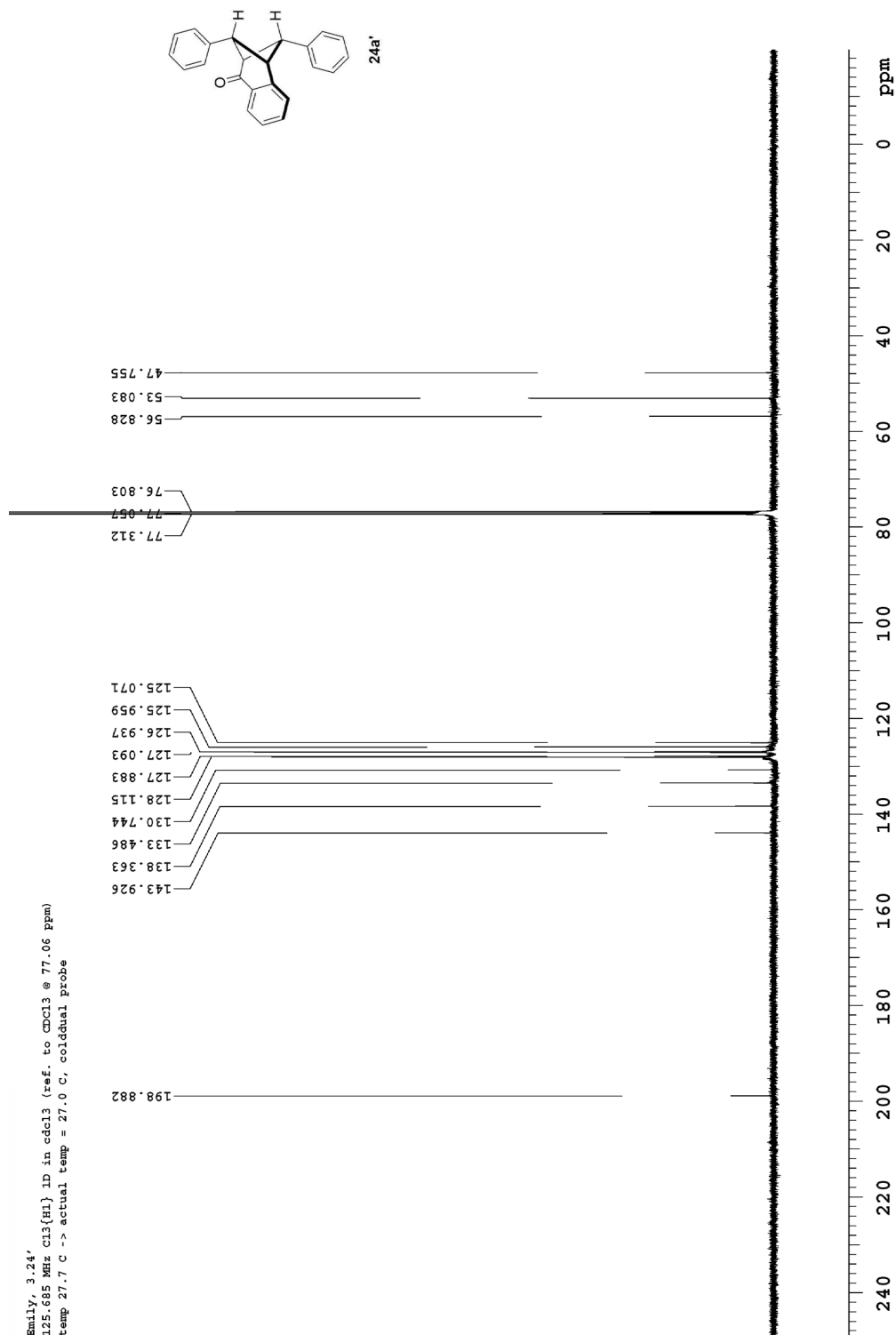


Enily, 3/24
 125.685 MHz C13{H1} 1D in cdcl3 (ref. to CDCl3 @ 77.06 ppm)
 temp 27.7 C -> actual temp = 27.0 C, cold dual probe





Emily, 3-24'
 125.685 MHz c13{h1} 1D in cdcl3 (ref. to CDCl3 @ 77.06 ppm)
 temp 27.7 C -> actual temp = 27.0 C, cold dual probe



Emily, 3.25g
 499.787 MHz ¹H 1D in cdcl3 (ref. to CDCl3 @ 7.26 ppm)
 temp 27.7 C -> actual temp = 27.0 C, coldlual probe

